

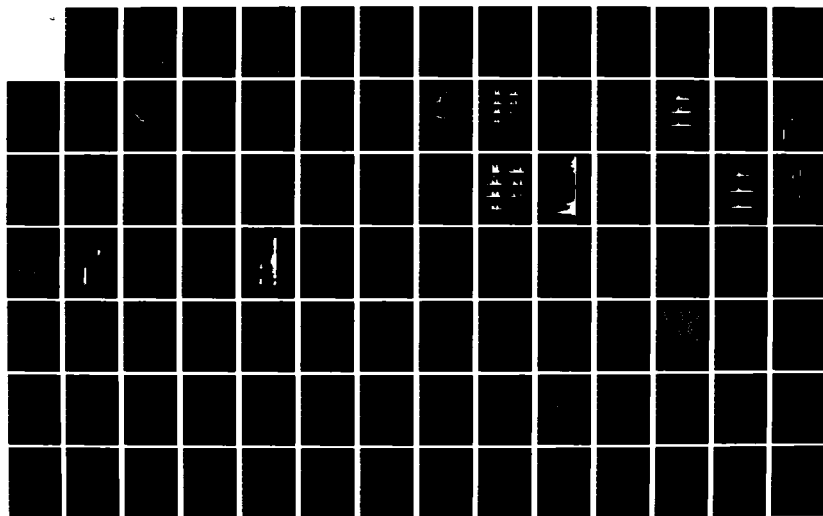
HD-A137 778

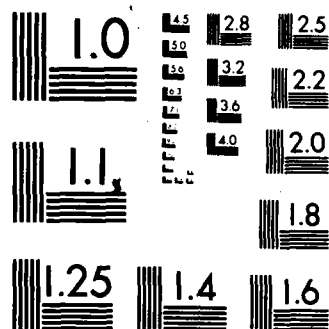
SPECTRAL ANALYSES OF HIGH-FREQUENCY PN SN PHASES FROM  
VERY SHALLOW FOCUS EARTHQUAKES(U) HAWAII INST OF  
GEOPHYSICS HONOLULU D A WALKER SEP 83 AFOSR-TR-84-0059  
F49620-81-C-0065 F/G 8/11

1/2

UNCLASSIFIED

NL





MICROCOPY RESOLUTION TEST CHART  
NATIONAL BUREAU OF STANDARDS-1963-A

AD A13778

AFOSR-TR. 84-0059

4

FINAL  
Technical Report

to the

Air Force Office of Scientific Research

from  
Daniel A. Walker

Hawaii Institute of Geophysics  
University of Hawaii  
Honolulu, Hawaii 96822

Name of Contractor: University of Hawaii

Effective Date of Contract: 3 March 1981

Contract Expiration Date: 30 September 1983

Total Amount of Contract Dollars: \$270,910

Contract Number: F49620-81-C-0065

Principal Investigator and Phone Number: Daniel A. Walker  
808-948-8767

Program Manager and Phone Number: John W. Shupe  
Interim Director of Research  
808-948-7541

Title of Work: Spectral Analyses of High-Frequency Pn, Sn Phases from Very  
Shallow Focus Earthquakes

The views and conclusions contained in this document are those of the authors and should not be interpreted as necessarily representing the official policies, either expressed or implied, of the Air Force Office of Scientific Research or the United States Government.

DTIC FILE COPY

DTIC  
ELECTE  
S FEB 13 1984 D

Approved for release;  
distribution unlimited.

84 02 10 126

**UNCLASSIFIED**

SECURITY CLASSIFICATION OF THIS PAGE (When Data Entered)

REPORT DOCUMENTATION PAGE		READ INSTRUCTIONS BEFORE COMPLETING FORM
1. REPORT NUMBER <b>AFOSR-TR- 84-0059</b>	2. GOVT ACCESSION NO. <b>AD-A137775</b>	3. RECIPIENT'S CATALOG NUMBER
4. TITLE (and Subtitle)  Spectral Analyses of High-Frequency Pn,Sn Phases from Very Shallow Focus Earthquakes		5. TYPE OF REPORT & PERIOD COVERED  Final Report
		6. PERFORMING ORG. REPORT NUMBER
7. AUTHOR(s)  D. A. Walker		8. CONTRACT OR GRANT NUMBER(s)  F49620-81-C-0065
9. PERFORMING ORGANIZATION NAME AND ADDRESS Hawaii Institute of Geophysics University of Hawaii Honolulu, Hawaii 96822		10. PROGRAM ELEMENT, PROJECT, TASK AREA & WORK UNIT NUMBERS  2309/A1 <b>6/102F</b>
11. CONTROLLING OFFICE NAME AND ADDRESS  Air Force Office of Scientific Research/ <b>NP</b> Bolling AFB, Washington, D.C. 20301		12. REPORT DATE  September 1983
		13. NUMBER OF PAGES  <b>182</b>
14. MONITORING AGENCY NAME & ADDRESS (if different from Controlling Office)		15. SECURITY CLASS. (of this report)  unclassified
		15a. DECLASSIFICATION/DOWNGRADING SCHEDULE N/A
16. DISTRIBUTION STATEMENT (of this Report)  <del>Approved for public release;</del> <del>distribution unlimited.</del>		
17. DISTRIBUTION STATEMENT (of the abstract entered in Block 20, if different from Report)		
18. SUPPLEMENTARY NOTES		
19. KEY WORDS (Continue on reverse side if necessary and identify by block number)  Underground Nuclear Explosions; Body-Waves; Spectral Analyses; Hydrophone Recording; Discrimination; Noise Levels		
20. ABSTRACT (Continue on reverse side if necessary and identify by block number)  The Wake Island Hydrophone Array has been successfully upgraded from a 3-channel slow-speed analog cassette system to an 11-channel computer controlled digital system for continuing research on Ocean P (Po) and Ocean S (So) phases, as well as normal, mantle-refracted P phases from underground nuclear explosions and earthquakes at great distances.		

DD FORM 1 JAN 73 1473

**UNCLASSIFIED**

SECURITY CLASSIFICATION OF THIS PAGE (When Data Entered)



UNCLASSIFIED

SECURITY CLASSIFICATION OF THIS PAGE(When Data Entered)

Features of the upgraded system are a large dynamic range (events from at least 4.0 to 8.0 mb can be recorded without distortion), absolute timing accuracy to 1 msec, interchannel timing accuracy to 1 msec, digital recording for ease of processing, and a 40 Hz Nyquist frequency for recording frequencies actually observed in Po/So at large distances.

Software development for compression and efficient management of the data has been successfully completed with master tapes sent to DARPA's Center for Seismic Studies for use by interested investigators.

Research papers on Po/So phases have reported on the frequency content and propagation velocities at the Wake hydrophones and across a 1600 km long deep ocean hydrophone array. At a distance of about  $18^{\circ}$  ( $\approx 2000$  km) frequencies for Po/So are as high as 30 and 35 Hz, respectively;

at a distance of about  $30^{\circ}$  ( $\approx 3,300$  km), as high as 15 and 20 Hz, respectively. The travel time equations which successfully model all Northwestern Pacific shallow-focus Po/So first arrival data collected by the Hawaii Institute of Geophysics since 1963 at epicentral distances greater than  $12^{\circ}$  are  $T = X/(7.96 \pm 0.05 \text{ km/sec}) - (7.14 \pm 2.38 \text{ sec})$  and  $T = X/(4.57 \pm 0.04 \text{ km/sec}) - (14.03 \pm 5.31 \text{ sec})$ , respectively. Values for a frequency dependent Q are found to range from  $625 \pm 469$  at 2 Hz to  $2106 \pm 473$  at 13 Hz for Po and from  $1401 \pm 296$  at 5 Hz to  $3953 \pm 863$  at 15 Hz for So. This could alternatively be described as an average attenuation of  $-21.5 \pm 0.9 \text{ dB}$  per 1000 km of travel path for both Po and So at all frequencies studied.

Regarding published research on normal-mantle refracted P phases, spectral comparisons for earthquakes and explosions have been completed and published. Expected differences between the spectral signatures of explosions and shallow focus earthquakes at great distances (the nuclear explosions being relatively stronger at high frequencies) are reported. The recording of a small explosion and improvement in its S/N ratio through some elementary enhancement techniques are also discussed.

Accession For	
NTIS GRA&I	<input checked="checked" type="checkbox"/>
DTIC TAB	<input type="checkbox"/>
Unannounced	<input type="checkbox"/>
Justification	
By	
Distribution/	
Availability Codes	
Dist	Avail and/or Special
A/1	



UNCLASSIFIED

SECURITY CLASSIFICATION OF THIS PAGE(When Data Entered)

# TABLE OF CONTENTS

Page

## INTRODUCTION

General Objectives . . . . .	1
Specific Objectives . . . . .	1
Reasons for Interest . . . . .	1

## PROGRESS

Upgrading of the Wake Island Hydrophone Array Recording System . . .	3
Po/So Spectra vs. Focal Depth and Source Parameters . . . . .	4
Spectral Comparisons for Earthquakes and Explosions . . . . .	4
Estimates of Coherence . . . . .	5
Comparisons of S/N Ratios . . . . .	5

SUMMARY OF ACCOMPLISHMENTS . . . . .	5
--------------------------------------	---

SIGNIFICANT TASKS REMAINING . . . . .	7
---------------------------------------	---

## APPENDICES

- I. "Spectra of nuclear explosions, earthquakes, and noise from Wake Island bottom hydrophones" by C. S. McCreery, D. A. Walker, and G. H. Sutton; Geophys. Res. Lett., 10, 59-62, 1983.
- II. "Spectral characteristics of high-frequency Pn. Sn phases in the Western Pacific" by D. A. Walker, C. S. McCreery, and G. H. Sutton, J. Geophys. Res., 88, 4289-4298, 1983.
- III. "Oceanic Pn/Sn: a qualitative expansion and reinterpretation of the T-phase" by D. A. Walker; HIG Report 82-6, 1982.
- IV. "A Preliminary Informal Comparison of Signal/Noise Capabilities Between the Wake Bottom Hydrophone Array, the Ocean Sub-Bottom Seismometer, and Ocean Bottom Seismometers" by C. S. McCreery and D. A. Walker.
- V. Po/So Phases: Propagation Velocity and Attenuation Across a 1600 km Long Deep Ocean Hydrophone Array by D. A. Walker and C. S. McCreery.
- VI. OPA Newsletter, no. 1, 15 September 1982.
- VII. OPA Newsletter, no. 2, 15 January 1983.
- VIII. OPA Newsletter, no. 3, 15 May 1983.
- IX. "The Continuous Digital Data Collection System for the Wake Island Hydrophones" by C. S. McCreery.
- X. List of Events Processed by the Wake Digital Data Collection System.

AIR FORCE  
NOTES  
This  
ap  
Dist  
limited.  
MATTHEW  
Chief, Technical Information Division

## INTRODUCTION

### General Objectives

General objectives of our research in deep ocean seismology can be summarized as follows:

- (1) to determine the mechanism for the generation and propagation of Po/So phases; and
- (2) to utilize the low noise levels at high frequencies (i.e.,  $> 2$  Hz) of the deep oceans and the relatively large amplitudes observed in P at those high frequencies from events at great distances (i.e.,  $>> 30^\circ$ ) to gain new insights into: (a) differences in spectra associated with source characteristics, and (b) the physical properties of the deep mantle.

In the past two years the principal means for achieving these objectives has been through the acquisition of data from hydrophones and ocean bottom seismometers located near Wake Island.

### Specific Objectives

Specific objectives of an applied nature which we believe may be of interest to AFOSR are the following:

- (1) the relationship of Po/So spectra to focal depth and source parameters;
- (2) spectral comparisons of normal, mantle-refracted P phases at great distances from earthquakes and explosions;
- (3) estimates of the coherence of seismic phases recorded on the deep ocean floor; and
- (4) comparisons of S/N ratios for phases recorded on the Wake hydrophones, ocean bottom seismometers, and ocean sub-bottom seismometers.

The specific means by which AFOSR has contributed to our efforts to achieve these objectives has been major support for the upgrading of our Wake Island hydrophone array (partial support being derived from ACDA) and for the analysis of data acquired by: (a) the upgraded station, (b) the original three channel Wake system, and (c) other ocean bottom instrumentation in the Western Pacific.

### Reasons for Interest

Reasons why these applied objectives may be of interest follow.

- (1) For oceanic travel paths out to distances of about 3000 km, Po/So phases have signal-to-noise ratios generally at least ten times greater than the ratios of their respective normal, mantle-refracted P and S phases; and, in many instances, no P's or S's can be found in spite of

the presence of very strong Po's and So's. Therefore, the detection and discrimination of underground nuclear explosions at distances less than about 3000 km in an ocean environment requires an understanding of Po/So. Most important could be any possible relationship of Po/So spectra to focal depth and/or source parameters.

- (2) Normal, mantle-refracted P phases recorded at great distances (i.e.,  $60^{\circ}$  to  $90^{\circ}$ , or approximately 6700 km to 10,000 km) have substantial amounts of energy at high frequencies (i.e., 2 Hz to 10 Hz). Such phases from earthquakes and explosions are well recorded in the low noise environment of the deep ocean. [Estimates of noise levels on the Wake bottom hydrophones in the 2 to 10 Hz range are comparable to those of the best continental sites.]
- (3) A major concern in the analysis of underground explosions by seismic methods is the reliability of yield estimates. Much of the scatter in yield estimates is due to inconsistencies between the waveforms from different stations, and even between the waveforms from elements of continental arrays with apertures the size of the Wake bottom array. These differences may be attributable to variations in the response of the continental crust underlying these arrays. Signals recorded in regions where the crust is very thin (i.e., under the deep ocean basins) may have higher coherencies--thereby providing a means for improved estimates of yield. The Wake array is an ideal tool for evaluating this hypothesis.
- (4) In recent years some members of the "detection and discrimination" community have demonstrated a substantial amount of interest in ocean sub-bottom instrumentation. The level of this interest may be best manifested in DARPA's commitment to develop a working sub-bottom system--the "Marine Seismic System" or MSS. Another sub-bottom instrument which has been developed (this at HIG through ONR sponsorship) is called the "Ocean Sub-Bottom Seismometer" (OSS). A reasonable presumption is that S/N ratios for ocean sub-bottom systems would be greater than for existing bottom systems (i.e., ocean bottom seismometers or ocean bottom hydrophones), resulting in a higher sensitivity (or lower detection threshold) for the sub-bottom instrument. A possible alternative to a sub-bottom instrument is an array of bottom instruments such as ocean bottom seismometers or ocean bottom hydrophones, with enough elements to make up the difference in S/N. Essential requirements to achieve an increase in S/N are incoherent noise and coherent signals in the frequency band of interest. Advantages of such an array over a sub-bottom instrument may be in cost, in ease of deployment, and in studies requiring an array. With the continued operation of the eleven element deep-ocean hydrophone array near Wake Island, these questions may be answered through further comparisons between signals recorded by the sub-bottom systems and those recorded by the Wake hydrophones.

## PROGRESS

### Upgrading of the Wake Island Hydrophone Array Recording System

Upgrading of the recording system for the Wake Hydrophone Array, from a 3-channel slow-speed analog cassette system to an 11-channel, 16 bit, computer-controlled digital system, was accomplished by September, 1982. Some of the advantages of this new system are: (1) a large dynamic range to record, without distortion, events ranging from at least  $mb = 4.0$  to  $mb = 8.0$  (i.e., 16 bits = 96 dB); (2) absolute timing generally accurate to 1 msec (for ease in processing, no time correction needs to be applied to achieve this accuracy); (3) interchannel timing accurate to within 1 msec; (4) a digital recording format such that only a minimal amount of processing is necessary to convert the data to a widely useable format; (5) the capability to record all eleven available hydrophones; (6) the recording of frequencies at least as high as those already observed at Wake in Po and So (i.e., a 40 Hz Nyquist); (7) operation of the system so simple that it can be accomplished by the personnel at Wake who are untrained in computer hardware and software; (8) required servicing (i.e., changing tapes) no more than once per day; and (9) the capability of restarting automatically after power failures (which occur frequently at Wake).

The recording of data from all eleven available hydrophones produces four full-reel computer tapes per day requiring four tape drives to maintain a maximum of once per day servicing by an operator. Several problems which have occurred with the tape drives have made it necessary to record only eight of the eleven hydrophones (thus producing only three tapes per day) during most of the recording period. All other losses of data, including those caused by power-failures, amount to less than 3% of the total data collected.

Once the data on computer tape are received by HIG, an efficient compression and management of the data must be accomplished. Uncompressed, the data could amount to 1460 tapes per year, requiring a large space for storage and being inefficient to access for study, or to copy and transmit to other scientists. Software has been developed to compress this data to approximately 15% of its original volume and at the same time catalog all of the saved data for easy accessibility. Sections of data saved correspond to arrivals from events, and the raw data are also randomly sampled for future quantification of the temporal characteristics of ambient noise levels.

Compressed data tapes have been sent to the DARPA Center for Seismic Studies (CSS) for use by other scientists.

A complete description of the digital recording system at Wake, the data compression software used at HIG, and the tape format for data sent to CSS is contained in Appendix IX. A list of events for which the times of possible arrivals have been saved on the CSS compressed data tapes is contained in Appendix X.

## Po/So Spectra vs. Focal Depth and Source Parameters

Although this was one of our original research objectives for AFOSR, no direct progress has been made in this area. Factors contributing to this lack of progress have been:

- (a) the re-direction of efforts towards topics more readily resolved, of more immediate interest, and/or of greater apparent importance;
- (b) anticipated improvements in instrumentation (i.e., the upgrading to a digital, rather than an analog system) which would greatly facilitate the data reduction required for this task; and
- (c) the small number of events with very shallow focal depths (<10 km).

Indirectly, a great deal of progress may have been made towards the achievement of this objective. [It is unlikely that relationships of spectra to focal depths and source parameters could be postulated in the absence of a generally acceptable model for the generation and propagation of Po/So phases.] Evidence of continuing progress in Po/So research may be found in: (a) recent publications ("Oceanic Pn/Sn: a qualitative explanation and reinterpretation of the T-phase" by D. Walker; HIG Report 82-6; and "Spectral characteristics of high-frequency Pn. Sn phases in the Western Pacific" by D. Walker, C. McCreery, and G. Sutton; op. cit.); (b) the formation of an Ocean P Alliance with the publication of an OPA newsletter; and, (c) important advances apparent in analyses of data acquired by the ONR sponsored OBS Wake array experiment reported at the recent fall AGU meeting and now in draft form in preparation for publication. ("Po/So Phases: Propagation Velocity and Attenuation Across A 1600 km Long Deep Ocean Hydrophone Array" by D. A. Walker and C. S. McCreery).

We should note that with the upgraded system we have recorded two shallow focus events (15 km and 17 km depth) from the Marianas at distances of about 18° and one intraplate (and presumably very-shallow focus) event from approximately 12° to the west of Wake. The Po/So phases from these, and other, events will be useful in evaluating Po/So as a possible discriminant.

## Spectral Comparison for Earthquakes and Explosions

Spectral comparisons between earthquakes and explosions have been completed and are the subject of a published paper ("Spectra of nuclear explosions, earthquakes, and noise from Wake Island bottom hydrophones" by C. McCreery, D. Walker, and G. Sutton, Geophys. Res. Lett., 10, 59-62, 1983.) The data examined show expected differences between the spectral signatures of explosions and shallow focus earthquakes at great distances--the nuclear explosions being relatively stronger at high-frequencies (or weaker at low-frequencies) than earthquakes. Also, a small explosion has been recorded with a significant S/N ratio on the Wake hydrophones. A unique aspect of hydrophone recordings is that the ocean surface reflection (recorded at a time after the main P corresponding to twice the water depth divided by the velocity of sound in water) can be used to increase S/N ratios.

## Estimates of Coherence

Comprehensive estimates of coherence and possible improvements in yield estimates are a major topic for investigation in the coming year using data acquired from the expanded hydrophone array. Some preliminary estimates of coherence have already been made. These estimates are appended to this report.

## Comparisons of S/N Ratios

In September of 1982, DARPA and ONR conducted tests (the "Downhole Experiment") in the Northwestern Pacific relating to sub-bottom seismic instrumentation. Successful deployments included OBS's and HIG's ocean sub-bottom seismometer (OSS). During the same time the expanded Wake system became operational. Preliminary comparisons of S/N ratios for the Wake system and the available downhole data have been made. They are appended to this report. Additional comparisons were (and are being) made after the OSS data was retrieved from its recording package on the ocean bottom in the summer of 1983. These comparisons will be the subject of a future report.

## SUMMARY OF ACCOMPLISHMENTS

Major accomplishments supported in whole, or in part, by AFOSR since 3 March 1982 follow.

- (1) Successful upgrading of the Wake Hydrophone Array recording system from a three-channel analog cassette system to a sixteen-channel digital system. Some of the advantages of this new system are: (a) the ability to simultaneously record all of the active hydrophones in the array; (b) a 96 dB dynamic range; (c) millisecond accurate absolute and cross-channel timing; and (d) a digital format which allows immediate processing of the data.
- (2) Development of software to compress and manage the digital data collected at Wake. This data is compressed by saving intervals of data in which seismic phases of interest are known or suspected to be present, and by saving regular intervals of data for sampling the ambient noise levels. These compressed data are stored on magnetic tape files which are catalogued on paper and in computer files for easy reference.
- (3) Preparation of a report on items 1 and 2 above ("The Continuous Digital Data Collection System for the Wake Island Hydrophones" by C. S. McCreery).
- (4) Distribution of the Wake digital data through the DARPA Center for Seismic Studies (CSS). Compressed data tapes containing known or suspected seismic phases are being routinely sent to CSS for access by others who may have an interest in this data. Investigators at Rondout Associates Inc. have successfully accessed the data through CSS. A list of intervals, and the events and phases, which they represent, is contained in Appendix X. The event format of the data also is described in Appendix IX.

- (5) The observation and characterization of differences in spectral signature between P from explosions and P from shallow focus earthquakes recorded on the Wake bottom hydrophones. The observations reflect differences in source spectra between explosions and shallow focus earthquakes. For similar magnitudes, explosions had more energy at frequencies above 2.0 Hz and less energy at frequencies below 1.5 Hz.
- (6) The enhancement of S/N of an extremely small explosion by signal stacking to a level near that for perfectly coherent signals.
- (7) The publication of a report on items "4" and "5" above ("Spectra of nuclear explosions, earthquakes, and noise from Wake Island bottom hydrophones" by C. McCreery, G. Sutton, and D. Walker; op. cit.).
- (8) Continuing analyses of Po/So phases with additional spectrograms and discussions submitted for publication ("Spectral characteristics of high-frequency Pn. Sn phases in the Western Pacific" by D. Walker, C. McCreery, and G. Sutton; op. cit.).
- (9) The formation of an "Ocean P Alliance" with the publication of an OPA Newsletter to stimulate interest in, and research on, Po/So phases.
- (10) The evolution of a qualitative explanation for the propagation of Po/So phases consistent with many observations of these phases throughout the western, northern, and central Pacific.
- (11) The discovery of a probable relationship between Po/So and T phases.
- (12) Publication of a report discussing item "9" and "10" above ("Oceanic Pn/Sn: a qualitative explanation and reinterpretation of the T-phase" by D. Walker; HIG Report 82-6.)
- (13) Preliminary comparisons, with available data, of the Wake hydrophones to ocean bottom seismometers and the OSS. It should be noted that these are merely preliminary studies and in some cases the comparisons made are of an indirect nature. Nonetheless, it would appear that the Wake hydrophones may be comparable to the OSS in terms of S/N ratios, considering possible improvements through array processing. Direct comparisons to MSS are not possible since that system was not successfully deployed in the Pacific. Regarding the comparisons of Wake to ocean bottom seismographs, we have observed with data from an ONR sponsored OBS experiment near Wake Island in 1981 that the Wake hydrophones have higher S/N ratios than OBS's by about 10 dB over the range 1-20Hz.
- (14) The presentation of studies on the spectra of nuclear explosions and earthquakes, as well as spectral studies of Po/So, at the 1982 DARPA/AFOSR annual review.
- (15) Preparation of a report (Po/So Phases: Propagation Velocity and Attenuation Across a 1600 km Long Deep Ocean Hydrophone Array by D. Walker and C. McCreery) which quantifies the variations in velocity and spectra of Po/So phases across a long deep ocean array.



### SIGNIFICANT TASKS REMAINING

- (1) Consistent with our efforts to determine the mechanism for the generation and propagation of Po/So phases, a comprehensive investigation of the relationship of the T phase to Po/So will be made. This study will include spectral studies of the entire T phase coda (i.e., forerunners as well as peak signals) and comparisons of these spectra to the spectra of Po/So phases.
- (2) Differences between the hydrophone/cable response (and possibly the lithosphere response) across the Wake array will be determined and removed from the data. This will be necessary to evaluate the stability of yield estimates from spectral or waveform data across the array. Such an evaluation will be made.
- (3) Research on coherence across the Wake array will be completed within the coming year, and the significance of these studies in terms of possible improvements in S/N will be evaluated.
- (4) S/N comparisons to the Wake hydrophones will be made with the OSS data which was retrieved from its recording package on the ocean bottom this past summer.
- (5) Profiles of Po/So spectra as a function of focal depth will be made. If sufficient data is available for very shallow focus events, the possible significance of the relationships in terms of nuclear detection and/or discrimination will be evaluated.

The expanded Wake Island Hydrophone Array was successfully installed with funds provided primarily by AFOSR. However, since supplementary support of critical importance was provided by ACDA, all studies utilizing data acquired by the upgraded system should acknowledge both agencies. In the coming year ACDA funds will be used primarily on item #2 above, with the possibility that supplementary support for this task may be provided by AFOSR. On all other tasks AFOSR will be the principal supporter, with some supplementary funds provided by ACDA.

APPENDIX I

SPECTRA OF NUCLEAR EXPLOSIONS, EARTHQUAKES, AND NOISE FROM WAKE ISLAND BOTTOM HYDROPHONES

Charles S. McCreery and Daniel A. Walker

Hawaii Institute of Geophysics, University of Hawaii, Honolulu, HI 96822

George H. Sutton

Rondout Associates, Inc., Stone Ridge, NY 12484

**Abstract.** Spectral characteristics of P phases from 4 shallow focus earthquakes and 8 underground explosions, and of 52 samples of ocean bottom background noise, are examined by using tape recordings of ocean bottom hydrophones near Wake Island from July 1979 through March 1981. Significant differences are found between spectra of large shallow focus earthquakes and explosions ( $5.7 < m_b < 6.3$ ) observed at  $61^\circ$  to  $77^\circ$  epicentral distance. For similar magnitudes, explosions were found to have less energy at frequencies below 1.5 Hz and more energy at frequencies above 2.0 Hz. Earthquakes were found to have a spectral slope of  $-28$  dB/octave (relative to pressure) over the band 1 to 6 Hz. Explosions were found to have the same spectral slope over the band 2.2 to 6 Hz, but a different slope of  $-12$  dB/octave over the band 1.1 to 2.2 Hz. High frequencies ( $>6$  Hz) observed in the teleseismic P phases indicate high Q values for the deep mantle. Ambient noise levels on the ocean bottom near Wake are comparable to levels at the quietest continental sites for frequencies between 3 and 15 Hz. Also high levels of coherence (at least as high as 0.85) have been observed for P phases recorded on sensors with 40-km separation.

# Introduction

In an earlier report (Walker, 1980), slow-speed paper recordings of hydrophones located near Wake Island were used in a study of P phases from underground nuclear explosions and earthquakes at comparable distances. That study was prompted by: (1) the work of Evernden (1977) and Evernden and Kohler (1979), which showed that P phases recorded in the  $60^\circ$  to  $90^\circ$  distance range from underground explosions were surprisingly rich in high-frequency energy (at least as high as 9 Hz); (2) the extreme sensitivity of the Wake hydrophones to high-frequency signals (Walker et al., 1978); and (3) the location of most known underground test sites in the  $60^\circ$  to  $90^\circ$  distance range from the Wake hydrophones. The major conclusion of Walker (1980) was that observable P phases were found for all Russian underground explosions with estimated yields in excess of 270 kilotons, whereas no such phases were found for earthquakes of comparable or greater magnitude at similar distances. Principal limitations of the investigation were that: (1) the slow-speed paper recordings were not suitable for detailed spectral analyses of either the recorded signals

or the noise; and (2) the filtering was not optimized for the recording of distant earthquakes and explosions.

This report discusses the spectra of P phases from underground explosions and earthquakes as well as the spectra of ambient noise derived from recent tape recordings of the Wake Island ocean bottom hydrophone array. This array consists of six hydrophones on relatively flat ocean bottom near Wake at about 5.5-km depth. The hydrophones are located at the vertices and center of a pentagon roughly 40 km across and are cabled directly to Wake Island. Only three of the hydrophones could be recorded simultaneously on the recording system used. This system was a four-channel (three data, one time code) slow-speed cassette recorder, with automatic gain-ranging amplifiers following low-noise preamps connected to the differential outputs (via cabling) of the moving coil hydrophones on the ocean bottom. These recorded signals were used to compute absolute spectra of the seismic phases and background noise by the following steps: (1) digitization at 80 samples per sec after anti-alias filtering; (2) normalization of the automatic gain levels; (3) computation of contiguous 512-point FFT's (6.4 sec per FFT) and their corresponding power spectra; (4) averaging of those spectra over the time window of interest; (5) normalization of the spectral bandwidth from 0.156 Hz to 1.0 Hz; and (6) removal of the hydrophone/recording system/anti-alias response. The recording system and anti-alias response were determined in situ. The hydrophone response was taken from the Columbia University OBS Calibration Manual (Thanos, 1966), which describes the estimated response between 0.05 and 100 Hz of an equivalent hydrophone. More specific information on the Wake hydrophone/cable responses at these frequencies is not available because of the age of the array (about 20 years), its formerly classified status, and the original bandwidth of interest ( $>10$  Hz) to those who installed the array.

## Spectra of Underground Explosions and Natural Earthquakes

The earthquakes and explosions investigated in this study are listed in Table 1. These events were chosen because they all occurred within  $60^\circ$  to  $90^\circ$  epicentral distance, were shallow focus, had large signal/noise ratios, and did not exceed the dynamic range of the recording system. Figure 1 shows the pressure spectra of some of these events, as well as composite pressure spectra for the earthquake and explosion groups. For purposes of comparison, pressure and vertical

Copyright 1983 by the American Geophysical Union.

Paper number 2L1384.  
0094-8276/83/ 002L-1384\$3.00

Table 1. Description of Events Used in Figure 1

No.	Date	Location	Distance (degrees)	Depth (km)	Magnitude (mb)	Type	Number of Hydrophones
1	07/24/79	S. of Java	65.7	31	6.3	Earthquake	3
2	08/04/79	E. Kazakh	73.2	0	6.1	Explosion	3
3	08/18/79	E. Kazakh	73.2	0	6.1	Explosion	3
4	09/24/79	Novaya Zemlya	76.7	0	5.7	Explosion	1
5	09/29/79	N. Sumatra	72.9	27	6.2	Earthquake	1
6	10/18/79	Novaya Zemlya	76.8	0	5.8	Explosion	1
7	10/28/79	E. Kazakh	73.2	0	6.0	Explosion	1
8	12/23/79	E. Kazakh	73.3	0	6.1	Explosion	1
9	07/29/80	Nepal	76.4	18	6.1	Earthquake	2
10	09/14/80	E. Kazakh	73.2	0	6.2	Explosion	2
11	10/12/80	E. Kazakh	73.2	0	5.9	Explosion	2
12	11/19/80	Sikkim	70.4	17	6.0	Earthquake	2

displacement may be related using the expression:  $P = \omega \rho v A$ , where  $P$  is pressure,  $\omega$  is angular frequency,  $\rho$  is seawater density,  $v$  is the speed of sound in seawater, and  $A$  is vertical

displacement. This relationship holds for compressional energy arriving vertically from below the hydrophone. The following differences in the spectral signatures between explosions and shallow focus earthquakes are evident: (1) lack of energy in explosion P relative to earthquake P at frequencies below 1.5 Hz, (2) changes in spectral slope (corner frequency?) for explosions from -12 to -28 dB/octave (equivalent to -18 and -34 dB/octave in ground displacement) at about 2.2 Hz, and (3) greater energy in explosion P relative to earthquake P at frequencies above 2.0 Hz, despite smaller magnitude of the average explosion (6.03) than that of the average earthquake (6.16). Differences between the explosion and earthquake P phases observed at these frequencies is not surprising. The high frequencies observed and the actual shape of these curves have implications regarding  $Q$  along the travel path. Although these implications will not be discussed here, it is pointed out that the observation of frequencies in excess of 6 Hz (and up to 9 Hz) at distances greater than 60° implies a high  $Q$  at least along the deep mantle part of the P travel path.

Although this study found a common high-frequency slope (-28 dB/octave) for both earthquakes and explosions, at least one other investigator (Evernden, 1977) has found earthquakes to fall off at least  $f^{-1}$  faster than explosions. This discrepancy might be explained by the small number of earthquakes used in the present study and the requirement in choosing those events of large signal/noise. Earthquakes having more high-frequency energy would have greater signal/noise because of much lower noise levels at high frequencies.

NTS events were not included in this study because they were rarely recorded with signal/noise greater than 2. Although signal levels near 1 Hz for NTS events are roughly equivalent to those observed for similar magnitude earthquakes and Soviet explosions, the signal fall-off above 1 Hz appears to be generally much greater for NTS. Therefore, little signal energy from NTS events is observed in the band above 2 Hz where lower ambient noise levels significantly enhanced the signal/noise of those events that were used. This rapid fall-off may be due to a recognized low  $Q$  effect in the source region (see for example Der et al., 1982).

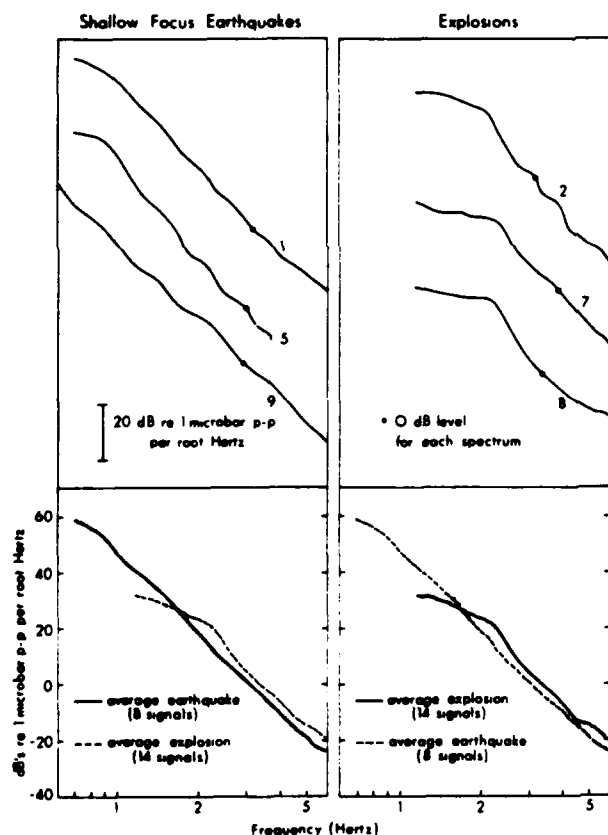


Figure 1. Sample spectra of P from some shallow focus earthquakes and nuclear explosions are shown in the upper portion of this figure. Numbers refer to the events as described in Table 1. The composite spectrum of each group, an average with  $\pm 1$  standard deviation, is shown in the lower portion of the figure. Before standard deviations were computed, individual spectrums were normalized by subtracting the difference between their mean dB value over the range 1.5-3.0 Hz and the mean dB value for all spectra over the same frequency range.

## Ocean Bottom Ambient Noise

The average background noise at the ocean bottom near Wake is shown in Figure 2 (labeled A). This average, along with its standard deviation, was determined from 52 samples of noise taken over 18 months of recording. Also plotted are an assortment of published noise curves for both ocean bottom and continental sites. When compared with noise levels from continental sites, the Wake ambient noise level could be described as: (1) high for frequencies between 0.2 Hz and 1.5 Hz; (2) average for frequencies between 1.5 Hz and 3.0 Hz; and (3) low for frequencies between 3.0 Hz and 15.0 Hz.

The observed low noise levels at higher frequencies affirm the ability of the Wake hydrophones to detect seismic signals at those frequencies. In addition, high-frequency phases recorded on the deep ocean bottom, which traverse only a few kilometers of homogeneous crust, may be less distorted than similar phases recorded on continents, which often traverse more than 40 km of crust. Consequently, coherence across the

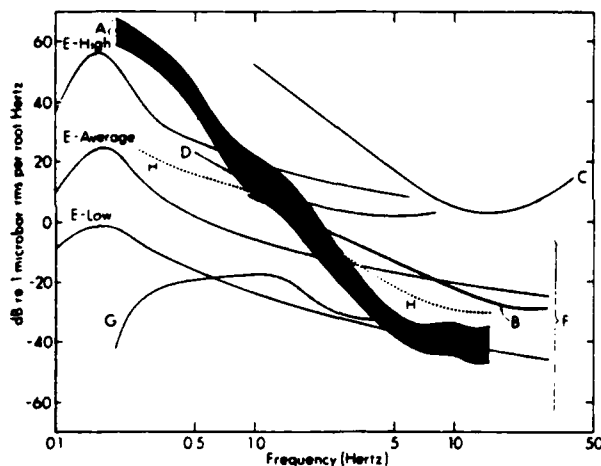


Figure 2. The average spectrum  $\pm 1$  standard deviation of 52 samples of background noise over 18 months from the Wake bottom hydrophones is labeled A. Also shown are some published noise curves for both ocean-bottom (B, C, D, and H) and continental (E, F, and G) environments, which have been converted from an assortment of units to the scale shown. B is a hypothetical "sample spectrum of deep-sea noise" (Urick, 1975; p. 188). C is a vertical seismometer measurement made in the Mariana Basin (Asada and Shimamura, 1976). D is a vertical seismometer measurement made at 46-km depth between Hawaii and California (Bradner and Dodds, 1964). H is a noise curve for a hydrophone bottomed off Eleuthera Island at 1200-m depth (Nichols, 1981). E represents low, average, and high noise levels estimated from curves compiled by Brune and Oliver (1959). F is an area bounded by the limits of noise curves measured on vertical seismometers for 16 locations within the United States and Germany (Frantti et al., 1962). G is the noise curve for the Oyer subarray of the Norwegian seismic array measured during a period "when most of the North Atlantic Ocean was very quiet" (Bungum et al., 1971).

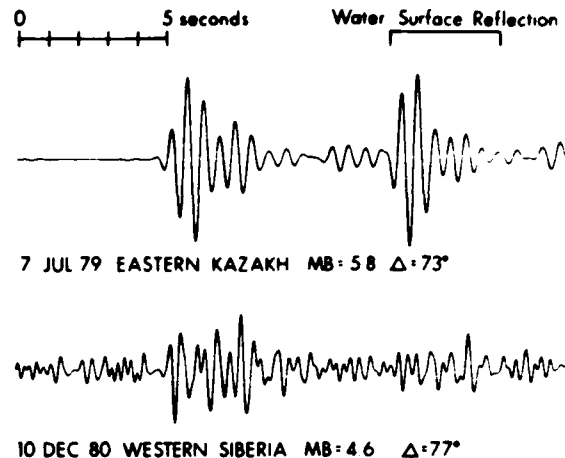


Figure 3. Sample time series of P, filtered to maximize signal/noise, from two nuclear explosions recorded on the Wake bottom hydrophones. The upper trace is from a single hydrophone and shows the direct arrival and its first water surface reflection. The lower trace is a composite of signals from two hydrophones with 40-km separation, obtained as follows: the filtered (1.5-5.0 Hz) time series from each hydrophone was inverted, shifted in time by the water surface reflection time, weighted to maximize the increase in signal/noise, and added to itself; the two resulting time series were then added with the appropriate propagation delay, and weighted to maximize the increase in signal/noise. Signal/noise was increased by 90% of the theoretical maximum with this method, indicating a high level of coherence between the signals added.

array appears to be high for teleseismic P. These factors (low noise levels and a thin, homogeneous crust) have enabled the Wake array to acquire some impressive recordings of underground nuclear explosions. Shown in Figure 3 is an Eastern Kazakh explosion at 73° with a body wave magnitude of 5.9. Its signal/noise ratio is approximately 50/1. Also shown in Figure 3 is a Western Siberian explosion at 77° with a body wave magnitude of 4.6. This arrival is the weighted sum of signals from two of the hydrophones, as explained in the figure caption. Coherence between the two hydrophone signals in the band 1.5 to 5 Hz was measured at 0.85 for this arrival.

## Summary

Significant differences are found between the spectra of P phases from explosions and from shallow focus earthquakes at 61° to 77° epicentral distance. Explosion spectra exhibit a change in spectral slope at about 2.2 Hz from -12 to -28 dB/octave relative to pressure. Earthquake spectra have a nearly constant slope of -28 dB/octave over the range of 1 to 6 Hz. High frequencies (>6 Hz) observed in these phases indicate a high Q in the deep mantle.

The ambient noise spectrum on the ocean bottom near Wake falls off at about -24 dB/octave over the range of 0.3 to 6 Hz. Between 3 and 15 Hz

the background noise levels are comparable to those at the quietest continental sites. Teleseismic P has been observed with a high level of coherence across a sensor separation of 40 km. The low level of ambient noise on the ocean floor at high frequencies and the high levels of coherence observed indicate that the ocean bottom may be an excellent observational regime for teleseismic P as well as other seismic phases rich in high frequencies.

**Acknowledgments.** This research was supported by the Advanced Research Projects Agency of the Department of Defense and was monitored by the Air Force Office of Scientific Research under Contract Nos. F 49620-79-C-0007 and F 49620-81-C-0065. Supplementary funds were provided by the U.S. Arms Control and Disarmament Agency. Installation of the recording system was partially funded by the Office of Naval Research (Code 425GG). The authors express special thanks to the Air Force and Kentron International for assistance in installing and maintaining the recording station at Wake, and to Al David for diligently changing tapes and making repairs. The authors thank Neil Frazer for critically reviewing this report and Rita Pujalet for editorial assistance. Hawaii Institute of Geophysics Contribution No. 1316.

#### References

- Asada, T., and H. Shimamura, Observation of earthquakes and explosions at the bottom of the western Pacific: Structure of oceanic lithosphere revealed by Longshot experiment, The Geophysics of the Pacific Ocean Basin and Its Margins, edited by G. H. Sutton, M. H. Manghnani, and R. Moberly, Am. Geophys. Union Monograph 19, p. 135-153, 1976.
- Bradner, H., and J. Dodds, Comparative seismic noise on the ocean bottom and land, J. Geophys. Res., **69**, 4339-4348, 1964.
- Brune, J., and J. Oliver, The seismic noise of the earth's surface, Bull. Seismol. Soc. Amer., **49**, 349-353, 1959.
- Bungum, H., E. Rygg, and L. Bruland, Short-period seismic noise structure at Norwegian seismic array, Bull. Seismol. Soc. Amer., **61**, 357-373, 1971.
- Der, Z. A., T. W. McElfresh, and A. O'Donnell, An investigation of the regional variations and frequency dependence of anelastic attenuation in the mantle under the United States in the 0.5-4 Hz band, Geophys. J. R. astr. Soc., **69**, 67-99, 1982.
- Evernden, J., Spectral characteristics of the P codas of Eurasian earthquakes and explosions, Bull. Seismol. Soc. Amer., **67**, 1153-1171, 1977.
- Evernden, J. and W. Kohler, Further study of spectral characteristics of P codas of earthquakes and explosions, Bull. Seismol. Soc. Amer., **69**, 483-511, 1979.
- Frantti, G., D. Willis, and J. Wilson, The spectrum of seismic noise, Bull. Seismol. Soc. Amer., **52**, 113-121, 1962.
- Nichols, R. H., Infrasonic ambient ocean noise measurements: Eleuthera, J. Acoustic. Soc. Am., **69**, 974-981, 1981.
- Thanos, S. M., OBS Calibration Manual, Lamont Geological Observatory, 1966.
- Urick, R., Principles of Underwater Sound, McGraw-Hill, 1975.
- Walker, D., Hydrophone recordings of underground nuclear explosions, Geophys. Res. Lett., **7**, 465-467, 1980.
- Walker, D., C. McCreery, G. Sutton, and F. Duennebier, Spectral analyses of high-frequency Pn and Sn phases observed at great distances in the western Pacific, Science, **199**, 1333-1335, 1978.

(Received August 6, 1982;  
accepted August 31, 1982.)

APPENDIX II

SPECTRAL CHARACTERISTICS OF HIGH-FREQUENCY  $P_N$ ,  $S_N$  PHASES

## IN THE WESTERN PACIFIC

Daniel A. Walker and Charles S. McCreery

Hawaii Institute of Geophysics, Honolulu, Hawaii 96822

George H. Sutton

Rondout Associates, Stone Ridge, New York 12484

**Abstract.**  $P_N$  and  $S_N$  phases from 25 selected earthquakes recorded since July of 1979 on ocean bottom hydrophones near Wake Island are used to complement and extend prior investigations of high-frequency  $P_N$ ,  $S_N$  spectra in the Western Pacific. At a distance of about  $18^\circ$  ( $\approx 2000$  km), frequencies for  $P_N$  and  $S_N$  are as high as 30 and 35 Hz, respectively; at a distance of about  $30^\circ$  ( $\approx 3300$  km), as high as 15 and 20 Hz, respectively.  $P_N$  phases lose their high-frequency energy more rapidly than  $S_N$  phases do, yet  $P_N$  wavetrains are much longer than  $S_N$  wavetrains.  $P_N$  wavetrains of longer duration, more energy, and higher frequencies are found for travel paths primarily in the Northwestern Pacific Basin than for travel paths across the transition zone from the shallow Ontong-Java Plateau to the deep Northwestern Pacific Basin.  $S_N$  phases are extremely weak or absent for travel paths crossing this transition zone from the shallower Ontong-Java Plateau to the deeper Northwestern Pacific Basin, whereas  $S_N$  phases are well recorded for travel paths crossing the transition zone in the opposite direction. Although normal, mantle-refracted P phases are well recorded beyond about  $21^\circ$  ( $\approx 2300$  km), available data indicate that detectable normal, mantle-refracted P phases may not exist at distances from about  $17^\circ$  to  $21^\circ$ .

## Introduction

Recent investigations of high-frequency  $P_N$ ,  $S_N$  in the Pacific (Walker, 1977; Walker et al., 1978; Sutton et al., 1978; Talandier and Bouchon, 1979; and McCreery, 1981) suggest that the real character of these phases is revealed at frequencies much higher than those traditionally associated with normal, mantle-refracted body waves at teleseismic distances (i.e.,  $\approx 1$  Hz). For example, in one investigation [Walker et al., 1978], frequencies as high as 12 and 15 Hz were found for the  $P_N$  and  $S_N$  phases, respectively, of an earthquake recorded at a distance of  $28.3^\circ$  (3147 km).

In this report we offer a more comprehensive analysis of the spectral characteristics of  $P_N$ ,  $S_N$  using additional data recorded since July of 1979 on ocean bottom hydrophones near Wake Island. Only undistorted arrivals with signal/noise ratios of at least 3/1 were used in this investigation. Epicentral distances, origin

times, depths, and magnitudes are given in Table 1; and locations of epicenters are shown in Figure 1.

## Northwestern Pacific Basin Travel Paths

Spectrograms for some of the  $P_N$ ,  $S_N$  phases having travel paths primarily under the deep Northwestern Pacific Basin (i.e., events 1 through 18) are shown in Figure 2. All reveal high frequencies, with values in excess of 20 Hz for both  $P_N$  and  $S_N$  at a distance of  $18.0^\circ$  (2000 km; event 2) and values of up to 15 and 20 Hz for  $P_N$  and  $S_N$ , respectively, at a distance of  $29.4^\circ$  (3270 km; event 17). (More detailed spectral analyses of the phases for event 2 at  $18.0^\circ$  indicate values as high as 30 and 35 Hz for  $P_N$  and  $S_N$ , respectively.)

Spectrograms for events 17 and 18 show the normal, mantle-refracted P phases as well as high-frequency  $P_N$  and  $S_N$  phases. Other events for which normal, mantle-refracted P phases have been clearly recorded are 11, 12, 13, 15, and 16. The fact that all of these events are at distances in excess of  $21^\circ$  is not coincidental, for it is only at these distances (the precise crossover depending, in part, on focal depth) that P phases begin to arrive ahead of the high-frequency  $P_N$  phase (Figure 3). With increasingly shorter distances, high-frequency  $P_N$  arrives increasingly ahead of the expected P.

Although it might seem reasonable to assume that P does arrive at distances less than about  $21^\circ$ , but is masked by  $P_N$ , such an assumption should be tested. One test is to compare spectrums where all of the P's energy, or large portions of it, might be suspected of being present within the  $P_N$  coda (i.e., events 1 through 10) to the spectrums where only  $P_N$  is known to exist (i.e., events 13 through 18; 11 and 12 could not be used due to  $P_N$  clipping). Composite spectrums have been made for the two groups of  $P_N$  arrivals (i.e.,  $P_N$  with P suspected, at distances from about  $17^\circ$  to  $22^\circ$ ; and  $P_N$  with P known to be absent, at distances from about  $26^\circ$  to  $33^\circ$ ), as well as for all P phases, at distances from about  $22^\circ$  to  $33^\circ$ , either clearly arriving well ahead of  $P_N$  (events 11, 12, 13, 15, 16, 17, and 18) or suspected of arriving close to, but ahead of,  $P_N$  (events 9 and 10). These composites and the individual absolute spectrums from which they were derived are shown in Figure 4.

Individual and composite P spectrums are obviously, and not unexpectedly, very different in character from individual and composite  $P_N$

Copyright 1983 by the American Geophysical Union.

Paper number 3B0272.

0148-0227/83/0038-0272\$05.00



TABLE 1. Epicentral Distances, Origin Times, Depths, and Magnitudes of Events 1-25 in Figure 1

Event Number	Distance, deg.	Date	Time	Depth, km	Magnitude, mb
1	17.8	July 8, 1980	1704:15.1	54	4.8
2	18.0	July 11, 1980	0942:00.2	33	5.3
3	18.7	June 9, 1980	1923:33.3	33	5.6
4	19.0	Dec. 8, 1979	1258:55.2	51	5.5
5	19.8	Dec. 16, 1979	1050:48.0	96	5.0
6	20.1	March 26, 1980	0722:37.0	45	5.5
7	20.7	Nov. 1, 1980	0440:37.7	109	5.6
8	20.9	Dec. 17, 1979	0728:48.2	33	5.1
9	21.2	Jan. 15, 1980	0523:25.7	120	5.1
10	21.7	Nov. 29, 1979	1708:21.3	109	5.4
11	24.9	Dec. 11, 1979	1726:22.1	161	5.9
12	25.4	Dec. 19, 1980	2332:41.6	79	6.2
13	26.5	Oct. 20, 1980	0329:21.3	81	5.5
14	27.1	Oct. 28, 1979	0539:36.0	88	5.4
15	28.5	Feb. 23, 1980	0551:03.5	47	6.4
16	28.5	Jan. 1, 1981	1032:13.1	53	6.2
17	29.4	Nov. 26, 1980	2348:59.9	77	5.8
18	32.7	Aug. 22, 1979	1828:55.7	128	5.5
19	28.0	Feb. 12, 1980	0320:23.2	75	5.9
20	28.0	Aug. 13, 1979	0303:47.9	88	5.8
21	28.6	May 14, 1980	1126:00.6	57	6.1
22	28.8	Sept. 28, 1980	1825:59.7	68	6.0
23	30.4	Nov. 6, 1979	1138:31.5	30	6.0
24	31.1	Oct. 23, 1979	0951:06.7	22	6.1
25	31.1	Feb. 22, 1980	2115:42.1	68	5.9

spectrums, in that the P has larger signal-to-noise ratios at lower frequencies (i.e., 1-2 Hz) than either Pn grouping (Figures 4 and 5), and the composite P is richer in lows, and weaker in highs, relative to the 26° to 33° Pn composite (Figure 5a). In comparing the composite 17° to 22° Pn spectrum to the composite 26° to 33° Pn spectrum (Figure 5b), we note that the 17° to 22° Pn is similar in character to the 26° to 33° Pn for frequencies higher than 2 Hz, but has lower signal-to-noise ratios at frequencies less than 2 Hz (i.e., values fall below the "4 dB above noise" requirement for plotting). This latter observation is also apparent in the individual spectrums (Figure 4). The fact that values for the 17° to 22° Pn spectrum fall below the 4 dB requirement for frequencies less than 2 Hz, coupled with values for the 22° to 33° P spectrum

above the 4 dB level at those frequencies, suggests that detectable normal, mantle refracted P phases may not exist in the Pn codas of events at distances of 17° to 22°.

Another important, though not surprising, observation to be made from the composite plots (Figure 5b) is that Pn phases at great distances appear to be weaker at higher frequencies (>10 Hz) than Pn phases at shorter distances.

Sn composite plots have also been made for the same events for which Pn composites have been made. These plots are shown in Figure 6. Although normal mantle-refracted P phases have been well recorded at great distances, normal mantle-refracted S phases from earthquakes have not been recorded by the Wake hydrophones. Presumably, this is due to the small pressure signal in the water resulting from S phases at

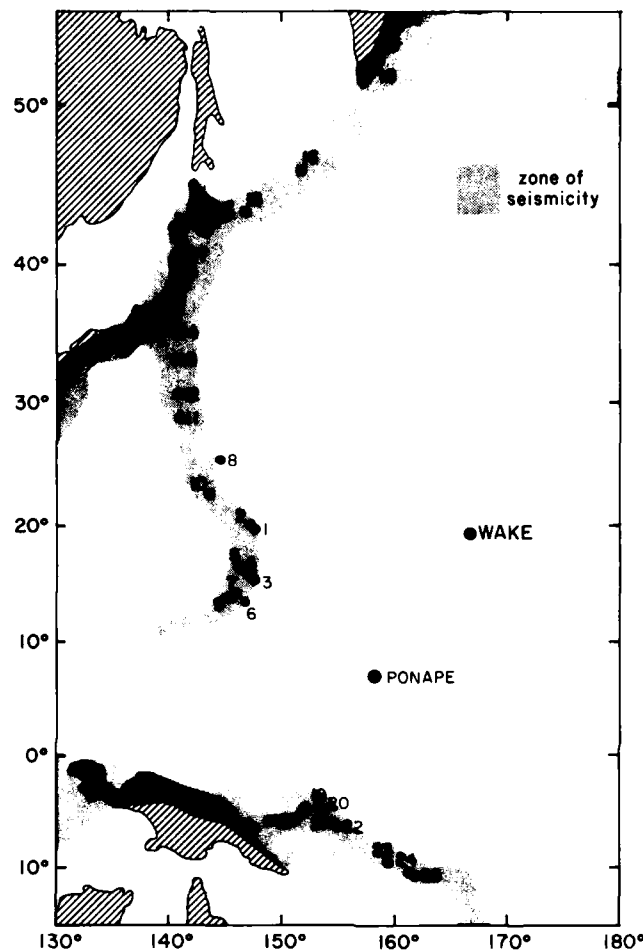


Fig. 1. Epicenter location map.

teleseismic distances. In addition, background noise levels are higher for those frequencies at which S would appear [McCreery et al., 1982].

In Figure 6a, Sn composite plots for the 17° to 22° and 26° to 33° distance ranges are compared to one another. Considering that the standard deviations of all of the composite plots presented in this paper are generally in the range of  $\pm 3$  dB, no significant differences are apparent in Figure 6a. In Figures 6b and 6c, Sn composite plots are compared to their respective Pn composite plots. Again, no statistically significant differences are indicated. In other words, Sn signal strength is generally comparable to Pn signal strength. This similarity of Pn and Sn spectrums was observed earlier for travel paths in the Western Pacific east of the Marianas [Ouchi, 1981].

Special mention should be made of the fact

that the composite Sn plot in Figure 6c is 4 dB above background noise at frequencies well above 8 Hz while the composite Pn plot is not. Also it should again be noted that the individual Pn's and Sn's used to formulate the composite plots were for the same earthquakes. These considerations suggest that Sn phases do not lose their high frequencies as rapidly as Pn phases.

It has been pointed out that some high frequencies observed elsewhere might be the result of instrumental nonlinearities [Sacks, 1980] and/or nonlinear seismic interactions in the vicinity of a receiving station [Nakamura and Koyama, 1982]. As the lower frequencies are of comparable amplitude for both Pn and Sn at both distance ranges considered (Figures 6b and 6c), it is unlikely that such nonlinearities could explain the data discussed here. We also note that P, which has higher average amplitudes than

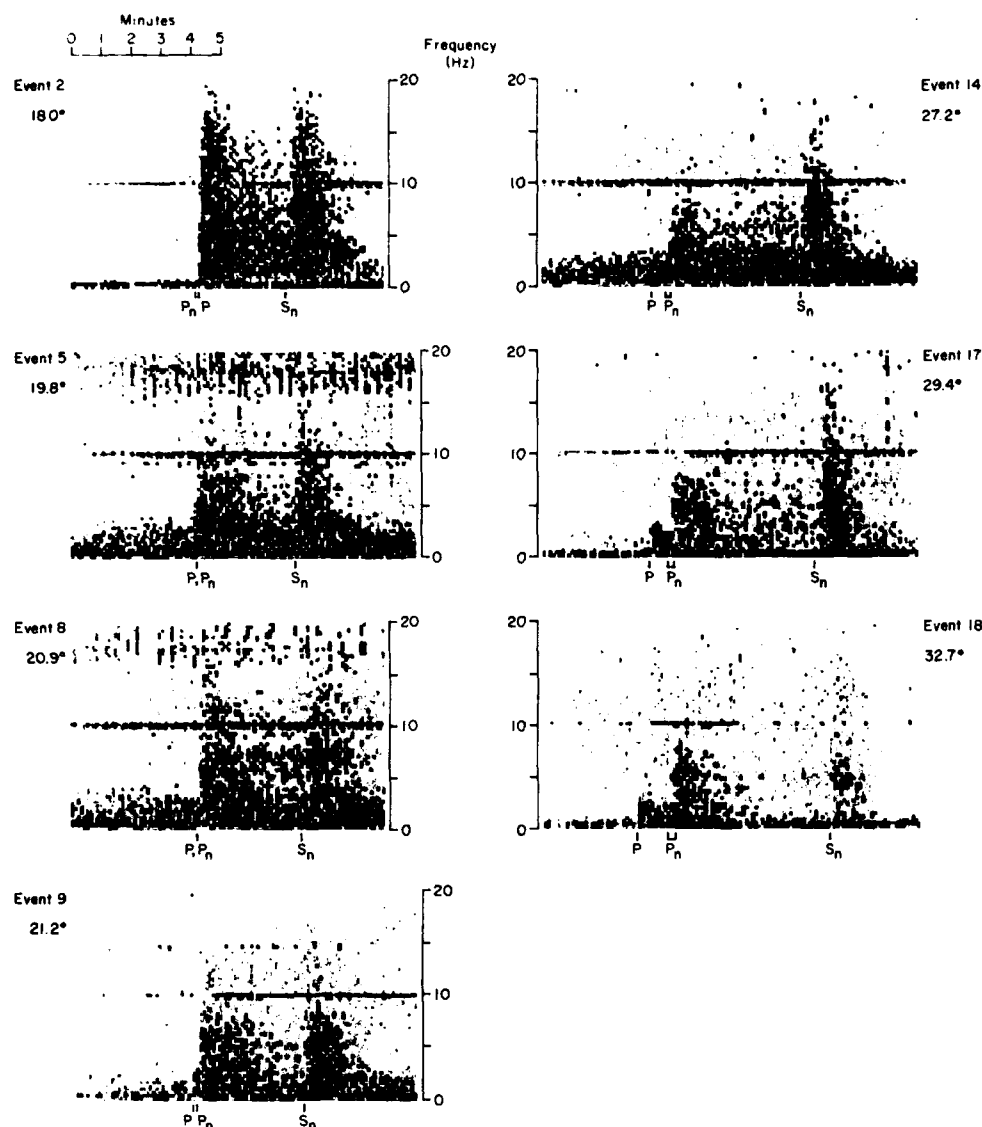


Fig. 2. Spectrograms for some earthquakes having travel paths to Wake under the Northwestern Pacific Basin. Expected times of arrivals are based on either the Jeffreys and Bullen [1958] tables for P or Pn/Sn travel time curves from Walker [1977]. These and succeeding spectrograms were made by dividing the time series into adjacent 512-point segments, Lanczos squared windowing the segments, and performing a fast Fourier transform (FFT) on each segment. In the horizontal direction, the width of each shaded block corresponds to one of the 512-point segments in the time series. In the vertical direction, each block is the average of two adjacent power spectral estimates out of the FFT. Only frequencies from 0 to 1/2 Nyquist are shown. The contour interval is 8 dB. The line at 10 Hz is due to time code cross talk. Instrument responses have not been removed.

Pn or Sn at the lower frequencies, has the most rapid falloff toward higher frequencies (Figure 5).

In all of these comparisons, another objection that could be made is that differences in source spectrums (and/or orientation of the source

relative to the recording station) were not considered. Although all of the events occurred within the subducting margin of the Northwestern Pacific and the Pn, Sn phases used were generated by earthquakes having focal depths of 128 km or less, differences in source spectrums might be

significant. We believe, however, that overall trends of the individual spectrums (Figure 4) used for the composite plots are similar (as opposed to specific details that may differ) and that such similarities could justify the general conclusions drawn from that data. We also note that source effects are minimized in those comparisons of composite Pn's and Sn's from the same earthquakes (Figures 6b and 6c).

Another interesting feature of Pn, Sn phases is that the Pn wavetrain is much longer than the Sn wavetrain (Figure 2). Spectral analyses indicate that energy is lost at all frequencies in the later arriving portions of these wavetrains, and that this loss is much greater in the Sn wavetrains than in the Pn wavetrains.

#### Ontong-Java Plateau Travel Paths

Spectrograms for some of the more interesting Pn phases with travel paths to Wake under the shallow Ontong-Java Plateau (as well as portions of the deep Northwestern Pacific Basin) are shown in Figure 7. (Refer also to Table 1, Figure 1, and Figure 8.) The most conspicuous feature of these spectrograms is that Sn phases are extremely weak, or absent, even though Pn phases are prominent.

Figure 9 compares the composite Pn spectrum for events having Ontong-Java Plateau travel paths (events 19 through 25) to the composite Pn spectrum for events at comparable distances having Northwestern Pacific Basin travel paths (events 15 through 18). The Northwestern Pacific Basin events appear to have more Pn energy at

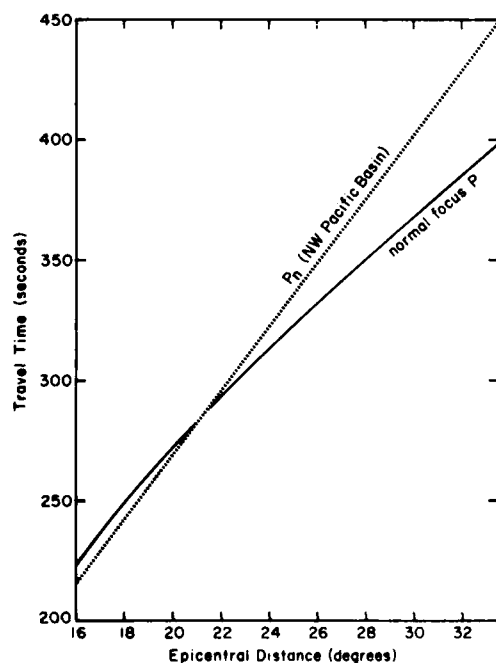


Fig. 3. Travel time curves for normal, mantle-refracted P phases and for Pn phases. P times are taken from Jeffreys and Bullen [1958], and Pn times are taken from Walker [1977].

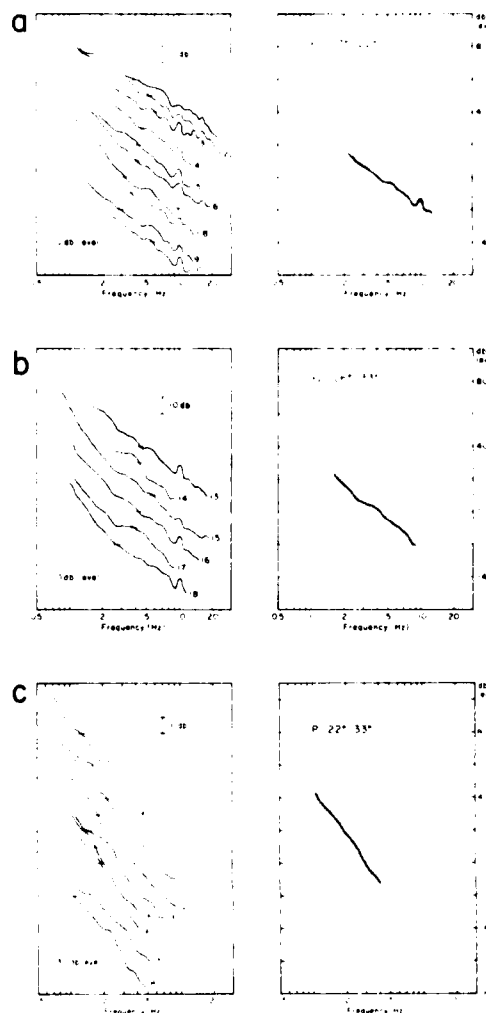


Fig. 4. Individual and composite spectrums for arrivals at Wake where (a) both Pn and P might be suspected of being present, at distances from about  $17^{\circ}$  to  $22^{\circ}$ , (b) only Pn is known to exist at distances from about  $26^{\circ}$  to  $33^{\circ}$ , and (c) only P is known to exist, at distances from about  $22^{\circ}$  to  $33^{\circ}$ . The spectrums are power level spectrums in decibels relative to one microbar peak-to-peak pressure per root hertz. Values for individual spectrums were plotted only if they were at least 4 dB above background noise. The composite curves are simply the averages for the individual curves, with the condition that composite values were used for those frequencies lacking at most only one individual curve. Standard deviations of composite values are indicated by shading. Values for standard deviations in these and succeeding spectrums are generally in the range of  $\pm 3$  dB. The peaks at 10 Hz are due to time code cross talk.

higher frequencies than the Ontong-Java Plateau events. However, because of the approximate  $\pm 3$  dB standard deviation on each of these curves, this suggestion is not statistically significant. Comparing Figures 2 and 7, the duration of the Pn

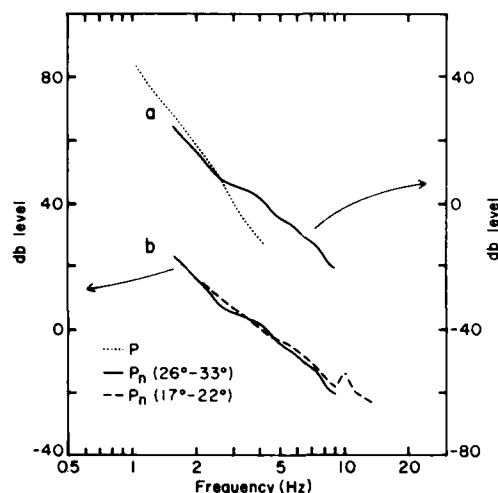


Fig. 5. Comparisons of composite spectrums: (a) P and the 26° to 33° Pn, and (b) the 17° to 22° Pn and the 26° to 33° Pn. Conclusions which can be drawn from these plots are (1) P and Pn spectrums are very different in character, (2) detectable P phases may not exist in the Pn codas of events at distances of 17° to 22°, and (3) Pn phases at great distances appear to be weaker at higher frequencies ( $\approx 10$  Hz) than Pn phases at shorter distances.

wavetrains appears to be greater for the Northwestern Pacific Basin events.

In such comparisons, the important question again arises of differences in source characteristics, in this instance for New Ireland-Solomon Island earthquakes and for Japan-Kuril Islands-Kamchatka earthquakes. It is not possible, however, to attribute the absence of Sn to differences in source characteristics, as Sn phases from New Ireland and the Solomons have been well recorded at Ponape on the northern margin of the Ontong-Java Plateau [Walker, 1977]. Examples of such phases are shown in Figure 10. Of the more than forty events from the New Ireland-Solomon Islands area recorded at Ponape, amplitudes of Sn phases are at least comparable to, and frequently larger than, those of their respective Pn phases.

The absence of Sn at Wake would, therefore, appear to be a result of Sn's inability to propagate efficiently across the transition zone from the shallower Ontong-Java Plateau to the deeper Northwestern Pacific Basin, and would suggest that much of the energy in Sn travels through portions of the lithosphere involved in the transition. On the other hand, Sn's that have crossed this transition zone from the other direction (i.e., from earthquakes in the Marianas, Japan, the Kuriles, and Kamchatka) are well recorded at Ponape (Figure 10). Differences in the crustal structure of the Ontong-Java Plateau and the Northwestern Pacific Basin are indicated by the section profile [Hussong et al., 1979] shown in Figure 11.

Another comparison of spectrums at Wake for the two differing types of travel paths

(Northwestern Pacific Basin and Ontong-Java Plateau travel paths) was made for the later arriving energy in the Pn wavetrains. For these comparisons, less energy at higher frequencies was present in those Pn's having travel paths that include the Ontong-Java Plateau. These deficiencies and the corresponding absence of Sn for paths across the transition zone from the shallow Ontong-Java Plateau to the deep Northwestern Pacific Basin suggest that the longer, stronger Pn phases observed for travel paths to Wake, primarily across the Northwestern Pacific Basin, may be the result of more efficient conversions of Pn to Sn (or Sn to Pn).

#### Concluding Remarks

The phenomenon of high-frequency Pn, Sn propagation is emerging as a major unresolved property of the oceanic crust and/or mantle. Others have described high-frequency Pn, Sn propagation as 'a challenge remaining to the theoretician' [Richards, 1979] and as 'the challenge to both explosion and earthquake

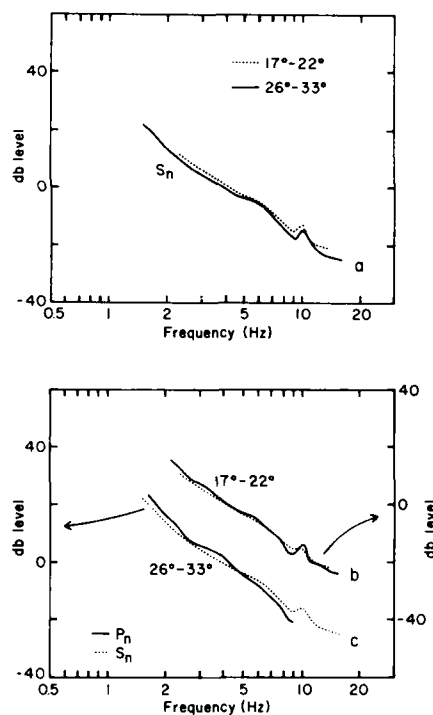


Fig. 6. Composite spectrums of Sn phases for those earthquakes with their Pn phases plotted in Figures 4a and 4b. Comparisons of spectrums are made (a) for the two Sn composites to one another, (b and c) and for each of the Sn composites to their respective Pn composite. A conclusion which can be drawn from these plots is that Sn signal strength is generally comparable to Pn signal strength except at high frequencies and large distances where Sn phases do not lose their energy as rapidly as Pn phases.

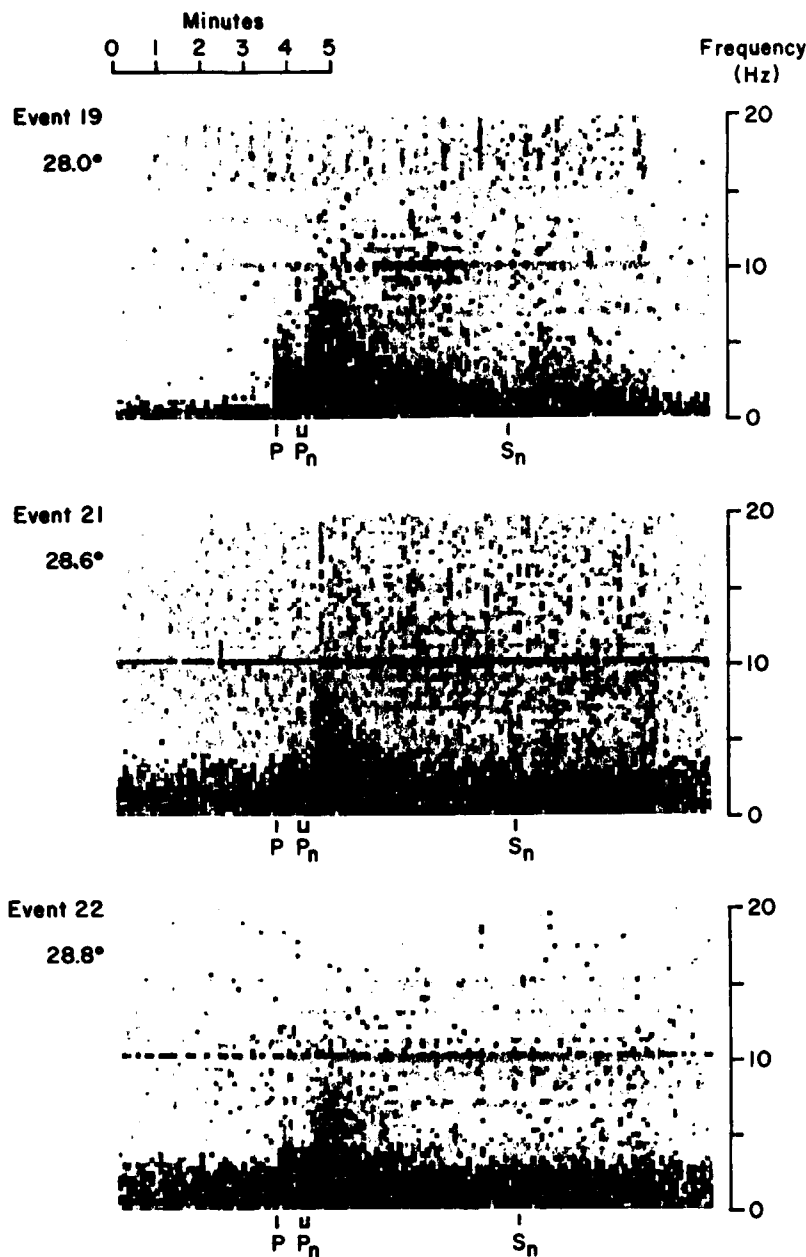


Fig. 7. Some spectrograms for earthquakes having portions of their travel paths to Wake under the Ontong-Java Plateau. In comparing these spectrograms to those of Figure 2, note the absence, or weakness, of Sn. Computational procedures are the same as used in Figure 2.

seismology for the coming decade' [Hirn et al., 1973]. These descriptions are supported not only by the unusual character of the phases but also by their probable occurrence throughout the world's oceans.

As important as recent efforts are to determine the mechanism of high-frequency Pn, Sn propagation [e.g., Stephens and Isacks, 1977; Menke and Richards, 1980; Sutton and Harvey, 1981; Gettrust and Frazer, 1981], we believe that

many essential characteristics of Pn, Sn phases (especially at very high frequencies) are not well known, and that accurate quantification of those characteristics through the acquisition of additional high-quality data is greatly needed. We hope that this report will further familiarize seismologists with high-frequency Pn, Sn propagation and will be viewed as a preliminary attempt to quantify, in a relative sense, some of the essential characteristics of these phases.

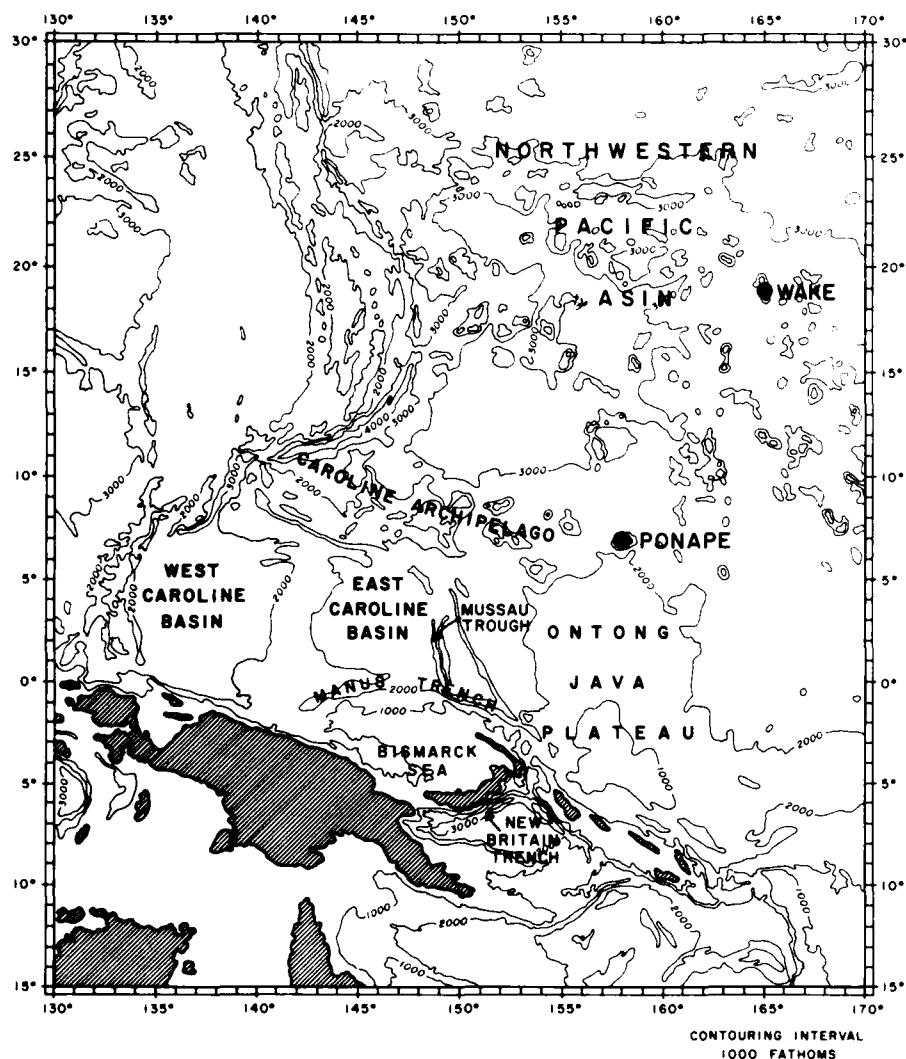


Fig. 8. Bathymetry map of the Northwestern Pacific area.

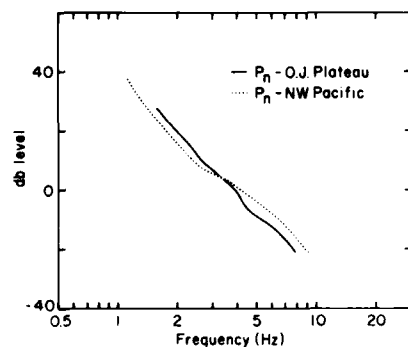


Fig. 9. Comparisons of composite Pn spectra for events having travel paths across the Ontong-Java Plateau and the Northwestern Pacific Basin.

summary of principal observations contained in this report follows.

The apparent absence of normal, mantle-refracted P phases at distances less than about  $21^\circ$  ( $\approx 2300$  km).

Frequencies as high as 30 and 35 Hz for Pn and Sn, respectively, at  $18.0^\circ$  (2000 km).

Frequencies as high as 15 and 20 Hz for Pn and Sn, respectively, at  $29.4^\circ$  (3270 km).

With increasing distance (i.e., from about  $20^\circ$  to  $30^\circ$ ), Sn phases not losing their high frequencies as rapidly as Pn phases do.

Pn wavetrains longer than Sn wavetrains.

The extreme weakness or absence of Sn phases for travel paths across the transition zone from the Ontong-Java Plateau to the Northwestern Pacific Basin and the presence of Sn phases for travel paths in the opposite direction across this transition zone.

Longer, more energetic Pn wavetrains for travel paths primarily in the Northwestern Pacific Basin than for travel paths across the transition zone from the Ontong-Java Plateau to the Northwestern Pacific Basin.

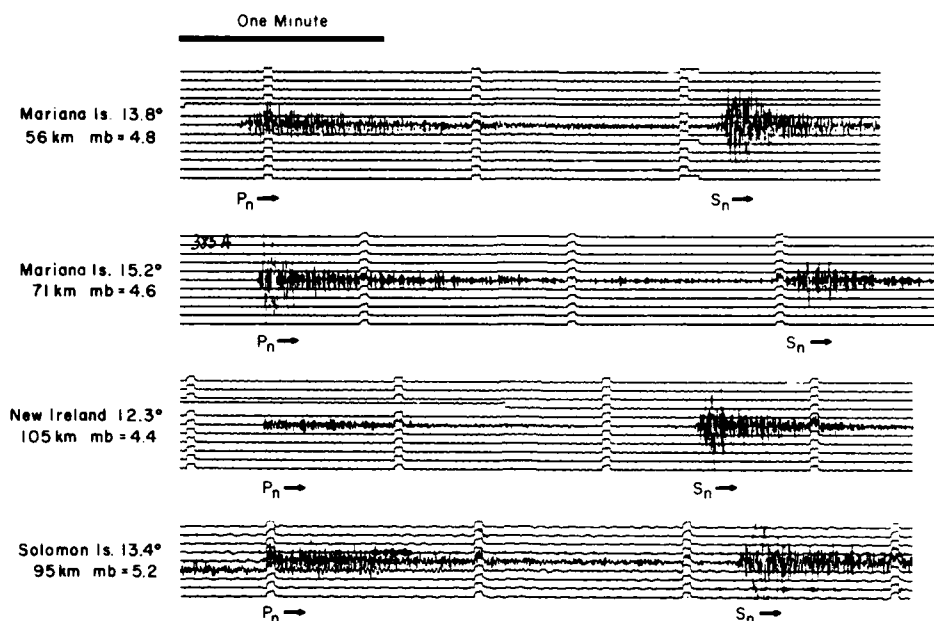


Fig. 10. Pn and Sn phases recorded at Ponape on the northern margin of the Ontong-Java Plateau.

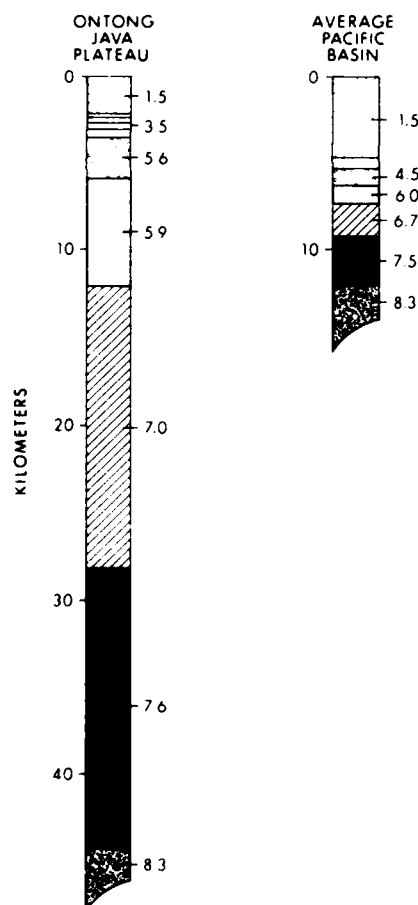


Fig. 11. Section profiles for the Ontong-Java Plateau and Pacific Basin as taken from Hussong et al. [1979].

**Acknowledgments.** This research was supported by the Advanced Research Projects Agency of the Department of Defense and was monitored by the Air Force Office of Scientific Research under contract F49620-79-C-0007. Supplementary funds were provided by the Air Force Office of Scientific Research (contract F49620-81-C-0065), the Office of Naval Research (Code 425GG), and the U.S. Arms Control and Disarmament Agency. The authors thank Fred Duennebler, Joe Gettrust, and Neil Frazer for reviewing a draft of this report. The editorial assistance of Rita Pujale is also acknowledged. Hawaii Institute of Geophysics contribution 1354.

#### References

- Gettrust, J., and L. Frazer, A computer model study of the propagation of the long-range Pn phase, *Geophys. Res. Lett.*, **8**, 749-752, 1981.
- Hirn, A., L. Steinmetz, R. Kind, and K. Fuchs, Long range profiles in western Europe, II, Fine structure of the lower lithosphere in France (southern Bretagne), *Z. Geophys.*, **39**, 363-384, 1973.
- Hussong, D., L. Wiperman, and L. Kroenke, The crustal structure of the Ontong-Java and Manihiki oceanic plateaus, *J. Geophys. Res.*, **84**, 6003-6010, 1979.
- Jeffreys, H., and K. Bullen, *Seismological Tables*, Office of the British Association, Burlington House, London, 1958.
- McCreery, C., High-frequency Pn, Sn phases recorded by ocean bottom seismometers on the Cocos Plate, *Geophys. Res. Lett.*, **8**, 489-492, 1981.
- McCreery, C., D. Walker, and G. Sutton, Spectra of nuclear explosions, earthquakes, and noise from Wake Island bottom hydrophones, *Geophys. Res. Lett.*, **10**, 59-62, 1983.



- Menke, W., and P. Richards, Crust-mantle whispering gallery phases: A deterministic model of teleseismic Pn wave propagation, J. Geophys. Res., **85**, 5416-5422, 1980.
- Nakamura, Y., and J. Koyama, Seismic Q of the lunar upper mantle, J. Geophys. Res., **87**, 4855-4861, 1982.
- Ouchi, T., Spectral structure of high frequency P and S phases observed by OBS's in the Mariana Basin, J. Phys. Earth, **29**, 305-326, 1981.
- Richards, P., Theoretical seismic wave propagation, Rev. Geophys. Space Phys., **17**, 312-328, 1979.
- Sacks, I., Mantle Qs from body waves-difficulties in determining frequency dependence, (abstract), Eos Trans. AGU, **61**, 298, 1980.
- Stephens, C., and B. Isacks, Toward an understanding of Sn: Normal modes of Love waves in an oceanic structure, Bull. Seismol. Soc. Am., **67**, 69-78, 1977.
- Sutton, G., and D. Harvey, Complete synthetic seismograms to 2 Hz and 1000 km for an oceanic lithosphere (abstract), Eos Trans. AGU, **62**, 327, 1981.
- Sutton, G., C. McCreery, F. Duennebier, and D. Walker, Spectral analyses of high-frequency Pn, Sn phases recorded on ocean bottom seismographs, Geophys. Res. Lett., **5**, 745-747, 1978.
- Talandier, J., and M. Bouchon, Propagation of high frequency Pn waves at great distances in the Central and South Pacific and its implications for the structure of the lower lithosphere, J. Geophys. Res., **84**, 5613-5619, 1979.
- Walker, D., High-frequency Pn and Sn phases recorded in the Western Pacific, J. Geophys. Res., **82**, 3350-3360, 1977.
- Walker, D., C. McCreery, G. Sutton, and F. Duennebier, Spectral analyses of high-frequency Pn and Sn phases observed at great distances in the Western Pacific, Science, **199**, 1333-1335, 1978.

(Received July 14, 1982;  
revised January 5, 1983;  
accepted February 7, 1983.)

APPENDIX III

OCEANIC PN/SN PHASES:  
A QUALITATIVE EXPLANATION  
AND REINTERPRETATION  
OF THE T-PHASE

Daniel A. Walker

November 1982

Prepared for  
OFFICE OF NAVAL RESEARCH  
Contract N00014-75-C-0209  
Project NR 083-603



Charles E. Helsley  
Director  
Hawaii Institute of Geophysics

## ABSTRACT

The combined effects of: (1) differing efficiencies between Pn and Sn energy transmission across the basement-sediment interface; (2) ocean surface reflections; (3) Pn to Sn conversions; and, (4) large lateral variations in the crust and upper mantle are used to formulate a working hypothesis which appears to explain, qualitatively, many observations of high-frequency Pn/Sn phases throughout the western, northern, and central Pacific. Also, the concept of Pn/Sn phases as sources of energy at the basement-sediment interface is suggested as a possible mechanism for T-phase generation through scattering or Stoneley wave generation.

## CONTENTS

	<u>Page</u>
ABSTRACT.....	111
LIST OF FIGURES.....	vi
INTRODUCTION.....	1
SN SIGNAL STRENGTH.....	1
PN WAVETRAINS.....	2
OCEAN-SURFACE REFLECTIONS.....	5
PN/SN PHASES AT GREAT DISTANCES.....	5
T-PHASE MECHANISMS.....	11
SUMMARY.....	12
CONCLUSIONS.....	15
ACKNOWLEDGMENTS.....	16
SUPPLEMENTARY NOTE.....	17
REFERENCES.....	18

## FIGURES

<u>Figure</u>	<u>Page</u>
1. Spectrograms for some earthquakes having travel paths to Wake under the Northwestern Pacific Basin.....	3
2. Digitally rectified and compressed plot of P, Pn, Sn, and T phases for an earthquake south of Japan recorded by the Wake Island hydrophones...	4
3. An example of ocean-surface reflections.....	6
4. Some spectrograms for earthquakes having portions of their travel paths to Wake under the Ontong-Java Plateau.....	7
5. Examples of Pn and Sn phases recorded at Ponape on the northern margin of the Ontong-Java Plateau.....	8
6. Bathymetry map of the Northwestern Pacific area...	9
7. Section profiles for the Ontong-Java Plateau and Pacific Basin (from Hussong et al. 1979).....	10
8. Sonogram of Pn, Sn, and T phases (after Duennebieer 1968).....	13
9. Spectrums for the P, Pn, Sn, and T phases shown in Figure 2.....	14

## INTRODUCTION

High-frequency Pn/Sn phases were first observed nearly fifty years ago for travel paths in the Atlantic from the West Indies to the northern east coast of the United States (Leet et al., 1951, reported that these observations were made as early as 1935). The history of research on these phases since that time has been given by several authors, with some of the more recent being Molnar and Oliver (1969) and Walker (1977a).

My interest in the phenomenon began in 1963 with the recording of long-range, high-frequency Pn/Sn phases on hydrophones of what was then known as the Pacific Missile Range facility. My efforts at trying to understand these unusual phases (Sn wavetrains greater than Pn wavetrains with frequencies as high as 15 Hz at distances in excess of 3000 km; Walker et al., 1978) has continued since those initial observations. A reasonable, concise summary of my accomplishments prior to this report might be that no answers were found--only more questions. Such methodology can only be rationally tolerated for a length of time much shorter than my tenure on the case. So, for the past few years, it has been hoped that a working hypothesis could be found that would permit many, if not all, of the diverse observational pieces to be fitted together in at least a qualitative sense. Such a hypothesis could then serve as an appropriate starting point for comprehensive and detailed quantitative analyses leading to a generally acceptable model for the generation and propagation of long-range, high-frequency Pn/Sn phases. A working hypothesis has now emerged and is the subject of this report.

## SN SIGNAL STRENGTH

One of the most interesting aspects of long-range, high-frequency Pn/Sn propagation in the northwestern Pacific is the strength of the Sn phase (Walker et al., in press). Relative to Pn, Sn often appears stronger at great distances--even at high frequencies (Fig. 1). A possible explanation for these observations begins with considerations of: (1) the efficiencies of Pn/Sn energy transmission across the basement-unconsolidated sediment interface; (2) possible conversions of Pn and Sn at the basement-sediment interface; and, (3) ocean-surface reflections. Observations of conversions upward and across the basement-sediment interface, as well as ocean-surface reflections for short travel paths

off the coast of California are reported in Auld et al. (1969), where data indicate that the percentage of P (perhaps actually Pn) energy converted to S is greater than the percentage of S (perhaps actually Sn) energy converted to P. Examples of ocean-surface reflections are also given in Shimamura et al. (1975) and McCreery et al. (in press).

The very recording of "Pn/Sn" phases on ocean-bottom sediments is evidence that Pn and Sn energy does propagate, by some means, into the sediments. Energy losses above the basement-sediment interface will occur, i.e. not all of the energy passing into the sediments will be returned to the interface by way of reflections from the ocean surface. These losses could be much greater than those produced within that portion of the waveguide below the basement-sediment interface. Furthermore, if the percentage of Sn energy lost after propagation up through the basement-sediment interface, as S or converted P or both, is less than the percentage of Pn energy similarly lost up through this interface, then Sn would retain a greater percentage of its initial energy within that portion of the waveguide below the basement-sediment interface.

Under these assumptions Sn signal strength could increase with distance relative to Pn signal strength--even at high frequencies.

#### PN WAVETRAINS

In spite of Sn's greater signal strength, its wavetrain is considerably shorter than Pn's (Figs. 1 and 2). This seemingly peculiar observation can be explained by considering other types of conversions.

Any phases, originally Pn or Sn, that pass upward through the basement-sediment interface may eventually be reflected by the ocean surface (or the sediment-water interface) and returned to the basement-sediment interface to continue, somewhat weakened, in the waveguide as Pn or Sn or both. Throughout the travel path to the station, original Pn's returning to the interface and continuing in part as Sn's, as well as original Sn's returning to the interface and continuing in part as Pn's, would arrive between the main Pn and Sn phases. The net effect of such conversions would be Pn wavetrains greater in their duration than Sn wavetrains.



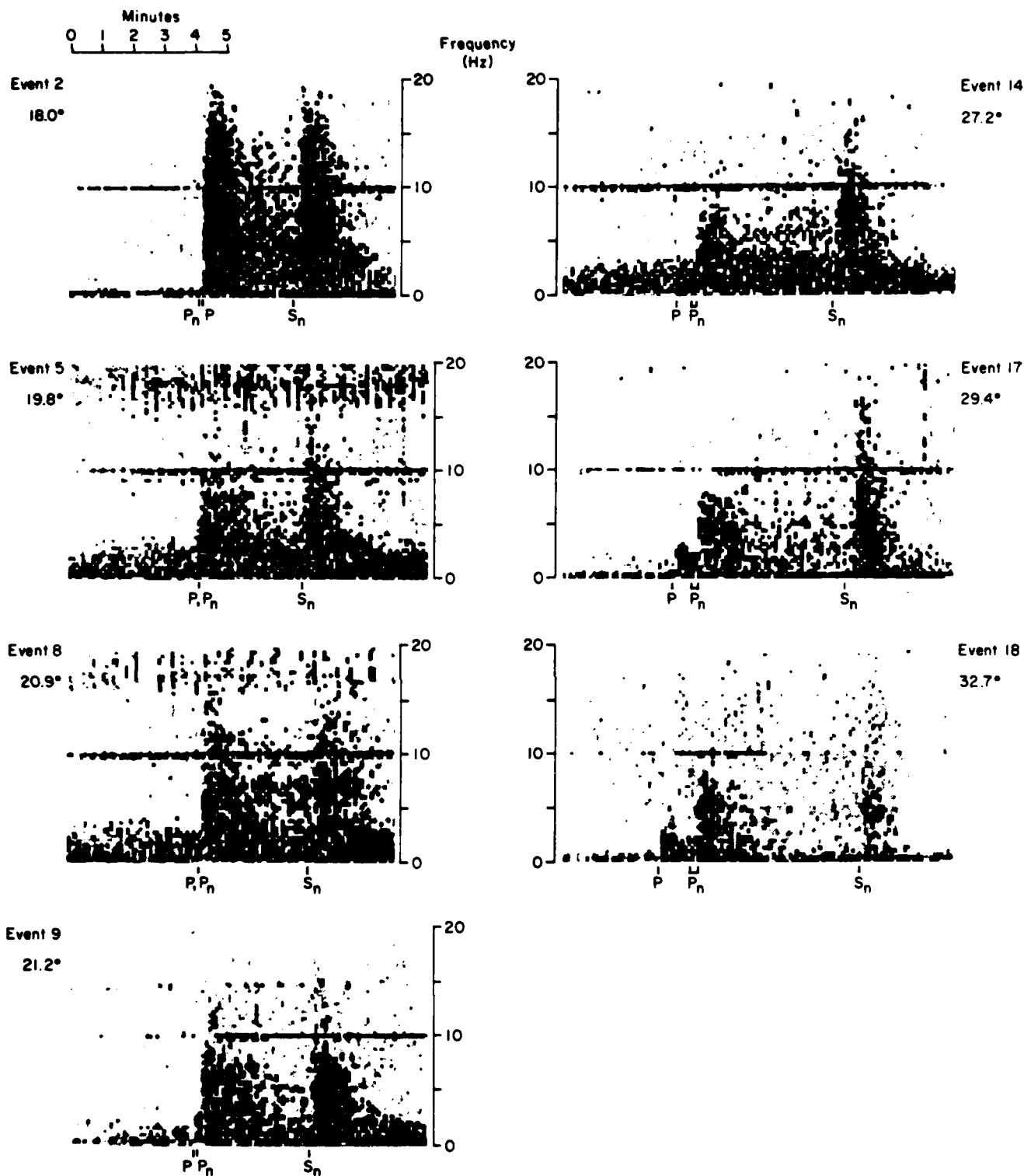


Fig. 1. Spectrograms for some earthquakes having travel paths to Wake under the Northwestern Pacific Basin. Expected times of arrivals are based on either the Jeffreys-Bullen tables (1958) for P or Pn/Sn travel time curves from Walker (1977a). The contour interval is 8 db. The line at 10 Hz is due to time code cross talk.

6 SEPTEMBER 1982; 01:47:02; 29.3N, 140.3E; 6.6  $M_B$ ; 167 KM; SOUTH OF HONSHU; DISTANCE = 25.2°

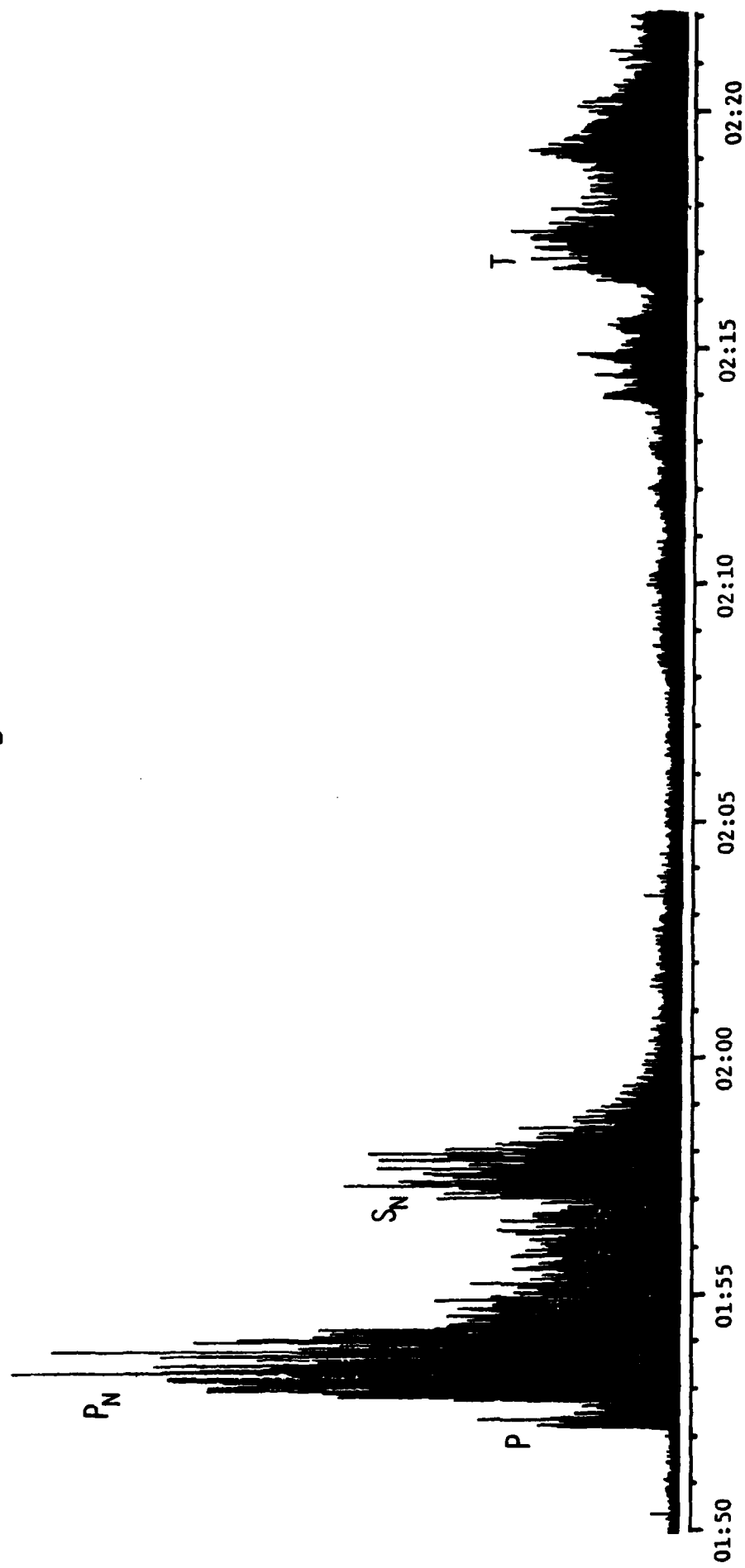


Fig. 2. Digitally rectified and compressed plot of P, Pn, Sn, and T phases for an earthquake south of Japan recorded by the Wake Island hydrophones.

## OCEAN-SURFACE REFLECTIONS

Other potentially significant contributors to the Pn, as well as Sn, wavetrains are multiple ocean-surface reflections of all Pn/Sn variations observed on the ocean bottom that are capable of becoming compressional water waves at the sediment-water interface. Such reflections have already been proposed in synthetic Pn model studies (Gettrust and Frazier, 1981). An example of an ocean-surface reflection is shown in Figure 3.

## PN/SN PHASES AT GREAT DISTANCES

Another puzzling aspect of Pn/Sn propagation is the frequent absence or weakness of Sn, yet presence of Pn, at great distances (often more than 4000 km) throughout the North Pacific (Walker, 1977a and b) and Central Pacific (Talandier and Bouchon, 1979), in spite of stronger Sn's than Pn's for relatively homogeneous travel paths across the deep Northwestern Pacific Basin.

A possible explanation is that paths other than those across the relatively homogeneous deep Northwestern Pacific Basin are likely to encounter relatively large lateral changes in the crust and upper mantle. These changes would have to be of such a nature so as to reduce Sn signal strength without seriously affecting the Pn phase. Large lateral changes could be produced by plateaus, rises, ridge systems, island and seamount chains, fracture zones, transform faults, fossil arcs and trenches, and rafted continental fragments.

Specific examples of Sn's severely attenuated by large lateral variations are found in recordings of earthquakes from the Solomon Islands area on the Wake hydrophones. Although these events are at distances comparable to events from Japan and the Kurils which have strong Pn/Sn phases (Fig. 1), only their Pn's are well recorded (Fig. 4). Furthermore, this effect cannot be attributed to differences in source mechanisms because Sn's from the area are well recorded at Ponape (examples of such recordings are shown in Fig. 5; refer to Fig. 6 for the location of Ponape). A reasonable explanation would appear to be the large structural changes associated with the transition from the shallow Ontong Java Plateau to the deeper Northwestern Pacific Basin (Figs. 6 and 7). An additional factor may be the extension of the Caroline Archipelago through this region.

# WAKE HYDROPHONE RECORDING OF UNDERGROUND EXPLOSION

7 JULY 1979 03:46:58.3 50.06N,79.11E E. KAZAKH

$M_B = 5.8$  YIELD = 100 KT DISTANCE = 73.1°

S/N RATIO = 50/1 ESTIMATED MAGNIFICATION @ 2 HZ =  $10^6$

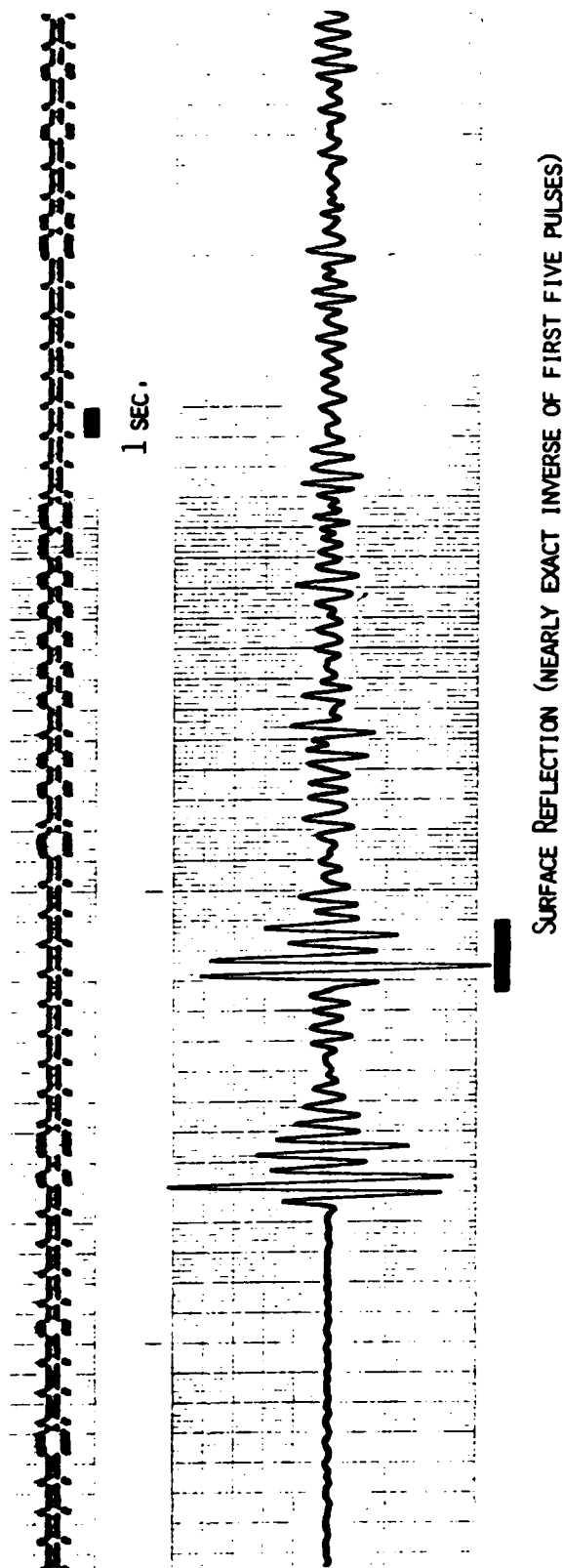


Fig. 3. An example of ocean-surface reflections.

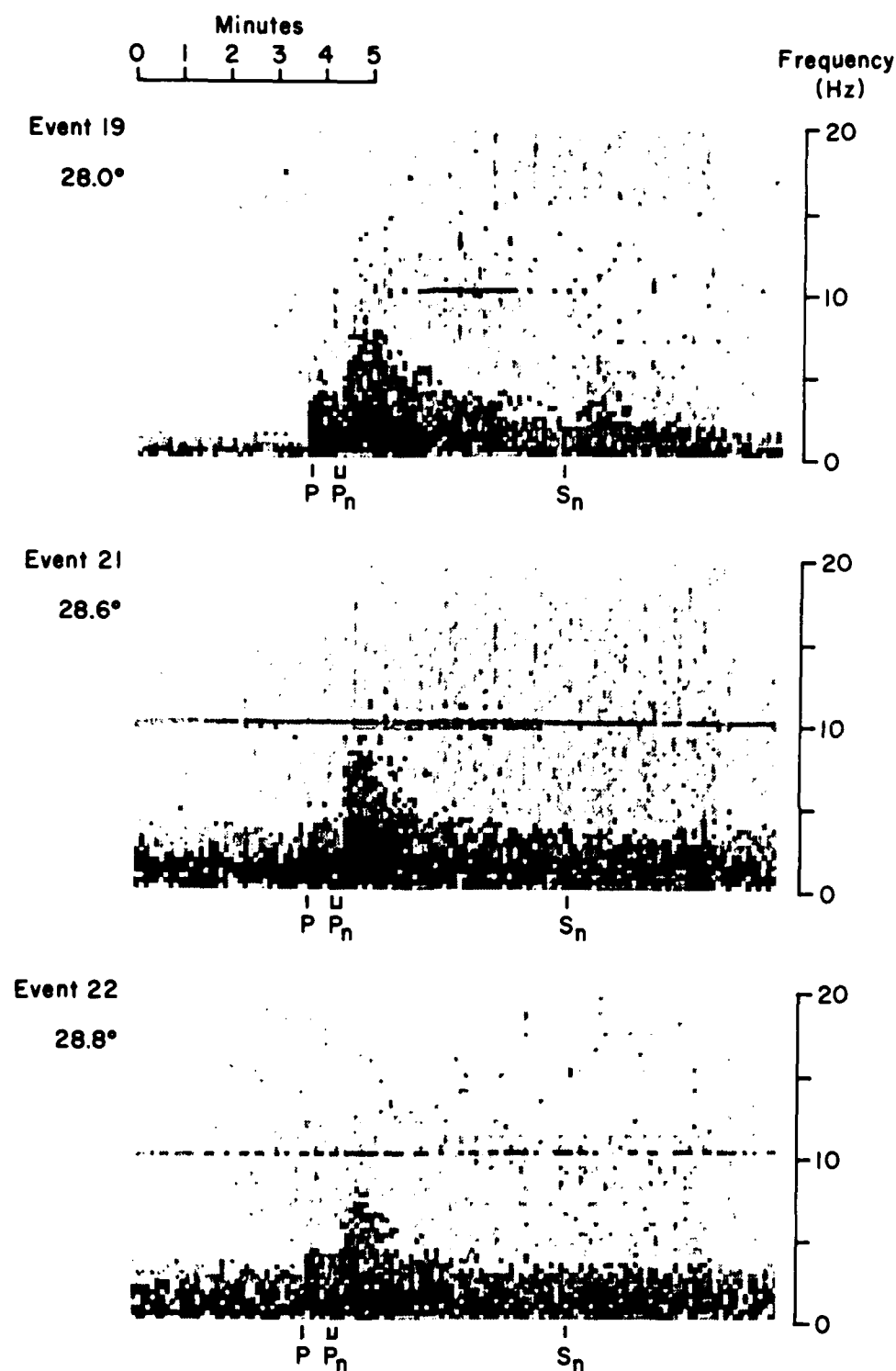


Fig. 4. Some spectrograms for earthquakes having portions of their travel paths to Wake under the Ontong-Java Plateau. Computational procedures are the same as used in Fig. 1.

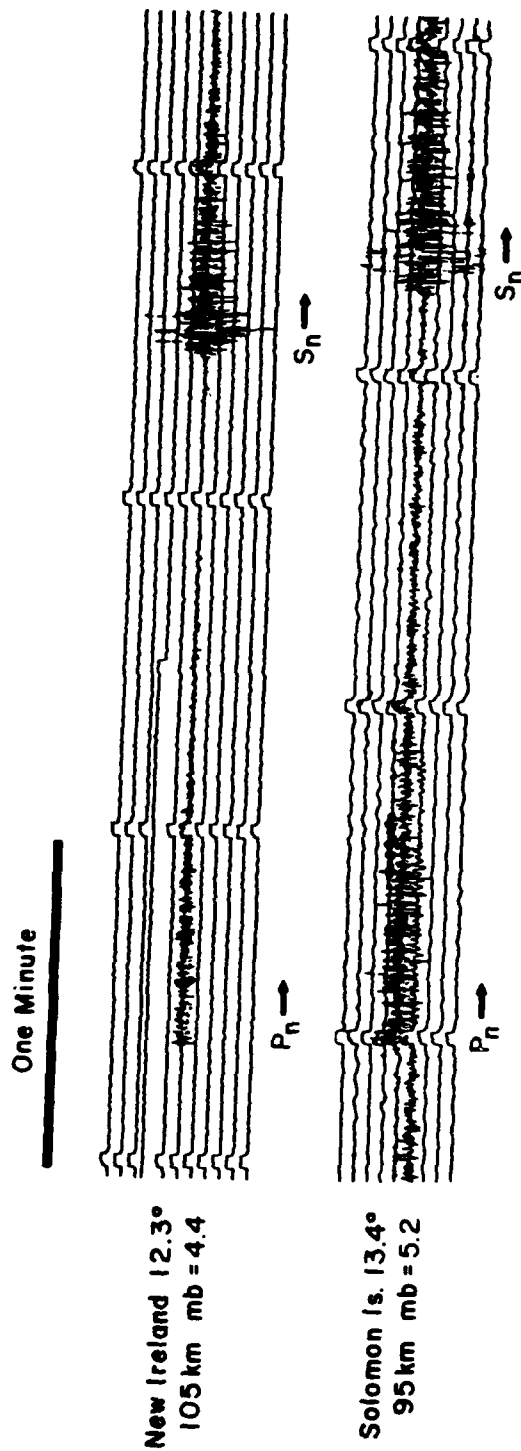


Fig. 5. Examples of  $P_n$  and  $S_n$  phases recorded at Ponape on the northern margin of the Ontong-Java Plateau. Of more than forty events from the New Ireland-Solomon Islands area, amplitudes of  $S_n$  phases are at least comparable to, and frequently larger than, those of their respective  $P_n$  phases.

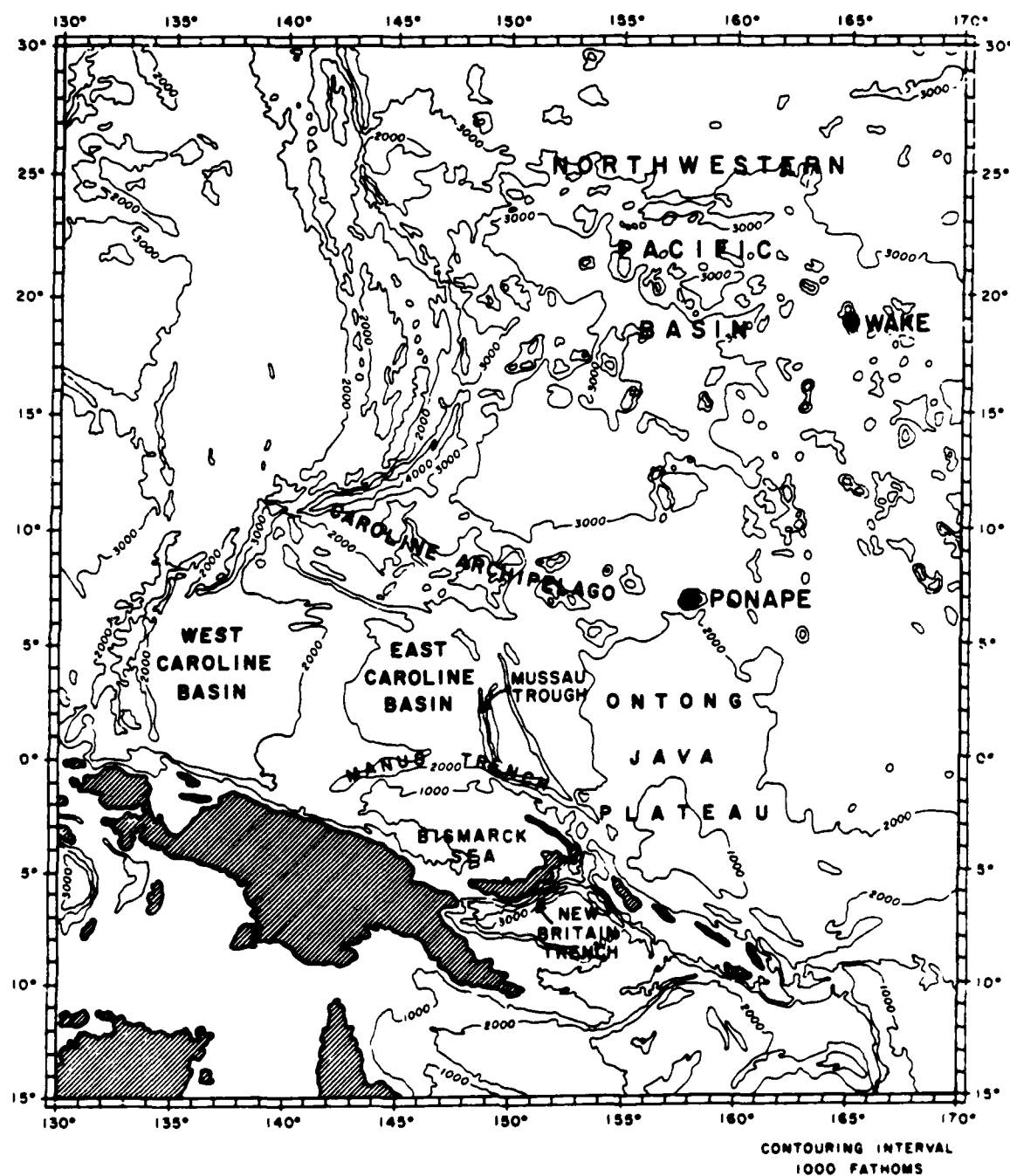


Fig. 6. Bathymetry map of the Northwestern Pacific area.

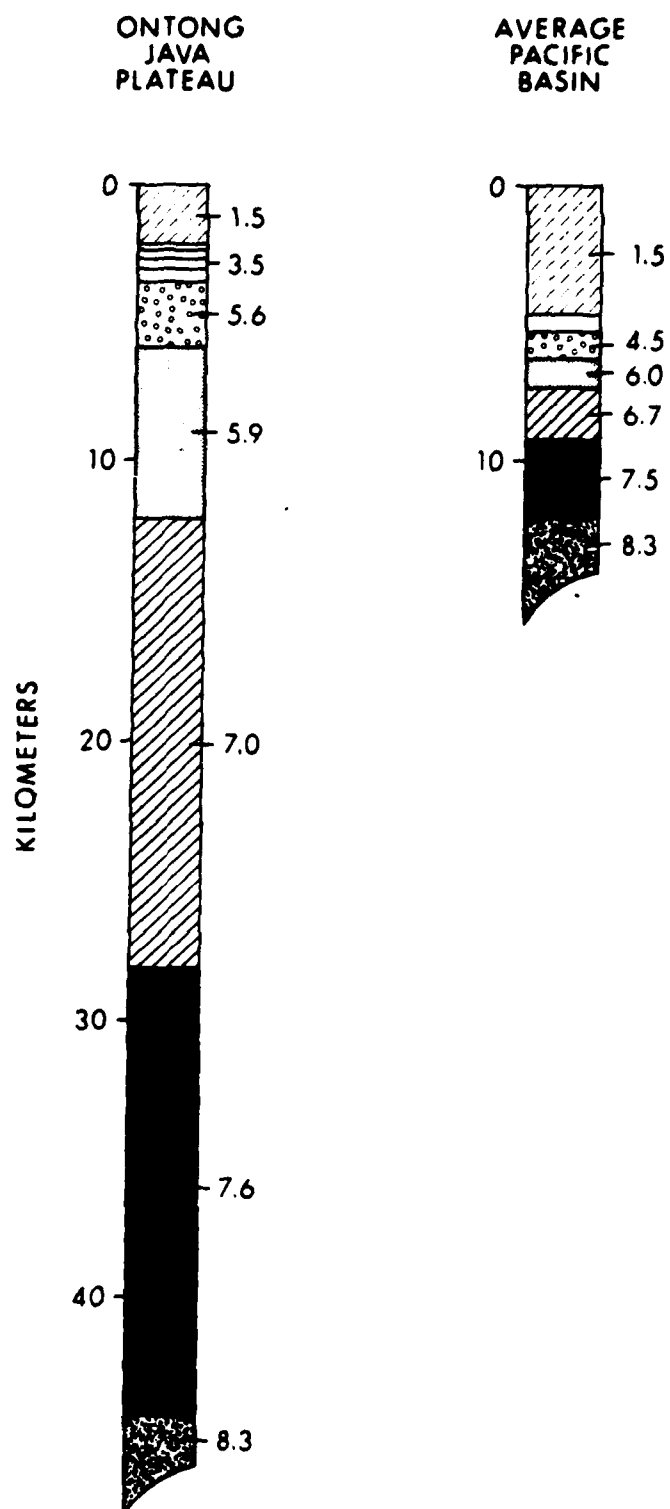


Fig. 7. Section profiles for the Ontong-Java Plateau and Pacific Basin (from Hussong *et al.* 1979).



## T-PHASE MECHANISMS

Tolstoy and Ewing (1950) recognized the importance of a sloping bottom in the production of T-phases, and Milne (1959) provided a specific mechanism involving multiple reflections between the surface of the ocean and its downward sloping bottom. Although such a mechanism could be significant for T-phases originating in areas with the appropriate downward sloping bottom, many strong T-phases have been observed from regions where the ocean floor is level or at a greater depth than adjacent areas in the direction of the receiver (Johnson *et al.*, 1968; Duennebie, 1968). Included among these regions are the deep ocean floor off the coast of California and Oregon, the deep ocean floor south of the subducting margins of the Northern Pacific and east of the Western Pacific, and the East Pacific Rise.

Because of these observations, a mechanism other than down-slope propagation is required. Some suggestions included ocean surface scattering (Johnson *et al.*, 1968), scattering from the sea floor by fault scarps near the source (Johnson and Norris, 1970), and coupling of Stoneley waves into the SOFAR channel (Biot, 1952; Duennebie, 1968). All of these proposed mechanisms, including downslope propagation, presume that the energy of the T-phase comes ultimately from P and, perhaps, S phases travelling upwards through the crust to the ocean bottom near the T-phase source location; however, with such a presumption, none of the proposed mechanisms is capable of explaining T-phase forerunners. In describing these forerunners, Johnson (1963) stated:

"The time of earliest perceptible arrival is probably primarily a function of magnitude as the signal emerges slowly from the ocean background noise...Early, low-level arrivals, undetected in most T-phase recordings, must be normal-mode ground waves or, at least, must have followed a ground path for a significant portion of their travel."

He also states that in one instance (a 7.0-Ms earthquake from the Kurils) the forerunners were so early that "the transformation from P or S waves to sound channel waves would have to occur at a distance of about 17 to 21° from the source toward the receiver." In describing a P, S, and T phase (Fig. 8; actually the P and S phases are P<sub>n</sub> and S<sub>n</sub> phases) from a large (6.2 mb) earthquake in the Marianas recorded on hydrophones near Enewetok Atoll at a distance of about 18°, Duennebie (1968) notes that "the T phase does not have a definite onset and that energy was continuously received at the hydrophone after the arrival of the P wave."

Both authors suggest that the apparent coupling into the SOFAR channel was due to normal, mantle P or S waves or both refracted by the Emperor Seamount Chain (Johnson, 1963) and by several groups of seamounts in the Northwestern Pacific Basin (Duennebier, 1968). In terms of frequency content and strength of signal, however, the energy from the long-range, high-frequency, guided Pn and Sn phases seems more likely to be coupled into the SOFAR channel than the mantle-refracted P and S phases which are extremely weak at high frequencies. At teleseismic distances frequencies of P and S generally do not exceed 3 or 4 Hz, while Pn, Sn, and T frequencies may be as high as 20 Hz (Figs. 8 and 9).

For large earthquakes sufficient energy could be contained in the Pn/Sn phases for coupling into the SOFAR channel throughout the travel path to the receiver. This coupling could occur by any of the mechanisms proposed for the generation of the T-phase (i.e., scattering or Stoneley waves or both), with seamount enhancement remaining as an important consideration. In effect the Pn/Sn phases would serve as potential sources of energy at the sediment-basement (or water-sediment) interface. As Pn/Sn energy declines with increasing distance, the amount of energy coupled into the SOFAR channel would also decline, thus producing a T-phase signal which would slowly emerge from the ocean background noise. A recently recorded example of such an emergent T-phase is shown in Figure 2. Energy arriving at 02:08 corresponds to a Pn path of  $9.6^\circ$  at 8.0 km/sec and a T-phase path of only  $15.6^\circ$  at 1.5 km/sec.

Finally, an additional explanation for Sn appearing to have relatively more energy than Pn with increasing distance could be that Pn energy is coupled more efficiently into the SOFAR channel than Sn energy is.

## SUMMARY

Vast regions of the world's oceans are characterized by thinly layered, homogeneous crustal and uppermost mantle structure. This report suggests that comprehensive observations of high-frequency phases, often referred to as Pn/Sn, throughout the Western, Northern, and Central Pacific may be explained by a waveguide which extends upward from the uppermost mantle through the crust and, to some extent, into the sedimentary layers and the entire water column. Pn energy is more efficiently propagated upward into the sedimentary column than

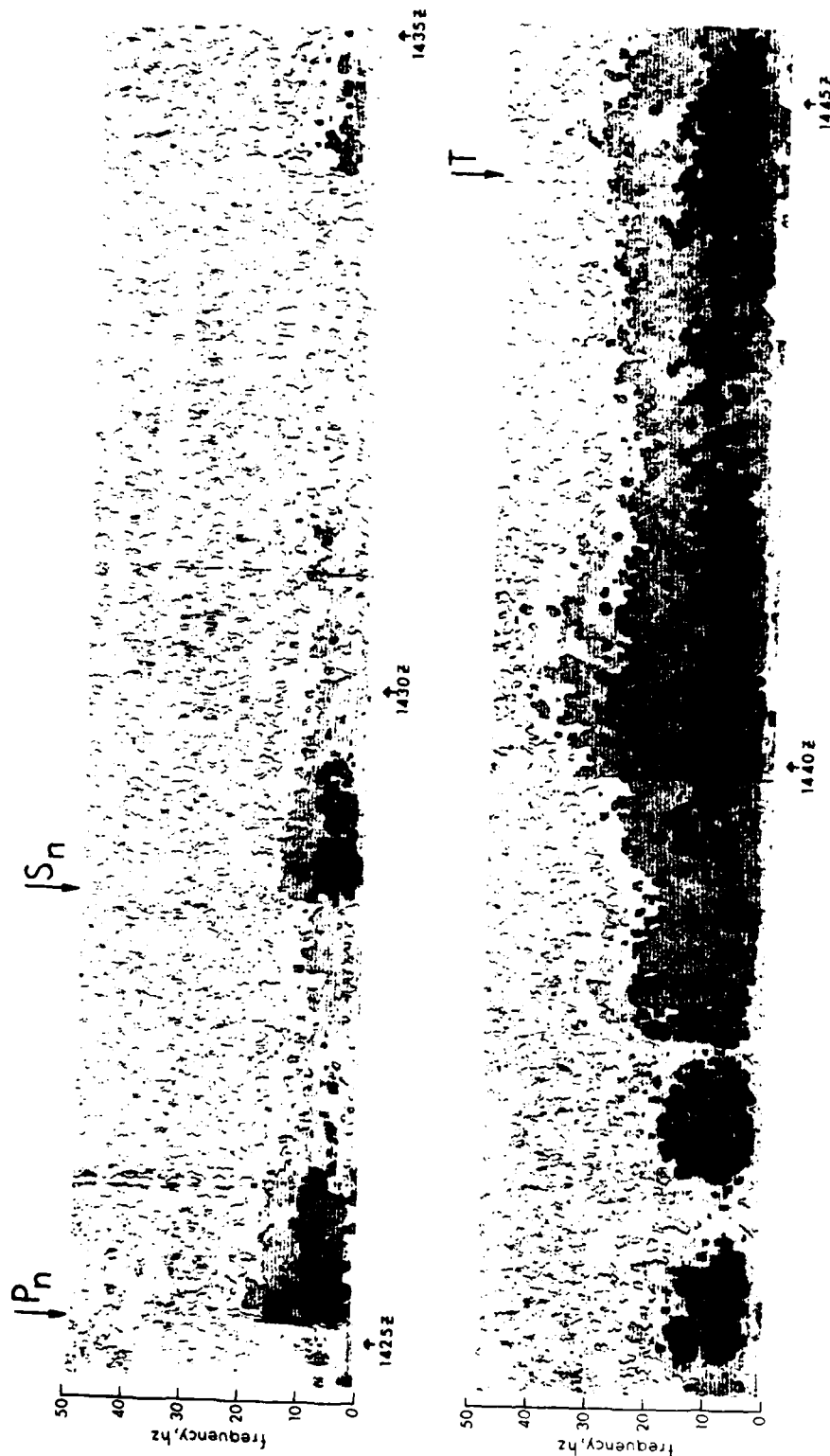


Fig. 8. Sonogram of  $P_n$ ,  $S_n$ , and  $T$  phases (after Duennebie 1968). Note that the  $T$ -phase does not have a definite onset. Instead, energy appears to be continuously received at the hydrophone after the arrival of the  $P$  wave.

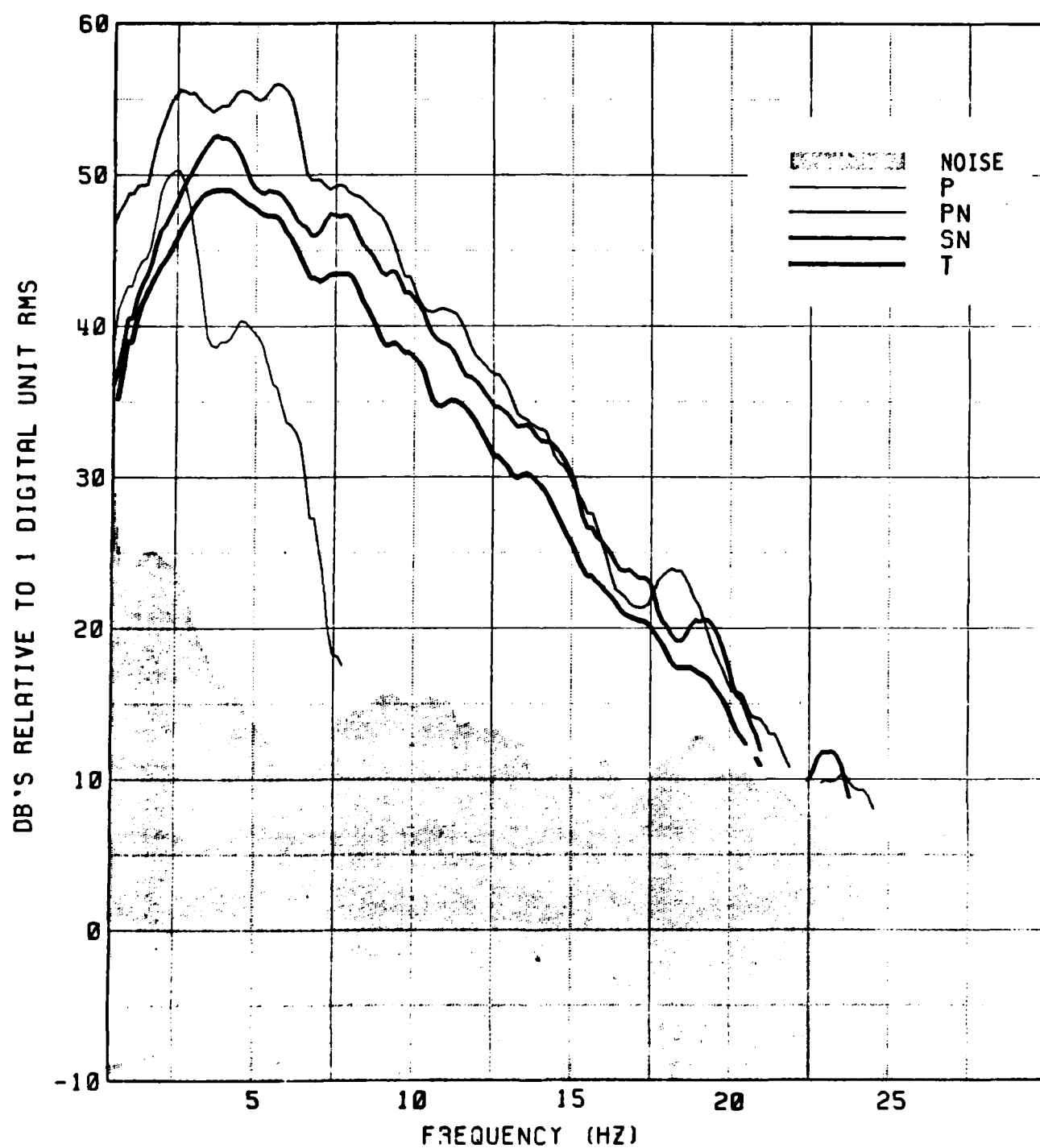


Fig. 9. Spectrums for the P, Pn, Sn, and T phases shown in Figure 2.

Sn energy, and, because of this, Pn is more rapidly attenuated than Sn. As distance increases, Pn's losses above the basement-sediment interface produce a relative strengthening of the Sn phase, such that Sn eventually has more energy than Pn.

The observed data also suggests that the long Pn/Sn wavetrains may, in part, be the result of multiple ocean-surface reflections near the receiver.

Pn to Sn and Sn to Pn conversions are suggested to explain Pn wavetrains consistently longer than the wavetrains of Sn. These conversions could occur when Pn or Sn energy passes through the basement-sediment interface and is returned to that interface by way of reflections from the ocean surface to continue in the waveguide, at least in part, as Sn or Pn phases. Such conversions might be produced at any of the interfaces encountered by Pn or Sn, or their converted phases.

In conjunction with the scattering mechanisms and Stoneley wave propagation already proposed to explain T-phase observations, Pn/Sn phases as sources of energy at the sediment-basement interface could explain: (1) the generation of T-phases in regions not having the downward sloping ocean bottom required by the classical downslope mechanism of Milne (1959) and (2) T-phase forerunners extending well ahead of the peak arrivals--occasionally beginning perhaps as early as the Pn and/or Sn phases. Also, another explanation for Sn having more energy than Pn is provided if Pn energy is more efficiently transmitted than Sn energy into the SOFAR channel.

Finally, the observed data suggest that large lateral variations in the crust and upper mantle may produce significant reductions in Sn signal strength without seriously affecting the Pn phase.

## CONCLUSIONS

Although many puzzling observations of long-range oceanic Pn/Sn phases may be resolved by the suggestions presented in this report, many of these suggestions can, and should, be tested quantitatively. These analyses could include the re-examination of existing data, new experiments, and theoretical modeling efforts leading to the generation of complete synthetic seismograms. Furthermore, one should not forget that the mechanisms for the generation and propagation of the main Pn and Sn phases are still not generally agreed

upon, nor have proposed models been matched in a comprehensive manner with observations. Such tasks are of utmost importance if the phenomenon is to finally achieve the status it deserves as a major geophysical feature and tool for mapping the crust and uppermost mantle of the world's oceans--this after nearly fifty years of being little more than an obscure curiosity.

Regarding the T-phase, it seems appropriate that the earth's most efficient acoustical waveguides, the SOFAR channel and the Pn/Sn waveguide, finally should be related; and in the hypothesis formulated in this report, the SOFAR channel is energized by leakage from the Pn/Sn waveguide. The recognition of this relationship could be an important, and perhaps critical, factor in arriving at a comprehensive understanding of these oceanic phases.

"In the bulletin of the Harvard Seismograph Station, under date of September 15, 1935 attention was directed to the unusual character of certain records from the vicinity of 17°N, 62°W. One of the novel features was a short-period phase about 23 minutes after P. It has become known as T, for third, with P and S constituting the first and second groups of short-period waves of similar general appearance...Actually, many features of P and S are abnormal on this and later records from certain areas at this distance range, and work on that part of the problem is in progress, but the investigation of T has been undertaken first." (Leet et al., 1951)

#### ACKNOWLEDGMENTS

This research was supported by the Office of Naval Research (Code 425GG). Supplementary funds were provided by the Air Force Office of Scientific Research and the U. S. Arms Control and Disarmament Agency. The Ponape Island Seismic Station which operated from May of 1972 through September of 1973 was supported by the National Science Foundation under grants GA-37118X1 and DES75-14814. The author thanks the U. S. Air Force (Detachment 4, 15th Air Base Wing) and Ken-tron International for assistance in installing and maintaining the recording stations at Wake.

Special appreciation goes to Charles McCreery, George Sutton, and Loren Kroenke for constructive comments and discussions. Editorial assistance was provided by Barbara Jones.

## SUPPLEMENTARY NOTE

It may be appropriate at this time to suggest that a new name be given to the high-frequency compressional and shear phases often observed at great distances in the world's oceans. The difficulty with the nomenclature used to date is that: (1) an, as yet, unsubstantiated relationship to the well known and much studied longer-period Pn/Sn phases of continents is inferred; and (2) the environmental feature most strongly linked to the observations is not cited. Thus, a more logical term would be "Ocean P" or "Ocean S" with the abbreviations being "Po/So." With this change, those unfamiliar with the phenomenon would not be as likely to make the false assumption that the phases are similar to continental Pn and Sn. Such assumptions in the past have been a major stumbling block in stimulating interest and support for "Po/So" research.

## REFERENCES

- Auld, B., G. Latham, A. Nowroozi, and L. Seeber, 1969. Seismicity off the coast of northern California determined from ocean bottom seismic measurements, Bull. Seismol. Soc. Am., 59, p. 2001-2015.
- Biot, M., 1952. The interaction of Rayleigh and Stoneley waves in the ocean bottom, Bull. Seismol. Soc. Am., 42, p. 81-93.
- Duennebie, F., 1968. Spectral variation of the T phase, Hawaii Inst. of Geophysics Rept. HIG-68-22, 18 pp., 11 figs.
- Gettrust, J. and L. Frazer, 1981. A computer model study of the propagation of long-range Pn phase, Geophys. Res. Lett., 8, p. 749-752.
- Husson, D., L. Wiperman, and L. Kroenke, 1979. The crustal structure of the Ontong-Java and Manihiki oceanic plateaus, J. Geophys. Res., 84, p. 6003-6010.
- Jeffreys, H. and K. Bullen, 1958. Seismological Tables, Office of the British Association, Burlington House, W. 1., London, 50 pp.
- Johnson, R., 1963. Spectrum and dispersion of Pacific T phases, Hawaii Inst. of Geophysics Rept. HIG-34, 12 pp.
- Johnson, R. and R. Norris, 1970. T wave generation mechanisms, Hawaii Inst. of Geophysics Rept. HIG-70-7, 16 pp, 6 figs., + Appen., 34 figs.
- Johnson, R., R. Norris, and F. Duennebie, 1968. Abyssally generated T phases, pp. 70-78 in L. Knopoff, C. Drake, and P. Hart (eds.), The Crust and Upper Mantle of the Pacific Area, Am. Geophys. Union Geophys. Mono. No. 12.
- Leet, L., D. Linehan, and P. Berger, 1951. Investigation of the T phase, Bull. Seismol. Soc. Am., 41, p. 123-141.
- McCreery, C., D. Walker, and G. Sutton, in press. Spectra of nuclear explosions, earthquakes, and noise from Wake Island bottom hydrophones, Geophys. Res. Lett.
- Milne, A., 1959. Comparison of spectra of an earthquake T phase with similar signals from nuclear explosions, Bull. Seismol. Soc. Am., 49, p. 317-329.



- Molnar, P. and J. Oliver, 1969. Lateral variations of attenuation in the upper mantle and discontinuities in the lithosphere, J. Geophys. Res., 74, p. 2648-2682.
- Shimamura, H., Y. Tomoda, and T. Asada, 1975. Seismograph observation at the bottom of the Central Basin Fault of the Philippine Sea, Nature, 253, p. 177-179.
- Talandier, J. and M. Bouchon, 1979. Propagation of high frequency Pn waves at great distances in the Central and South Pacific and its implications for the structure of the lower lithosphere, J. Geophys. Res., 84, p. 5613-5619.
- Tolstoy, I., and M. Ewing, 1950. The T phase of shallow focus earthquakes, Bull. Seismol. Soc. Am., 40, p. 25-51.
- Walker, D., 1977a. High frequency Pn and Sn phases recorded in the western Pacific, J. Geophys. Res., 82, p. 3350-3360.
- Walker, D., 1977b. High frequency Pn phases observed in the Pacific at great distances, Science, 197, p. 257-259.
- Walker, D., C. McCreery, G. Sutton, and F. Duennebier, 1978. Spectral analysis of high-frequency Pn and Sn phases observed at great distances in the Western Pacific, Science, 197, p. 1333-1335.
- Walker, D., C. McCreery, and G. Sutton, in press. Spectral characteristics of high-frequency Pn, Sn phases in the Western Pacific, J. Geophys. Res.

Unclassified

SECURITY CLASSIFICATION OF THIS PAGE (When Data Entered)

REPORT DOCUMENTATION PAGE		READ INSTRUCTIONS BEFORE COMPLETING FORM
1. REPORT NUMBER HIG Technical Report No. 82-6	2. GOVT ACCESSION NO.	3. RECIPIENT'S CATALOG NUMBER
4. TITLE (and Subtitle) Oceanic Pn/Sn Phases: A Qualitative Explanation and Reinterpretation of the T-Phase		5. TYPE OF REPORT & PERIOD COVERED
		6. PERFORMING ORG. REPORT NUMBER HIG Technical Report No. 82-6
7. AUTHOR(s) Daniel A. Walker		8. CONTRACT OR GRANT NUMBER(s) N00014-75-C-0209
9. PERFORMING ORGANIZATION NAME AND ADDRESS Hawaii Institute of Geophysics 2525 Correa Road Honolulu, Hawaii 96822		10. PROGRAM ELEMENT, PROJECT, TASK AREA & WORK UNIT NUMBERS Project No. 083 603
11. CONTROLLING OFFICE NAME AND ADDRESS Office of Naval Research Code 425 GG Ocean Sciences and Technology Division Bay St. Louis, MS 39520		12. REPORT DATE November 1982
14. MONITORING AGENCY NAME & ADDRESS (if different from Controlling Office) Office of Naval Research Branch Office 1030 East Green St. Pasadena, CA 91106		13. NUMBER OF PAGES
		15. SECURITY CLASS. (of this report) Unclassified
		15a. DECLASSIFICATION/DOWNGRADING SCHEDULE
16. DISTRIBUTION STATEMENT (of this Report)  Approved for public release; distribution unlimited.		
17. DISTRIBUTION STATEMENT (of the abstract entered in Block 20, if different from Report)		
18. SUPPLEMENTARY NOTES  Published as Hawaii Institute of Geophysics Technical Report 82-6		
19. KEY WORDS (Continue on reverse side if necessary and identify by block number)  Marine geophysics Western Pacific Seismic waves Waveguide SOFAR		
20. ABSTRACT (Continue on reverse side if necessary and identify by block number)  The combined effects of: (1) differing efficiencies between Pn and Sn energy transmission across the basement-sediment interface; (2) ocean surface reflections; (3) Pn to Sn conversions; and, (4) large lateral variations in the crust and upper mantle are used to formulate a working hypothesis which appears to explain, qualitatively, many observations of high frequency Pn/Sn phases throughout the western, northern, and central Pacific. Also, the concept of Pn/Sn phases as sources of energy at the basement-sediment interface is suggested as a possible mechanism for T-phase generation through scattering or Stoneley wave generation.		

DD FORM 1 JAN 73 1473

EDITION OF 1 NOV 65 IS OBSOLETE  
S/N 0102-014-6601

Unclassified  
SECURITY CLASSIFICATION OF THIS PAGE (When Data Entered)

CORRECTIONS AND ADDITIONS

- pg. 12 line 5  
after "... (Duennebier, 1968)."  
add " Northrop (1972) also suggests a transformation from P to T  
at a distance of about  $17^\circ$  to explain the earliest  
perceptible T phase arrivals on Oahu hydrophones from the 28  
March 1964 Alaskan earthquake."
- pg. 12 line 27 (last sentence of 2<sup>nd</sup> paragraph)  
"... path of  $9.6^\circ$  at 8.0 km/sec and a T-phase path of only  
 $15.6^\circ$ ..."  
should read "... path of  $10.1^\circ$  at 8.0 km/sec and a T-phase path of  
only  $15.1^\circ$ ..."
- pg. 12 line 32 (last sentence of 3<sup>rd</sup> paragraph)  
after "... than Sn energy is."  
add " Conversions of Pn or Sn to T near the receiver could also  
strengthen and extend the Pn and Sn wavetrains."
- pg. 15 line 28 (last sentence of 4<sup>th</sup> paragraph)  
after "... the SOFAR channel."  
add " Conversions of Pn or Sn to T near the receiver could  
strengthen and extend the Pn and Sn wavetrains."
- pg. 18 McCreery et al. has since been published in volume 10, p. 59-62, of  
Geophysical Research Letters, 1983.
- pg. 19 add " Northrop, J. 1972. T-phases, in The Great Alaskan Earthquake  
of 1964: Oceanography and Coastal Engineering, Nat. Acad. of  
Sci., Washington, D.C., p. 19-24."

*Dan Walker*

APPENDIX IV

**A Preliminary Informal Comparison  
of Signal/Noise Capabilities  
Between The Wake Bottom Hydrophone Array,  
The Ocean Sub-Bottom Seismometer,  
And Ocean Bottom Seismometers**

**by  
Charles S. McCreery and Daniel A. Walker**

**both at  
Hawaii Institute of Geophysics  
2525 Correa Road  
Honolulu, Hawaii 96822  
(808) 948-8767**

Abstract. A comparison has been made between noise levels and signal/noise (S/N) ratios of the Wake Bottom Hydrophone Array (WBHA), the Ocean Sub-Bottom Seismometer (OSS), and Ocean Bottom Seismometers (OBS's) using data which has recently become available. The general purpose of this comparison is to evaluate WBHA as a possible alternative or complement to deep sea drillhole seismometers such as the Marine Seismic System (MSS) now being developed and tested for possible deployment in the Northwestern Pacific Basin. Absolute noise measurements show roughly comparable levels between WBHA and OSS, although the OSS data was scant. S/N ratios were found to be approximately 17 dB greater on the OSS than on a nearby OBS over the band 2-20 Hz, and 10 dB greater on WBHA than on a nearby OBS over the band 1-20 Hz. Improvements in WBHA S/N ratios of at least 3 dB and up to 11 dB, by stacking the water surface reflections and all 6 hydrophone signals, may be gained depending upon the level of coherence between signals. An evaluation of coherence levels has revealed apparent differences between the individual hydrophone/cable responses. Appropriate correction factors for these differences will have to be determined and then applied to the data before coherence levels are accurately known. The limited amount of data available for the noise and S/N ratio comparisons, and the indirect route by which the comparisons were made are arguments for attaching a certain amount of skepticism to the results. Additional OSS data which will become available after May 1983 should provide for a more direct and statistically stronger comparison.

Introduction. Considerable effort has been expended in recent years to develop a deep-sea borehole seismometer such as DARPA's Marine Seismic System (MSS) and the Hawaii Institute of Geophysics (HIG) Ocean Sub-Bottom Seismometer (OSS), which can be deployed down drillholes in the ocean bottom. Impetus for this effort has come from a desire to make high quality seismic observations on the vast portions of the earth covered by oceans. Although seismic observations in the oceans are capable of being made more or less routinely using Ocean Bottom Seismometers (OBS's) sitting on top of the sediments, it has often been presumed that an instrument located below the sediment-basalt interface would have significantly greater signal/noise (S/N) ratios, at least for upwardly arriving signals. This is because such an instrument should receive more energy from seismic signals arriving from below, and less energy from noise propagating downward through the water column and sediments.

Since July of 1979, HIG has monitored on a nearly continuous basis, an array of hydrophones located near Wake Island in the Northwestern Pacific Ocean. This array consists of six hydrophones on the ocean bottom at 5.5 km water depth in a 40 km, 2-dimensional grouping, and 3 pairs of hydrophones at 1 km water depth (SOFAR channel) spread over 300 km. Recordings from only two or three of the hydrophones were made prior to September 1982; subsequently recordings from eight of the hydrophones have been made. The array was installed with the hydrophones hardwired to Wake Island more than 20 years ago for the purpose of recording transient, non-tectonic signals at frequencies above 10 Hz. Recordings made by HIG indicate that the hydrophones are also excellent seismic sensors in at least the band 0.5-20 Hz. The capability to evaluate the full potential of this array as a seismic tool has only been possible since the September

1982 upgrading. One aspect of this evaluation is to compare the noise levels and the S/N ratios between the Wake Bottom Hydrophone Array (WBHA), a sub-bottom seismometer (the OSS), and an OBS. Although data for a direct comparison does not yet exist, a somewhat indirect comparison has been made using data collected recently. That comparison is the subject of this report.

Absolute Background Noise Levels. In September 1982, during Leg 88 of the R/V Glomar Challenger, the OSS was successfully deployed off of the Kuril Islands, 378 m below the ocean floor and 20 m below the sediment-basalt interface. For a period of about 2.5 days, data was recorded from the OSS directly on the ship. Then a 2 month continuous recording package was dropped over the side for pickup sometime in May 1983. Briefly overlapping this 2.5 day period was the nearby deployment of several HIG OBS's. Noise levels measured at about the same time by the OSS vertical seismometer and a representative OBS vertical seismometer are shown in Figure 1. Although the general shape of the curves is similar, the difference in absolute levels is striking. Some of this difference is due to the impedance difference between the basalt and the top of the sediment. Smaller signals, as well as lower noise levels, would be associated with the higher impedance of the basalt. If normalized to the sediment impedance by a  $\sqrt{\rho c}$  correction, where  $\rho$  is density and  $c$  is compressional velocity, the OSS noise curve moves up by about 9 dB to the position of the dashed curve. The remaining differences between these two noise curves may reflect the attenuation of downwardly propagating noise energy. Some of this noise is certainly generated by the research vessels which were operating overhead.



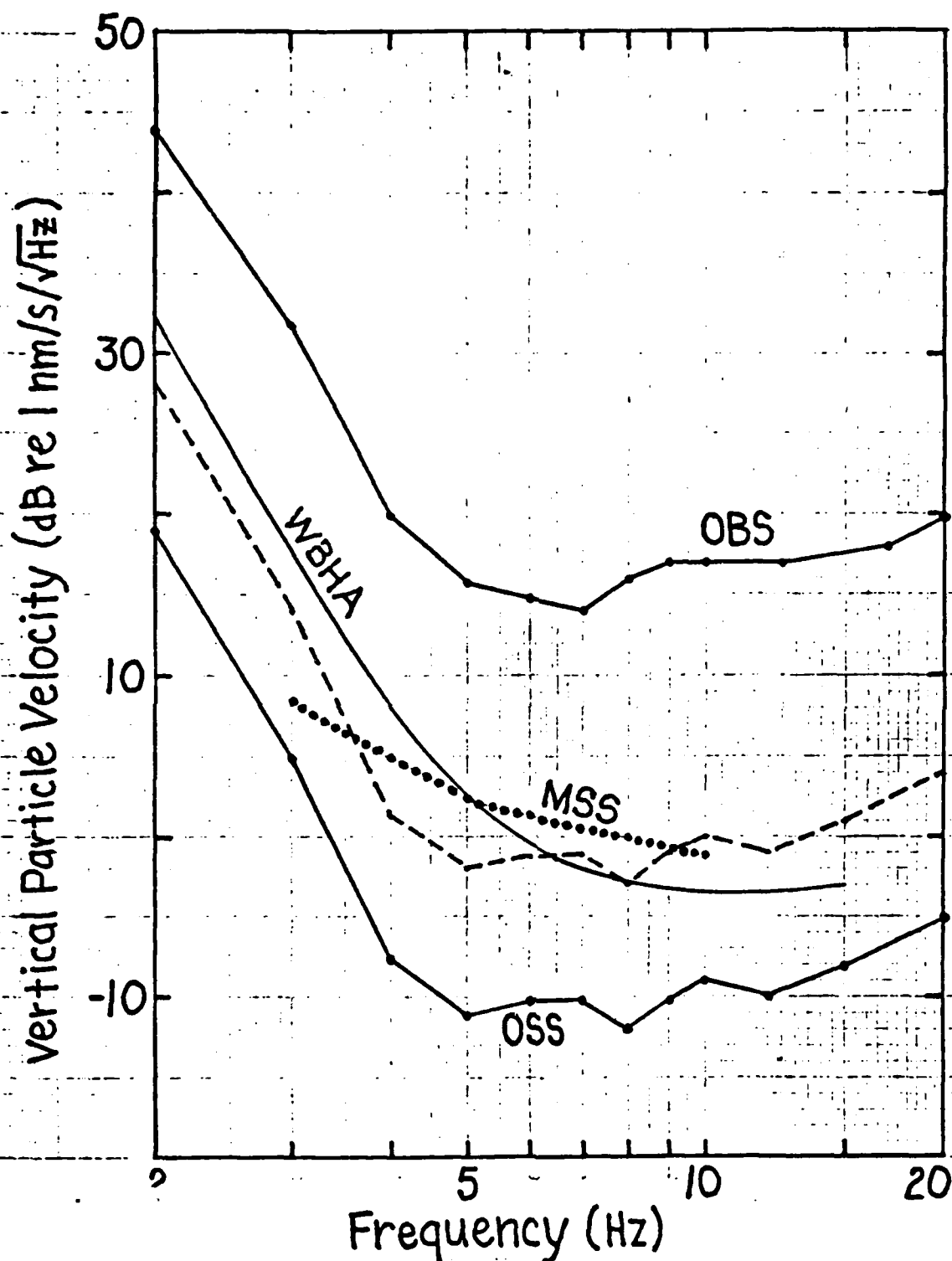


Figure 1. Background noise level measurements from WBHA (one hydrophone, 52 samples over 18 months), from an OBS and the OSS deployed in the NW Pacific Basin (vertical component-1 simultaneous sample) and the MSS in the Atlantic (vertical component-1 sample). The dashed curve is the OSS curve adjusted by 9 dB to normalize it to sediment impedance.

Also shown in Figure 1 is the average background noise for one of the Wake bottom hydrophones, determined from 52-2 minute random noise samples taken over a period of 18 months. Pressure has been converted to vertical particle velocity by the expression  $\dot{x} = P/\rho c$ , where  $\dot{x}$  is vertical particle velocity,  $P$  is the pressure,  $\rho$  is seawater density, and  $c$  is the speed of sound in seawater. Although the hydrophone noise is certainly not generated entirely by vertically arriving pressure waves (thus vertical particle velocity), this conversion is useful to determine an equivalent noise level for comparison.

For reference purposes, the noise curve for MSS in the Atlantic has also been plotted. It is not known if an impedance correction need be applied to this curve and so none has been.

The OBS and OSS noise curves may not be representative of average noise levels because they are only 1 sample and because of the ship generated noise. The relationship between these two curves however, is probably significant, and illustrates the decrease in noise level which can be achieved by a downhole instrument. The average noise level of the Wake bottom hydrophone is similar to that of the normalized OSS curve. These two curves are also comparable to the MSS curve for frequencies between about 4 and 10 Hz.

Signal/Noise. Although absolute noise levels are important for evaluating the usefulness of a seismic sensor, a more important parameter is S/N. Ideally, a comparison should be made of an earthquake or explosion signal recorded simultaneously on the Wake hydrophones, an OBS, and a downhole instrument, all located in close proximity. Unfortunately, these data do

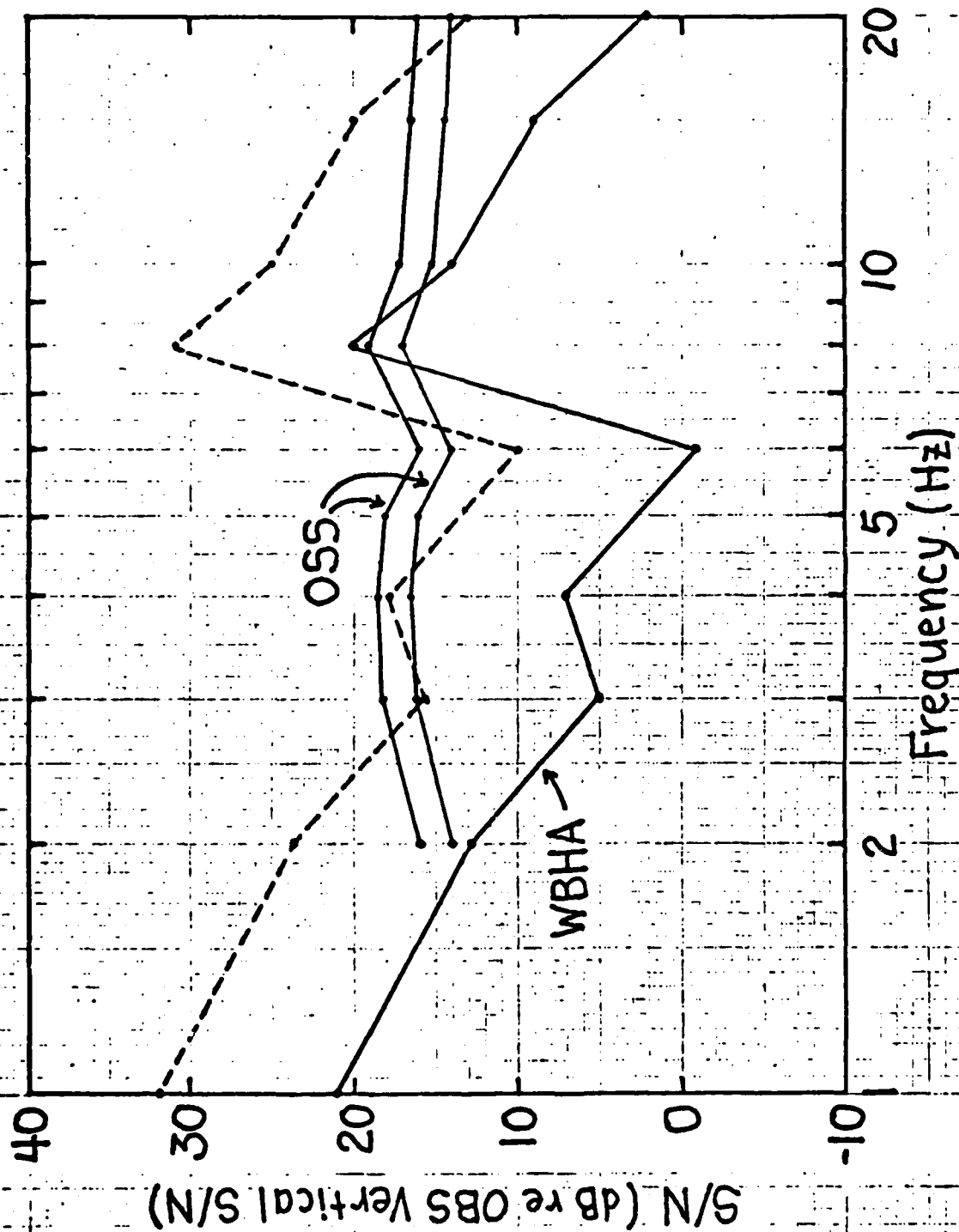


Figure 2. S/N measured on WBHA and on the OSS relative to S/N measured on nearby OBS's as described in the text. The lower OSS curve is based on shot S/N data, while the upper OSS curve is based strictly on noise data. The dashed curve is the WBHA curve raised by 11 dB to show the potential S/N by signal stacking.

not exist. With a few assumptions however, an indirect comparison can be made using data which do exist.

Within the 2.5 day period of OSS data previously mentioned is the record of a 126 pound shot at 80 km distance. It occurred, however, after the last of the nearby OBS's had been recovered. Fortunately, during the OBS deployment there was an 1800 pound shot also at 80 km distance from one of the OBS's. After making some assumptions and corrections, a comparison between ground arrivals on these records may yield information about the improvement in S/N between the OBS and OSS. The first correction is one for shot size, equal to the ratio of the shot weights to the power 0.66, or 15 dB. The spectral shape of the two shot records is very similar so a common shape was assumed. The second correction is for temporal changes in background noise which occurred during the time between the shots. These effects were compensated for by assuming the same OBS/OSS noise ratios found for the simultaneous data discussed in the previous section. The resulting ratio of  $(OSS\ S/N)/(OBS\ S/N)$  is plotted in Figure 2.

Also shown is a curve which represents the possible gain in S/N of the OSS relative to the OBS based strictly on the simultaneous noise data. A correction for the impedance difference between the sediment and basalt has been applied. No assumptions were made about possible losses in upcoming signal levels between the OSS and OBS, and the effect of these would be to raise this curve by some amount. However, the near agreement in absolute level between this curve and the one based on the shot data may imply that these losses are not significant for the frequencies observed. (The parallel nature of the two curves is not significant but is due to having used the simultaneous noise data to correct for temporal differences in the

shot data.) On the average, these data support an improvement in S/N over the range 2-20 Hz of about 17 db.

A more direct comparison can be made between WBHA and an OBS. In August of 1981, HIG deployed an OBS array along a 1500 km line in the NW Pacific, and one of these OBS's was located within the bounds of WBHA. A strong Po (i.e., "Ocean P"; formerly called high-frequency Pn) signal from a large earthquake in the Kuril Islands was recorded simultaneously by this OBS and by a recording system connected to 3 of the hydrophones of WBHA. A comparison between the OBS vertical geophone and WBHA could not be made because that sensor was not working properly on the OBS. Consequently, the OBS hydrophone signal has been used. To correct for any difference in S/N between the OBS vertical and OBS hydrophone, a factor equal to the actual measured difference in S/N between the vertical geophone and hydrophone for this same signal recorded on another OBS at a closer epicentral distance was added to the S/N of the hydrophone. This factor averaged 1 dB over the range 1-20 Hz. Plotted in Figure 2 is the ratio between the average S/N of the 3 Wake hydrophones and the S/N measured on the OBS hydrophone with the previously described correction added. The somewhat wild behavior of this curve, such as the jump from -1 dB at 6 Hz to 20 dB at 8 Hz, is not entirely understood. It may be related to resonances in the OBS package which contribute to the OBS noise level, or it may be due to other factors which could not be identified by the analysis of only this one signal. For most frequencies, however, the WBHA data show an improvement in S/N, and this improvement averages roughly 10 dB over the range 1-20 Hz.

A natural question to ask is: "Why should there be any difference at all in S/N between the OBS hydrophone and the nearby WBHA hydrophones, since they are both lying at the top of the sediment column?" One explanation

might be that the OBS used for comparison was particularly noisy due to noise sources in the water very close by or due to electrical noise in the amplification and recording system. Evidence which generally contradicts this hypothesis is that the noise levels measured on the other OBS's in the array were comparable. An alternate explanation may be related to the 20 year age of the array, and the possibility that the bottom hydrophones are now buried under a layer of sediment. Burial of the hydrophones would isolate them from noise generated by bottom water currents flowing around them, and also possibly from sediment surface phenomena such as Stonely waves. Although these explanations are not supported by direct evidence at this time, it would certainly be worthwhile to learn that shallow burial of a hydrophone under the sea floor sediment would greatly improve its S/N capabilities.

Coherence Across WBHA. An important aspect of current research at HIG is the investigation of coherence of teleseismic body waves across the 40 km aperture of WBHA. The impact of near receiver structure on these signals may be small due to the thin and relatively undisturbed nature of the oceanic lithosphere underlying WBHA. High coherency would have important implications for: (a) the planning of any future ocean seismic arrays; (b) studies of first arrivals requiring a great deal of timing precision; (c) studies requiring precise determination of seismic amplitudes (such as yield determination), and especially (d) studies of small signals where enhancement of S/N is desired (such as detection). Highly coherent signals may be added (with appropriate propagation delays) to yield an increase in S/N equal to the square root of the number of sensors (for uncorrelated noise). At WBHA the theoretical increase in S/N would be equal to about 11

dB (3 dB of which comes from the first water surface reflection which is well established as having nearly perfect coherence with the initial arrival). Data from 3 WBHA hydrophones, collected prior to September 1982 on slow-speed cassettes, indicated high levels of coherence for a sampling of teleseismic P arrivals. Unfortunately, these data were not especially suited for this type of analysis because of timing inaccuracies and the suspect fidelity of the recording medium. Since September 1982, however, continuous data from 5 of the 6 bottom hydrophones have been collected digitally, essentially solving the timing and fidelity problem, and providing a format for a much speedier and more accurate analysis of the data. Software for the necessary quantitative analysis is still under development. However, "eyeball" checks for coherency have been made for a few of the digitally recorded teleseismic P phases with large S/N. The results are encouraging although not entirely conclusive.

Figure 3 illustrates the kind of broadband coherency which seems to be characteristic of the different P arrivals examined. Some features are "in phase" across the array while others are not. Certain pairs appear more coherent than other pairs. This relationship does not seem to be a function of epicentral distance or azimuth. Certainly a large improvement in S/N would not be expected from the stacking of these signals as they are.

Possible reasons for the observed difference in signals may be classified into the following categories: (a) major differences in the coda exist for very small changes in takeoff angle (for Figure 3, much less than  $1^\circ$ ); (b) variations in lithospheric structure directly beneath the array have a significant impact on the signals; and (c) the hydrophone/cable responses differ significantly across the array. If the

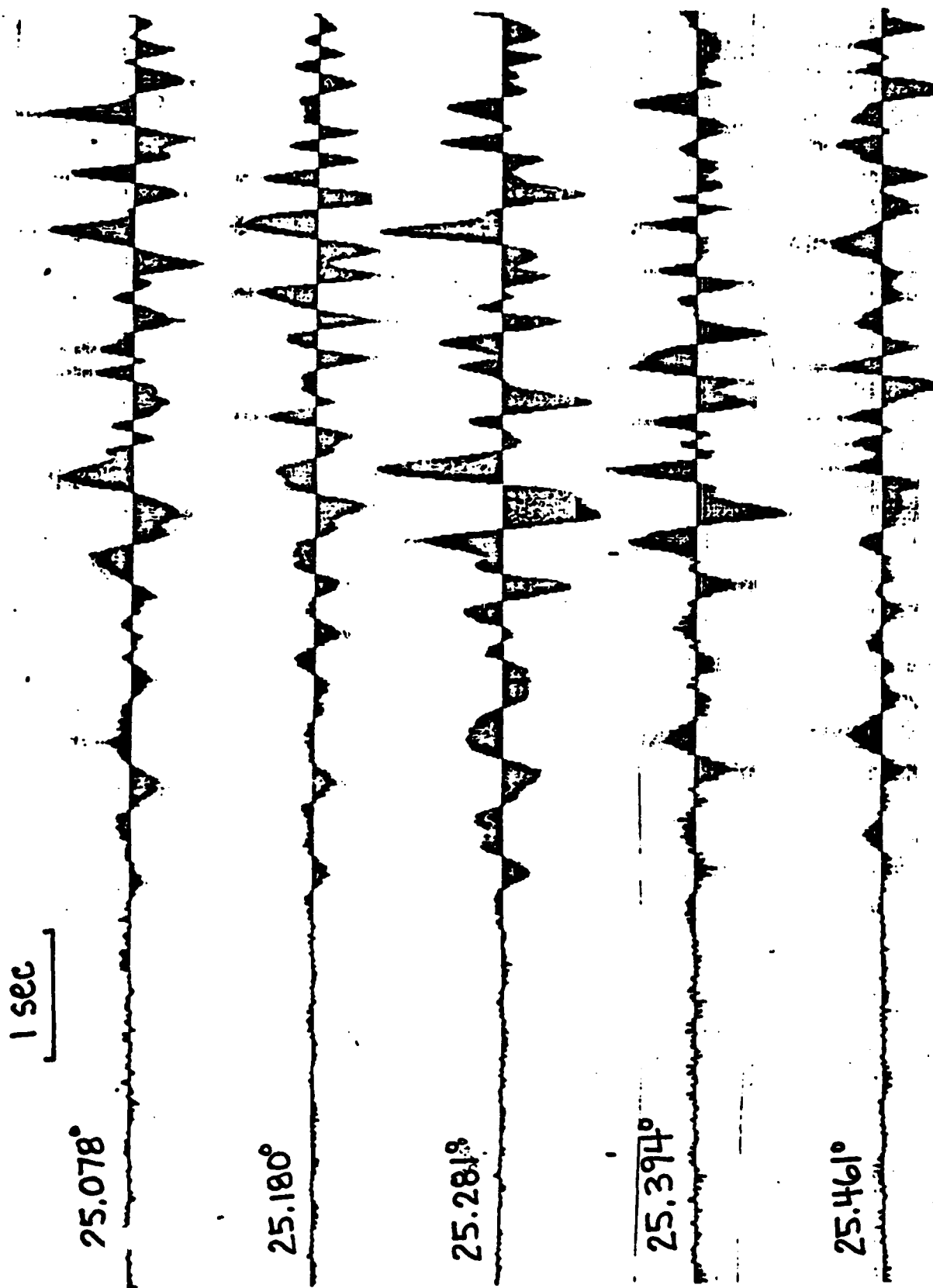


Figure 3. Unfiltered first arrivals of P across the Wake bottom hydrophones from an earthquake south of Honshu, Japan (6 Sept. 1981,  $h=167$  km,  $m=6.6$ ). Traces have been offset by travel time differences.



explanation is (a) then little, if any, improvement in coherence can be expected by massaging the data. If the explanation is (b) then significant improvements in coherence are possible, provided the lithospheric response does not vary greatly with small changes in azimuth or angle of incidence of incoming P arrivals. If the explanation is (c) then an even more significant improvement in coherence is possible. The technique which will be used to investigate (b) and (c) is basically a calculation of amplitude and phase differences between hydrophones for a given signal as a function of frequency. If (c) is true, then these differences should be consistent regardless of what kind of signal is being recorded - P, Po, So, T, or noise. If (b) is true, then the differences should be consistent for P and possibly Po and/or So. If both (b) and (c) are true, the effects should be separable. These effects may then be removed by a deconvolution of the observed signals with the empirically determined impulse responses of the lithosphere and hydrophone/cable. Determination of these responses to a level of statistical significance will require the recording and analysis of a variety of signals at assorted azimuths and epicentral distances which have strong S/N. Evidence exists to suggest that at least (c) is true.

Figure 4 shows amplitude differences observed across WBHA for a 10 minute section of record which includes a P, Po, and So signal. The upper curve is the absolute value of the maximum difference in amplitude observed between the six hydrophone signals as a function of frequency. Energy below about 0.5 Hz is from microseisms while between 0.5 Hz and 20 Hz it is mostly an average of the P, Po, and So. The lower curve shows amplitude differences between two particular hydrophones. Although it may seem unusual to have combined energy from all of these different types of signals, the individual signals, P, Po, So, and noise, exhibit the same

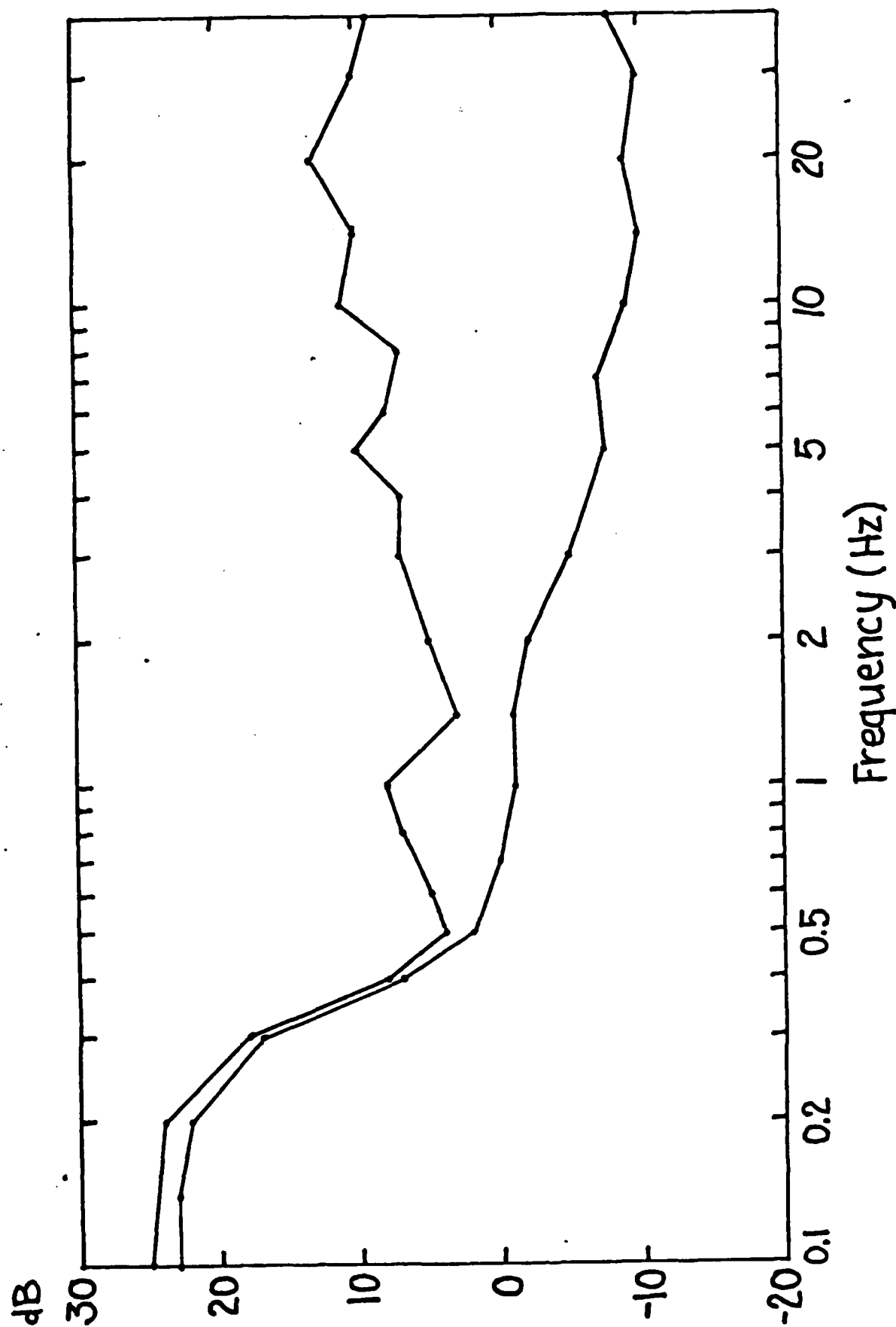


Figure 4. Plot of differences between spectra across the Wake bottom hydrophone array for a 10 minute section of record containing P, Po and So signal and noise. The upper curve shows the maximum value of variation in level between all of the hydrophones. The lower curve shows the difference in level between two of the hydrophones.

relationships although with a somewhat greater scatter. This strongly suggests that there are at least differences in the hydrophone/cable responses which are removable. These differences might easily produce the incoherencies seen in Figure 3. Further and more careful analysis of other events will necessary to precisely determine the differences in amplitude and especially phase. The reward may be stronger coherency and thus an increase in S/N.

Conclusions. The data presented in this report indicate that WBHA, the OSS, and, by inference, the MSS, are seismic tools of comparable quality. Noise levels measured were similar for all three although the data were somewhat limited. S/N ratios measured for OSS were greater than that for individual WBHA hydrophones by an average of about 7 dB. Gains in S/N levels, through stacking of the WBHA signals, will reduce, if not eliminate or reverse, that difference. Precise estimation of the coherence across WBHA will not be made until recently discovered differences in the hydrophone/cable responses have been more accurately determined so that their effects may be removed from the signals.

Many of the comparisons in this report were made via rather indirect routes due to the limited amount of data. Additional data should become available sometime this summer after the OSS recording package has been picked up and the data returned, reduced, and distributed. More data from the August 1981 Wake OBS Experiment will be in a reduced form soon. Also, data from OBS's deployed during the OSS experiment by Oregon State University should be available later this year. All of these future data should be examined and added or compared to those data presented here to

further understand these results.

Acknowledgements. This preliminary and informal report was sponsored by the Air Force Office of Scientific Research, with supplementary funds provided by the U.S. Arms Control and Disarmament Agency. Major upgrading of the Wake system in September of 1982, just prior to the Downhole Experiment, was made possible through the timely support of those agencies.

APPENDIX V

**Po/So Phases: Propagation Velocity and Attenuation  
Across a 1600 Km Long Deep Ocean Hydrophone Array**

by

**Daniel A. Walker and Charles S. McCreery**

both at

**Hawaii Institute of Geophysics  
2525 Correa Road  
Honolulu, Hawaii 96822**

**Abstract.** Po/So phases from numerous earthquakes along the margin of the Northwestern Pacific Basin were successfully recorded by a linear, 1500 km ocean bottom hydrophone (OBH) array deployed for two months near Wake Island. Data from ten shallow-focus ( $<100$  km) events at  $18^\circ$  (2000 km) to  $33^\circ$  (3700 km) epicentral distance were used to compute propagation velocities for Po and So. The resulting travel-time equations  $T=X/(7.96 \pm 0.05 \text{ km/sec}) - (7.14 \pm 2.38 \text{ sec})$  and  $T=X/(4.57 \pm 0.04 \text{ km/sec}) - (14.03 \pm 5.31 \text{ sec})$  for Po and So, respectively, successfully model all Northwestern Pacific Basin shallow-focus Po/So first arrival data collected by the Hawaii Institute of Geophysics since 1963 at epicentral distances greater than  $12^\circ$ . Also, arrivals from an event in the Kuril Islands ( $m_b = 6.6$ ,  $h = 45$  km), which propagated down the axis of the array, were used to estimate the attenuation of Po and So between  $25^\circ$  (2800 km) and  $33^\circ$  (3700 km) epicentral distance. After a correction for cylindrical spreading, values for a frequency dependent  $Q$  are found to range from  $625 \pm 469$  at 2 Hz to  $2106 \pm 473$  at 13 Hz for Po and from  $1401 \pm 296$  at 5 Hz to  $3953 \pm 863$  at 15 Hz for So. These same data may be alternatively described as exhibiting an average attenuation of  $-21.5 \pm 0.9$  dB per 1000 km of travel path, which applies to both Po and So at all frequencies studied.

## Introduction

Late in the summer of 1981, the Hawaii Institute of Geophysics (HIG) successfully deployed a 1500 km long linear array of twelve ocean bottom hydrophones (OBH's) near Wake Island (Fig. 1). Half of the instruments (indicated by open circles) started recording on 12 August and ended on 23 September. The remaining half started on 3 September and ended on 15 October. The total recording time was about 65 days, with all twelve instruments in operation from 3 September through 23 September. Of the twelve OBH's deployed, ten were successfully recovered, and nine of these had quality data throughout their operational period. Recorded concurrently were three bottom hydrophones of the Wake Hydrophone Array (WHA), a 40 km array of sensors located near, and cabled directly to, Wake Island. WHA data were used in the study of first arrivals, and were considered to be part of the OBH array data. All of the OBH and WHA instruments were in ocean depths between 5265 m and 5657 m. Of more than 130 events identified from seismic phases in the recordings, 108 were located by the National Earthquake Information Service (NEIS; Table 1 and Fig. 1). The primary purpose of the experiment was to acquire data of critical importance in understanding a phenomenon known as high-frequency Pn/Sn, long-range Pn/Sn, or Ph.f./Sh.f.; but referred to here as Po/So or Ocean P/Ocean S after Walker (1982).

Po/So phases were first observed in the North Atlantic and have been found throughout the North, Western, and Central Pacific. First arriving Po/So energy travels with a fairly constant apparent velocity (epicentral distance/travel time) of about 8.0 and 4.6 km/sec, respectively, while peak amplitude arrivals have apparent velocities of about 7.6 and 4.5 km/sec, respectively, which are comparable to basal crustal rates. At distances of about  $18^\circ$  ( $\approx 2000$  km), observed frequencies of Po/So are as high as 30 and 35 Hz, respectively; and at distances of about  $30^\circ$  ( $\approx 3300$  km), as high as 15 and 20 Hz, respectively. The signal/noise ratios for Po/So phases are generally at least ten times greater than the ratios of their respective normal, mantle-refracted P and S phases; and in many instances no P's or S's can be found in spite of the presence of very strong Po's and So's. Aside from the SOFAR channel of the world's oceans, the Po/So waveguide appears to be the earth's most efficient acoustical waveguide. Also, it seems probable that the phenomenon is a dominant feature of all of the world's oceans and marginal seas.

Recent efforts have been made, using synthetics, to determine the mechanism of Po/So propagation (e.g., Stephens and Isacks, 1977; Menke and Richards, 1980; Sutton and Harvey, 1981; and Gettrust and Frazer, 1981), although many essential characteristics of these phases are still poorly known. Data collected before this experiment, composed almost entirely of events recorded at single stations and over an unevenly distributed range of epicentral distances, made difficult the precise determination of the travel-time curve between  $0^\circ$  and  $40^\circ$ , as well as the attenuation of these phases as a function of frequency and distance. These parameters need to be accurately determined so that a unique model can eventually be found.

To exemplify this point consider Fig. 2: a plot of apparent velocity versus epicentral distance for Po and So having Northwestern Pacific travel paths and source focal depths of 100 km or less which is based on data collected and published (Walker, 1981) by HIG before this experiment. Two



Table 1. Events Recorded by the OBH Array  
(Data from NEIS Monthly Lists)

No.	Date	Time	Location	h	m	M	n	Po	So
1	Aug.	12	22:35	Solomon Is.	33	4.9	-	3	-
2		13	02:57	Tonga Is.	191	5.4	-	3	-
3		14	05:42	Volcano Is.	33	4.7	-	3	-
4		14	06:24	Molucca Passage	38	5.5	5.3	1	-
5		14	09:05	Honshu, Japan	58	-	-	2	-
6		15	10:30	Alaska	53	5.1	-	2	-
7		15	19:53	Philippine Is.	152	4.8	-	1	-
8		16	23:54	Kuril Is.	33	5.6	5.0	3	-
9		17	02:17	West Irian	34	5.7	5.8	3	-
10		17	17:07	Fiji Is.	383	5.5	-	2	-
11		18	05:29	Banda Sea	34	5.1	4.8	1	-
12		19	01:41	Kermadec Is.	185	5.1	-	1	-
13		19	03:01	Fiji Is.	507	4.8	-	1	-
14		19	06:06	Loyalty Is.	25	5.6	4.9	1	-
15		20	02:19	Santa Cruz Is.	71	5.0	-	3	-
16		20	12:53	Mariana Is.	193	3.8	-	4	-
17		20	15:10	Kermadec Is.	347	4.9	-	1	-
18		21	14:29	Bonin Is.	509	4.6	-	1	-
19		23	01:59	Loyalty Is.	100	5.8	-	1	-
20		23	12:00	Kuril Is.	40	6.0	5.8	4	3
21		24	15:46	Aleutian Is.	56	5.2	-	2	-
22		25	06:56	Honshu, Japan	325	4.8	-	4	-
23		25	07:16	Tonga Is.	33	5.9	5.7	1	-
24		25	07:22	Tonga Is.	33	5.7	-	1	-
25		25	20:07	Mariana Is.	33	4.9	4.4	1	-
26		26	04:51	Mariana Is.	40	5.2	5.1	5	-
27		26	16:32	New Britain	74	5.7	-	6	-
28		26	18:56	Honshu, Japan	230	4.4	-	3	-
29		28	09:04	Alaska	71	5.1	-	3	-
30		30	11:36	Fiji Is.	609	5.4	-	6	-
31		31	06:14	Komandorsky Is.	33	4.7	3.8	1	-
32	Sept.	1	07:23	Tonga Is.	33	5.8	5.7	4	-
33		1	09:29	Samoa Is.	25	7.0	7.7	6	-
34		1	18:38	Tonga Is.	33	5.7	5.3	3	-
35		1	23:55	Tonga Is.	33	5.6	5.4	3	-
36		2	08:44	Samoa Is.	33	5.3	5.5	1	-

Legend: h - event depth (km); m - body-wave magnitude; M - surface-wave magnitude; n - number of instruments in array which recorded body-wave phases P, Po, or So from this event; Po - number of Po arrivals from this event used in first-arrival study; So - number of So arrivals from this event used in first-arrival study.

No.	Date	Time	Location	h	m	M	n	Po	So
37	Sept. 2	09:24	Honshu, Japan	58	5.5	-	2	-	-
38	3	03:59	Hokkaido, Japan	52	4.7	-	4	-	-
39	3	04:29	Philippine Is.	93	5.8	-	4	-	-
40	3	05:35	Kuril Is.	45	6.6	6.6	10	6	8
41	3	19:39	Honshu, Japan	44	5.6	5.4	4	-	-
42	3	19:44	New Guinea	136	4.8	-	5	-	-
43	4	11:15	Philippine Is.	645	6.0	-	10	-	-
44	4	23:44	Solomon Is.	38	5.4	5.3	9	-	-
45	6	11:02	Loyalty Is.	31	5.9	6.2	1	-	-
46	7	15:11	Fiji Is.	231	5.2	-	3	-	-
47	7	16:20	Honshu, Japan	440	4.9	-	3	-	-
48	7	19:06	Honshu, Japan	33	5.8	5.5	7	6	5
49	7	20:07	Honshu, Japan	29	5.1	4.7	7	5	4
50	8	19:26	Kuril Is.	46	5.7	5.4	5	-	3
51	10	03:29	Solomon Is.	110	4.9	-	3	-	-
52	10	23:21	Mariana Is.	13	5.6	5.2	10	5	-
53	11	08:33	Fiji Is.	554	5.2	-	5	-	-
54	12	03:40	Fiji Is.	302	5.2	-	3	-	-
55	12	07:15	Kashmir	33	6.2	5.9	3	-	-
56	12	14:51	Hokkaido, Japan	111	4.9	-	7	-	-
57	12	16:14	Bonin Is.	33	4.6	-	2	-	-
58	13	01:20	Honshu, Japan	39	4.8	4.8	4	-	-
59	13	02:17	Eastern Kazakh	0	6.0	4.5	4	-	-
60	13	20:24	Honshu, Japan	87	4.9	-	3	-	-
61	14	15:08	Honshu, Japan	33	5.4	5.0	4	4	-
62	15	14:12	Banda Sea	102	5.9	-	2	-	-
63	15	20:43	Taiwan	167	4.9	-	3	-	-
64	17	06:19	Banda Sea	33	5.7	5.8	1	-	-
65	17	08:23	Loyalty Is.	30	5.7	6.6	2	-	-
66	17	12:42	Fiji Is.	356	5.2	-	10	-	-
67	17	21:12	Kamchatka	33	4.9	3.9	2	-	-
68	19	07:27	China	561	4.4	-	3	-	-
69	20	04:39	Honshu, Japan	33	4.4	-	2	-	-
70	22	06:55	Mariana Is.	33	4.2	-	6	-	-
71	24	17:20	Bonin Is.	33	5.7	5.3	5	3	2
72	25	03:25	New Guinea	116	4.8	-	1	-	-
73	25	10:21	Bonin Is.	33	4.4	-	2	-	-
74	25	14:30	Kermadec Is.	45	5.9	5.9	5	-	-
75	25	15:01	Honshu, Japan	25	5.5	6.1	2	-	-
76	28	03:36	Honshu, Japan	31	5.5	5.3	5	-	-
77	28	17:56	Kermadec Is.	323	6.0	-	5	-	-
78	29	23:02	Tonga Is.	226	5.1	-	5	-	-

Legend: h - event depth (km); m - body-wave magnitude; M - surface-wave magnitude; n - number of instruments in array which recorded body-wave phases P, Po, or So from this event; Po - number of Po arrivals from this event used in first-arrival study; So - number of So arrivals from this event used in first-arrival study.

No.	Date	Time	Location	h	m	M	n	Po	So
79	Sept. 30	07:04	New Guinea	123	5.4	-	4	-	-
80	30	23:03	Pacific Ocean	10	5.9	5.2	2	-	-
81	30	23:37	Hokkaido, Japan	52	4.9	4.9	2	-	-
82	Oct. 1	12:14	Novaya Zemlya	0	5.9	3.8	4	-	-
83	1	13:10	New Ireland	85	5.0	-	2	-	-
84	1	16:02	Kermadec Is.	33	5.6	5.1	5	-	-
85	1	17:04	Kuril Is.	33	5.9	5.7	5	4	4
86	1	19:00	S. Nevada	0	4.9	-	2	-	-
87	2	05:51	Savu Sea	109	4.6	-	4	-	-
88	2	15:13	Mariana Is.	113	5.0	-	5	-	-
89	3	07:21	Kuril Is.	75	5.1	-	4	-	-
90	3	08:26	Hokkaido, Japan	62	4.4	-	2	-	-
91	3	16:48	Philippine Is.	238	5.0	-	2	-	-
92	4	00:01	New Guinea	33	5.9	6.3	4	-	-
93	4	04:11	Honshu, Japan	38	5.2	5.0	4	-	2
94	4	10:18	Solomon Is.	58	5.1	-	2	-	-
95	4	10:27	Solomon Is.	24	5.7	5.4	5	-	-
96	5	04:28	China	534	4.7	-	2	-	-
97	6	07:40	Aleutian Is.	23	5.2	4.3	3	-	-
98	7	03:02	Fiji Is.	620	5.8	-	5	-	-
99	7	08:32	Solomon Is.	41	5.8	5.3	5	-	-
100	7	15:03	Samoa Is.	33	4.8	-	2	-	-
101	7	17:48	Philippine Is.	595	5.3	-	4	-	-
102	9	12:19	Solomon Is.	50	6.0	6.4	5	-	-
103	9	19:46	Mariana Is.	96	4.7	-	5	-	-
104	11	00:36	Minahassa Pen.	94	5.6	-	4	-	-
105	13	15:53	Kamchatka	112	5.3	-	3	-	-
106	14	12:29	Mariana Is.	205	5.0	-	5	-	-
107	14	20:09	Mariana Is.	131	4.9	-	5	-	-
108	15	01:47	Honshu, Japan	47	6.0	5.4	5	-	-

Legend: h - event depth (km); m - body-wave magnitude; M - surface-wave magnitude; n - number of instruments in array which recorded body-wave phases P, Po, or So from this event; Po - number of Po arrivals from this event used in first-arrival study; So - number of So arrivals from this event used in first-arrival study.

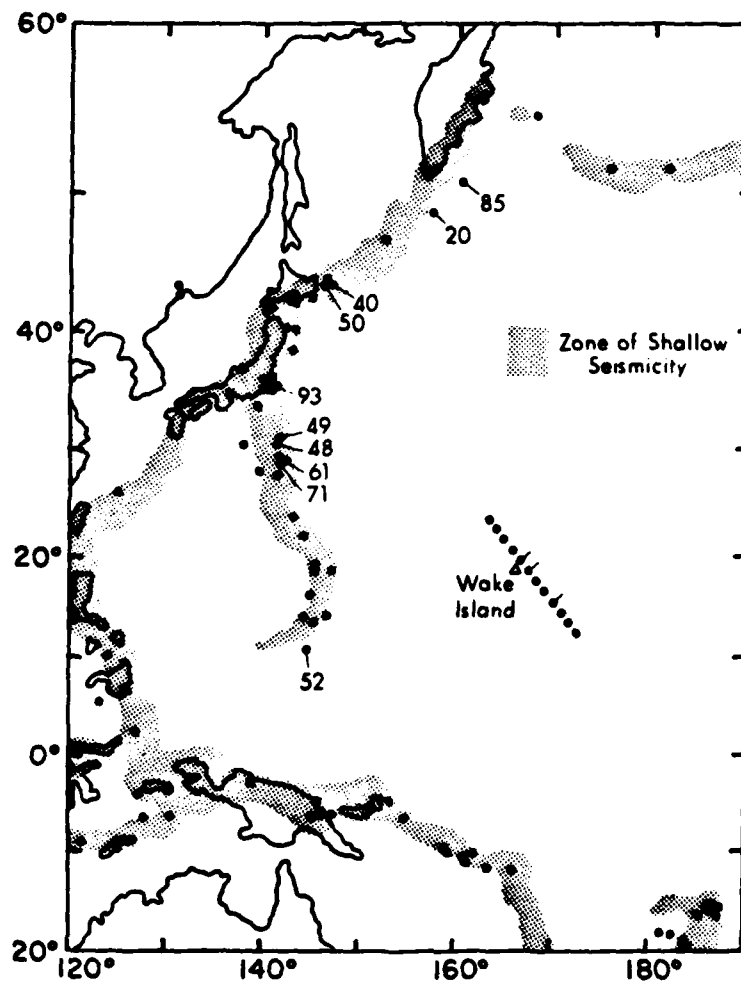


Figure 1. Map showing OBH locations and epicenters of earthquakes recorded by the array (see Table 1). Instruments operating from 12 August through 23 September are indicated by open circles. Those operating from 3 September through 15 October are indicated by closed circles. Three instruments which did not work properly are flagged. Event numbers (from Table 1) are indicated for epicenters of events specifically used in this study.

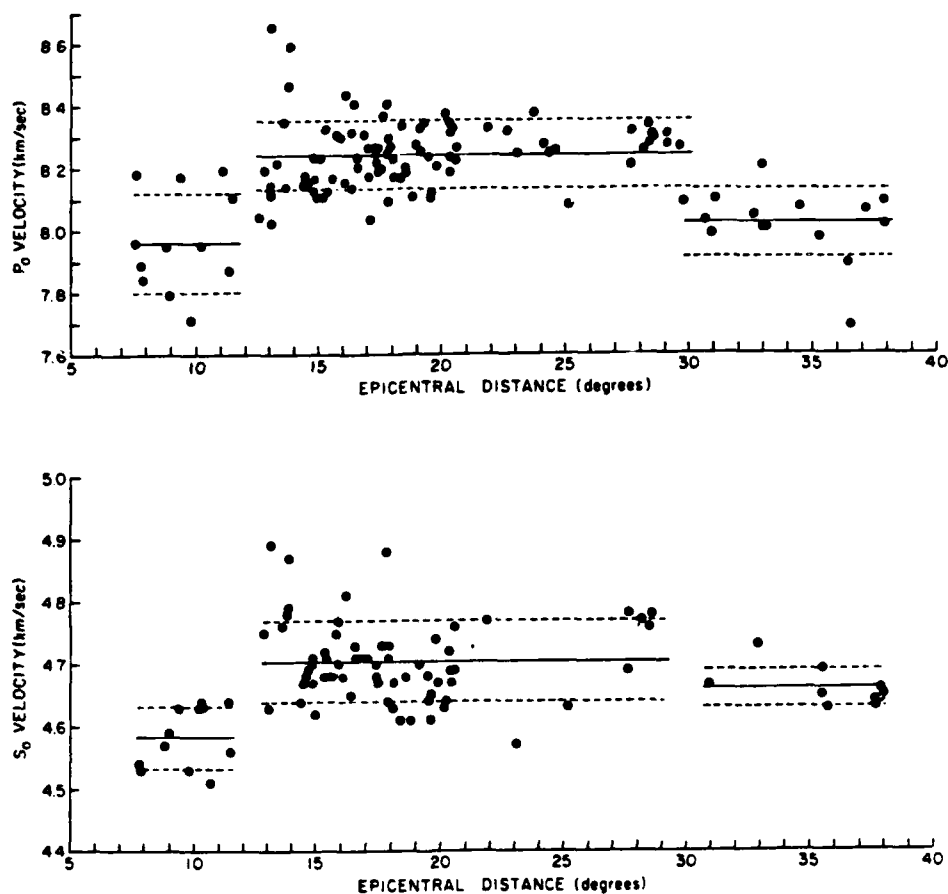


Figure 2. Apparent velocity ( $X/T$ ) versus epicentral distance ( $X$ ) for  $P_0$  and  $S_0$  with Northwestern Pacific travel paths and focal depths of 100 km or less. Note the discontinuities at  $12^\circ$  and  $30^\circ$ . Solid and dashed lines represent the mean apparent velocity plus and minus one standard deviation over the three distance ranges. This plot is based on data compiled before the OBH experiment.

significant features of this plot are the lower apparent velocity values at distances less than  $12^\circ$  and greater than  $30^\circ$  in comparison to values within the  $12^\circ$  to  $30^\circ$  range. The large amount of scatter coupled with insufficient sampling near  $12^\circ$  and  $30^\circ$ , however, make the exact nature of these velocity transitions unknown. For the purpose of modeling, it is important to know if these transitions are smooth or abrupt, and might therefore represent a gradual increase in velocity with depth or a discontinuity in velocity at some depth.

Similar difficulties arise when attempting to use older data to estimate the attenuation of Po/So energy as a function of travel-time (or distance). The high frequencies and large signal/noise ratios observed would indicate that their attenuation must be significantly smaller than that of normal, mantle-refracted P or S phases at similar distances. However, these observations might also be due in part to a frequency-dependent Q combined with low noise levels at the higher frequencies ( $> 4$  Hz) where Po/So are most prominent. Unfortunately, the mix of data (i.e., different earthquakes recorded at only single stations) make it hard to separate attenuation from other factors which influence the observed amplitudes such as magnitude, focal depth, epicentral distance, source orientation, and possibly azimuth.

To help clarify these uncertainties, an experiment was designed to record Po/So across a linear, 1500 km array consisting of 12 OBH's. The data provided by such an experiment would permit determination of Po and So phase velocities independent of the source parameters, thus hopefully eliminating the major source of scatter in velocity estimates. Data from the experiment would also facilitate a nearly direct measure of attenuation as a function of frequency and travel-time (only a spreading term would have to be assumed in order to determine the apparent Q). In addition, any other changes in the Po/So coda would for the first time be observed at several distances along approximately the same azimuth.

The array was aimed towards northern Japan and the southern-most islands of the Kuril chain (Fig. 1), and was positioned to provide data across the  $30^\circ$  transition zone previously described. This target was chosen because of its long history of moderate-to-large earthquakes and several successful recordings of Po/So phases from this region on the hydrophone installation at Wake Island. Of the events recorded by the OBH array in the Marianas through Kuril portion of the circum-Pacific arc, the largest (a 6.6 mb; event 40 in Table 1) occurred in the target area while all of the instruments were recording.

#### Po/So Propagation and Apparent Velocity

To confirm the assumption that much of the scatter in Fig. 2 can be attributed to errors in the epicenters and/or origin times of these single station data points (i.e., no more than one station recorded any given earthquake), a similar plot has been constructed for some of the OBH data (Fig. 3). Although this data as a whole exhibits scatter of about the same magnitude as that shown in Fig. 2, there is significantly less scatter within each subset of data representing individual events at several OBH's. Thus, the larger source of scatter may be attributed to apparent velocity differences between events; and a strong possibility is that these

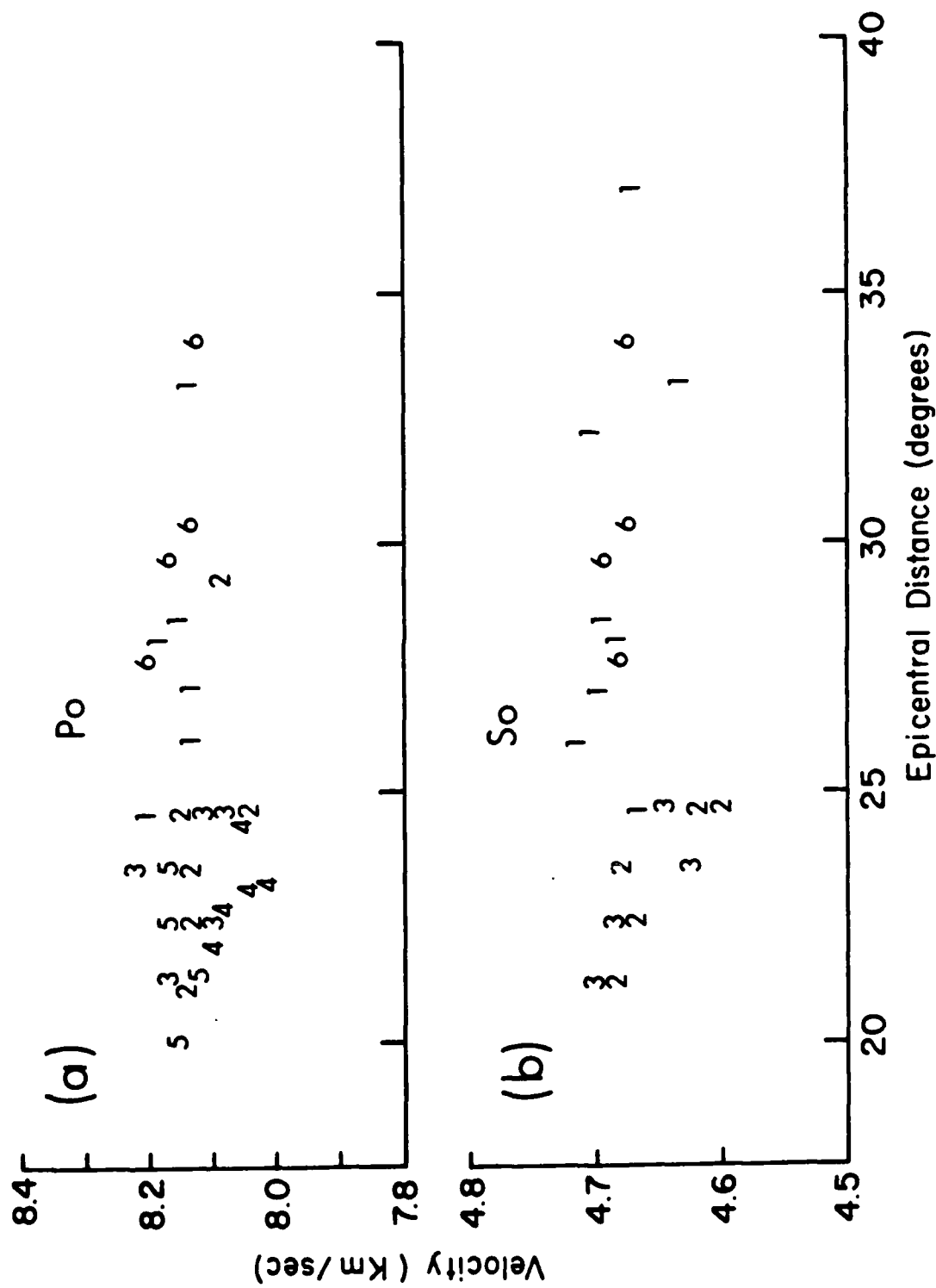


Figure 3. Apparent velocity (X/T) versus epicentral distance (X) for some of the Po and So data collected during the OBH experiment. Data points numbered 1 through 6 represent each set of first arrivals recorded across the OBH array from events 40, 48, 49, 52, 61, and 85, respectively. Note that the scatter of each subset is less than the scatter of the combined data.

differences are a result of errors in NEIS origin times and hypocenter locations. The remaining scatter within each subset may be the result of: (1) uncertainty in the time of onset, (2) OBH location errors, (3) OBH clock correction errors, and/or (4) local differences in crustal and sediment structure between OBH's. Unfortunately, the magnitude of this remaining scatter is enough to cause an unacceptable level of uncertainty in the propagation velocity of Po or So for any given event. An uncertainty of 1 sec in travel-time over 500 km of the array at a phase velocity of 8.0 km/sec will produce an uncertainty of 0.13 km/sec in the determination of that phase velocity, as well as an uncertainty of 5.0 sec in the travel-time intercept for data taken at an average epicentral distance of 2500 km. To reduce this uncertainty, a method was sought to determine propagation velocity and travel-time intercept by combining the first arrival data of all the events in a way which would have the following important properties: (1) propagation velocity would be determined from the differences in travel time between OBH's for a given event and would be independent of the NEIS origin time published for the event; (2) events recorded on more instruments would be weighted more heavily; (3) events recorded over a larger range of epicentral distance would also be weighted more heavily; and (4) the travel-time - epicentral distance relationships within the data set of each individual event would be maintained. The following method satisfactorily meets those requirements.

Using only those events with focal depths of 100 km or less, having Northwestern Pacific Basin travel paths, and recorded with distinct onsets at two or more stations (see Table 1), the raw epicentral distance and travel time data were computed using NEIS epicenters. For each subset of data associated with a single event, the mean epicentral distance and travel time was computed and subtracted from the raw data for that event to yield zero-measured data for each event, as well as for the data as a whole. From these combined data the slope of the travel-time line could be computed, but the intercept would be lost (it would be exactly zero). Consequently, the mean for all of the raw epicentral distance and travel-time data was computed and added to each point of the zero-measured data set to restore the intercept. The travel-time lines computed from these data, and shown in Fig. 4, represent the best available estimates of Po/So velocities at distances between about 2400 and 3400 km. These values (i.e., inverse slopes) are  $7.96 \pm 0.05$  km/sec and  $4.57 \pm 0.04$  km/sec for Po and So, respectively. The large negative intercepts found,  $-7.14 \pm 2.38$  sec and  $-14.03 \pm 5.31$  sec for Po and So respectively, imply that the first arriving energy propagates at a higher velocity than indicated by the inverse slopes over some portion of the travel path nearer to the source than where the observations were made.

In Fig. 5, we have superimposed Po/So data from the Wake OBH experiment (solid triangles) on Fig. 2. It is obvious that these data do not support the discontinuity in apparent velocity at  $30^\circ$  which was a feature of the older data; but they appear, instead, to describe a smooth transition across this boundary. A re-examination of the older data, especially those data points near the offset, was made to determine if the cause of this discrepancy could be found. Consequently, the original computer cards used to calculate epicentral distances for data collected in 1963 and 1964 were found to contain systematic errors in the coordinates of some recording sites. The formerly classified status of these sites and



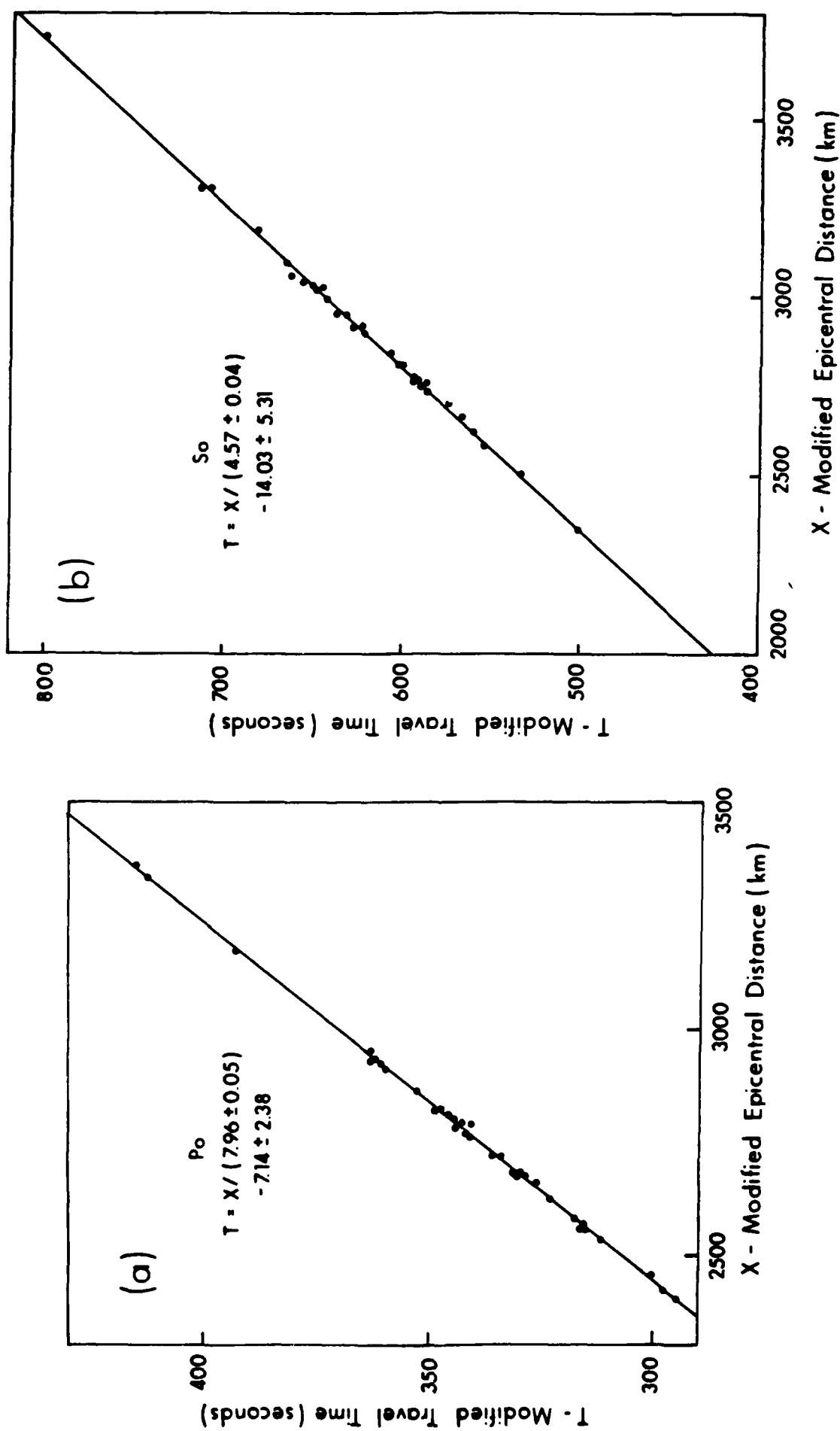


Figure 4. Modified travel-time plots for  $P_o$  and  $S_o$  as described in the text.

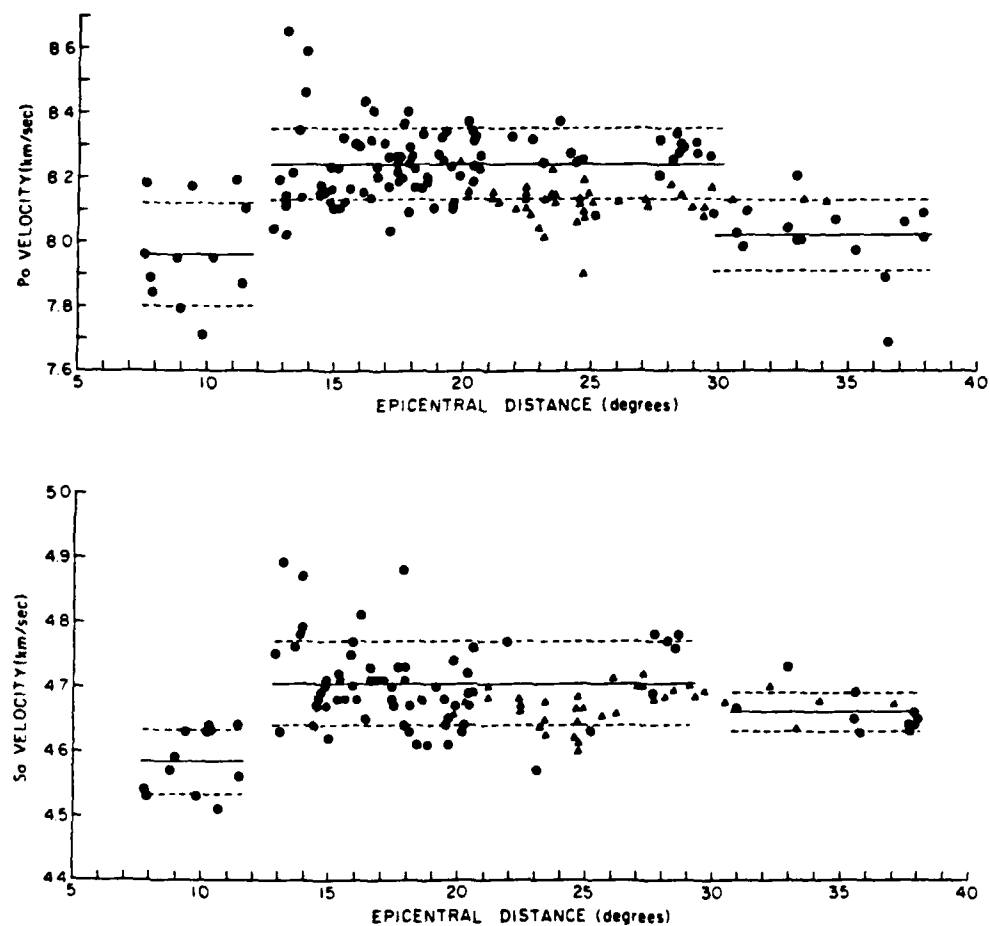


Figure 5.  $P_o$  and  $S_o$  data from the OBH experiment (solid triangles) superimposed on Fig. 2a and Fig. 2b, respectively. Note that these data do not support a discontinuity in apparent velocity at  $30^\circ$ .

the circuitous route by which these coordinates had been previously obtained may be an explanation for these errors. The erroneous data have been plotted as open circles and the corrected data as solid circles (along with the rest of the older data) in Fig. 6. Also plotted in Fig. 6 (as open triangles) are some additional hydrophone data from the analog cassette recording system at Wake, collected since 1978. It is clear from this comprehensive data set that an apparent velocity discontinuity at  $30^\circ$  is no longer supported by the data. Instead, a gradual decrease of apparent velocity with distance is observed between about  $12^\circ$  and  $38^\circ$  for both  $P_o$  and  $S_o$ . This characteristic of apparent velocity is entirely compatible with the inverse slope propagation velocity and intercept values computed from the OBH data and shown in Fig. 4.

To illustrate this compatibility, the travel-time equations have been converted into relationships between apparent velocity and epicentral distance as follows:

$$T = X/V + I$$

Travel-time equation where  $T$  is travel-time,  $X$  is epicentral distance,  $V$  is propagation velocity, and  $I$  is the travel-time intercept.

$$A = X/T = X/(X/V + I)$$

Apparent velocity equation where  $A$  is the apparent velocity.

$$S_A^2 = \frac{(X/V+I)^2 V^4 S_X^2 + X^4 S_V^2 + X^2 V^4 (S_I^2 + S_O^2)}{V^4 (X/V+I)^4}$$

Mean-squared error in

apparent velocity,  $S_A^2$ , resulting from errors in: the propagation velocity,  $S_V$ ; the travel-time intercept,  $S_I$ ; the epicentral distance,  $S_X$ , due to epicenter errors; and the observed travel-time,  $S_O$ , due to errors in origin-time.

Plotted in Fig. 7 are  $A$ , and  $A \pm S_A$  versus epicentral distance,  $X$ . Values for  $V$ ,  $S_V$ ,  $I$ , and  $S_I$  are those given in Fig. 4;  $S_X$  is 10 km; and  $S_O$  is 1 sec. Values used for  $S_X$  and  $S_O$  are reasonable for epicenter/origin-time data taken from the NEIS listings, and these lists have been used for all of the data in the figure. The figure shows that approximately one standard deviation of the data (ie. 68 percent for normally distributed

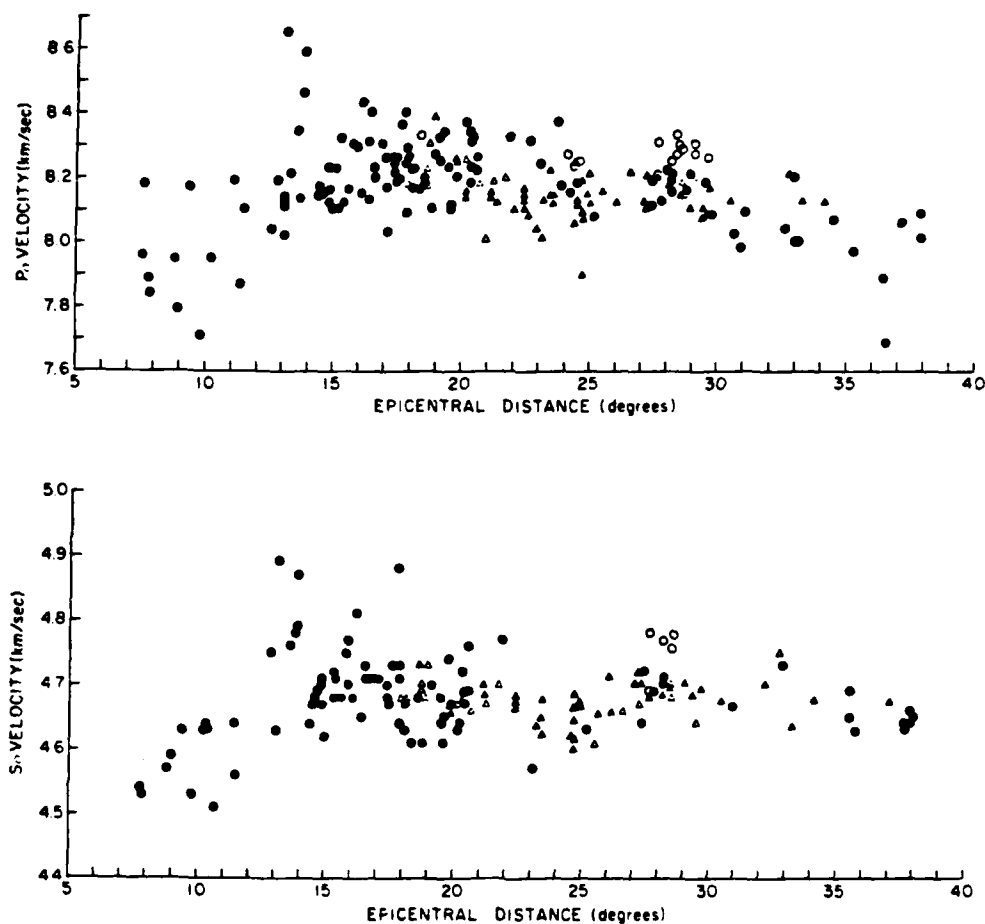


**Figure 6.** This figure is the same as Fig. 5 except that: (1) erroneous data from 1963 and 1964 (open circles) have been replotted as closed circles; and (2) addition hydrophone data from Wake, collected since 1978, are plotted as open triangles.

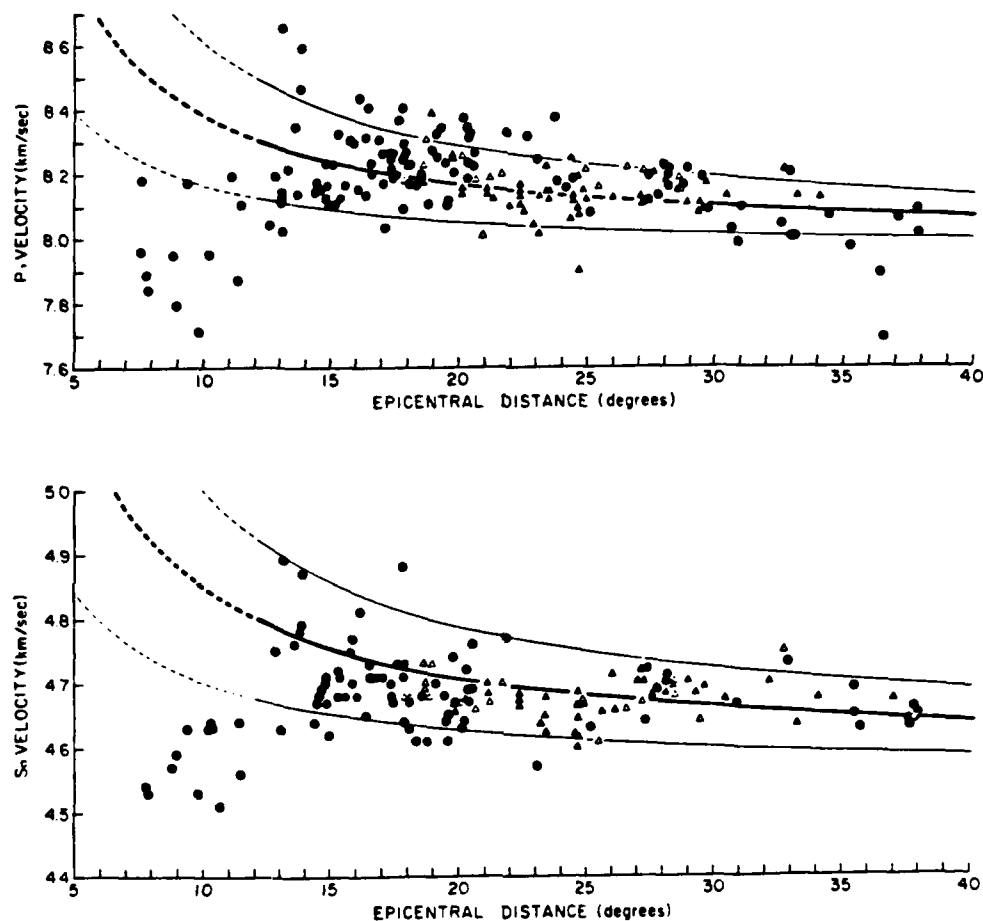


Figure 7. This figure contains the data from Fig. 6. representing all of the Po and So first arrival data from shallow-focus events with Northwestern Pacific Basin travel paths collected by HIG since 1963. Superimposed on these data are curves representing the Po and So travel-time equations (Fig. 4). with plus and minus one standard deviation, determined strictly from the OBH data. Note that most of the data beyond  $12^{\circ}$  epicentral distance falls within the bounds described by these curves.

data) falls within the bounds of  $A S_A$ . It is concluded, therefore, that the first arrival times of Po and So phases from shallow-focus (i.e., focal depths less than 100 km) earthquakes occurring along the margin of the Northwestern Pacific Basin with travel paths greater than  $12^\circ$  epicentral distance across the Northwestern Pacific Basin, may be successfully modeled by the travel-time equations given in Fig. 4.

An important question which remains to be answered is: By what methods of generation and propagation are the first arrivals on both sides of the  $12^\circ$  apparent velocity discontinuity produced? In spite of those modeling efforts mentioned previously, which have successfully reproduced certain aspects of Po/So travel-time and coda, no model as yet exists which addresses this question or reproduces the observations which led to this question. A hypothesis proposed here, which seems to contain some

credibility, is that energy observed at less than  $12^\circ$  has propagated from near the source to near the receiver entirely within the waveguide (i.e., up the descending lithosphere and across the plate), while first-arriving energy observed at greater than  $12^\circ$  has propagated along a higher velocity,

or deeper, P or S type path over distances less than  $12^\circ$  before coupling into the waveguide at a distance greater than  $12^\circ$ . (The term "waveguide" refers here to the structure within which Po/So energy propagates at the constant velocity value given in Fig. 4.) Evidence which supports this hypothesis is: (1) the apparent velocity data observed for Po and So at distances less than  $12^\circ$  could reasonably be fit by a zero-intercept linear travel-time equation with a propagation velocity equal to the propagation

velocity found for the data beyond  $12^\circ$  (This would imply that the propagation velocity and thus the structure of the waveguide are continuous across  $12^\circ$  - an intuitively pleasing result.); and (2) the apparent

velocities for shallow-focus P and S at  $12^\circ$  (from Jeffreys and Bullen, 1958) are near those required for P and S to couple into the Po/So

waveguide and produce the observed arrival times beyond  $12^\circ$ . Although a propagation mechanism of this type might fit the data quite well, a velocity model of the oceanic crust and upper mantle which produces this phenomena has not been found. It is probable that such a velocity model would contain lateral heterogeneities associated with the downgoing slab in order to propagate energy between  $0^\circ$  and  $12^\circ$  with an average velocity greater than the waveguide velocity, and still couple this energy into the waveguide. This requirement is not easy to satisfy (and may be impossible to satisfy) with a radially symmetric velocity model.

One test of this proposed hypothesis could be made by examining Po/So arrivals from earthquakes with depths greater than 100 km. Po/So energy has been observed and recorded by HIG for many earthquakes with focal depths greater than 100 km and up to 600 km. Energy which has propagated along a P or S type path before coupling into the waveguide should contain a depth dependence in travel-time, coda, and/or frequency content. The precise nature of such a dependence would serve to either confirm or deny the hypothesis, or to generate a new one.

## Attenuation of Po and So

As stated earlier, one of the more remarkable features of Po/So is their high-frequency content; therefore, a major goal of Po/So research in recent years has been to quantify those properties within the earth in terms of  $Q$  which permit the efficient transmission of these frequencies over great distances. When a frequency-independent model for  $Q$  was fit to some older Po/So data with frequencies between about 2 and 10 Hz, the resulting  $Q$  values were greater than 5000 in most cases (Walker et al., 1978 and Sutton et al., 1978). These values are much higher than those generally found for upper mantle travel paths using P and S data at frequencies below 2 or 3 Hz. A frequency-dependent  $Q$ , however, might satisfy both sets of observations. Sutton et al. (1983) found two methods for extracting a relationship between  $Q$  and frequency from single-station Po/So data. They found that  $Q$  was approximately proportional to frequency over the range 2-9 Hz and that the  $Q$  of So was higher than the  $Q$  of Po for any given frequency.

Data collected during the OBH experiment provided, for the first time, the opportunity to observe Po/So energy propagating across a large array of instruments. Although Po/So phases from numerous events were recorded, the magnitude 6.6, Kuril Is. event noted earlier (event 40, Table 1) was especially well suited for a study of attenuation. Its large magnitude and its location in the area targeted by the array produced Po/So phases which travelled down the axis of the 1500 km deployment line with sufficient energy to be observed with high signal/noise ratios on many of the instruments.

Fig. 8 shows the spectra of the Po and So coda from the Kuril event at five epicentral distances corresponding to the five OBH's that were used. These spectra have been computed from a series of contiguous 512 point FFT's taken on the time series data which was digitized at 80 samples per sec. The spectral energy has been summed over an apparent velocity window extending from 8.2-7.0 km/sec and from 4.7-4.0 km/sec for Po and So, respectively, and has also been summed over a 1 Hz band at any given frequency. Instrument response has not been removed; however, the response of each individual OBH is presumed to be identical so that intercomparison of the spectra is valid. Only signal levels which were at least 4 dB above background noise levels, at any given frequency, have been plotted. A correction for cylindrical spreading has also been applied to these spectra so that the losses observed in the figure represent attenuation due to anelasticity, scattering, tunneling, and/or any mechanism other than cylindrical spreading. Note that in general the energy level falls off at a constant rate with distance, regardless of frequency. Also note that the attenuation of So with distance is about the same as that for Po.

A general expression for the observed amplitude of seismic signals of this type is:

$$A(f) = A_0(f)r^{-b}e^{-\pi f p q(f)[r-1]}$$

where  $A(f)$  is the observed signal amplitude at a given frequency,

$A_0(f)$  is the source amplitude ( $r=1$ ) at a given frequency,

$f$  is the given frequency,

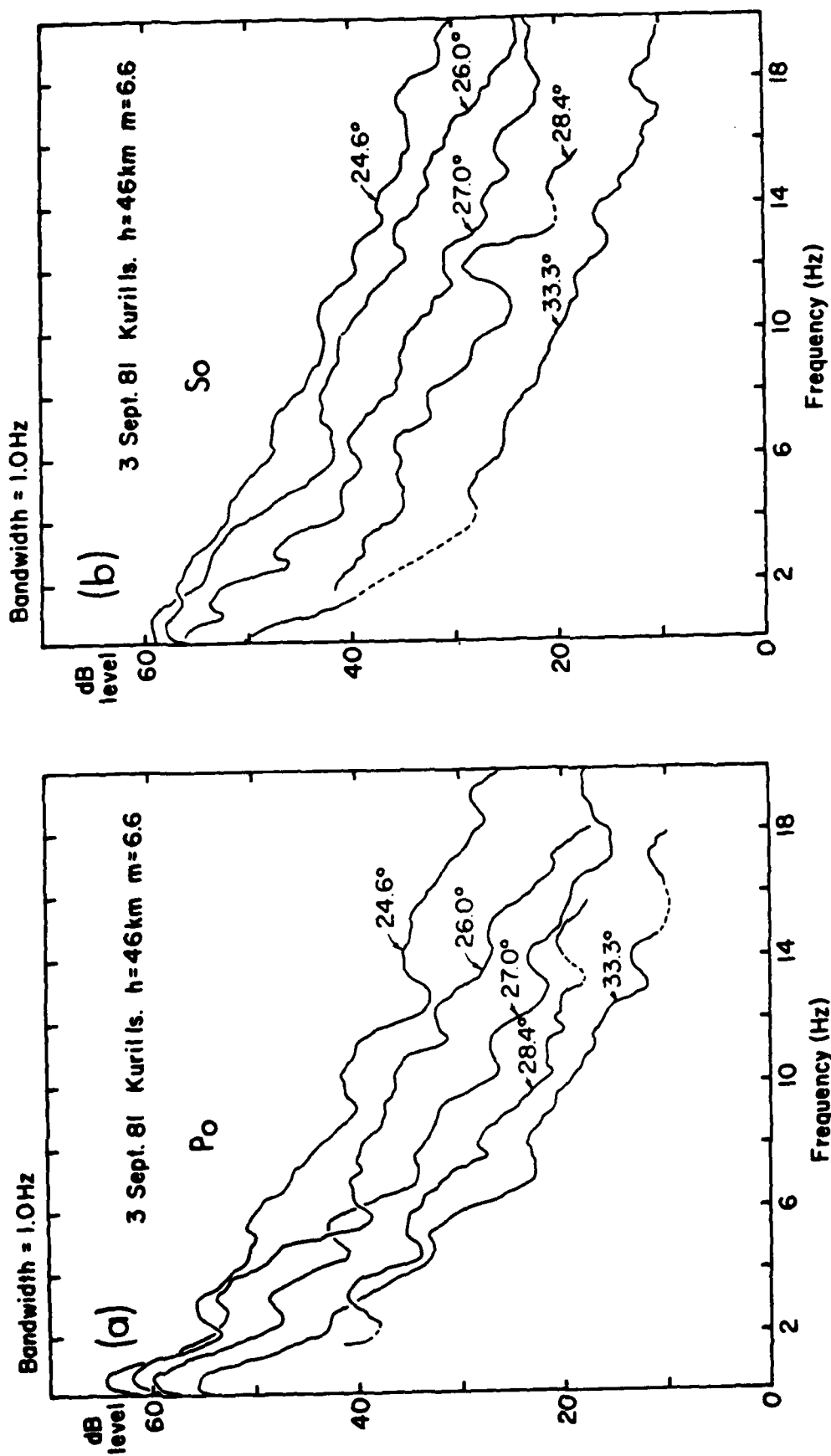


Figure 8. Spectra of Po and So from a large event in the Kuril Is. observed at five epicentral distances corresponding to five OBH's. Spectral energy has been summed over the apparent velocity ranges 8.0 - 7.2 km/sec and 4.7 - 4.0 km/sec for Po and So, respectively. The effect of cylindrical spreading, amounting to only 1.3 dB between 24.6° and 33.3°, has been removed from the data. Only signal levels at least 4 dB above ambient noise levels have been plotted. Dashed portions of the spectra are for continuity only, and do not represent actual data at those frequencies.



$r$  is the epicentral distance,  
 $b$  is the spreading parameter (0.5 for cylindrical spreading;  
 1.0 for spherical spreading),  
 $p$  is slowness (i.e., travel-time/epicentral distance),  
 and  $q(f) = Q(f)^{-1}$  is the apparent anelastic attenuation coefficient.

Conversion of the observed amplitude into decibels gives:

$$20\log_{10}A(f) = 20\log_{10}A_0(f) - 20b\log_{10}(r) - 20\pi fpq(f)[r-1]\log_{10}(e)$$

Rearranging terms and differentiating with respect to  $r$  gives:

$$\frac{d(20\log_{10}A(f) + 20b\log_{10}(r))}{dr} = -20\pi fpq(f)\log_{10}(e)$$

Therefore:

$$Q(f) = q(f)^{-1} = \frac{-20\pi fp\log_{10}(e)}{\frac{d(20\log_{10}(A(f)r^b))}{dr}}$$

Each curve plotted in Fig. 8 represents  $20\log_{10}[A(f)r^{0.5}]$  at a given  $r$  for a range of frequencies. At any given frequency, we know  $20\log_{10}[A(f)r^{0.5}]$

at several  $r$ 's and can thus determine  $\frac{d\{20\log_{10}[A(f)r^{0.5}]\}}{dr}$  by simple linear regression. All other quantities in the equation for  $Q(f)$  are known.  $Q(f)$  has thus been found for data sampled in one Hertz bands, and these values are plotted in Fig. 9. Although cylindrical spreading ( $b = 0.5$ ) has been assumed, the spreading term plays only a minor role in these calculations. A choice of spherical spreading would raise the values of  $Q(f)$  by no more than about 10 percent. Only frequencies where data exist at all five distances have been used. The standard deviations shown include contributions from the error in the determination of  $\frac{d(20\log_{10}[A(f)r^{0.5}])}{dr}$ , the error in slowness which is due to sampling the

data over a range of slownesses, and the error in frequency due to sampling over a 1 Hz band. This method gives values for  $Q(f)$  roughly proportional to frequency, and gives higher values of  $Q(f)$  for  $S_0$  relative to those for  $P_0$  at any given frequency. These results are consistent with those found by Sutton et al. (1983) mentioned earlier, although the absolute levels for  $Q(f)$  are lower at any given frequency in this study. The relationship between the  $Q(f)$  values of  $P_0$  and  $S_0$ ,  $Q_{S_0}(f) \approx 1.4Q_{P_0}(f)$ , is markedly different from the relationship  $t_{S_0}^* = 4t_{P_0}^*$ , which implies  $Q_{S_0}(f) = 0.44Q_{P_0}(f)$ , found by others (see for example Cormier, 1982).

The nature of the  $Q(f)$  values suggests that a simpler mathematical model might be used to describe the attenuation of  $P_0/S_0$ . This is because

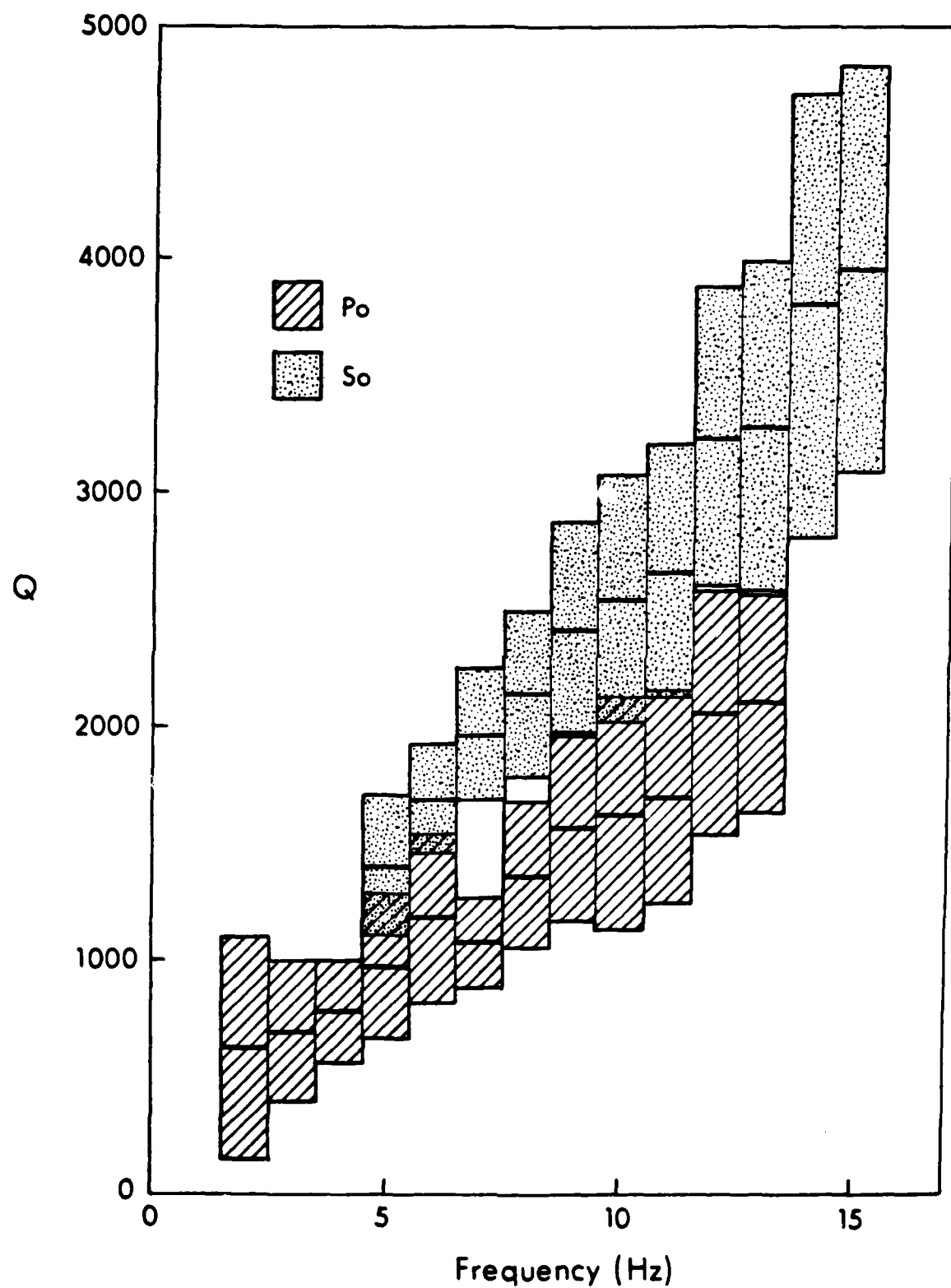


Figure 9. Values for  $Q(f)$  plus and minus one standard deviation as explained in the text are plotted versus frequency for both  $P_o$  and  $S_o$ .

values for  $fpq(f)$  are approximately the same for any given frequency and slowness (ie.,  $P_0$  or  $S_0$ ). Thus, the form of this model is:  $A(f) = A_0(f)r^{-b}e^{-a(r-1)}$ , where "a" is the coefficient of attenuation. In this expression, the change in signal amplitude over some propagation distance is not a function of frequency or slowness as in the previous expression containing "q". By a method similar to that described earlier it can be

shown that:  $-20\log_{10}(e) = \frac{d\{20\log_{10}[A(f)r^{0.5}]\}}{dr}$ , where  $-20\log_{10}(e)$

equals the decibel change in amplitude, after a cylindrical spreading correction, per unit propagation distance. The right-hand side of the above equation may be evaluated by linear regression, using the set of values for  $20\log_{10}[A(f)r^{0.5}]$ , which can be computed from the observed

values for A at a given r (and for a given frequency band), versus r. Values for  $-20\log_{10}(e)$  have been computed and tabulated in Table 2. The

same data set used to determine the  $Q(f)$  values discussed previously has been used to compute values in the table. With the exception of two lower values for  $P_0$  at 2 Hz and 3 Hz and the slightly higher average values for  $P_0$  relative to  $S_0$ , it could be said that the data generally support the assumption that "a" is nearly a constant value for both  $P_0$  and  $S_0$  at any of the frequencies examined.

All of the data can be combined by a zero-meaning method, similar to that described for combining the first arrival data, to yield a single value for  $-20\log_{10}(e)$ . These modified data are shown in Fig. 10, and the regression line fit to them has a slope of  $-21.5 \pm 0.9$  dB per 1000 km of travel path. Also shown are regression lines fit to the subsets of  $P_0$  and  $S_0$  data which have slopes of  $-19.7 \pm 1.4$  and  $-23.6 \pm 1.1$  dB per 1000 km, respectively. Differences between the  $P_0$  and  $S_0$  values reflect those differences observed in Table 2. Note that all of the data lie at five distances corresponding to the five OBH's. Also note that the data points at each distance do not cluster about the central regression line, but tend to cluster about some value away from the line. It is possible that these shifts, amounting to a few dB at most, are due to differences between individual OBH responses. These differences may exist because of complexities in processing the slow-speed cassette tapes, and uncertainties in the absolute calibration of the individual hydrophones. Computation of new regression lines, under the assumption that the data of each OBH contain a constant but unknown bias, and under the condition that the sum of the squares of the biases are minimized, results in exactly the same regression lines shown in the figure with somewhat smaller variances. This result is due to the mathematics, and not to any unique property of the data.

### Conclusions

Data collected by a 1500 km OBH array deployed for two months in the Northwestern Pacific Basin near Wake Island has provided important new information about the propagation of  $P_0/S_0$  phases. Using this array, propagation velocities of first arrivals from shallow-focus (<100 km)

Table 2. Attenuation of Po and So as a Function of Frequency and Propagation Distance

f (Hz)	Attenuation (dB/1000 km)	
	Po	So
2	-11.5 ± 8.4	- -
3	-15.4 ± 6.1	- -
4	-18.5 ± 4.7	- -
5	-18.4 ± 5.6	-22.4 ± 4.3
6	-18.3 ± 5.4	-22.3 ± 2.6
7	-23.4 ± 3.8	-22.3 ± 2.8
8	-21.1 ± 4.6	-23.4 ± 3.4
9	-20.6 ± 5.1	-23.4 ± 4.1
10	-22.1 ± 6.7	-24.7 ± 4.8
11	-23.4 ± 6.0	-25.9 ± 4.9
12	-21.0 ± 5.2	-23.3 ± 4.3
13	-22.2 ± 4.8	-24.8 ± 5.1
14	- -	-23.1 ± 5.2
15	- -	-23.8 ± 5.0

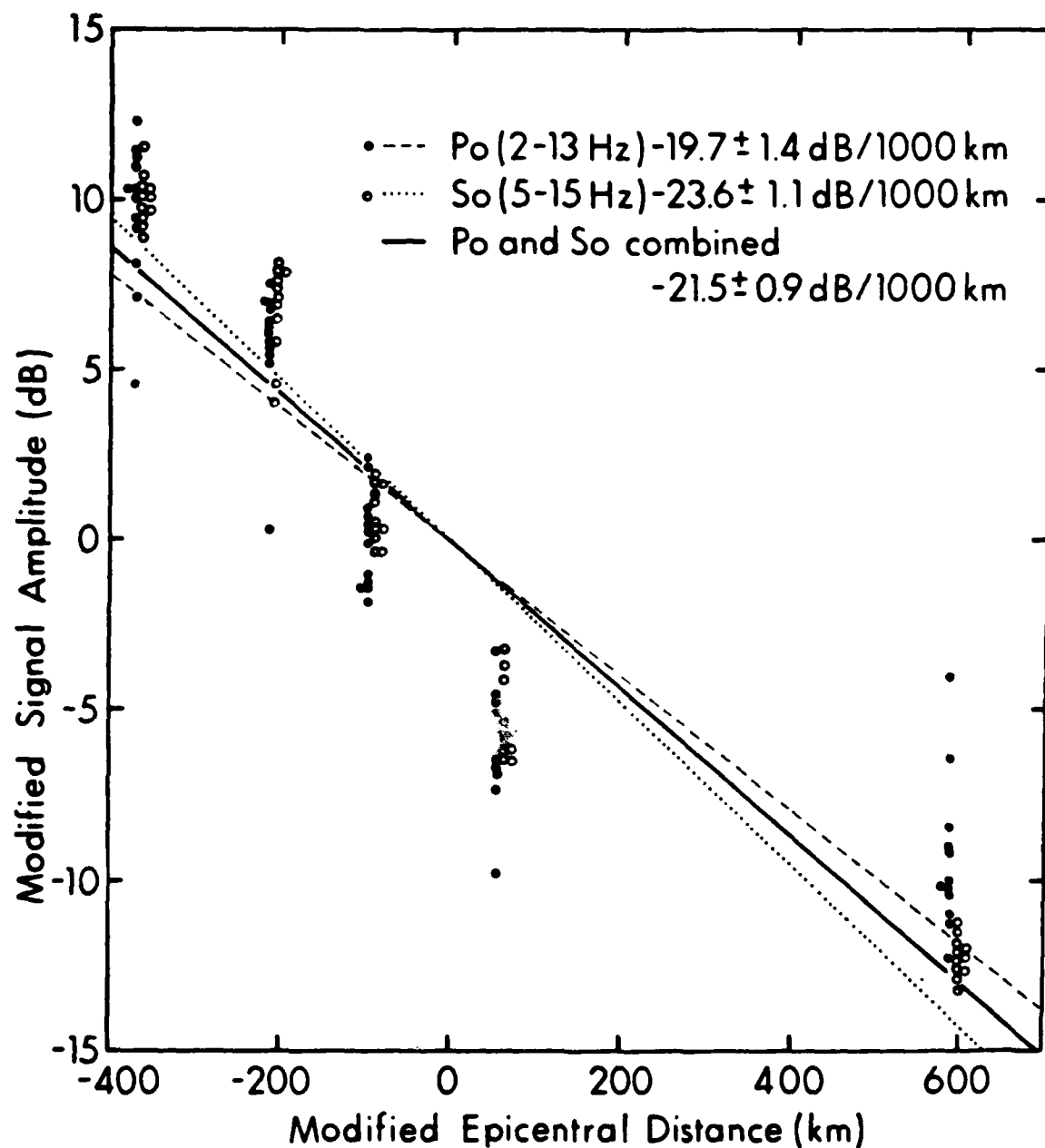


Figure 10. Spectral amplitudes at each frequency studied (Po: 2-13 Hz and So: 5-15 Hz) are plotted versus epicentral distance after modification by zero-meaning as explained in the text. The five data clusters represent the five OBH's used. Note that the data of both Po and So, at all frequencies, follow the same general trend, which is attenuation as a function of distance. For reference, attenuation as a function of distance at each individual frequency in Po and So is listed in Table 2.

events have been measured by a more accurate method than was previously possible using single station data. The velocities found are  $7.96 \pm 0.05$  km/sec and  $4.57 \pm 0.04$  km/sec for Po and So, respectively.

measured at epicentral distances between  $18^\circ$  (2000 km) and  $33^\circ$  (3700 km). Associated with these propagation velocities in the linear travel-time equation are intercepts equal to  $-7.14 \pm 2.38$  sec and  $-14.03 \pm 5.31$  sec for Po and So, respectively. These large negative intercepts imply higher propagation velocities over some part of the travel path nearer to the source than where the data were recorded. Travel times of all Po/So first arrivals collected by HIG since 1963, from shallow-focus events with

Northwestern Pacific Basin travel paths greater than  $12^\circ$  epicentral distance, are successfully modeled by the linear travel-time equation:  $T = X/V + I$ , using those values for V (propagation velocity) and I (travel-time intercept) reported here. Data at epicentral distances less

than  $12^\circ$  (collected prior to this experiment) appear to follow a different Po/So travel-time branch than the one described by the OBH data. The exact nature of this branch is not clear due to deficiencies in the quantity and quality of this data. Additional insight into this transition may be found through the examination of Po/So arrivals from numerous deeper-focus events (up to 600 km focal depth) which have been recorded but not yet studied.

The OBH data have also been used to directly measure the attenuation of Po and So. An event which occurred in the Kuril Islands ( $m_b = 6.6$ ,  $h = 45$  km) and generated Po and So arrivals which propagated almost exactly down the axis of the array, was used to quantify attenuation in terms of a frequency-dependent Q. Values found for  $Q(f)$  range from  $625 \pm 469$  at 2 Hz to  $2106 \pm 473$  at 13 Hz for Po, and from  $1401 \pm 296$  at 5 Hz to  $3953 \pm 863$  at 15 Hz for So. This attenuation may be more simply described in terms of the single value  $-21.5 \pm 0.9$  decibels per 1000 km of travel path, which in general applies to all the frequencies studied in both Po and So.

AD-A137 778

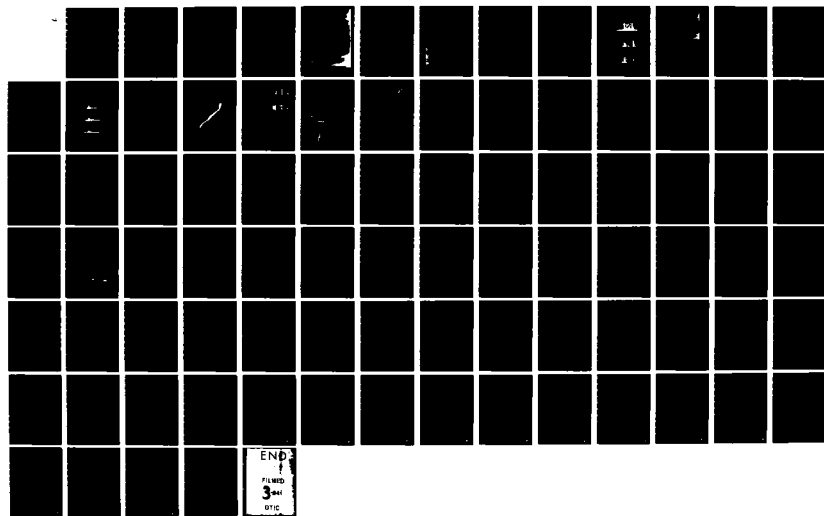
SPECTRAL ANALYSES OF HIGH-FREQUENCY PN SN PHASES FROM  
VERY SHALLOW FOCUS EARTHQUAKES(U) HAWAII INST OF  
GEOPHYSICS HONOLULU D A WALKER SEP 83 AFOSR-TR-84-0059  
F49620-81-C-0065

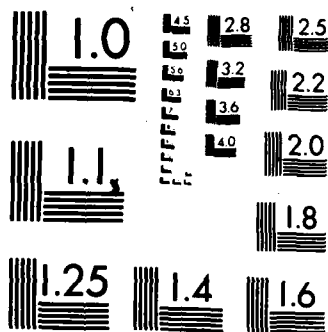
2/2

UNCLASSIFIED

F/G 8/11

NL





MICROCOPY RESOLUTION TEST CHART  
NATIONAL BUREAU OF STANDARDS-1963-A



Acknowledgements. This research was supported by the Office of Naval Research (code 425GG). Funds for support of the hydrophone station at Wake Island were provided primarily by the Air Force Office of Scientific Research under Contract No. F-49620-81-C-0065, with supplementary support from the U.S. Arms Control and Disarmament Agency. The authors express thanks to Dave Byrne, Grant Blackinton, Bob Mitiguy, Dave Barrett, and Fred Duennebier for their help in modifying, testing, launching, and recovering the OBH's. Appreciation is also expressed to Al David and Kentron Corporation for their part in maintaining the recording station at Wake. The authors also thank George Sutton for reviewing this manuscript, and Rita Pujalet for editorial assistance. Hawaii Institute of Geophysics Contribution No. 0000.

References

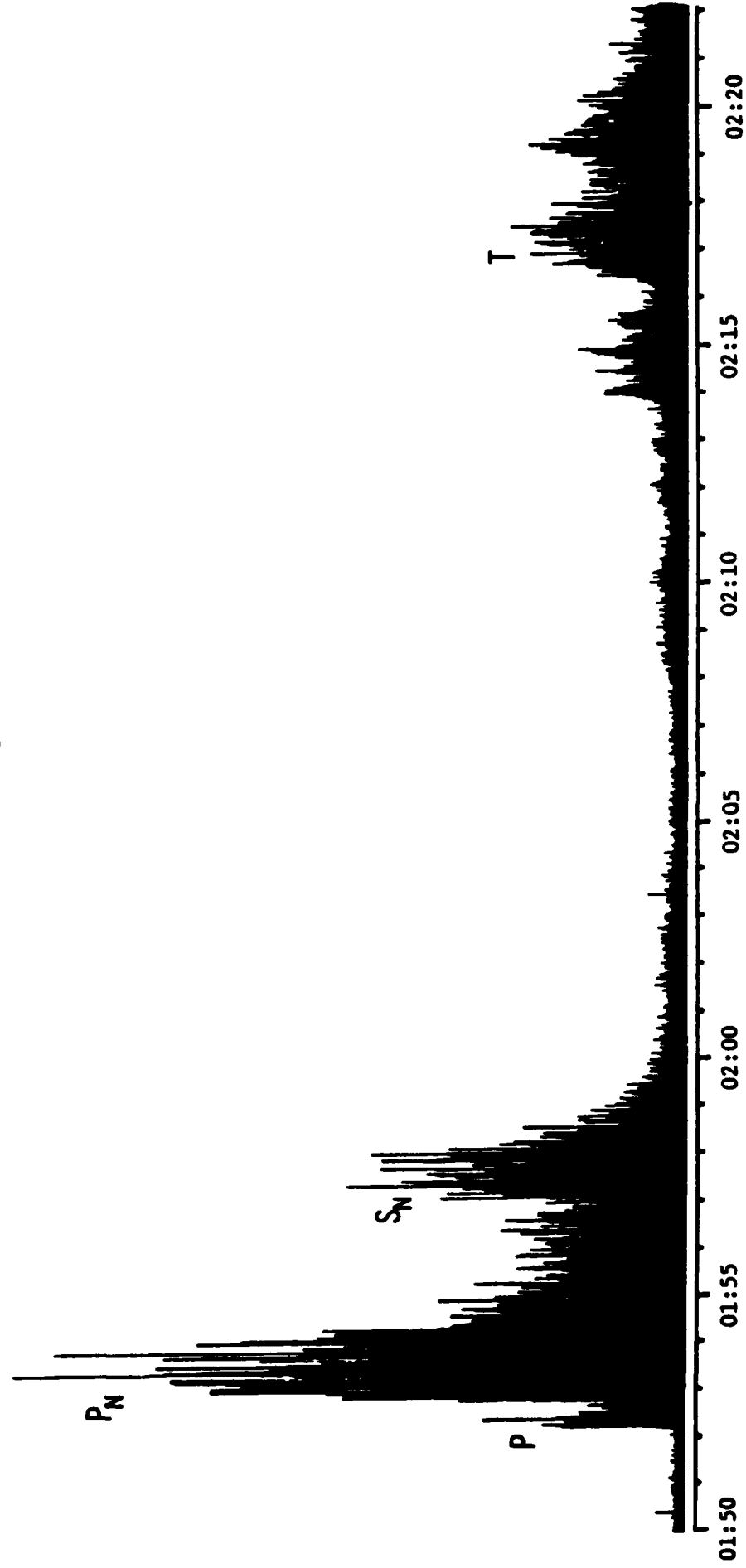
- Cormier, V., The effect of attenuation on seismic body waves. Bull. Seismol. Soc. Am., 72. S169-S200. 1982.
- Gettrust, J., and L. Frazer. A computer model study of the propagation of the long-range Pn phase. Geophys. Res. Lett., 8, 749-752. 1981.
- Jeffreys, H., and K. Bullen. Seismological Tables. Office of the British Association, Burlington House. London. 1958.
- Menke, W., and P. Richards. Crust-mantle whispering gallery phases: a deterministic model of teleseismic Pn wave propagation. J. Geophys. Res., 85. 5416-5422. 1980.
- Stephens, C., and B. Isacks. Toward an understanding of Sn: normal modes of Love waves in an oceanic structure. Bull. Seismol. Soc. Am., 67. 69-78, 1977.
- Sutton, G., and D. Harvey. Complete synthetic seismograms to 2 Hz and 1000 km for an oceanic lithosphere (abstract). EOS Trans. AGU. 62. 327. 1981.
- Sutton, G., C. McCreery, F. Duennebier, and D. Walker. Spectral analyses of high-frequency Pn, Sn phases recorded on ocean bottom seismographs. Geophys. Res. Lett., 5. 745-747. 1978.
- Sutton, G., P. Pomeroy, J. Carter, and C. McCreery. Short period guided waves over oceanic and continental paths. DARPA Annual Program Review. 1983.
- Walker, D., High-frequency Pn, Sn velocities: some comparisons for the Western, Central, and South Pacific, Geophys. Res. Lett., 8, 207-209, 1981.
- Walker, D., Oceanic Pn/Sn phases: a qualitative explanation and reinterpretation of the T-Phase. Hawaii Inst. of Geophysics Rept. HIG-82-6. 1982.
- Walker, D., C. McCreery, G. Sutton, and F. Duennebier. Spectral analyses of high-frequency Pn and Sn phases observed at great distances in the Western Pacific, Science. 199, 1333-1335, 1978.

APPENDIX VI

# OPA

Newsletter of the Ocean P Alliance  
Number 1 September 15, 1982

6 SEPTEMBER 1982; 01:47:02; 29.3N, 140.3E; 6.6  $M_b$ ; 167 km; SOUTH OF HONSHU; DISTANCE = 25.2°



# OPA

## NEWSLETTER OF THE OCEAN P ALLIANCE

The purpose of OPA, the newsletter of the "Ocean P Alliance," is to stimulate interest in a seismic phase known as "Ocean P." This phase, Po, and its associated S phase, So, were first observed in the North Atlantic and have since been found throughout the North, Western, and Central Pacific. First arriving Po/So phases travel with fairly constant apparent velocities of about 8.0 and 4.6 km/sec, respectively, while peak arrivals have velocities (about 7.6 and 4.5 km/sec) comparable to basal crustal rates. At distances of about 180 (~ 2000 km), observed frequencies of Po and So are as high as 30 and 35 Hz, respectively; and at distances of about 300, as high as 15 and 20 Hz, respectively. The signal-to-noise ratios for Po/So phases are generally at least ten times greater than the ratios of their respective normal, mantle-refracted P and S phases; and, in many instances no P's and S's can be found in spite of the presence of very strong Po's and So's.

Aside from the SOFAR channel of the world's oceans, the Po/So waveguide appears to be the earth's most efficient acoustical waveguide (estimates of Q are as high as 20,000). Also it seems probable that the phenomenon is a dominant feature of all of the world's oceans and marginal seas.

In spite of these remarkable and extensive observations, Po/So research has not yet received the general recognition, interest, and support that it deserves. Recent observations indicate the phenomenon is not just of interest in terms of basic science, but applied science as well. The applied aspects include the detection and discrimination of underground nuclear explosions along subduction zones and/or continental margins, large-scale mapping of the crust and uppermost mantle of the world's oceans and marginal seas, and acoustical studies of ocean sediments and crust at high frequencies.

In view of the foregoing discussions, the intent of this newsletter is to promote interest in Po/So research by providing an additional, and more effective, forum for the exchange of observations and ideas. Contributions or correspondence should be addressed to:

Dan Walker, OPA  
Rm. 432, HIG, U. of H.  
2525 Correa Rd.  
Honolulu, HI 96822

Views expressed in this publication are those of the authors only and do not reflect official positions of the Ocean P Alliance unless expressly stated.

Acknowledgments. The concept of a newsletter to improve communications among those interested in Po/So research grew directly out of responses to my 30 March letter. I thank all of those who provided this encouragement. I would also like to express

my appreciation to a few visionary program managers at the National Science Foundation, the Office of Naval Research, the Air Force Office of Scientific Research, and the U.S. Arms Control and Disarmament Agency.

### Dear Potential Ocean P Alliance Members:

On 30 March 1982, I wrote a rather lengthy letter to some of you concerning seismic phases variously referred to as high-frequency Pn/Sn, long-range Pn/Sn, or Ph.f./Sh.f. It was, and is, my opinion that the level of interest in, and support for, research on these phases was far less than commensurate with their potential importance to geophysics. [In the event that your may have misplaced the 30 March letter, some of the more significant observations are summarized in the masthead.] To share this concern and to obtain an objective assessment, I requested that you reciprocate and express your views to me.

As you may have guessed, the response has been very encouraging--so much so that you have before you a new means for the exchange of observations and ideas on the phenomenon of "high-frequency Pn/Sn" propagation.

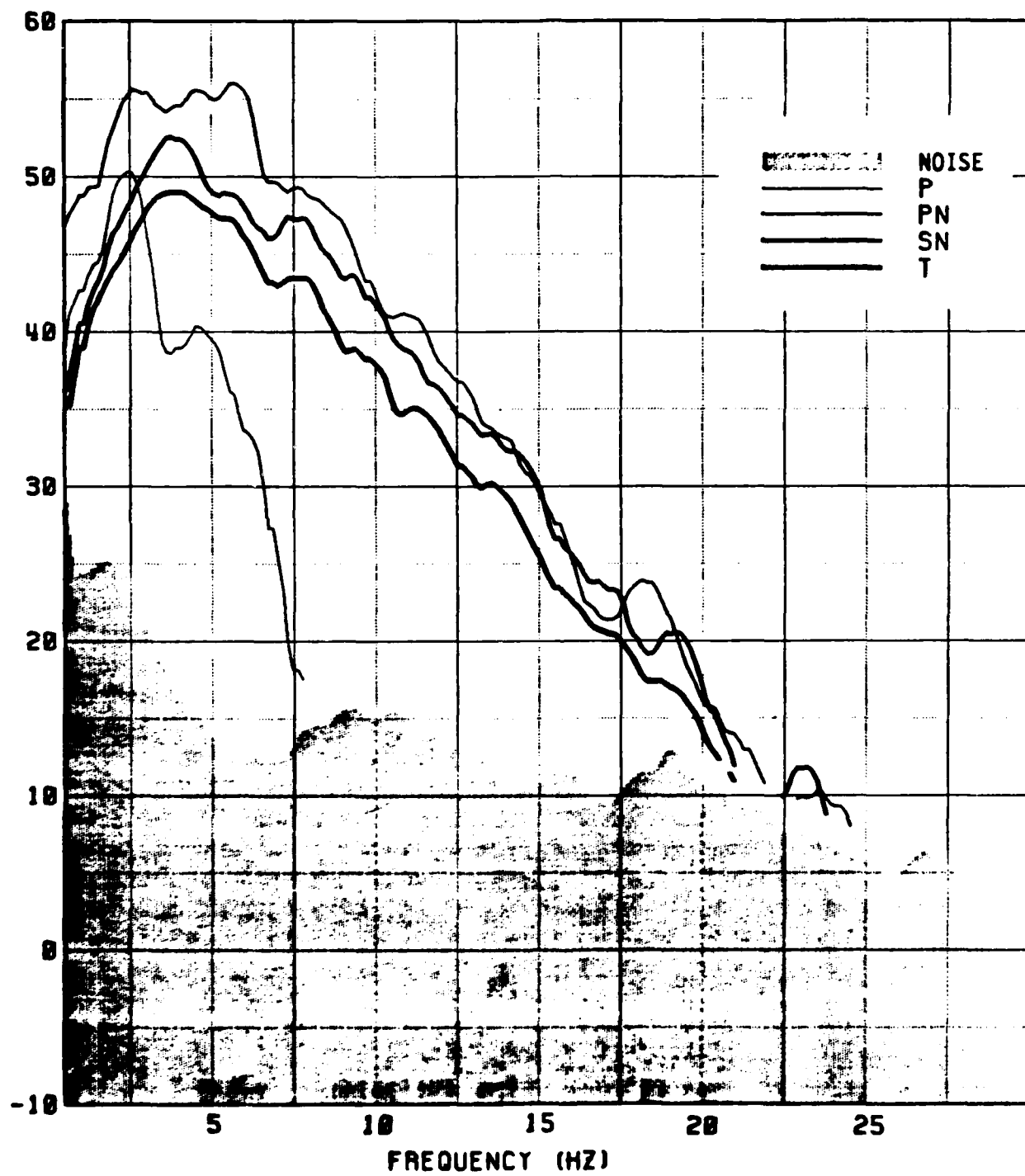
Rationale. The history of research on these phases since they were first recognized nearly fifty years ago could best be described as sporadic--with only a small number (often zero) of researchers actively studying the phenomenon at any given time. Such efforts for those early years are understandable. Unfortunately, even with the advent of ocean-bottom hydrophones, digital systems which greatly facilitate spectral analyses, and rapidly evolving computer techniques for modeling complex seismic phases, the number of researchers actively studying the phenomenon is still small. As a result much of what we publish is given little attention, or is totally ignored; and this situation is exacerbated by the large number of journals ("haystacks") in which these studies ("needles") can be published.

Thus, the timing now seems appropriate for building a larger constituency and pushing for a solution. Legitimate means are increased communications, as well as continuing quality research. Without such an effort at this time, I am fearful that research on the phenomenon will still be dangerously close to the "sporadic mode," making hard times and additional periods of dormancy very real possibilities.

I believe the assessment that high-frequency Pn/Sn propagation is "a challenge remaining to the theoretician," (Richards, 1979, Rev. Geophys. Space Phys., 17, 312-328) and is "the challenge to both explosion and earthquake seismology for the coming decade" (Hirn et al., 1973, Z. Geophys., 39, 363-384). I also believe that the opportunities for widespread participation in the solution of major geophysical problems are increasingly rare and that such opportunities should be seized.

Name Change. It may be advantageous at this time to suggest that a new name be given to the high-frequency compressional and shear phases observed at great distances in the world's oceans. The

DB'S RELATIVE TO 1 DIGITAL UNIT RMS



difficulty with the nomenclature used to date is that: (1) an, as yet, unsubstantiated relationship to the well known longer-period Pa/Sa phases of continents is inferred; and (2) the environmental feature most strongly linked to the observations is not cited. Thus, a more logical term would be "Ocean P" or "Ocean S" with the abbreviations being "Po/So." With this change, those unfamiliar with the phenomenon would not be as likely to make the false assumption that the phases are similar to continental Pn and Sn. Such assumptions in the past have been a major stumbling block in stimulating interest and support for "Po/So" research.

**Our Birthday.** You may have noticed something special about the date of this inaugural newsletter--15 September 1982 commemorates the 47th anniversary of the first known published report of Po/So phases.

"In the bulletin of the Harvard Seismograph Station, under date of September 15, 1935, attention was directed to the unusual character of certain records from the vicinity of 17°N, 62°W. One of the novel features was a short-period phase about 23 minutes after P. It has become known as T, for third, with P and S constituting the first and second groups of short-period waves of similar general appearance. The problem was discussed with Weston, and since that time those two stations have been working on it. Lindehan published in 1940 the first description outside station bulletins." [Leet et al., 1951, Bull. Seismol. Soc. Am., 41, 123-141].

"At the 1939 meeting of the Eastern Section of the Seismological Society of America, the author presented a paper on earthquakes occurring about 15° to 30° distance from Weston, Massachusetts. The difficulty of locating these quakes was stressed in the paper, due to the strange characteristics of the recordings. Observers of many stations thought of them as a series of locals. As has been mentioned, the records from this area are quite different from those we have recorded from other locations. The predominant characteristic is the multiplicity of their extremely short period. The so-called P-group may last as long as three or four minutes due to the multiplicity mentioned and frequently runs into the S-group: The second group lasts about the same length of time as the former. About 20 minutes after the P-group is a third unidentified group which we have labelled as T." [Lindehan, 1940, EOS Trans. AGU, 21, 229-232].

"Actually, many features of P and S are abnormal on this and later records from certain areas at this distance range, and work on that part of the problem is in progress, but the investigation of T has been undertaken first." [Leet et al., op. cit.]

As I stated in my 30 March letter, although the T-phase was accurately identified in a relatively short time as compressional energy traveling in the sound channel of the world's oceans, one could best describe work on the other "part of the problem" (i.e.,

the "abnormal" P and S phases), 47 years later, as still being "in progress."

It is my hope that on the 50th anniversary of the first reported observations of Po and So, the need for a special newsletter would no longer exist.

**Success.** The minimum objective of the newsletter is nothing more than the stimulation of deserved interest in Po/So research. Achievements beyond the minimum objective will be strongly dependent on contributions and correspondence from members and their "lobbying efforts" with program managers.

**Membership.** The "Ocean P Alliance" is not at the moment a formal organization. If no useful purpose would be achieved by "formalization" then this current status should remain unchanged. Anyone wishing to be considered as a member of the Alliance is automatically "in." Anyone wishing to remain skeptical, but nonetheless interested, could consider themselves, if they wish as non-members and still receive the newsletter. I may at some later date directly ask you for your opinions on the newsletter.

I would hope that those receiving the newsletter would provide: (1) The names and addresses of individuals who should be added to our mailing list, and (2) Po/So publications which should be added to our Po/So bibliography, as well as news of forthcoming publications. If you have some other newsworthy items or comments on topics discussed in OPA, please send them to me. I would also like to know if you have been mistakenly placed on the mailing list. **Format.** We hope that you will save all issues of OPA for future reference. To that end we have a format conducive to storage in a 3-hole binder.

**Future Topics.** Items for future issues include the OPA mailing list, correspondence from members, a bibliography of Po/So research, more amazing Po/So recordings, news of upcoming publications, and interesting questions for debate.

**Our Covers.** To further commemorate the first reported observation of Po, So, and T phases in September of 1935 across the North Atlantic Basin, we have covered our newsletter with Po, So, and T phases which were generated in September of 1982 across the Northwestern Pacific Basin. In addition, the normal, mantle-refracted P is also shown. These phases were recorded on a twelve channel hydrophone array located near Wake Island. Do you see any similarities between these Pacific phases and those from the Atlantic discussed by Leet et al. (op.cit) and Lindehan (op. cit.)? What significant observations can be made from these plots? For answers, "tune in" to the next issue of OPA!

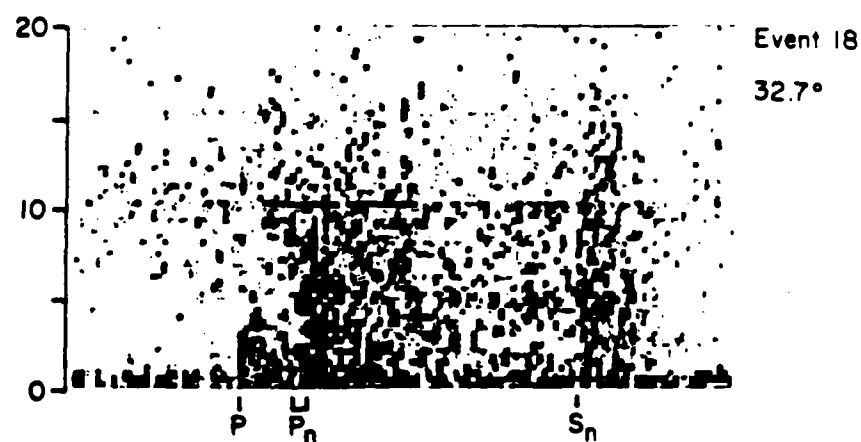
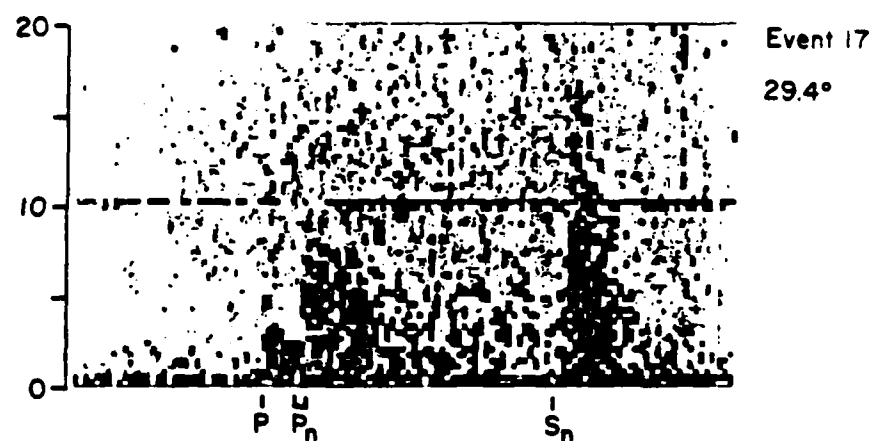
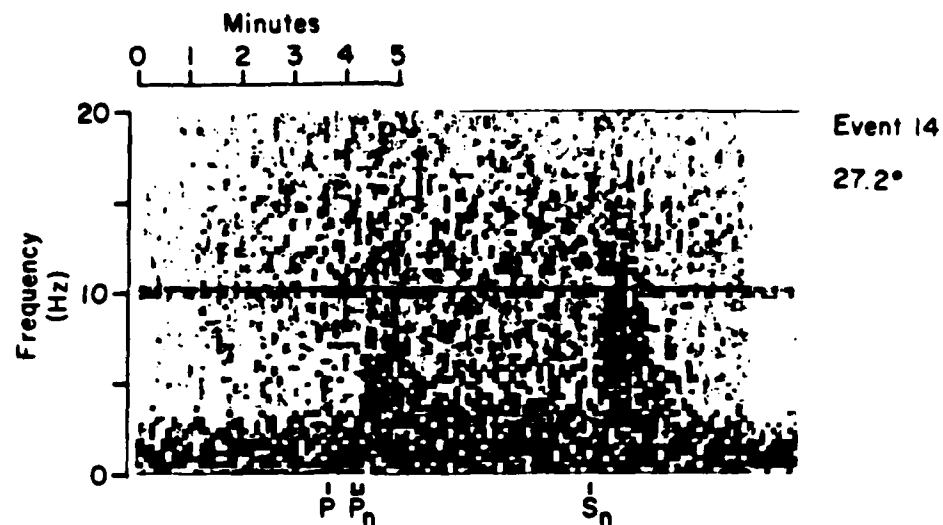
Dan Walker

APPENDIX VII



# OPA

Newsletter of the Ocean P Alliance  
Number 2 January 15, 1983



# OPA

## NEWSLETTER OF THE OCEAN P ALLIANCE

The purpose of OPA, the newsletter of the "Ocean P Alliance," is to stimulate interest in a seismic phase known as "Ocean P." This phase, Po, and its associated S phase, So, were first observed in the North Atlantic and have since been found throughout the North, Western, and Central Pacific. First arriving Po/So phases travel with fairly constant apparent velocities of about 8.0 and 4.6 km/sec, respectively, while peak arrivals have velocities (about 7.6 and 4.5 km/sec) comparable to basal crustal rates. At distances of about 180 (~ 2000 km), observed frequencies of Po and So are as high as 30 and 35 Hz, respectively; and at distances of about 300, as high as 15 and 20 Hz, respectively. The signal-to-noise ratios for Po/So phases are generally at least ten times greater than the ratios of their respective normal, mantle-refracted P and S phases; and, in many instances no P's and S's can be found in spite of the presence of very strong Po's and So's.

Aside from the SOPAR channel of the world's oceans, the Po/So waveguide appears to be the earth's most efficient acoustical waveguide (estimates of Q are as high as 20,000). Also it seems probable that the phenomenon is a dominant feature of all of the world's oceans and marginal seas.

In spite of these remarkable and extensive observations, Po/So research has not yet received the general recognition, interest, and support that it deserves. Recent observations indicate the phenomenon is not just of interest in terms of basic science, but applied science as well. The applied aspects include the detection and discrimination of underground nuclear explosions along subduction zones and/or continental margins, large-scale mapping of the crust and uppermost mantle of the world's oceans and marginal seas, and acoustical studies of ocean sediments and crust at high frequencies.

In view of the foregoing discussions, the intent of this newsletter is to promote interest in Po/So research by providing an additional, and more effective, forum for the exchange of observations and ideas. Contributions or correspondence should be addressed to:

Dan Walker, OPA  
Rm. 432, HIG, U. of H.  
2525 Correa Rd.  
Honolulu, HI 96822

Views expressed in this publication are those of the authors only and do not reflect official positions of the Ocean P Alliance unless expressly stated.

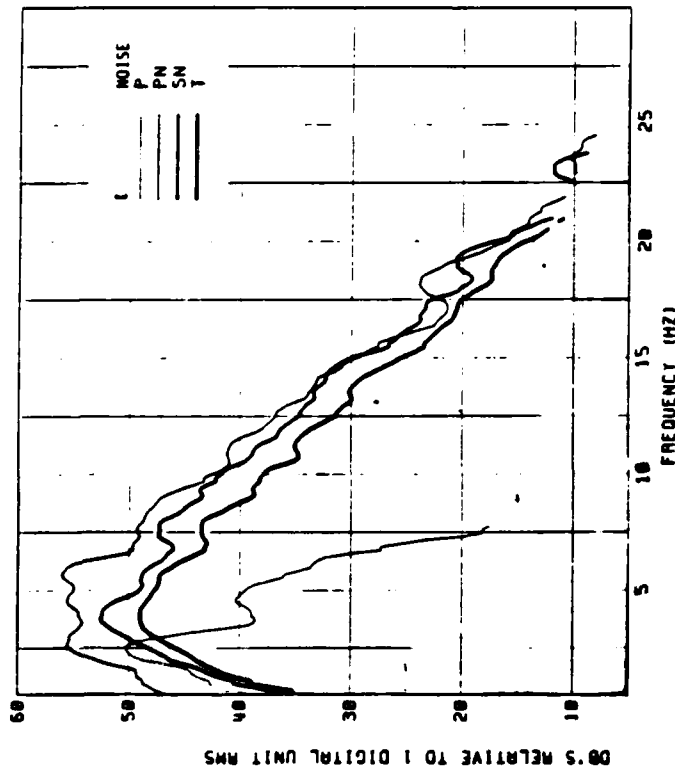
Dear Colleague:

As you may recall, the covers for our inaugural issue consisted of a digitally rectified and compressed plot of P, Po, So, and T phases for an earthquake south of Japan recorded by the Wake hydrophones (front cover) and spectrums for these same phases (back cover). For purposes of the discussion which will follow these figures are repeated here in a severely reduced form. In closing the inaugural issue, I asked whether you could see any similarities between these Pacific phases and those from the Atlantic discussed by Leet, Linchen, and Berger (1951) and Linchen (1940). The unusual characteristics mentioned by these authors are the similar general appearance of their so-called P (primary) and S (secondary) groups to the later arriving T (tertiary) group, the multiplicity of their extremely short period with the P frequently running into the S group, and S about as long as P.

Certainly all of these characteristics have been seen in the Pacific as exemplified in the figures shown here. The P, S, and T groups are of the same general appearance, the P group runs into the S group, in some respects the S group may be about as long as P, and the phases are of extremely short period. The striking and remarkable similarities of these phases are most evident in the spectrums, which also serve to quantify their short period content.

6 SEPTEMBER 1982 (11:47:02; 29.3N, 140.3E; 6.6 M<sub>L</sub>; 157 Km; SOURCE OF MOMENTUM DISTANCE = 25.2°





**The T Phase: A New Approach to Po/So Research.** Especially intriguing is the detailed correlation of the T spectrum to the So spectrum. This and the general correlation of the T and Po spectra suggest a possible new approach to Po/So research. In the future it would seem appropriate to consider the possible relationship of Po and So to T. [Other evidence suggesting a possible relationship of Po and So to T is contained in the report "Oceanic Pn/Sn Phases: A Qualitative Explanation and Reinterpretation of the T-Phase" (D. Walker, WIG Report 82-6, 1982). [Topics from this report are discussed in this newsletter].

**Spectra for Atlantic Po, So, and T Phases: A Challenge for East and Gulf Coast Seismologists.** I believe that Leet, Linehan, and Berger would be surprised at just how short the periods were for the phases they observed. Unfortunately, the recordings and instrumentation which they had (in all probability 60 mm/minute analog recordings from standard 1 Hz instrumentation) did not permit them to see just how high the frequencies were. In the deep ocean near Wake, forty years later, we have the advantages of lower noise in the 3 Hz to 15 Hz range than most continental stations, a better system response to those frequencies than conventional 1 Hz instrumentation, digital recordings, and computers which facilitate

the derivation of spectra. It is nonetheless surprising that spectra of Atlantic Po, So, and T phases have not been published. (If I am mistaken, I hope someone will write and provide references.) It would be interesting to compare these spectra to those from the Pacific. I hope that some east or Gulf coast seismologists will take the challenge and be the first to quantify the frequency content of Atlantic Po/So phases.

**Continuing Japanese Research on Po/So.** I was pleased to meet recently with Drs. Nagumo and Kasahara and to review a preprint of their new paper, with Drs. Ouchi and Koresawa, on OBS observations of Po/So phases. The report contains important information on Po/So velocities. I wish them every success in efforts to publish this important paper.

**Po/So Bibliography.** One of the major objectives of the OPA Newsletter is to acquire a comprehensive and up-to-date bibliography of Po/So research. A preliminary attempt to achieve this objective follows. I hope that readers aware of omissions will bring them to my attention so that they can be added to the listings.

**Our Covers: Now you see "it". Now you don't!** The covers are spectrograms from the Wake Island hydrophones. Expected times of arrivals are based on either the Jeffreys-Bullen tables for P or Po/So travel time curves. The contour interval is 8 db. The line at 10 Hz is due to time code cross talk.

**What's "it"?** The So - very strong on the front cover, but weak or absent on the back cover. Phases shown on the front cover are typical of events from the Japan, Kuril, Kamchatka portion of the circum-Pacific arc; and, therefore, these phases have travel paths to Wake under the deep Northwestern Pacific Basin. Phases shown on the back cover are typical of events from the New Ireland and Solomon Islands area; and, therefore, these phases have travel paths to Wake under the shallow Ontong-Java Plateau as well as portions of the deep Northwestern Pacific Basin.

An obvious explanation is differences in source characteristics. Unfortunately, this seemingly reasonable explanation cannot be correct, since So phases from the New Ireland and Solomon Islands area are well recorded at Ponape on the northern margin of the Ontong-Java Plateau (roughly mid-way between the source locations and the receivers at Wake). [Of the more than forty events from the New Ireland and Solomon Islands area recorded at Ponape during an approximate seventeen month experiment, amplitudes of So phases are at least comparable to, and frequently larger than, those of their respective Po phases.]

What, then, could be the explanation? Possible clues are: (1) the transition from So to Po, allowing Ontong-Java Plateau to the deeper Northwest Pacific; and (2) the frequent absence or weakness of So, presence of Po, at great distances (often more

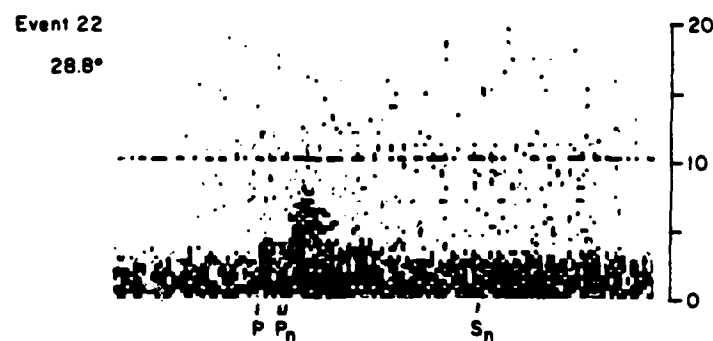
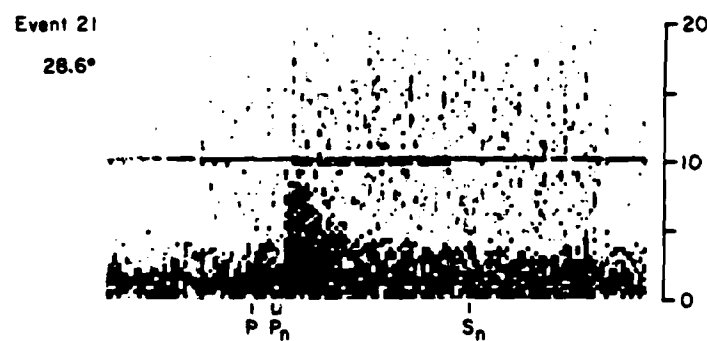
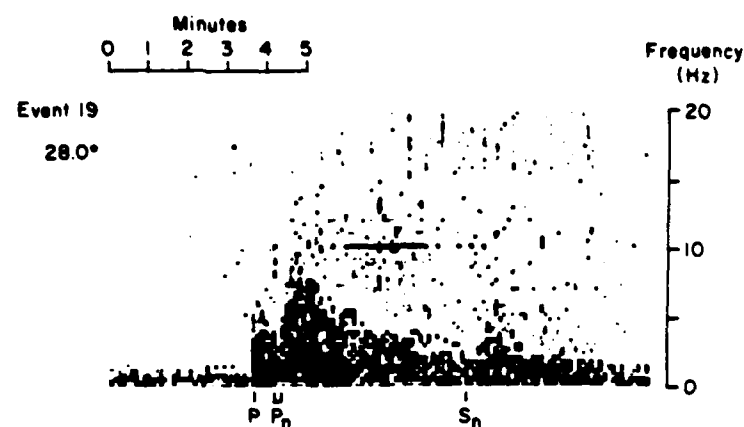
than 4000 km) throughout the North Pacific (Walker, 1977a and b) and Central Pacific (Talandier and Bouchon, 1979), in spite of stronger  $S_o$ 's than  $P_o$ 's for relatively homogeneous travel paths across the deep Northwestern Pacific Basin.

A possible explanation will be given in the next issue of OPA. Please send any comments or suggestions on this or other items.

## Po/So Bibliography

- Asada, T. and M. Shimamura, 1976, Observation of earthquakes and explosions at the bottom of the Western Pacific: Structure of the oceanic lithosphere revealed by longshot experiment, in The Geophysics of the Pacific Ocean Basin and Its Margin, Geophys. Monogr. Ser., ed. G. Sutton, M. Manghoni, and R. Moberly, Vol. 19, Am. Geophys. Union, Washington, D.C., 135-153.
- Auld, B., G. Latham, A. Morroosi, and L. Seeber, 1969, Seismicity off the coast of northern California determined from ocean bottom seismic measurements, Bull. Seismol. Soc. Am., **59**, 2001-2015.
- Barzaghi, M., B. Isacks, and J. Oliver, 1972, Propagation of seismic waves through and beneath the lithosphere that descends under the Tonga Island arc, J. Geophys. Res., **77**, 952-958.
- Bath, M., 1966, Propagation of  $S_u$  and  $P_u$  to teleseismic distances, Pure Appl. Geophys., **53**, 19-30.
- Brune, J., and J. Dorman, 1963, Seismic waves and earth structure in the Canadian shield, Bull. Seismol. Soc. Amer., **53**, 167-210.
- Fuchs, K., and K. Schulz, 1976, Tunneling of low-frequency waves through the subcrustal lithosphere, J. Geophys. Res., **81**, 175-190.
- Gettrust, J., and L. Fraser, 1981, A computer model study of the propagation of the long-range  $P_u$  phase, Geophys. Res. Lett., **8**, 749-752.
- Hales, A., G. Healey, and J. Ratior, 1970,  $P$  travel times for an oceanic path, J. Geophys. Res., **75**, 7362-7381.
- Hart, R., and V. Press, 1973,  $S_u$  velocities and the composition of the lithosphere in the regionalized Atlantic, J. Geophys. Res., **78**, 407-411.
- Hirn, A., L. Steimetz, B. Kind, and K. Fuchs, 1973, Long range profiles in western Europe, II, Fine structure of the lower lithosphere in France (southern Bretagne), J. Geophys. Res., **78**, 363-386.
- Isacks, B., and J. Oliver, 1964, Seismic waves with frequencies from 1 to 100 cycles per second recorded in a deep mine in northern New Jersey, Bull. Seismol. Soc. Amer., **54**, 1941-1979.
- Kasahara, J., and B. Harvey, 1977, Seismological evidence for the high-velocity zone in the Kuril trench area from ocean bottom seismometer observations, J. Geophys. Res., **82**, 3805-3816.
- Kalutrin, V., T. Bastian, and P. Molnar, 1977, The spectral content of Penit-Mandu Kush intermediate depth earthquakes: Evidence for a high- $Q$  zone in the upper mantle, J. Geophys. Res., **82**, 2931-2943.
- Kind, R., 1974, Long range propagation of seismic energy in the lower lithosphere, J. Geophys. Res., **79**, 189-202.
- Latham, G., and G. Sutton, 1966, Seismic measurements of the ocean floor, J. Geophys. Res., **71**, 2545-2573.
- Leet, L., D. Linshan, and P. Berger, 1951, Investigation of the T phase, Bull. Seismol. Soc. Amer., **41**, 123-141.
- Linshan, D., 1940, Earthquakes in the West Indian region, EOS Trans. AGU, **21**, 229-232.
- Mantovani, E., Z. Schwab, M. Liao, and L. Knopoff, 1977, Teleseismic  $S_u$  guided wave in the mantle, Geophys. J. R. Astron. Soc., **51**, 709-726.
- McCreery, C., 1981, High-frequency  $P_u$ ,  $S_u$  phases recorded by ocean bottom seismometers on the Cocos Plate, Geophys. Res. Lett., **8**, 489-492.
- McCreery, C. and G. Sutton, 1980, Wave train characteristics of long-range, high-frequency  $P_u$ ,  $S_u$  crossing an ocean bottom hydrophone array, Bull. Seismol. Soc. Amer., **70**, 437-446.
- Menke, W., and P. Richards, 1980, Crust-mantle whispering gallery phases: a deterministic model of teleseismic  $P_u$  wave propagation, J. Geophys. Res., **85**, 5416-5422.
- Mitrovnas, W., B. Isacks, and L. Seeber, 1969, Earthquake locations and seismic wave propagation in the upper 250 km of the Tonga Island arc, Bull. Seismol. Soc. Amer., **59**, 1115-1135.
- Molnar, P., and J. Oliver, 1969, Lateral variations of attenuation in the upper mantle and discontinuities in the lithosphere, J. Geophys. Res., **74**, 2648-2682.
- Nagumo, S., and J. Kasahara, 1976, Ocean-bottom seismograph study of the western margin of the Pacific, in The Geophysics of the Pacific Ocean Basin and Its Margin, Geophys. Monogr. Ser., ed. G. Sutton, Washington, D.C., 155-167.
- Odegard, M., 1975, Upper mantle structure of the North Pacific, Ph.D. thesis, Univ. of Hawaii, Honolulu.
- Oliver, J., and B. Isacks, 1967, Deep earthquake zones, anomalous structures in the upper mantle, and the lithosphere, J. Geophys. Res., **72**, 4259-4275.
- Ouchi, T., 1981, Spectral structure of high frequency  $P$  and  $S$  phases observed by OBS's in the Mariana Basin, J. Phys. Earth., **29**, 305-326.
- Ouchi, T., S. Nagumo, and S. Koresawa, 1981, Ocean bottom seismometer study on the seismic activity in the Mariana Island arc region, Bull. Earth. Res. Inst., **26**, 43-65.
- Press, F., and M. Ewing, 1955, Waves with  $P_u$  and  $S_u$  velocity at great distances, Proc. Nat. Acad. Sci., **41**, 24-27.

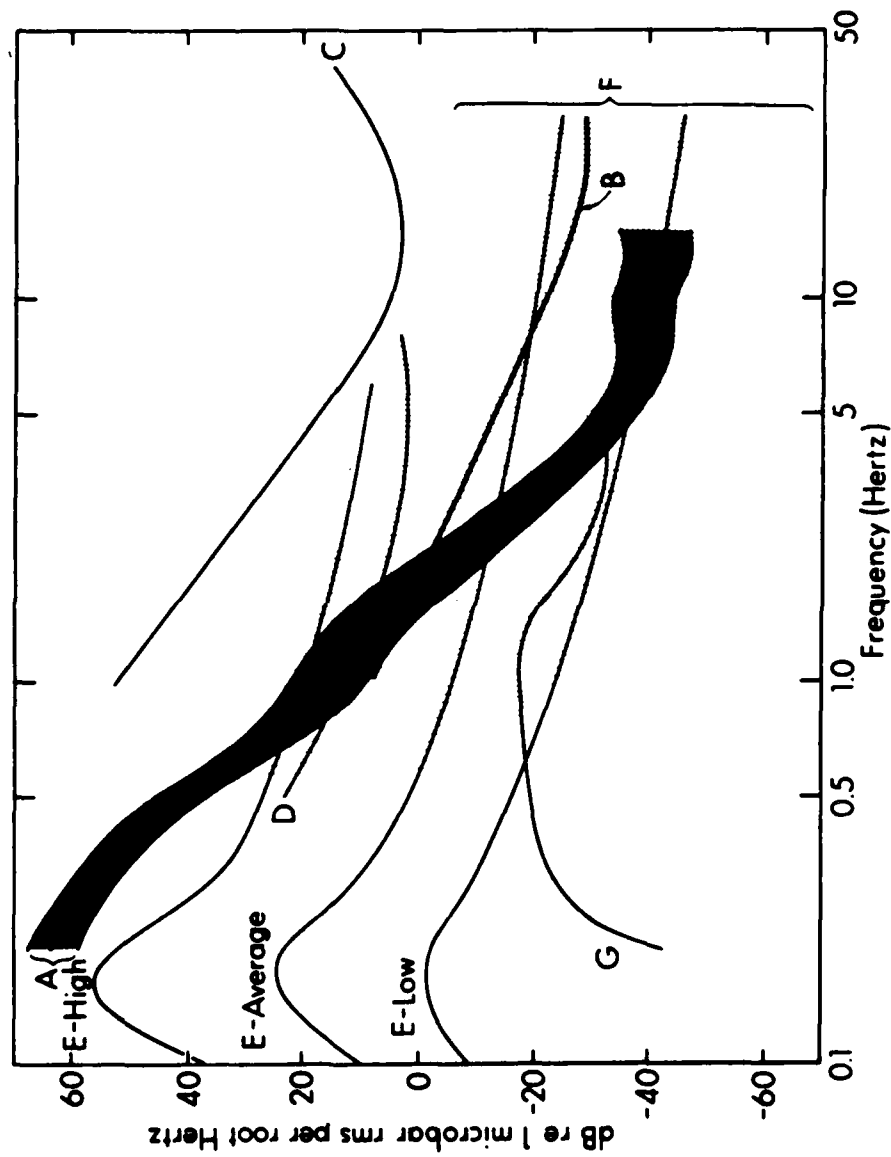
- Richards, P., 1979, Theoretical seismic wave propagation, Rev. Geophys. Space Phys., **17**, 312-328.
- Shimmura, N., and T. Asada, 1975, T waves from deep earthquakes generated exactly at the bottom of deep-sea trenches, Earth and Planet. Sci. Lett., **22**, 137-142.
- Shimmura, N., and T. Asada, 1976, Apparent velocity measurements on an oceanic lithosphere, Phys. Earth Planet. Int., **13**, 15-22.
- Shimmura, N., T. Asada, and M. Kumazawa, 1977, High shear velocity layer in the upper mantle of the western Pacific, Nature, **265**, 680-682.
- Shimmura, N., Y. Tomoda, and T. Asada, 1975, Seismographic observations at the bottom of the Central Basin Fault of the Philippine Sea, Nature, **253**, 177-179.
- Shurbet, D., 1962, The high-frequency P and S phases from the West Indies, Bull. Seismol. Soc. Amer., **52**, 957-962.
- Shurbet, D., 1964, The high-frequency S phase and structure of the upper mantle, J. Geophys. Res., **69**, 2065-2070.
- Stephens, C., and B. Isacks, 1977, Toward an understanding of Sn: Normal modes of Love waves in an oceanic structure, Bull. Seismol. Soc. Amer., **67**, 69-78.
- Sutton, G., C. McCreery, F. Duennbier, and D. Walker, 1978, Spectral analyses of high-frequency Pn and Sn phases recorded on ocean bottom seismographs, Geophys. Res. Lett., **5**, 745-747.
- Sutton, G., and D. Harvey, 1981, Complete synthetic seismograms to 2 Hz and 1000 km for an oceanic lithosphere, EOS Trans. AGU, **62**, p. 327.
- Sutton, G., and D. Walker, 1972, Oceanic mantle phases recorded on seismographs in the Northwestern Pacific at distances between 7° and 40°, Bull. Seismol. Soc. Amer., **62**, 631-655.
- Talandier, J., and M. Rouchon, 1979, Propagation of high frequency Pn waves at great distances in the Central and South Pacific and its implications for the structure of the lower lithosphere, J. Geophys. Res., **84**, 5613-5619.
- Utau, T., 1967, Anomalies in a seismic wave velocity and attenuation associated with a deep earthquake zone (1), J. Fac. Sci. Hokkaido Univ., Ser. I, Geophysics, **3**, 1-25.
- Walker, D., 1977, High-frequency Pn and Sn phases recorded in the Western Pacific, J. Geophys. Res., **82**, 3350-3360.
- Walker, D., 1977, High-frequency Pn phases observed in the Pacific at great distances, Science, **197**, 257-259.
- Walker, D., 1981, High-frequency Pn, Sn velocities: some comparisons for the Western, Central, and South Pacific, Geophys. Res. Lett., **8**, 207-209.
- Walker, D., 1982, Oceanic Pn/Sn phases: a qualitative explanation and reinterpretation of the T-phase, Hawaii Inst. of Geophysics Rept. HIG-82-6, 19 pp.
- Walker, D., C. McCreery, G. Sutton, and F. Duennbier, 1978, Spectral analyses of high-frequency Pn and Sn phases observed at great distances in the Western Pacific, Science, **199**, 1333-1335.
- Walker, D., and G. Sutton, 1971, Oceanic mantle phases recorded on hydrophones in the Northwestern Pacific at distances between 9° and 40°, Bull. Seismol. Soc. Amer., **61**, 65-78.



APPENDIX VIII

# OPA

Newsletter of the Ocean P Alliance  
Number 3 May 15, 1983





# OPA

## NEWSLETTER OF THE OCEAN P ALLIANCE

The purpose of OPA, the newsletter of the "Ocean P Alliance," is to stimulate interest in a seismic phase known as "Ocean P." This phase, Po, and its associated S phase, So, were first observed in the North Atlantic and have since been found throughout the North, Western, and Central Pacific. First arriving Po/So phases travel with fairly constant apparent velocities of about 8.0 and 4.6 km/sec, respectively, while peak arrivals have velocities (about 7.6 and 4.3 km/sec) comparable to basal crustal rates. At distances of about 18° (~2000 km), observed frequencies of Po and So are as high as 30 and 35 Hz, respectively; and at distances of about 30°, as high as 15 and 20 Hz, respectively. The signal-to-noise ratios for Po/So phases are generally at least ten times greater than the ratios of their respective normal, mantle-refracted P and S phases; and, in many instances no P's and S's can be found in spite of the presence of very strong Po's and So's.

Aside from the SOFAR channel of the world's oceans, the Po/So waveguide appears to be the earth's most efficient acoustical waveguide (estimates of Q are as high as 20,000). Also it seems probable that the phenomenon is a dominant feature of all of the world's oceans and marginal seas.

In spite of these remarkable and extensive observations, Po/So research has not yet received the general recognition, interest, and support that it deserves. Recent observations indicate the phenomenon is not just of interest in terms of basic science, but applied science as well. The applied aspects include the detection and discrimination of underground nuclear explosions along subduction zones and/or continental margins, large-scale mapping of the crust and uppermost mantle of the world's oceans and marginal seas, and acoustical studies of ocean sediments and crust at high frequencies.

In view of the foregoing discussions, the intent of this newsletter is to promote interest in Po/So research by providing an additional, and more effective, forum for the exchange of observations and ideas. Contributions or correspondence should be addressed to:

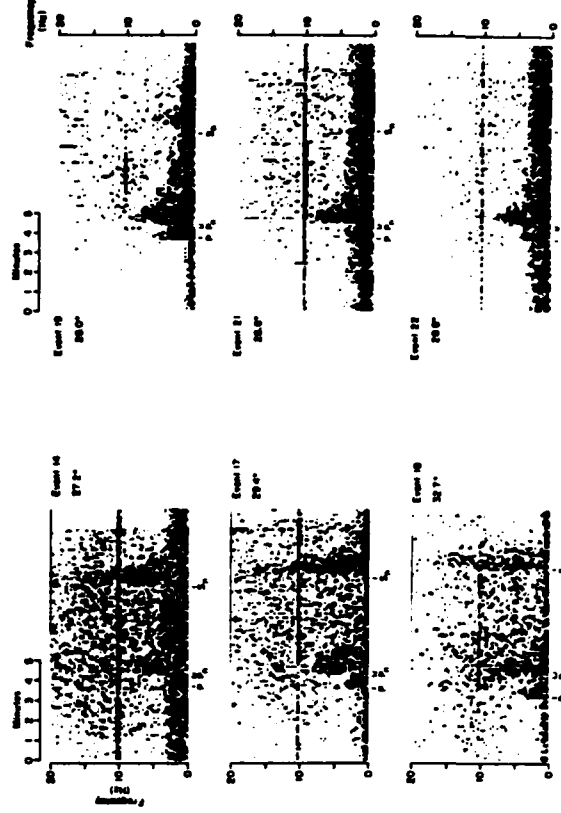
Dan Walker, OPA  
Rm. 432, HIG, U. of H.  
2525 Correa Rd.  
Honolulu, HI 96822

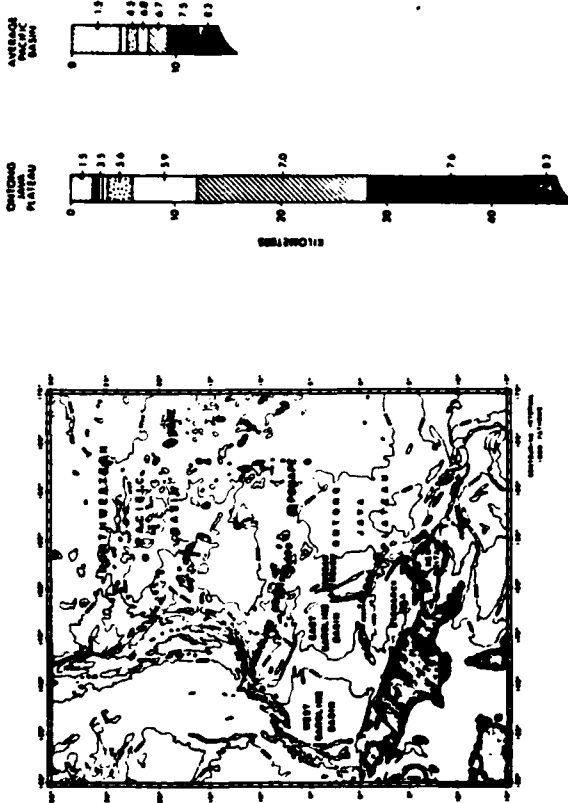
Views expressed in this publication are those of the authors only and do not reflect official positions of the Ocean P Alliance unless expressly stated.

Dear Colleague:

The covers of our last issue, shown here in reduced form, are spectrograms for phases with travel paths to the Wake Island hydrophones under the deep Northwestern Pacific Basin (front cover) and under the shallow Ontong Java Plateau (back cover). An obvious explanation for the absence, or weakness, of So (labeled Sn) on the back cover is differences in source characteristics. However, recordings made during an earlier experiment at Pohnpei, roughly midway between the receivers at Wake and the source locations of earthquakes in the New Ireland and Solomon Island area (see accompanying map), indicate that this explanation can not be correct. Over an approximate seventeen month recording period, more than forty events from the New Ireland and Solomon Island area were recorded, with the amplitudes of So at least comparable to, and frequently larger than, those of their respective Po phases.

An observation which contributes to a possible explanation is the frequent absence or weakness of So, yet presence of Po, at great distances (often more than 4000 km) throughout the North Pacific (Walker, 1977a and b) and Central Pacific (Talandier and Bouchon, 1979), in spite of stronger So's than Po's for relatively homogeneous travel paths across the deep Northwestern Pacific Basin.





The explanation arising from these observations, then, is that paths other than those across relatively homogeneous ocean basins are likely to encounter large lateral changes in the crust and upper mantle. Observations require that the changes be such that S<sub>o</sub> signal strength is reduced without seriously affecting the P<sub>o</sub> phase. Large lateral changes could be produced by plateaus, rises, ridge systems, island and seamount chains, fracture zones, transform faults, fossil arcs and trenches, and rafted continental fragments. The transition from the shallow Ontong Java Plateau to the deeper Northwestern Pacific Basin (see accompanying figure), as well as the extension of the Caroline Archipelago through this region, could be features responsible for the weak, or absent, S<sub>o</sub>'s at Wake from events in the New Ireland and Solomon Island area. [This interpretation has been taken from a recent attempt (Walker, 1982) to provide a qualitative framework consistent with all of the diverse observational aspects of Po/S<sub>o</sub> - hoping that this would eventually lead to comprehensive and detailed quantitative analyses and, ultimately, a generally acceptable model for the generation and propagation of Po/S<sub>o</sub>.]

**Nuclear Connections.** In the masthead of this newsletter, reference is made to Po/S<sub>o</sub> being of interest in terms of the detection and discrimination of underground nuclear explosions. It may be worthwhile at this time to be more explicit as to possible reasons for such interest.

**A. Obvious - Large S/P Ratios for Po/S<sub>o</sub>.** An examination of the covers of previous OPA newsletters is all that is needed to suggest that S/P ratios for Po/S<sub>o</sub> may be larger than the ratios for mantle refracted P (S is not generally apparent for distances of up to about

20°). Indeed, numerous observations from the deep ocean, as well as hard rock island sites, in the Western Pacific indicate the S/P ratios for Po/S<sub>o</sub> at their dominant frequencies (about 4 to 8 Hz) are generally from 5 to 10X greater than the S/P ratios for P at its dominant frequencies (about 1.5 to 2.5 Hz). This dominance may extend out to distances of 3000 km, with P increasing in strength relative to Po/S<sub>o</sub> beyond this range. Also, at distances less than about 20°, the travel times of P<sub>o</sub> phases are such that they may arrive ahead of the mantle refracted P, thus masking whatever P energy may be present.

Although some of the most extensive observations of Po/S<sub>o</sub> phases have been in the Western Pacific, these phases have also been observed in other portions of the Pacific and the North Atlantic. The nature and extent of these observations suggest that the phenomenon could be a dominant feature of all the world's oceans and marginal seas.

**Thus, regional detection and discrimination of underground explosions with seismic instrumentation in an ocean environment (islands, the water column, bottom, or sub-bottom) may in large part be based on Po/S<sub>o</sub> recordings.**

As to why detection and discrimination in an ocean environment should be important, one has only to look at a globe. As to whether, in fact, detection and discrimination in an ocean environment is important, one has only to consider recent investments in ocean sub-bottom seismometers.

**B. Less Obvious - Lg/Pg Connections.** Just as Po/S<sub>o</sub> are the most prominent phases recorded at regional distances for oceanic travel paths, Lg and Pg are prominent phases recorded at regional distances for continental travel paths. Certainly Lg/Pg are of great importance in regional detection using continental stations (just as Po/S<sub>o</sub> should be of great importance in regional detection using oceanic stations). Surprisingly, the much studied phenomenon of Lg/Pg suffers problems of understanding not unlike those associated with Po/S<sub>o</sub>. In a recent publication (1983) Gupta and Blandford state:

"The mechanism for the generation of transverse component motion from explosions is still not clearly understood in spite of the large number of studies on the subject." [p. 571] and "... no convincing explanation has so far been offered for the generation of short-period (about 1 sec or less) transverse motion from explosions." [p. 572.]

[In their report they propose a scattering mechanism for the generation of short period transverse motion (including Lg) from explosions.]

Regarding the utility of Lg/Pg in the discrimination of nuclear explosions, several theoretical studies suggest a strong dependence of Lg/Pg signal character on focal depth. Also, Gupta and Blandford note that "the observed differences in the spectra of shear waves

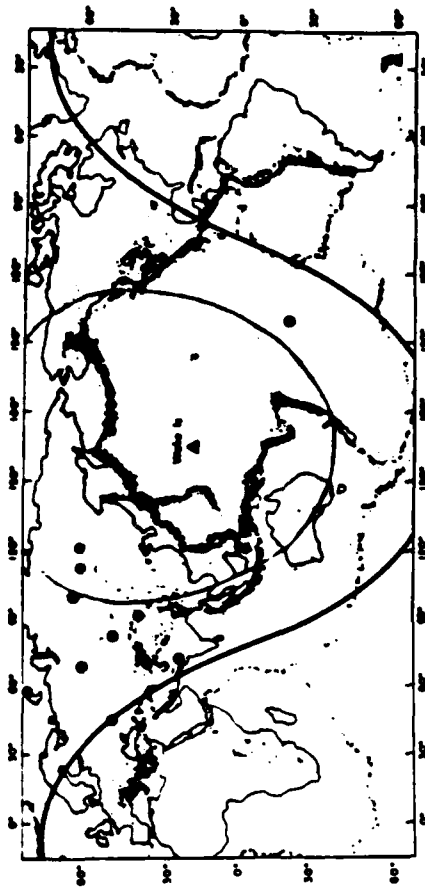
(i.e.,  $L_g$ ) from explosions and earthquakes seem to be large enough to be useful for source discrimination". [p. 589].

Could it be that  $L_g/P_g$  investigators might better understand certain aspects of  $L_g/P_g$  by turning their attention to  $Po/So$ ? Or, conversely, might  $Po/So$  investigators better understand  $Po/So$  by turning their attention to  $L_g/P_g$ ? Because of the thinness and uniformity of the oceanic crust and upper mantle under the deep ocean basins relative to that under large portions of continents, could  $Po/So$  be viewed as less adulterated (and, therefore, less complex) forms of  $L_g/P_g$ ? And, finally, could comparative studies of  $L_g/P_g$  and  $Po/So$  lead to important breakthroughs in detection and discrimination capabilities on continents and in the oceans?

In my opinion all of these questions are very important. If you share this view, I hope that you will bring the phenomenon of  $Po/So$  to the attention of your associates who may be working on  $L_g/P_g$ . I am happy to report that at least one organization (Rondout Associates Incorporated) has recognized the potential of comparative studies between  $Po/So$  and  $L_g/P_g$  in the form of a research proposal submitted to AFOSR. [Indeed, most of my views on this topic were based on discussions presented in that proposal.]

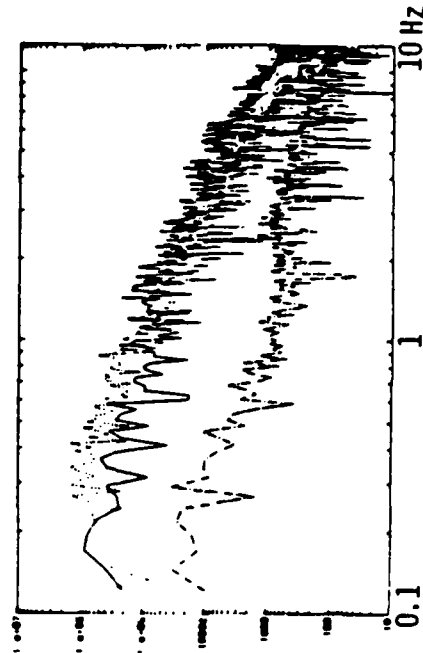
**C. Indirect - Mantle-Refracted Explosion  $P'$ 's.** Our front cover is a plot of estimated ocean bottom background noise (shaded region "A") near Wake Island compared to other measurements. [A detailed description of this figure is given at the end of the newsletter.] It is apparent from this plot that the noise levels near Wake for frequencies from about 3 to 15 Hz are comparable to, or better than, levels for some of the best continental sites. This would be of little significance if there were no signals at these frequencies. However, by some fortuitous accident of nature (my apologies to those of you who may be new to the field),  $Po/So$  phases (as has already been mentioned) have strong signals in the 4 to 8 Hz range. Further compounding this accident, (a) mantle-refracted P phases from underground nuclear explosions recorded at great distances (i.e., at distances from about  $60^\circ$  to  $90^\circ$ ) have surprisingly large amounts of energy at frequencies above 3 Hz, with higher corner frequencies than earthquakes at comparable distances; (b) explosions with smaller yields are believed to be relatively richer at higher frequencies; (c) the Wake hydrophones are ideally located in the  $60^\circ$  to  $90^\circ$  distance range from most of the known nuclear test sites (see accompanying figure: the shaded area represents the  $60^\circ$  to  $90^\circ$  distance range; solid circles represent underground nuclear test sites; the  $90^\circ$  boundary is firm since no P energy is observed beyond this distance; the  $60^\circ$  boundary is not firm since high frequency P energy has been observed at shorter distances); and, (d) ocean surface reflections can be used in signal enhancement (see back cover; a thorough description of this figure is given at the end of the newsletter).

The connection, then, is that sites ideal for the study of  $Po/So$  may also be of great value in recording underground explosions at great distances. [More detailed discussions of hydrophone recorded explosion  $P'$ 's may be found in a recent publication by McCreery et al. (1983).]

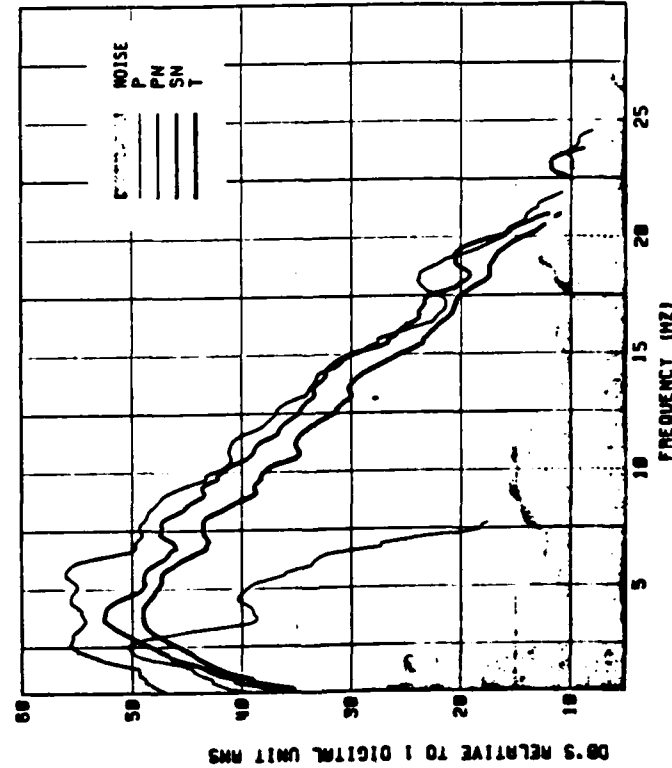


**Challenger Arrayed.** Although  $Po/So$  phases were first observed nearly fifty years ago on the east coast from an earthquake in the West Indies, I noted in the last newsletter that I had never seen spectra for  $Po/So$  phases from an Atlantic event. Therefore, in the last newsletter, east and gulf coast seismologists were "challenged" to spectrally analyze  $Po/So$  phases for Atlantic travel paths.

Surprisingly, that challenge has already been met by Rondout Associates Incorporated (RAI), and they have generously permitted the publication of their spectra in this newsletter (see accompanying figure). The event occurred near Puerto Rico ( $h = 189\text{km}$ ;  $mb = 5.7$ ) and was recorded by RAI's Catekill (New York) Seismic Array (CSA) at a distance of  $27.8^\circ$ . Shown are the ground velocity spectra for  $Po$  (solid line),  $So$  (dotted line), and background noise (dot-dash line).



Comparisons of these spectra, those on the back cover of OPA No. 1 (shown here in reduced form), and the front cover of this newsletter are most interesting. For both sets of spectra, Po's and So's are well above background noise out to about 10 Hz. The greater S/N ratios recorded on the ocean bottom (Wake hydrophone) at frequencies above 10 Hz may be the result of stronger signals, the lower noise levels of the ocean bottom at those frequencies, and/or greater attenuation of high frequencies by the continental portion of the Puerto Rico to GSA path. The greater S/N ratios recorded on the continent (GSA) at frequencies below 1 Hz is almost certainly a result of the lower noise levels of continents at those values. Therefore, the S/N ratios indicated in the spectra do appear to be consistent with the noise curves for continents and oceans shown on the front cover of this newsletter.



It is hoped that the publication of the Atlantic Po/So spectra is just the beginning of many comparative studies with Pacific Po/So phases (e.g.: velocities, spectra, Q's, effects of continental paths, structural interpretations, etc.).

**Po/So Bibliography.** Some additions to the bibliography published in the last issue of OPA can already be made. Item #1 is a tentative addition since this modeling effort is applicable only down to periods of 5 seconds and no direct references are made to the "Pn/Sn" phases observed at much higher frequencies for oceanic travel paths (i.e. Po/So). Item #3 was mistakenly omitted from the original list.

1. Menke, W., and P. Richards, 1983, The horizontal propagation of P waves through scattering media: analog model studies relevant to long-range Pn propagation, *Bull. Seismol. Soc. Amer.*, **73**, 125-142.

2. Walter, D., C. McGeery, and G. Sutton, 1983, Spectral characteristics of high-frequency Pn, Sn phases in the Western Pacific, *J. Geophys. Res.*, **88**, 4289-4298.

3. Walter, D., C. McGeery, G. Sutton, and P. Duenebier, 1978, Spectral analyses of high-frequency Pn and Sn phases observed at great distances in the Western Pacific, *Science*, **199**, 1333-1335.

**OUR COVER.** The front cover shows the average spectrum  $\pm 1$  standard deviation of 52 samples of background noise over 18 months from the Wake bottom hydrophones (A). Also shown are some published noise curves for both ocean-bottom (B, C, D, and E) and continental (F, G, and H) environments, which have been converted from an assortment of units to the scale shown. B is a hypothetical "sample spectrum of deep-sea noise" (Urick, 1975; p. 188). C is a vertical seismometer measurement made in the Mariana Basin (Asada and Shimamura, 1976). D is a vertical seismometer measurement made at 4.6-km depth between Hawaii and California (Bradner and Dodds, 1964). E is a noise curve for a hydrophone bottomed off Eleuthera Island at 1200-m depth (Nichols, 1981). F represents low, average, and high noise levels estimated from curves compiled by Brune and Oliver (1959). G is an area bounded by the limits of noise curves measured on vertical seismometers for 16 locations within the United States and Germany (Frantti et al., 1962). H is the noise curve for the Oyer subarray of the Norwegian seismic array measured during a period "when most of the North Atlantic Ocean was very quiet" (Dungum et al., 1971). The back cover shows a sample time series of P, filtered to maximize signal/noise, from two nuclear explosions recorded on the Wake bottom hydrophones. The upper trace is from a single hydrophone and shows the direct arrival and its first water surface reflection. The lower trace is a composite of signals from two hydrophones with 40-km separation, obtained as follows: the filtered (1.5-5.0 Hz) time series from each hydrophone was inverted, shifted in time by the water surface reflection time, weighted to maximize the increase in signal/noise, and added to itself; the two resulting time series were then added with the appropriate propagation delay, and weighted to maximize the increase in signal/noise. Signal/noise was increased by 90% of the theoretical maximum with this method, indicating a high level of coherence between the signals added.

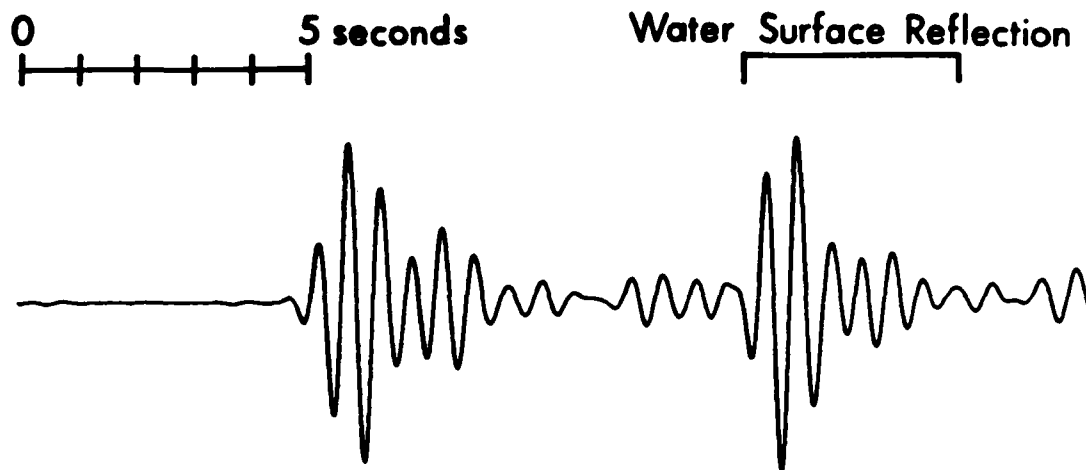
Both covers are discussed elsewhere in the newsletter. An interesting question posed by the front cover is this:

"Would instruments with responses comparable to those of the short period components of the World-Wide Seismograph Network (WWSN) be appropriate for the studies of regional and teleseismic body phases recorded on, or in, the ocean bottom?"

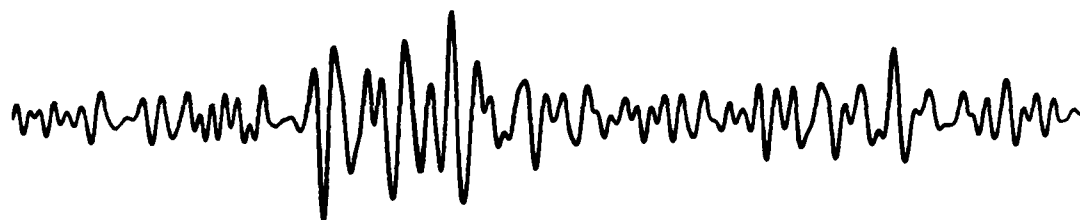
Reminder: You are invited to comment on topics presented in the newsletter and to provide other items of interest. Also, since it is difficult to be aware of all papers published in the many differing geophysical journals, advice on any omissions in the Po/So bibliography would be appreciated. Again, special thanks to RAI for sharing their Po/So spectrums with us.

#### References

- Asada, T., and H. Shimamura, 1976, Observations of earthquakes and explosions at the bottom of the western Pacific: Structure of oceanic lithosphere revealed by Longshot experiment, *The Geophysics of the Pacific Ocean Basin and Its Margins*, edited by G. H. Sutton, M. H. Manghuni, and R. Moberly, Am. Geophys. Union Monograph 19, p. 135-153.
- Bradner, H., and J. Dodds, 1966, Comparative seismic noise on the ocean bottom and land, *J. Geophys. Res.*, **62**, 4339-4348.
- Brune, J., and J. Oliver, 1959, The seismic noise of the earth's surface, *Bull. Seismol. Soc. Amer.*, **49**, 349-353.
- Bungum, H., E. Rysg, and L. Draland, 1971, Short-period seismic noise structure at Norwegian seismic array, *Bull. Seismol. Soc. Amer.*, **61**, 357-373.
- Frankti, G., D. Willis, and J. Wilson, 1962, The spectrum of seismic noise, *Bull. Seismol. Soc. Amer.*, **52**, 113-121.
- Gupta, I., and R. Blandford, 1983, A mechanism for generation of short-period transverse motion from explosions, *Bull. Seismol. Soc. Amer.*, **73**, 571-591.
- McCreery, C., D. Walker, and G. Sutton, 1983, Spectra of nuclear explosions, earthquakes, and noise from Wake Island bottom hydrophones, *Geophys. Res. Lett.*, **10**, 59-62.
- Nichols, R., 1981, Infrasonic ambient ocean noise measurements: Eleuthera, *J. Acoustical Soc. Am.*, **69**, 974-981.
- Talandier, J., and M. Bouchon, 1979, Propagation of high frequency Pn waves at great distances in the Central and South Pacific and its implications for the structure of the lower lithosphere, *J. Geophys. Res.*, **84**, 5613-5619.
- Urick, R., *Principles of Underwater Sound*, McGraw-Hill, 1975.
- Walker, D., 1977a, High-frequency Pn and Sn phases recorded in the Western Pacific, *J. Geophys. Res.*, **82**, 3350-3360.
- Walker, D., 1977b, High-frequency Pn phases observed in the Pacific at great distances, *Science*, **197**, 257-259.
- Walker, D., 1982, Oceanic Pn/Sn phases: a qualitative explanation and reinterpretation of the T-phases, *Hawaii Inst. of Geophysics Rept. HIG-82-6*, 19 pp.



7 JUL 79 EASTERN KAZAKH MB=5.8  $\Delta=73^\circ$



10 DEC 80 WESTERN SIBERIA MB=4.6  $\Delta=77^\circ$

APPENDIX IX

The Continuous Digital Data Collection System for the  
Wake Island Hydrophones

by  
Charles S. McCreery

at  
Hawaii Institute of Geophysics  
2525 Correa Road  
Honolulu, Hawaii 96822  
(808) 948-8767

## ABSTRACT

A continuous digital data collection system was installed on Wake Island in August, 1982, to record seismic signals from an array of nearby hydrophones. Most of the hardware has been purchased "off-the-shelf" from various nationally known vendors. A few components have been built at the Hawaii Institute of Geophysics (HIG). Software for both the data collection and data reduction has been written at HIG. Some key features of the data collection system are: 1) 96 dB dynamic range (i.e., 16 bits), 2) up to 16 data channels, 3) accurate absolute timing ( $\pm 1$  msec, generally), 4) accurate interchannel timing, 5) power-failure recoverability, 6) up to 80 samples per second per channel (variable), 7) ease of operation (only four operator commands necessary), 8) operator intervention only once per day (to change up to 4 full reels of 9 track tape), and 9) common tape format (blocked data, 2 bytes per word, 2's complement notation). The preliminary data reduction consists of: 1) stripping off intervals of data for which seismic phases from known events are suspected of being present; and 2) stripping off randomly spaced 3-minute intervals (1 per hour on the average) as ambient noise samples. These tasks are accomplished by a series of programs run at HIG on a Harris H800 computer. This paper is primarily intended for the reader who wants to build a digital data acquisition system, or who wants to use the data collected by this particular system at Wake.



## TABLE OF CONTENTS

Introduction .....	3
Recording System Hardware .....	5
Wake Hydrophones .....	5
Preamp/Pre-whitening Filters .....	5
A/D Convertor .....	6
Satellite Clock .....	6
A/D Sampling Pulse Generator .....	7
Mounting Enclosure .....	7
LSI-11/2 Computer .....	8
64K-byte Memory .....	8
Bootstrap Module .....	8
64 Bit I/O Controller .....	8
Floppy Disk Drive Controller .....	8
Dual 512K-byte Floppy Disk Drive .....	8
EIA Line Controller .....	9
Console and Printer .....	9
Tape Controller and Formatter .....	9
Tape Drives .....	10
2-5 Hz Filter .....	10
Helicorder Amplifier and Drum Recorder .....	10
Continuous Data Acquisition Software .....	11
WAKEUP Parameters .....	11
Digitization Rate .....	11
Seconds Per Tape Block .....	12

Channel Number .....	12
Hydrophone .....	12
Amplifier .....	12
Gain .....	12
Blocks Per Tape .....	13
Unit - Drive Serial Number .....	13
Starting Tape Unit Number .....	13
Year and Julian Day .....	13
Current WAKEUP Configuration .....	14
WAKEUP Operator Commands .....	14
Switch Drives (S) .....	14
Reset (R) .....	15
Terminate (T) .....	15
Display (D) .....	16
Power Fail Recovery .....	16
WAKEUP Log .....	16
WAKEUP Tape Format .....	17
Preliminary Data Reduction Software .....	17
WAKEUP Log Entry .....	18
Event Data Entry .....	18
XSTRIP Parameters .....	20
Extracting the Data .....	21
Events Download to Strip Tapes .....	22
Random Interval Download to Interval Tapes .....	23
Checking Procedures .....	23
Strip Tape Copies .....	25

## INTRODUCTION

In June, 1979, HIG began operation of a four-channel (3 data, 1 time-code), slow-speed, cassette recording system for continuous monitoring of hydrophones located near Wake Island. The seismic data collected from this system have provided much needed information about ambient noise in the deep ocean, Po/So propagation, and the spectra at high frequencies (i.e.,  $> 2$  Hz) of deep mantle P phases from earthquakes and explosions recorded at great distances. However, the recording system itself had limitations which prevented more quantitative types of data analysis. These limitations included: 1) a dynamic recording range of only about 40 dB - this caused many signals to be clipped; 2) poor timing due to clock drift - absolute timing was accurate to only  $\pm 0.3$  sec.; 3) poor interchannel timing - differences in skew between the recording and playback heads could easily result in a 0.1 sec. timing error between channels; 4) analog format - a sophisticated, time consuming and data degenerating process was necessary to convert the analog signals to digital time series for further processing; and 5) only three of at least eleven working hydrophones could be recorded.

To eliminate these problems, a system was sought with the following general capabilities and constraints: 1) a large dynamic range to record, without distortion, events ranging from at least  $m_b = 4.0$  to  $m_b = 8.0$  (i.e., at least 80 dB); 2) Absolute timing accurate to less than 0.1 sec (for ease in processing, no time correction should need to be applied to achieve this accuracy); 3) Interchannel timing accurate to within only a small change in phase of the highest frequency of interest (e.g., 0.002 sec for a  $\pi/8$  phase change at 30 Hz); 4) a digital recording format such that only a minimal amount of processing is necessary to convert the data to a widely

useable format; 5) the capability to record all eleven available hydrophones; 6) the recording of frequencies at least as high as those already observed at Wake in Po and So (i.e., 30 Hz); 7) operation of the system so simple that it can be accomplished by personnel untrained in computer hardware and software; 8) required servicing (i.e., changing tapes) no more than once per day; and 9) the capability of restarting automatically after power failures (which occur frequently at Wake). After exploring numerous options, a design was chosen which met the specifications outlined above, and also appeared to have the best chance for success in terms of the reliability and intercompatability of its components and the feasibility of writing the necessary data acquisition software. This system was purchased, assembled, software and tested between March and August, 1982, and was installed at Wake during the last week of August, 1982.

Because of the large volume of raw data which would be collected by this system (i.e., up to 1460 full reel, 9-track, computer tapes per year) a scheme was desired for compressing the data. Data types which were considered the highest priority for saving are: 1) seismic phases applicable to ongoing research topics, 2) ambient noise samples, and 3) seismic phases for future research topics. A system of programs was written to extract and save those intervals in the raw data which contain these priority events. These programs also manage the data for easy accessibility and transmission to other scientists.

## RECORDING SYSTEM HARDWARE

The hardware used for the digital recording system is outlined in the flow chart of Fig. 1. The hydrophone signals are first amplified and shaped by the preamps and pre-whitening filters. Two of these signals are filtered further and used to create a helicorder-style seismogram. All of the signals from the preamps are converted to discrete time series by the A/D (analog to digital) convertor. The digitized data is then assembled into blocks and output to the tape drives by the LSI-11/2 computer. The satellite clock provides a time code for the helicorder, a synchronization signal for the A/D sampling pulse generator, and the date and time in digital format for inclusion with the data blocks written to tape. A more detailed description of the function of each component in Fig. 1 is given below:

Wake Hydrophones

The hydrophones are passive, moving-coil type, which are connected via cable to Wake Island. The estimated response is shown in Fig. 2. The hydrophones are located in two arrays. One array contains six sensors on the ocean floor at 5.5 km depth, and has an aperture of 40 km. The other array consists of five hydrophone pairs at SOFAR depth (1 km) and has an aperture of 300 km. Of the ten hydrophones in the SOFAR array, at least five of them at three sites appear to be working.

Preamp/Pre-Whitening Filters (HIG built)

The preamps are designed to have very low intrinsic noise levels because the hydrophone outputs are very small [as small as  $10 \text{ nVolts}/(\text{Hz})^{1/2}$  at 10 Hz]. The pre-whitening filters are designed to flatten the ambient



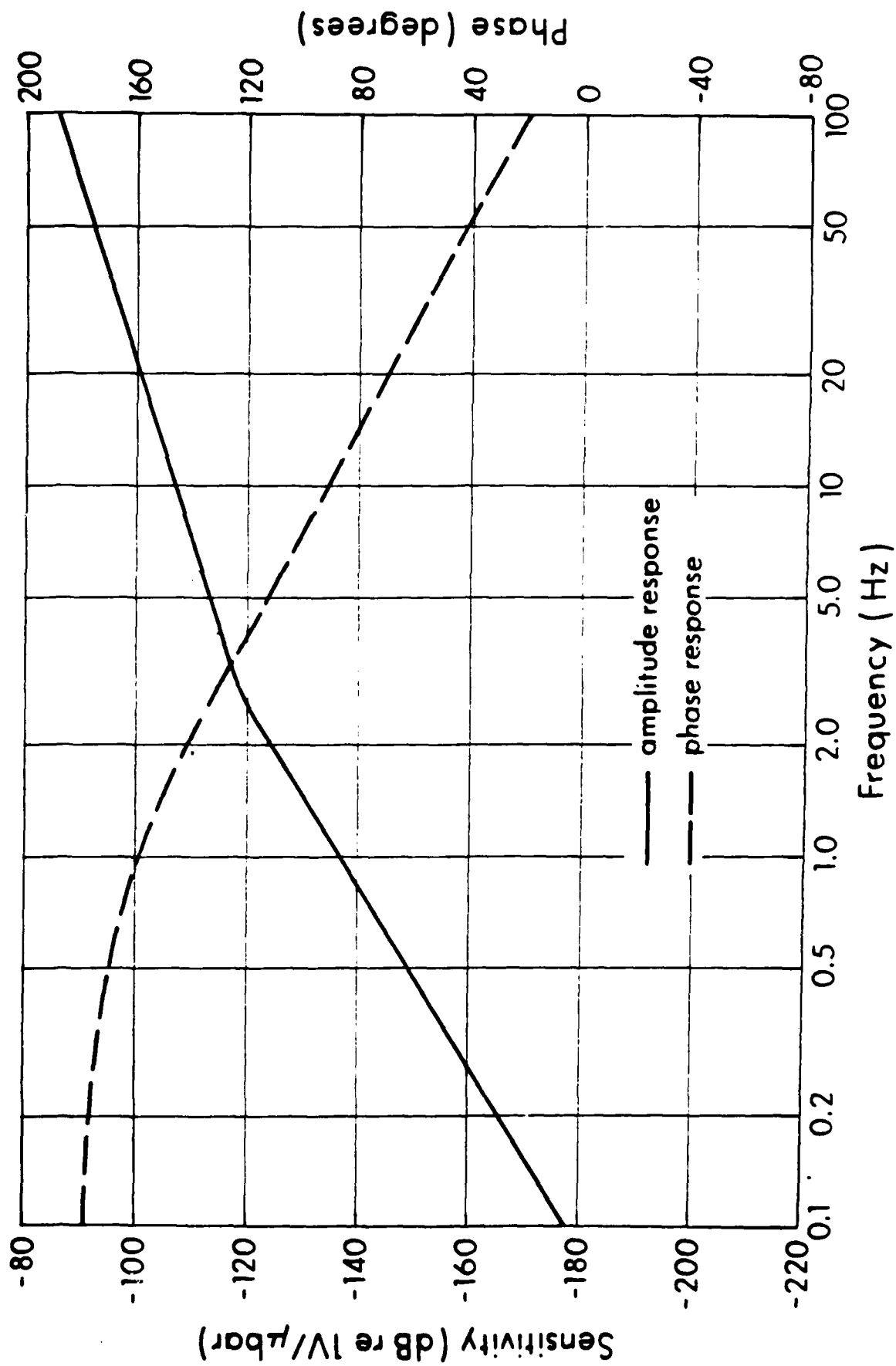


Figure 2. The estimated response of the Wake hydrophones (taken from the Columbia University's OBS Calibration Manual by S. N. Thanos, 1966).

ocean-bottom noise spectrum out of the hydrophone (measured previously using analog data), for the purpose of maximizing the dynamic recording range at all frequencies. Anti-aliasing filters and a 60 Hz notch filter are also included. The output amplifier stage has 10 gain steps (0-9), each 3 dB apart, which can be manually set. The response of the preamp/pre-whitening filters is shown in Fig. 3 (for gain step 9).

#### A/D Convertor (Data Translation Model DT2784SE/DT5716-B)

The A/D convertor is designed to fit into the backplane of the LSI-11/2 computer (i.e., into QBUS), with a cable and connector for receiving the signals to be digitized. The resolution is 16 bits, giving decimal values between -32,768 and +32,767 for inputs between -10.0 and +10.0 Volts, respectively. Up to 16 single ended inputs are acceptable, and the maximum throughput rate is 2.5 kHz (i.e., a minimum of 0.4 msec between samples). Simultaneous sample and hold of all channels is not available on this board, so the 16 channels are sampled sequentially. Furthermore, the design of this device actually requires that all 16 channels be sampled sequentially; the data of unwanted channels being discarded by the software. The trigger which causes a sample to be taken is provided externally by the A/D sampling pulse generator. An example of the temporal spacing between data points which is created by this scheme is shown in Fig. 4. Digital output from the A/D convertor is loaded directly into the LSI-11/2 core memory via direct memory access (DMA).

#### Satellite Clock (Kinematics model 468 DC)

The satellite clock provides inexpensive accurate time at a remote site by monitoring signals from the GOES satellites (East or West). Accuracy is



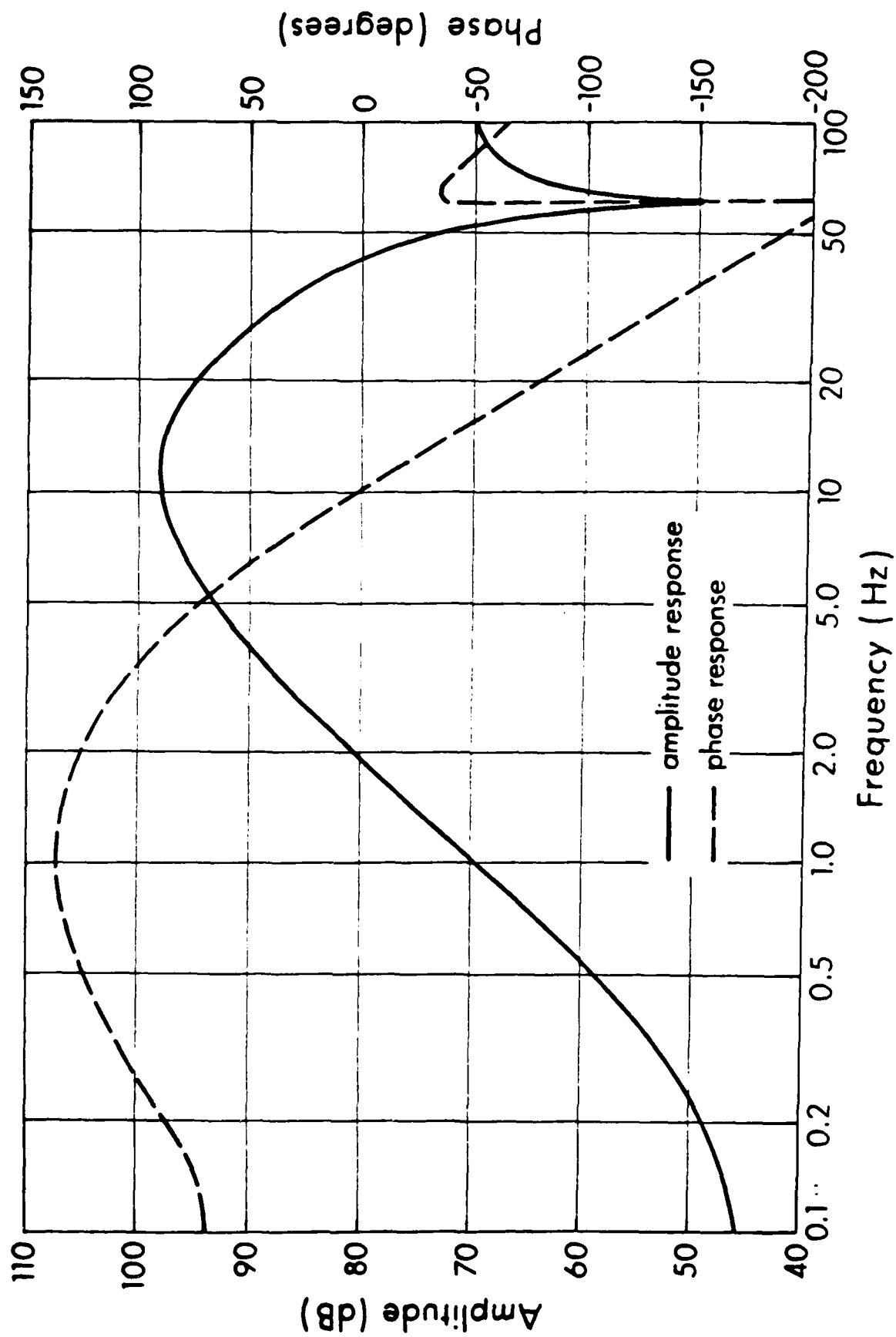


Figure 3. The response of the preamp/pre-whitening filters at gain step 9 (of 0-9). Subtract 3 dB from the amplitude response for each gain step down from 9.

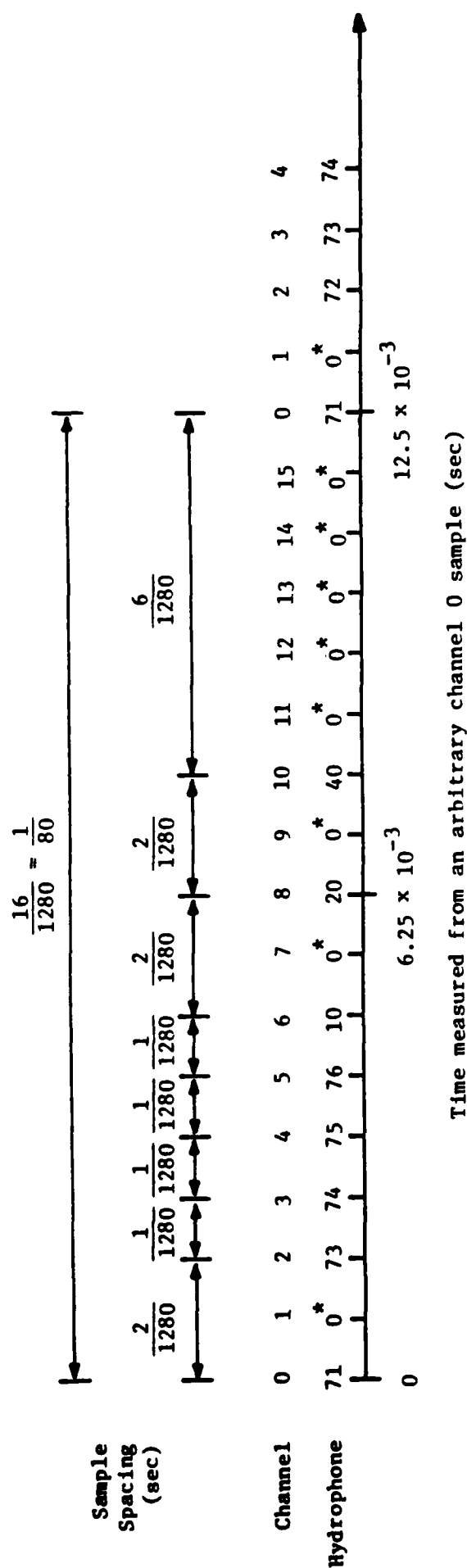


Figure 4. An example of the temporal spacing between data channels created by the data acquisition hardware and software for a sampling rate of 80 samples/second/channel. Hydrophones numbered 0 (also starred, \*) are for unwanted data channels which are sampled by the A/D converter but later discarded by the WAKEUP software. This channel/hydrophone information is written into the header part of each data block. The configuration shown is one which has been in use since the system was installed.

better than  $\pm 1$  msec when the satellite signal is being received. The time, in Julian days through milliseconds, is output in parallel BCD format through 45 pins of a 50 pin connector. This connector also contains 4 pins for the clock status (i.e., the worst case clock accuracy based on the amount of time since satellite synchronization was lost), and 1 pin with a 1 kHz square-wave used to determine when the other pins can be read (i.e., are not changing states). Also output (on BNC connectors) are a 1 Hz square-wave used to synchronize A/D sampling with the clock, and a slow code used for marking time on the helicorder record.

#### A/D Sampling Pulse Generator (HIG built)

This device is used to create precisely timed pulses (downward zero-crossings) which are synchronized with the satellite clock and trigger A/D conversions. The front panel has thumbwheel selectors for setting the number of channels of data to be sampled (always 16 in this system due to the A/D convertor; software discards unwanted channels), and the sampling rate (in samples/sec/channel). For 16 channels of data, sampled at 80 samples/sec/channel, the pulse generator produces a 1280 Hz square-wave. A/D synchronization with the clock is necessary so that the starting times of output data blocks, which are assembled for a constant number of A/D conversions, will also remain synchronized over long periods of time.

#### Mounting Enclosure (DEC model BA11-NE)

The mounting enclosure contains the power supply, backplane (QBUS), and cooling fan for the LSI-11/2 computer. The backplane has quad connectors for nine boards, all of which are occupied in this system configuration.

These nine boards, and the order in which they are placed from top to bottom in the enclosure, are noted in Fig. 1.

LSI-11/2 Computer (DEC model KD11-HA)

This is the central processing unit of the computer.

64 K-byte memory (DEC model MSV11-DD)

This is the core memory for the computer, consisting of 32K 2-byte words.

Bootstrap module (DEC model BDV11-AA)

This module brings up the computer from a down or power fail status, and causes the RT-11 operating system to be loaded from the disk.

64 Bit I/O Controller (DEC model DRV11-J)

This board is necessary to interface the LSI-11/2 with the 50 pin output of the satellite clock. The 64 bits of I/O correspond to four two-byte words which may be accessed by the software to read the clock.

Floppy Disk Drive Controller (DEC model RXV21-BA)

This board interfaces the disk drive to the computer.

Dual 512K Byte Floppy Disk Drive (DEC model RXV21-BA)

The floppy disks contain all of the software necessary for performing data acquisition with the hardware. Under the present configuration, one disk contains the DEC RT-11 operating system software, while the other disk contains the programs written at HIG for collecting the data and a

parameters file which describes the exact configuration to be run (i.e., number of channels of data, blocksize, etc.). It is possible, should one disk drive become faulty, to combine all of the programs and data on one disk, and run from a single drive. A special function of the disk drive is to record the number of the current tape drive to which the data are being written. In the case of a power failure, which causes the core memory of the LSI-11/2 to be lost, the current tape drive number is necessary to safely and efficiently resume recording.

#### EIA Line Controller (DEC model DLV11-J)

This device provides four ports (0 to 3) for serial I/O (RS-232C, RS-422, or RS-423) to the LSI-11/2. Port 3 is the only one in use under the current operating configuration and interfaces to the DEC LA38-GA which is serving as both a line printer and operator console at 300 baud. Separate ports for the line printer and a CRT operator console were used during program development to facilitate higher baud rates.

#### Console and Printer (DEC model LA38-GA)

This device is used for all operator input and output (I/O) with the system, and for all program messages. Since there is actually very little I/O to this device, its slow speed is not a problem. Also, there is a distinct advantage in having a hardcopy record of certain essential I/O, especially since the system is at a remote site. Sample I/O is shown in Fig. 5.

#### Tape Controller and Formatter (DATUM model 15221)

WAKE HYDROPHONE ARRAY CONTINUOUS DIGITAL SEISMIC RECORDING SYSTEM

USING DRIVE 2 10781 DATE 1983:153 TIME/08:06:00:000 CLOCK/00  
 USING TAPE 10781  
 DRIVE 2 END OF TAPE REACHED  
 05820 BLOCKS WRITTEN  
 USING DRIVE 3 10782 DATE/1983:153 TIME/18:10:59:999 CLOCK/00  
 USING TAPE 10782  
 DRIVE 3 END OF TAPE REACHED  
 05824 BLOCKS WRITTEN  
 DRIVE 0 OFFLINE  
 USING DRIVE 1 10783 DATE/1983:154 TIME/00:16:19:999 CLOCK/00  
 USING TAPE 10783  
 SWITCH DRIVES  
 DRIVE 1 05217 BLOCKS WRITTEN

WAKE HYDROPHONE ARRAY CONTINUOUS DIGITAL SEISMIC RECORDING SYSTEM

USING DRIVE 2 10784 DATE 1983:154 TIME/07:31:04:999 CLOCK/00  
 USING TAPE 10784  
 DRIVE 2 END OF TAPE REACHED  
 05824 BLOCKS WRITTEN  
 USING DRIVE 3 10785 DATE/1983:154 TIME/15:36:24:999 CLOCK/00  
 USING TAPE 10785  
 DRIVE 3 END OF TAPE REACHED  
 05804 BLOCKS WRITTEN  
 DRIVE 0 OFFLINE  
 USING DRIVE 1 10786 DATE/1983:154 TIME/23:40:04:999 CLOCK/00  
 USING TAPE 10786  
 RESET-WAIT FOR MINUTE  
 DRIVE 1 06065 BLOCKS WRITTEN

WAKE HYDROPHONE ARRAY CONTINUOUS DIGITAL SEISMIC RECORDING SYSTEM

USING DRIVE 2 10787 DATE 1983:155 TIME/08:11:00:000 CLOCK/00  
 USING TAPE 10787  
 DRIVE 2 END OF TAPE REACHED  
 05822 BLOCKS WRITTEN  
 USING DRIVE 3 10788 DATE/1983:155 TIME/16:16:10:000 CLOCK/00  
 USING TAPE 10788  
 DRIVE 3 END OF TAPE REACHED  
 05807 BLOCKS WRITTEN  
 DRIVE 0 OFFLINE  
 USING DRIVE 1 10789 DATE/1983:156 TIME/00:20:05:000 CLOCK/00  
 USING TAPE 10789  
 SWITCH DRIVES  
 DRIVE 1 05063 BLOCKS WRITTEN

Figure 5. A sample of 3 consecutive days of I/O through the console at Wake. Operator input has been underlined (S, R, and S). The operator writes-in the WAKEUP tape identification numbers.

The tape controller interfaces the tape drives with the LSI-11/2. Only one controller is necessary for the four tape drives used. The formatter encodes the blocks of data written to tape, and decodes the blocks read from the tape. Only one formatter is necessary for the four tape drives.

#### Tape Drives (DATUM model D451)

Four 1600 bpi tape drives (0-3) are available for writing out the digitized data. Data is written to one drive until its tape is full (or until a specified number of blocks have been written), then data is written to the next drive in the sequence until its tape is full, and so on. Four tape drives are required if tapes are changed only once per day, since one day's data (11 channels at 80 samples/sec/channel) fills four tapes. An important feature which these tape drives have, is that they re-tension the tape, advance the tape several inches for safety, and put themselves "on line" after a power failure. This is an important factor which allows the system to start collecting data again without operator intervention or the unnecessary loss of data.

#### 2-5 Hz Filter (HIG built)

The two-channel 2-5 Hz bandpass filter is for filtering the two signals going to the drum recorder in a way which enhances signal to noise ratios of teleseismic P from underground nuclear tests. The filters are a two-pole passive RC design with the response shown in Fig. 6

#### Helicorder Amplifier and Drum Recorder (Teledyne Geotech models AR-311 and RV-301)

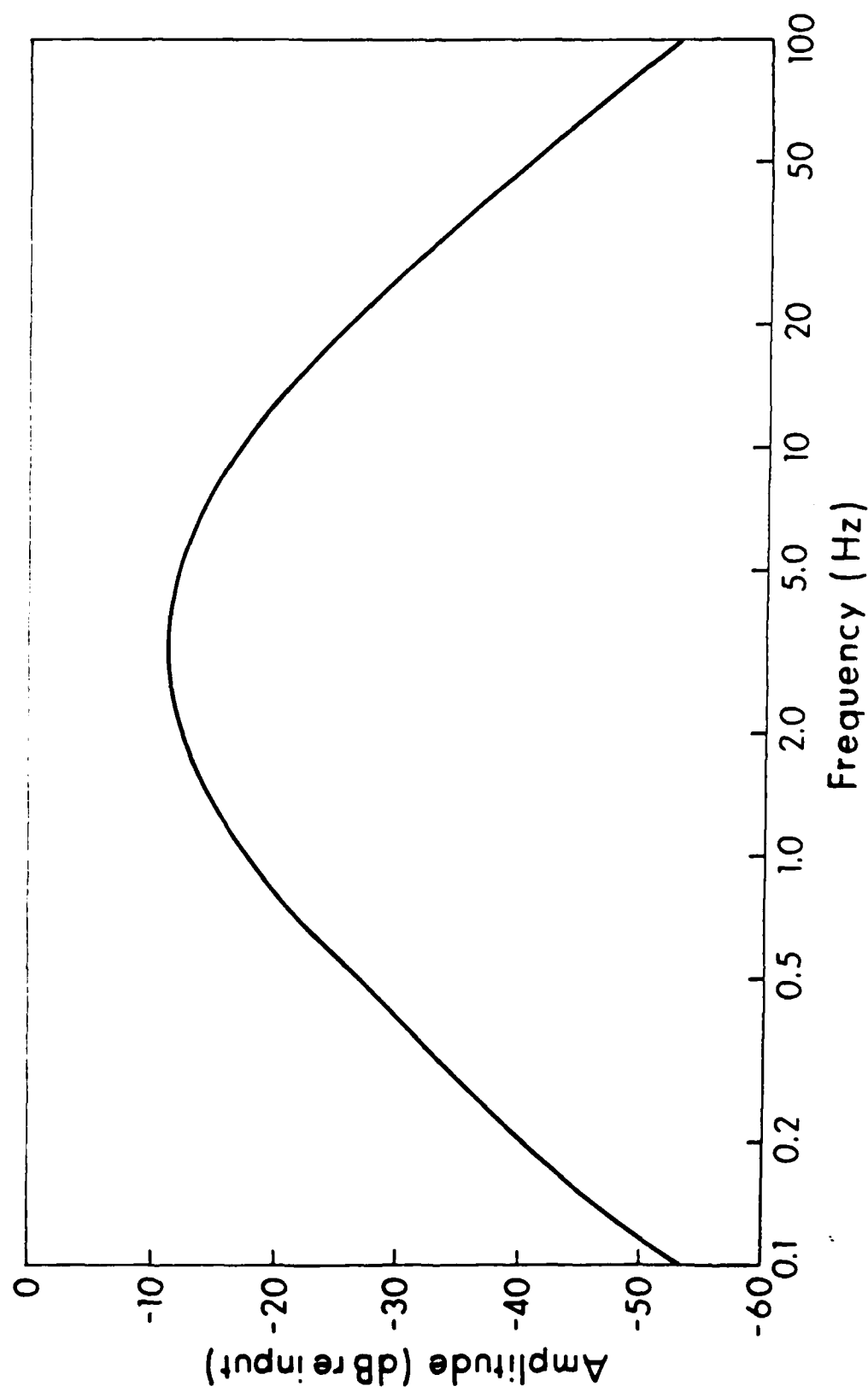


Figure 6. Response curve for the 2-5 Hz filter which precedes the helicorder.



This equipment is used to provide easily scanable visible records of the continuous seismic data. The recorder has two pens for the two input signals, and is geared so that one recording sheet lasts 24 hours. Additionally, the amplifiers and drum recorder are powered by a trickle charged, automobile battery backup system to provide continuous operation through power failures. Time code is input from the satellite clock. A sample helicorder record is shown in Fig. 7.

#### CONTINUOUS DATA ACQUISITION SOFTWARE

The data acquisition program, titled WAKEUP, is written in assembler code and executed under the RT-11 operating system. A simplified flow chart of this software is shown in Fig. 8. Some key features of program WAKEUP are: 1) it is controlled by an input parameters file which can be changed to satisfy differing data collection requirements; 2) it is extremely simple to run - only four, one-letter, operator commands (to be discussed later) are recognized; 3) it can restart itself after a power failure; and 4) it makes a hardcopy log of important program events.

#### WAKEUP Parameters

The WAKEUP running parameters can be displayed and changed by an interactive fortran program called PARAMS. A sample run of PARAMS is shown in Fig. 9. The parameters and their meanings are described below:

**Digitization Rate.** The value set here should be the same as the value set on the A/D sampling pulse generator for samples/sec/channel.

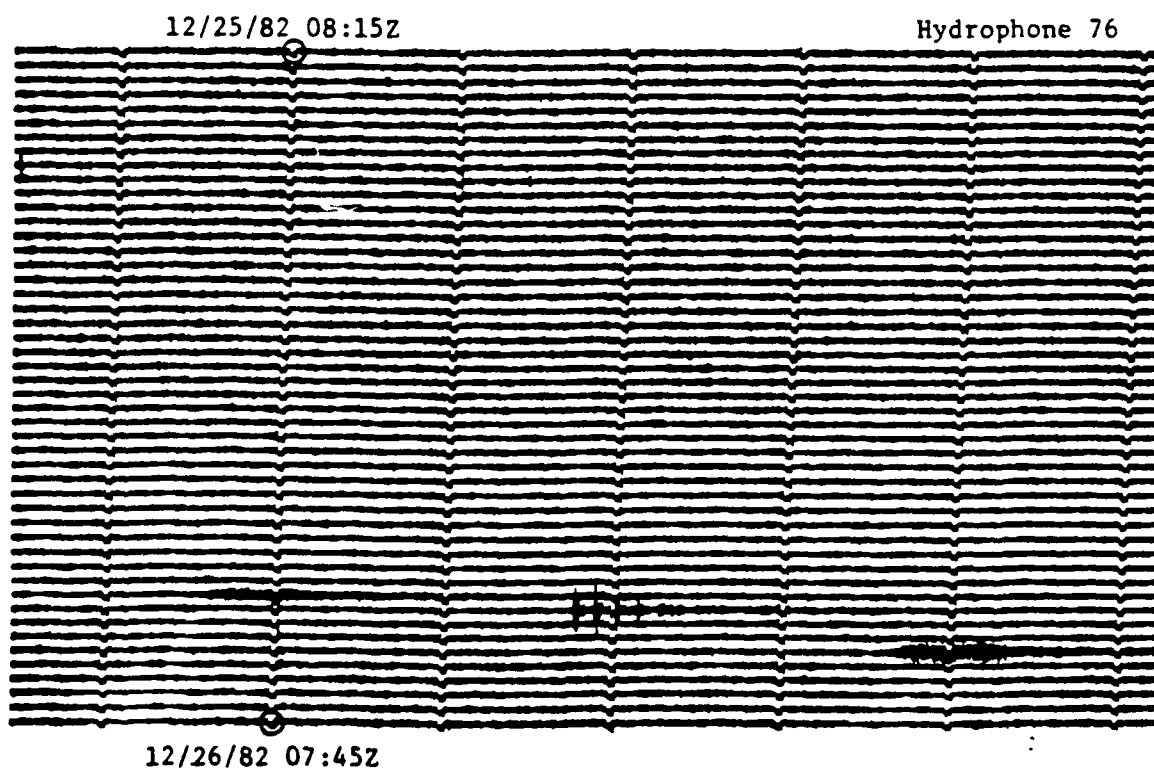
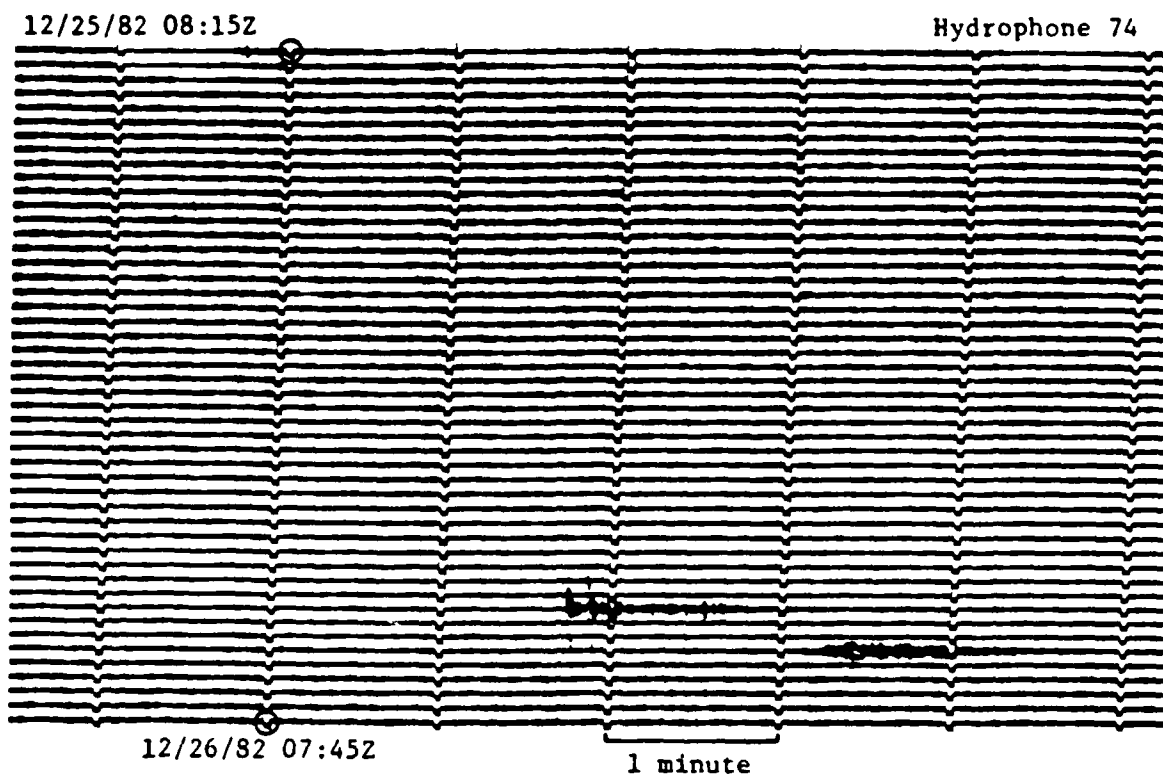


Figure 7. A section of helicorder record from Wake showing the P arrival from an Eastern Kazakh explosion (the impulsive arrival) and some other unidentified arrivals which are probably T-phases. There are 30 minutes between each trace.

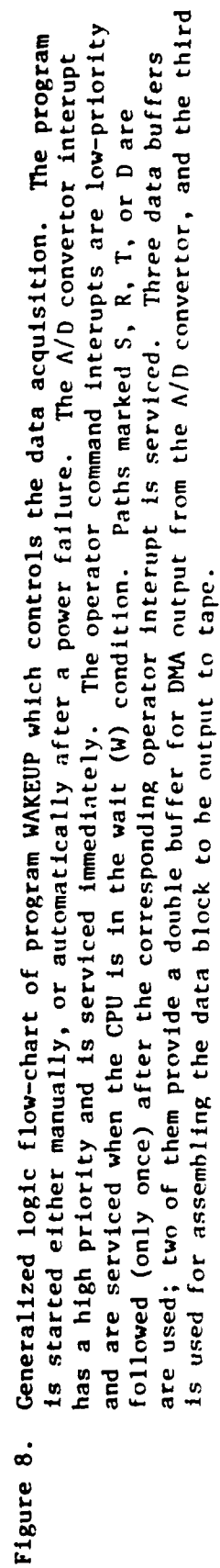


Figure 8. Generalized logic flow-chart of program WAKEUP which controls the data acquisition. The program is started either manually, or automatically after a power failure. The A/D converter interrupt has a high priority and is serviced immediately. The operator command interrupts are low-priority and are serviced when the CPU is in the wait (W) condition. Paths marked S, R, T, or D are followed (only once) after the corresponding operator interrupt is serviced. Three data buffers are used; two of them provide a double buffer for DMA output from the A/D converter, and the third is used for assembling the data block to be output to tape.

.RUN PARAMS

PARAMS - SETTING WAKEUP PARAMETERS

CURRENT PARAMETER VALUES

DIGITIZATION RATE: 80 SAMPLES/CHANNEL/SEC

SECONDS PER TAPE BLOCK: 5

CH	HYD	AMP	GN	CH	HYD	AMP	GN	CH	HYD	AMP	GN	CH	HYD	AMP	GN
0	71	6	9	1	72	8	9	2	73	9	9	3	74	0	9
4	75	19	9	5	76	1	9	6	10	13	9	7	11	16	9
8	20	11	9	9	21	3	9	10	40	18	9	11	0	0	0
12	0	0	0	13	0	0	0	14	0	0	0	15	0	0	0

BLOCKS PER TAPE: 32000

UNIT - DRIVE SERIAL NUMBER: 0-318 1-319 2-322 3-326

STARTING TAPE UNIT NUMBER: 0

YEAR: 1982 JULIAN DAY: 250

ENTER COMMAND (8 TO DISPLAY COMMANDS). 8

COMMAND - FUNCTION

- 0 - CHANGE DIGITIZATION RATE.
- 1 - CHANGE SECONDS PER BLOCK.
- 2 - CHANGE A/D CHANNEL ASSIGNMENTS.
- 3 - CHANGE BLOCKS PER TAPE.
- 4 - CHANGE TAPE UNIT SERIAL NUMBER.
- 5 - CHANGE STARTING UNIT NUMBER.
- 6 - CHANGE YEAR/JULIAN DAY.
- 7 - DISPLAY CURRENT PARAMETER VALUES.
- 8 - DISPLAY COMMAND FUNCTIONS.
- 9 - UPDATE AND DISPLAY WKPARM AND RCOVRY.
- 10 - CHANGES COMPLETE. UPDATE AND EXIT.

ENTER COMMAND (8 TO DISPLAY COMMANDS). 10

DK:WKPARM.BIN

80	400	4400	71	69	72	89	73
99	74	9	75	199	76	19	10
139	11	169	20	119	21	39	40
189	0	0	0	0	0	0	0
0	0	0	6400	32000	318	319	322
326	5	0	0	0	0	0	0

DK:RCOVRY.BIN

0	1982	250	0	0	0	0	0
0	0	0	0	0	0	0	0
0	0	0	0	0	0	0	0
0	0	0	0	0	0	0	0
0	0	0	0	0	0	0	0
0	0	0	0	0	0	0	0

DK:WKPARM.BIN AND DK:RCOVRY.BIN UPDATED.

STOP --

Figure 9. A sample run of program PARAMS which is used to change (or view) the running parameters of program WAKEUP. These parameters are stored on disk files DK:WKPARM.BIN and DK:RCOVRY.BIN. Operator commands have been underlined.

**Seconds Per Tape Block.** This value, multiplied by the sampling rate and by the number of active data channels, will determine the total number of samples per block. The number of samples per block should not exceed 5000 due to size limitations in the core memory containing the buffers. Very small block sizes should also be avoided, since the time to write a very small block to tape may exceed the time necessary to collect the data block.

**Channel Number (CH).** This is not a changeable parameter, but merely indicates which channel (0-15), of the A/D convertor, is being referred to.

**Hydrophone (HYD).** This parameter indicates which hydrophone (71-76 for the bottom array, and 10, 11, 20, 21, 40, and 41 for the SOFAR array) is connected to the A/D channel. If 0 is specified, then the channel is considered inactive. To compute the number of active channels, simply count the number of channels with non-zero values for this parameter (11 for the example in the figure). It is not necessary that the active channels be contiguous as shown in the figure.

**Amplifier (AMP).** This parameter indicates which of the preamp/pre-whitening filters (1-20) the hydrophone signal is connected to.

**Gain (GN) .** This parameter indicates the gain step (0-9) manually set on the final stage of the preamp/pre-whitening filters.

**Blocks Per Tape.** This parameter will set the number of blocks written to any tape drive before the next tape drive is used. When the value is set to a large number, as shown in the example, the program will write to a drive until the end-of-tape mark is sensed before switching drives. Estimates of how many blocks may fit on a tape can be computed by dividing the block length in bytes by 1600 bytes per inch, adding the length of the preamble, postamble and inter-record gap ( $\sim 0.6$  inches), and dividing into the tape length (28800 inches for a full-reel).

**Unit-Drive Serial Number.** This information is used to indicate which physical tape drive is connected to the tape drive unit (0-3) recognized by the computer.

**Starting Tape Unit Number.** This parameter is used to determine which tape drive to write to at the start of program WAKEUP. It is continually updated by WAKEUP to facilitate a smooth recovery after a power failure.

**Year and Julian Day -** These parameters are necessary because the satellite clock does not output the year. WAKEUP continually reads the Julian day from the parameters file and then updates it with the value output by the satellite clock. When the satellite clock Julian day is less than the Julian day in the parameters file (i.e., at the beginning of a new year), then the year is incremented by one.

Next in the example shown in Fig. 9, the user has typed 8 to display all the commands. No changes were necessary so a 10 was then typed to exit PARAMS.

The values in the parameters file (actually two files, DK:WKPARM.BIN and DK:RCOVRY.BIN) are displayed and control returned to the system.

#### Current WAKEUP Configuration

The WAKEUP configuration, set up by PARAMS, which has been in operation from 8 September 82 to the present (16 June 83) has the following key features: 1) data is digitized at a rate of 80 samples/sec/channel; 2) there are 8 active channels which are (given in the order in which they are multiplexed) 71, 73, 74, 75, 76, 10, 20, and 40 as previously described in Fig. 4; 3) each block contains 5 seconds of data which produces a block size of 3300 2-byte words (i.e., 3200 words of data plus a 100 word block header) and 4) the number of blocks per tape is large so that tapes are always written to their end-of-tape marks. Although it had been intended to digitize and record 11 hydrophones, which would produce 4 tapes per day, assorted problems with the tape drives have made it necessary to only record 8 hydrophones, which produces 3 tapes per day.

#### WAKEUP Operator Commands

Because Wake Island is such a remote place, and because those who must operate the system are untrained in computer hardware or software, program WAKEUP has been designed to handle many unusual situations without operator intervention. Only four operator commands are necessary during continuous data collection under WAKEUP, and these are described below:

**Switch Drives(S).** This command is used to force WAKEUP to write to the next available tape drive. This command is normally executed once per day when the operator comes in to change tapes. First he changes tapes on

those drives which have tapes full of data, and allows WAKEUP to continue writing onto the current drive. When fresh tapes are mounted, he executes the S, which causes WAKEUP to start writing to a fresh tape, and then he changes tapes on that last drive. A sample of S is shown in Fig. 5.

**Reset(R).** The reset command is nearly identical to the switch drives command, except that WAKEUP will wait for the satellite clock to indicate a change in the minute before it starts the A/D convertor collecting data for the next block. It is desirable to have data blocks which start on an integral second, (or integral minute) because it makes the measurement of time on plots, made later on during data reduction, somewhat simpler. Under ideal conditions, once the block beginnings are synchronized with the minute (i.e., if the number of seconds per block is 5, then all blocks should begin at 0, 5, 10, 15, 20, 25, 30, 35, 40, 45, 50, or 55 seconds after the minute) they should stay that way forever. Unfortunately, the satellite clock sometimes loses synchronization with the satellite for a while and begins to drift. When resynchronization occurs, the accumulated error gets propagated into the starting times of the blocks. When the operator notices this condition, he can correct it by using reset instead of switch drives. A sample of R is shown in Fig. 5.

**Terminate (T).** This command is used to terminate WAKEUP and return control to the RT-11 operating system.



Display (D). This command is used to display the date, time, and clock status at the beginning of the last data block collected.

### Power Fail Recovery

Probably the most harmful abnormal condition, in terms of potential loss of data, from which WAKEUP can recover without operator intervention is a power failure. Temporary periods without power are fairly common on Wake and can be due to storms, construction, and generator problems. Since an operator is only present once per day, an irrecoverable system crash due to a short power failure could cause the loss of the entire day's data. Fortunately, with the help of some unique features in the Datum tape drives (described previously), the DEC LSI-11/2 hardware, and the RT-11 operating system, it was possible to write the WAKEUP program with the capability to resume collecting data after a power failure, without wasting tape (which could cause the system to run out of tape before the operator arrived) and without writing over old data. An essential element of this recovery capability is that the particular tape drive being written to is stored on a disk file. When power comes back after a failure, WAKEUP reads this file and then resumes writing to the proper drive.

### WAKEUP Log

All operator input as well as RT-11 and WAKEUP messages and operator prompts go through the printer/console to create a log of events. A sample of this log is shown in Fig. 5, and has already been referred to several times. This log is essential for keeping track of normal system operations as well as problems which occur from time to time. The operator is

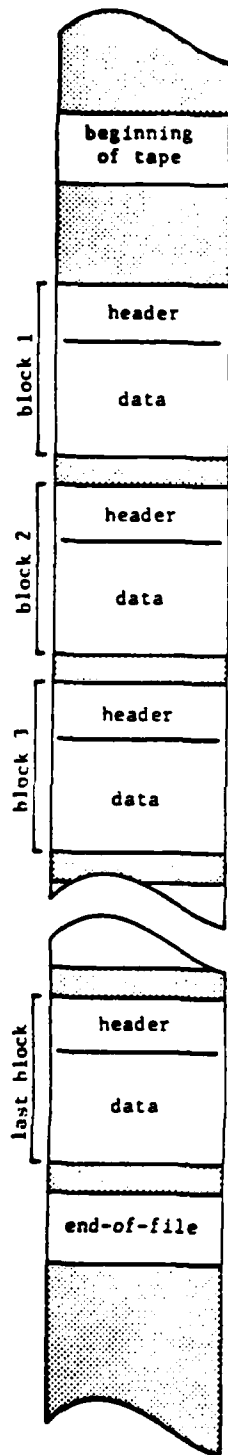
responsible for filling in the identification numbers of tapes mounted on each drive.

#### WAKEUP Tape Format

The WAKEUP tapes are numbered sequentially beginning with 10001. A detailed description of the format of the tapes and the blocks contained within the tapes is given in Fig. 10. The date and time given in the header are for the first data point in the block.

#### PRELIMINARY DATA REDUCTION SOFTWARE - WAKE HYDROPHONE INFORMATION PROCESSING SYSTEM (WHIPS)

Because of the large amount of data which is collected by this system (i.e., 50 billion bytes per year or 1500 tapes per year for 11 channels at 80 samples/sec/channel) it was realized that some sort of data compression scheme would have to be implemented in order to efficiently store, manage, retrieve, and distribute those data of current and future interest. These data have been defined in two general categories: 1) seismic phases such as P, S, Po, So, and T, and 2) ambient background noise. Software to sample these categories has been written and its structure is diagramed in the flow chart of Fig. 11. Intervals of data are saved when seismic phases from particular events are suspected of being present; and, in addition, 3-minute intervals of data selected at random times, with an average of one interval per hour, are also saved in order to sample the ambient noise. Three minutes of data is long enough to view several cycles at the longest periods thus far observed on the hydrophones - 20 seconds, and also long enough to provide reasonable statistics on the higher frequencies (1-20 Hz) where most of the oceanic, short-period seismic data are present. By sampling at



# WAKEUP Tape Description

General Format: 1600 BPI  
 2 bytes per word  
 IBM format  
 2's complement notation

All Blocks	
header: words 1-100 data: words 101-end	
Word(s)	Description
1	Year (e.g., 1983)
2	Julian day (1-366)
3	Hour
4	Minute
5	Second
6	Millisecond
7	Digitization rate (samples/sec/channel)
8	Number of samples/channel/block
9	Total number of samples/block
10-41	A/D channel information - 16 channels, 2 words per channel 1st word - hydrophone I.D. number (0 if channel not used) 2nd word - hundreds and tens digit is the amplifier I.D. number, units digit is the amplifier gain step
42	Tape unit (0-3)
43	Tape drive serial number
44	Clock status
45	A/D buffer size
46-100	Not used
101-end	Digitized hydrophone data (multiplexed-order of hydrophones is the same as the order of the active channels described in words 10-41)

Figure 10. The WAKEUP tape format.

## Wake Hydrophone Information Processing System (WHIPS)

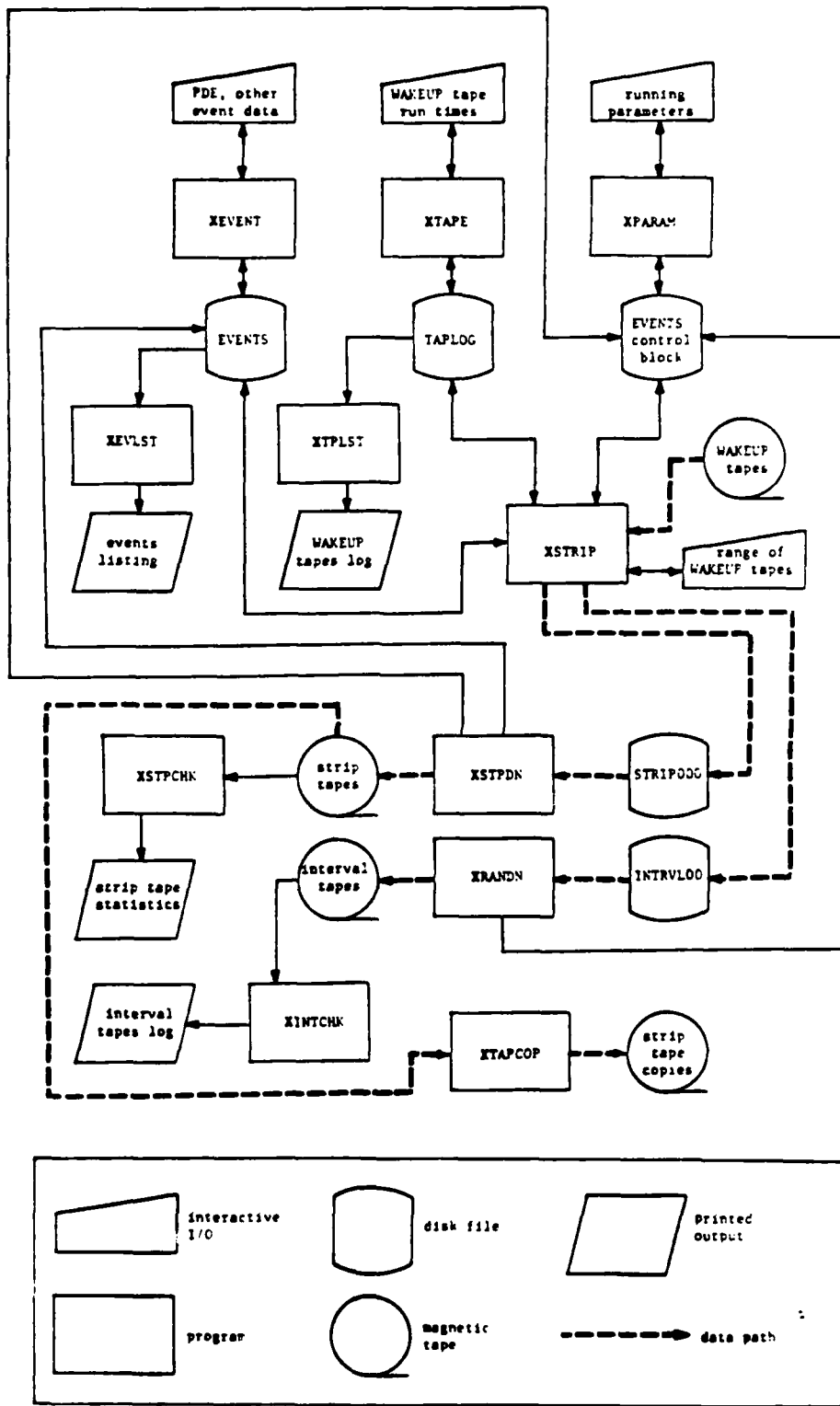


Figure 11. Generalized flow chart of the programs and files used in the preliminary reduction of the Wake digital data.

random time intervals, periodic noise of artificial nature is hopefully avoided. This system of programs and files which performs processing of the WAKEUP data is called WHIPS for Wake Hydrophone Information Processing System, and is run on a Harris model H800 computer.

#### WAKEUP Log Entry (XTAPE)

An initial step in the WHIPS procedure is to create or update file TAPLOG, which contains an identification number, starting time, block count, and status of each tape created by WAKEUP. This information is entered from the WAKEUP log (Fig. 5), using interactive program XTAPE. The data is necessary, as input to program STRIP, for calculating the time window to be processed for the compression of a given range of WAKEUP tape. Some sample data contained in TAPLOG, and printed out using program XTPLST is shown in Fig. 12. The total time represented on an individual tape can be found by multiplying the number of blocks by the number of seconds per block (which is 5 seconds per block for the tapes shown). The tape status indicates whether the tape is available for current or further processing (ACTIVE), or has been recycled (RECYCL).

#### Event Data Entry (XEVENT)

Another initial step in the WHIPS procedure is to create or update file EVENTS, which contains data about each earthquake for which an interval of data is to be saved. A sample of data contained in this file has been listed using program XEVLST and is shown in Fig. 13. Hypocenter/origin-time data are taken mostly from the Preliminary Determination of Epicenter (PDE) lists, published by the National Earthquake Information Service (NEIS), although other sources of data are used to complement the PDE's when

PAGE 001  
5 JUL 83

WAKE HYDROPHONE INFORMATION PROCESSING SYSTEM

WAKEUP TAPE LOG LIST

TAPE#	----START TIME----							#BLKS	STATUS
	YR	JLN	HR	MN	SC	MIL			
10561	83	076	05	27	25	000	5783	ACTIVE	
10562	83	076	13	29	20	000	5791	ACTIVE	
10563	83	077	05	12	40	000	5766	ACTIVE	
10564	83	077	13	13	10	000	5824	ACTIVE	
10565	83	078	05	15	15	000	5922	ACTIVE	
10566	83	078	13	28	45	000	5829	ACTIVE	
10567	83	079	04	34	45	000	5862	ACTIVE	
10568	83	079	12	43	15	000	5796	ACTIVE	
10569	83	080	05	17	25	000	5857	ACTIVE	
10570	83	080	13	25	30	000	5805	ACTIVE	
10571	83	081	06	15	50	000	5874	ACTIVE	
10572	83	081	14	25	20	000	5827	ACTIVE	
10573	83	081	22	30	55	000	4895	ACTIVE	
10574	83	082	05	18	50	000	5860	ACTIVE	
10575	83	082	13	27	10	000	5787	ACTIVE	
10576	83	082	21	29	25	000	5605	ACTIVE	
10577	83	083	05	16	30	000	5755	ACTIVE	
10578	83	083	13	16	05	000	5805	ACTIVE	
10579	83	083	21	19	50	000	5696	ACTIVE	
10580	83	084	05	14	30	000	5856	ACTIVE	

Figure 12. A sample of the WAKEUP tape information contained within WHIPS file TAPLOG which has been printed using program XTPLST. A detailed description of this printout is contained in the text.

# NAVE HYDROPHONE INFORMATION PROCESSING SYSTEM (WHIPS) EVENT LISTING

27 JUN 83

KEY: INFORMATION SOURCES - PDE=NETS PDECARD, MON=NETS MONTHLY LIST, L=LOCALS LIST, MEL=HELICORDER, OTH=OTHER  
 EVENT TYPE - E=ARTIFICIAL, M=NUCLEAR EXPLOSION, SA=SCIENTIFIC EXPLOSION, OT=OTHER, UN=UNKNOWN  
 PHASES - A=P, B=PO, C=S, D=SO, E=T, F=OTHER

EVNT	VR	MO	DA	JUL	HR	MM	SS	COORDINAT	LOC	TIME	DEP	MAGNI	INF	EV	TP	PHASES	SAVED	INTERVAL	STRIP
NO	FILE							LA	LO	LONG	TIME	TP	FILE						
0001	03	03	19	07	22	59	47.1	4.8265	151.812E	NW IRELAND REGION	119	4.9	0.0	PDE	TO A	21:00-23:15	15	200421-11	
0002	03	03	19	07	22	59	47.1	4.8265	151.812E	NW IRELAND REGION	119	4.9	0.0	PDE	TO A	21:00-23:15	15	200421-11	
0003	03	03	20	07	13	45	49.8	4.7275	153.125E	NW IRELAND REGION	119	4.9	0.0	PDE	TO A	21:00-23:15	15	200421-11	
0004	03	03	20	07	13	45	49.8	4.7275	153.125E	NW IRELAND REGION	119	4.9	0.0	PDE	TO A	21:00-23:15	15	200421-11	
0005	03	03	20	07	13	45	49.8	4.7275	153.125E	NW IRELAND REGION	119	4.9	0.0	PDE	TO A	21:00-23:15	15	200421-11	
0006	03	03	20	07	13	45	49.8	4.7275	153.125E	NW IRELAND REGION	119	4.9	0.0	PDE	TO A	21:00-23:15	15	200421-11	
0007	03	03	20	07	13	45	49.8	4.7275	153.125E	NW IRELAND REGION	119	4.9	0.0	PDE	TO A	21:00-23:15	15	200421-11	
0008	03	03	20	07	13	45	49.8	4.7275	153.125E	NW IRELAND REGION	119	4.9	0.0	PDE	TO A	21:00-23:15	15	200421-11	
0009	03	03	20	07	13	45	49.8	4.7275	153.125E	NW IRELAND REGION	119	4.9	0.0	PDE	TO A	21:00-23:15	15	200421-11	
0010	03	03	20	07	13	45	49.8	4.7275	153.125E	NW IRELAND REGION	119	4.9	0.0	PDE	TO A	21:00-23:15	15	200421-11	
0011	03	03	20	07	13	45	49.8	4.7275	153.125E	NW IRELAND REGION	119	4.9	0.0	PDE	TO A	21:00-23:15	15	200421-11	
0012	03	03	20	07	13	45	49.8	4.7275	153.125E	NW IRELAND REGION	119	4.9	0.0	PDE	TO A	21:00-23:15	15	200421-11	
0013	03	03	20	07	13	45	49.8	4.7275	153.125E	NW IRELAND REGION	119	4.9	0.0	PDE	TO A	21:00-23:15	15	200421-11	
0014	03	03	20	07	13	45	49.8	4.7275	153.125E	NW IRELAND REGION	119	4.9	0.0	PDE	TO A	21:00-23:15	15	200421-11	
0015	03	03	20	07	13	45	49.8	4.7275	153.125E	NW IRELAND REGION	119	4.9	0.0	PDE	TO A	21:00-23:15	15	200421-11	
0016	03	03	20	07	13	45	49.8	4.7275	153.125E	NW IRELAND REGION	119	4.9	0.0	PDE	TO A	21:00-23:15	15	200421-11	
0017	03	03	20	07	13	45	49.8	4.7275	153.125E	NW IRELAND REGION	119	4.9	0.0	PDE	TO A	21:00-23:15	15	200421-11	
0018	03	03	20	07	13	45	49.8	4.7275	153.125E	NW IRELAND REGION	119	4.9	0.0	PDE	TO A	21:00-23:15	15	200421-11	
0019	03	03	20	07	13	45	49.8	4.7275	153.125E	NW IRELAND REGION	119	4.9	0.0	PDE	TO A	21:00-23:15	15	200421-11	
0020	03	03	20	07	13	45	49.8	4.7275	153.125E	NW IRELAND REGION	119	4.9	0.0	PDE	TO A	21:00-23:15	15	200421-11	
0021	03	03	20	07	13	45	49.8	4.7275	153.125E	NW IRELAND REGION	119	4.9	0.0	PDE	TO A	21:00-23:15	15	200421-11	
0022	03	03	20	07	13	45	49.8	4.7275	153.125E	NW IRELAND REGION	119	4.9	0.0	PDE	TO A	21:00-23:15	15	200421-11	
0023	03	03	20	07	13	45	49.8	4.7275	153.125E	NW IRELAND REGION	119	4.9	0.0	PDE	TO A	21:00-23:15	15	200421-11	
0024	03	03	20	07	13	45	49.8	4.7275	153.125E	NW IRELAND REGION	119	4.9	0.0	PDE	TO A	21:00-23:15	15	200421-11	
0025	03	03	20	07	13	45	49.8	4.7275	153.125E	NW IRELAND REGION	119	4.9	0.0	PDE	TO A	21:00-23:15	15	200421-11	
0026	03	03	20	07	13	45	49.8	4.7275	153.125E	NW IRELAND REGION	119	4.9	0.0	PDE	TO A	21:00-23:15	15	200421-11	
0027	03	03	20	07	13	45	49.8	4.7275	153.125E	NW IRELAND REGION	119	4.9	0.0	PDE	TO A	21:00-23:15	15	200421-11	
0028	03	03	20	07	13	45	49.8	4.7275	153.125E	NW IRELAND REGION	119	4.9	0.0	PDE	TO A	21:00-23:15	15	200421-11	
0029	03	03	20	07	13	45	49.8	4.7275	153.125E	NW IRELAND REGION	119	4.9	0.0	PDE	TO A	21:00-23:15	15	200421-11	
0030	03	03	20	07	13	45	49.8	4.7275	153.125E	NW IRELAND REGION	119	4.9	0.0	PDE	TO A	21:00-23:15	15	200421-11	
0031	03	03	20	07	13	45	49.8	4.7275	153.125E	NW IRELAND REGION	119	4.9	0.0	PDE	TO A	21:00-23:15	15	200421-11	
0032	03	03	20	07	13	45	49.8	4.7275	153.125E	NW IRELAND REGION	119	4.9	0.0	PDE	TO A	21:00-23:15	15	200421-11	
0033	03	03	20	07	13	45	49.8	4.7275	153.125E	NW IRELAND REGION	119	4.9	0.0	PDE	TO A	21:00-23:15	15	200421-11	
0034	03	03	20	07	13	45	49.8	4.7275	153.125E	NW IRELAND REGION	119	4.9	0.0	PDE	TO A	21:00-23:15	15	200421-11	
0035	03	03	20	07	13	45	49.8	4.7275	153.125E	NW IRELAND REGION	119	4.9	0.0	PDE	TO A	21:00-23:15	15	200421-11	
0036	03	03	20	07	13	45	49.8	4.7275	153.125E	NW IRELAND REGION	119	4.9	0.0	PDE	TO A	21:00-23:15	15	200421-11	
0037	03	03	20	07	13	45	49.8	4.7275	153.125E	NW IRELAND REGION	119	4.9	0.0	PDE	TO A	21:00-23:15	15	200421-11	
0038	03	03	20	07	13	45	49.8	4.7275	153.125E	NW IRELAND REGION	119	4.9	0.0	PDE	TO A	21:00-23:15	15	200421-11	
0039	03	03	20	07	13	45	49.8	4.7275	153.125E	NW IRELAND REGION	119	4.9	0.0	PDE	TO A	21:00-23:15	15	200421-11	
0040	03	03	20	07	13	45	49.8	4.7275	153.125E	NW IRELAND REGION	119	4.9	0.0	PDE	TO A	21:00-23:15	15	200421-11	
0041	03	03	20	07	13	45	49.8	4.7275	153.125E	NW IRELAND REGION	119	4.9	0.0	PDE	TO A	21:00-23:15	15	200421-11	
0042	03	03	20	07	13	45	49.8	4.7275	153.125E	NW IRELAND REGION	119	4.9	0.0	PDE	TO A	21:00-23:15	15	200421-11	
0043	03	03	20	07	13	45	49.8	4.7275	153.125E	NW IRELAND REGION	119	4.9	0.0	PDE	TO A	21:00-23:15	15	200421-11	
0044	03	03	20	07	13	45	49.8	4.7275	153.125E	NW IRELAND REGION	119	4.9	0.0	PDE	TO A	21:00-23:15	15	200421-11	
0045	03	03	20	07	13	45	49.8	4.7275	153.125E	NW IRELAND REGION	119	4.9	0.0	PDE	TO A	21:00-23:15	15	200421-11	
0046	03	03	20	07	13	45	49.8	4.7275	153.125E	NW IRELAND REGION	119	4.9	0.0	PDE	TO A	21:00-23:15	15	200421-11	
0047	03	03	20	07	13	45	49.8	4.7275	153.125E	NW IRELAND REGION	119	4.9	0.0	PDE	TO A	21:00-23:15	15	200421-11	
0048	03	03	20	07	13	45	49.8	4.7275	153.125E	NW IRELAND REGION	119	4.9	0.0	PDE	TO A	21:00-23:15	15	200421-11	
0049	03	03	20	07	13	45	49.8	4.7275	153.125E	NW IRELAND REGION	119	4.9	0.0	PDE	TO A	21:00-23:15	15	200421-11	
0050	03	03	20	07	13	45	49.8	4.7275	153.125E	NW IRELAND REGION	119	4.9	0.0	PDE	TO A	21:00-23:15	15	200421-11	

Figure 13. A sample of event information contained within WHIPS file EVENTS, which has been printed using program XEVLST. A detailed description of this printout is contained in the text.

Reproduced from  
best available copy.

necessary. A general procedure has been formulated for determining which events from the PDE lists might produce seismic energy observable at Wake, based on experience gained from scanning the analog data collected since 1979. An outline of event types and their corresponding phases is presented in Fig. 14. Intervals to save for these events and phases are computed automatically by program XEVENT, at the time the hypocenter data are entered, and may be altered manually if necessary. The only seismic energy from events which is deliberately discarded is that of T-phases from smaller magnitude and unknown events. T-phase energy is generally so abundant (it is estimated that at least 10 times as many circum-Pacific events may be detected using T-phases than may be detected using other seismic phases) that very little data compression would be possible if all of these T-phase data were saved. This procedure is weighted towards saving more data than necessary (i.e., many of these events may not have observable energy at Wake, but this is hard to determine without scanning all the channels in particular frequency bands) so that a) unusual events are not discarded, b) data from small events may be enhanced with array processing, and c) data from events which are not of current interest but may be of future interest are saved. The helicorder records from Wake are also scanned for seismic phases such as P, Po, S, and So which do not correspond to known events, and intervals are saved to capture these phases. Two such intervals, corresponding to events 820 and 826, appear in Fig. 13. The final column of the listing shown in Fig. 13 gives the strip tape and file number which contains the corresponding interval of data. Some data intervals are contiguous or overlap and have therefore been saved in a single file (for example: events 807 and 808, and events 813 and 814). Other events have not yet been extracted from the WAKEUP tapes and are noted



Source Region(s)	Magnitude	Depth(km)	$\sim \Delta$	Phases
1. Nuclear Explosions Anywhere	all	all	$0^{\circ}-35^{\circ}$	P,Po,So,T
	all	all	$> 35^{\circ}$	P
2. Mariana Is., Bonin Is., Volcano Is., Honshu, and Gilbert Islands	$m_b < 5.0$	$<100$	$18^{\circ}-25^{\circ}$	P,Po,So
	$m_b > 5.0$	$<100$	$18^{\circ}-25^{\circ}$	P,Po,So,T
	all	$>100$	$18^{\circ}-25^{\circ}$	P,Po,So,T
3. Kuril Is., Kamchatka, Aleutian Is., New Guinea, New Britain, Solomon Is., and Santa Cruz Islands	$m_b > 5.0$	$<100$	$25^{\circ}-35^{\circ}$	P,Po,So,T
	all	$>100$	$25^{\circ}-35^{\circ}$	P,Po,So,T
4. Asian Continent	$m_b > 4.5$	all	$30^{\circ}-90^{\circ}$	P
5. Mid Pacific Plate Events	all	all	$0^{\circ}-35^{\circ}$	P,Po,So,T
	$m_b > 4.5$	all	$>35^{\circ}$	P,Po,So,T
6. Not Regions 2, 3, 4, or 5.	$m_b > 5.0$	all	$<90^{\circ}$	P
7. Mid Atlantic Antipode	all	all	$340^{\circ}-360^{\circ}$	P
8. Anywhere	$M > 6.0$	all	all	P
	$m_b > 6.5$	all	$340^{\circ}-360^{\circ}$	P

Figure 14. The general criteria used for deciding which phases (if any) to save for a known event. Time intervals which contain those phases are computed automatically by XEVENT or may be entered manually.

by a tape and file number of 0 (such as event 850). Some events, such as 801, 806, and 811, could not be extracted because there was no WAKEUP data available (in this case, due to a tape drive failure at WAKE). A file for these events, containing only header and trailer records, exists on the strip tape indicated, and the file number has been flagged as negative on the XEVLST listing.

#### XSTRIP Parameters (XPARAM)

The last initial step in the WHIPS procedure is to set up the running parameters for program XSTRIP which are stored in the header block of the EVENTS file. These parameters may be viewed and changed using program XPARAM, and a sample output from this program is shown in Fig. 15. Many of these parameters (D, E, F, G, H, and I) are continually updated by programs XSTRIP, XSTPDN, and XRANDN; and these parameters may be changed manually when necessary. Other parameters (A, B, and C) must always be entered and changed manually as the situation warrants. The "WAKEUP tape record length" (A) is equal to the WAKEUP sampling rate times the number of channels, times the number of seconds per block, plus 100 words for the block header (i.e.,  $[80 \times 8 \times 5] + 100 = 3300$ ). The "strip/interval disk record length" (A) is the block length used for disk files STRIP000 and INTRVL00; and it must be a multiple of 112 words (Harris sector size = 112 words) which is greater than or equal to the WAKEUP tape record length. The "maximum records ..." (B) is a conservative estimate of how many blocks of data (in this case, 3300 word blocks), will fit onto a tape created by XSTPDN or XRANDN. This parameter is necessary for XSTPDN to organize its output data so that individual intervals which are saved do not cross XSTPDN tape boundaries. The "seconds per WAKEUP tape block" (C) is used to convert terms which refer to a

A.	WAKEUP TAPE RECORD LENGTH IS	3300
	STRIP/INTERVAL DISC RECORD LENGTH IS	3360
B.	MAXIMUM RECORDS ON EVENT/INTERVAL TAPE IS	5580
C.	SECONDS PER WAKEUP TAPE BLOCK IS	5
D.	NEXT WAKEUP TAPE TO STRIP IS	10588
	LAST WAKEUP TAPE TO STRIP IS	0
E.	LAST RECORD ON STRIP DISC FILE IS	0
F.	CURRENT STRIP TAPE NUMBER IS	20044
	LAST FILE WRITTEN IS	5
	NUMBER OF TAPE RECORDS IS	1222
G.	LAST RECORD ON INTERVAL DISC FILE IS	0
H.	CURRENT INTERVAL TAPE NUMBER IS	30029
	NUMBER OF TAPE RECORDS IS	3856
I.	RANDOM INTERVAL	26266680000000 2626668179995

ENTER A-J, U (UPDATE), OR X (EXIT).

Figure 15. A part of the interactive I/O generated by WHIPS program XPARAM which is used to view or change the running parameters of program XSTRIP. More detailed explanation of these parameters is given in the text.

particular block on a WAKEUP tape into absolute times (for example - to calculate the ending time of a WAKEUP tape, given its starting time and total number of blocks). The "next" and "last WAKEUP tape to strip"

(D) refers to the range of WAKEUP tapes which are to be processed during a particular run of XSTRIP. These parameters are continually updated during the XSTRIP run to facilitate recovery in case of a system crash. At the completion of the run, the last tape which was processed becomes the "next WAKEUP tape to strip", and the "last WAKEUP tape to strip" is set to 0, as shown in the figure. The "last record on the strip disk file" (E) allows XSTRIP to begin writing into STRIP000 where it last left off. This parameter is set to 0 after a successful downloading of the data using XSTPDN, as is shown in the figure. The "current strip tape", "last file", and "number of tape records" (F), allows XSTPDN to download the data onto tape from the point on the tape at which it left off after the last run. G and H serve the same function for the random interval data as did E and F for the stripped events data. The "random interval" (I) gives the 3 minute time range, in century-milliseconds, of the next random interval to be stripped.

#### Extracting the data (XSTRIP)

XSTRIP is the program which extracts and stores data of events and of random intervals on disk for later downloading. The only operator input required is specification of the range of WAKEUP tapes to be processed. Normally, this processing takes place in contiguous chronological order. After the total time interval represented by the WAKEUP tapes has been computed from the TAPLOG file, a search of the EVENTS file is made to determine which event intervals, not yet extracted, lie entirely within the

total time interval. From these individual event intervals, grand intervals are computed which combine the times of overlapping event intervals. As the WAKEUP tapes are read one by one (the operator is prompted to mount each tape), the grand intervals are extracted and stored on disk file STRIP000. Concurrently, the random, three-minute intervals are being extracted and stored on disk file INTRVL00. The timing of these intervals is computed "on the fly" and the number of minutes of data between the beginnings of one 3-minute interval and the next is computed using a random variable with a uniform distribution between 3 (i.e., no overlap) and 117, giving an average separation of 60 minutes. The parameters list at the beginning of the EVENTS file is updated after the extraction of each grand interval and each random interval. This facilitates a smooth and efficient recovery after an XSTRIP abortion of any kind and provides information for later downloading of the data to tape. XSTRIP is complete after the last WAKEUP tape has been run. It should be noted that a typical XSTRIP run at HIG processes from 10 to 20 WAKEUP tapes, and requires approximately 20 million words of disk storage for the STRIP000 and INTRVL00 files.

#### Events Download to Strip Tapes (XSTPDN)

The STRIP000 disk file containing the event data is downloaded to tape using program XSTPDN. This program first accesses the running parameters in the EVENT file to find out which tape to download to, and how many files to advance into that tape before writing. As each grand interval in the STRIP000 file is downloaded to tape, the running parameters are updated, and the EVENTS file is updated with the strip tape number and file for those events contained in the grand interval. If the grand interval contains too many records to completely fit on the strip tape (based on "B" in the

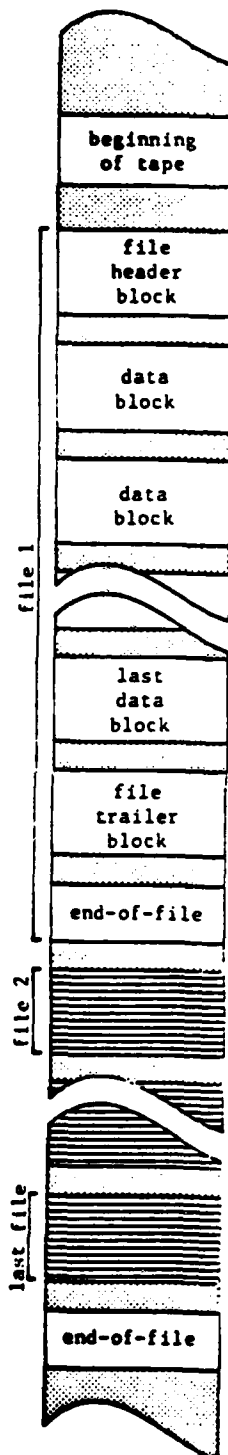
running parameters). then an end-of-file is written to the strip tape and a new strip tape is mounted following a prompt to the operator. Strip tapes are numbered sequentially beginning with 20001. The XSTPDN run is complete when all the grand intervals have been downloaded. and at that time the "last record on strip disk file" (E) in the running parameters is set to 0 as shown in Fig. 15. The format of the strip tape, and format of the blocks contained on the strip tape is given in Fig. 16.

#### Random Interval Download to Interval Tapes (XRANDN)

The INTRVL00 disk file, containing the 3-minute randomly spaced ambient noise samples, is downloaded to tape using program XRANDN. This program first accesses the running parameters to determine which interval tape to download to, and how many records from the INTRVL00 file to tape until the maximum number of records on tape ("B" in the running parameters) is reached. There are no end-of-files between the 3-minute intervals, however, an end-of-file is written after the last record on the interval tape. Interval tapes are numbered sequentially beginning with 30001. The XRANDN run is complete when all of the records in INTRVL00 have been downloaded, at which time item "G" in the running partameters is set to 0 as shown in Fig. 15. The format of the interval tape, and the format of the blocks contained on the interval tape is given in Fig. 17.

#### Checking Procedures (XSTPCHK and XINTCHK)

As a safety measure, and as a way of accumulating some preliminary statistics on the data, all strip and interval tapes are checked using programs XSTPCHK and XINTCHK. respectively. The outputs from these programs are viewed before the STRIP000 and INTRVL00 files are eliminated from disk



### WHIPS Strip Tape Description

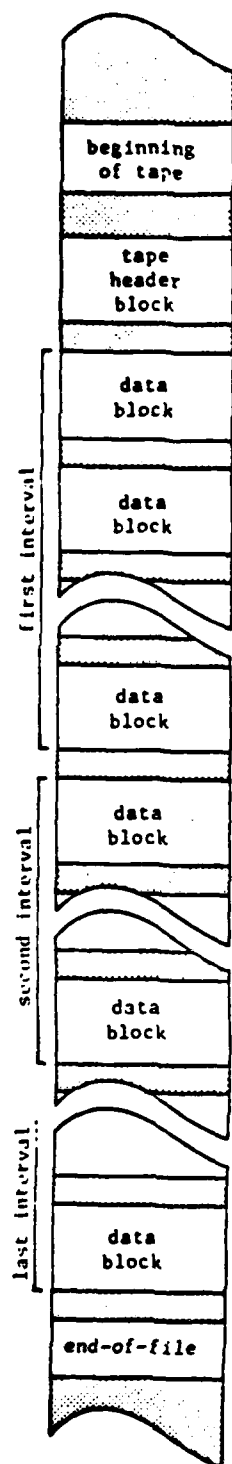
General Format: 1600 BPI  
 2 bytes per word  
 IBM format  
 2's complement notation

File Header Block	
Word(s)	Description
1	Always 0 to identify block as a header/trailer
2	Strip tape I.D. number
3	Strip file number
4-56	Not used
57	Estimated number of data block in this file
58-62	Not used
63	Total number of events (n) represented in this file
64-100	Not used
101-(101+n)	Event number(s)
(102+n)-end	Not used
Note: header block is the same size as the data block	

Data Block
The format of the strip tape data blocks is exactly the same as the format of the WAKEUP tape blocks.

File Trailer Block	
Word(s)	Description
1-3	Same as header block words 1-3
4-56	Not used
57	Actual number of data blocks in file
58	Number of words per block
59-63	Same as header block words 59-63
64-65	WAKEUP tape I.D. number(s)
66	Number of WAKEUP tape read errors
67-86	Block numbers with WAKEUP tape read errors
87-end	Same as header block words 87-end
Note: trailer block is the same size as the data block.	

Figure 16. Format for the WHIPS strip tapes which contain the event data.



#### WHIPS Interval Tape Description

General Format: 1600 BPI  
 2 bytes per word  
 IBM format  
 2's complement notation

Tape Header Block	
Word(s)	Description
1	Always 0 to identify block as a tape header
2	Interval tape I.D. number
3-end	Not used
Note: tape header block is the same size as the data block	

Data Block
The format of the interval tape data blocks is exactly the same as the format of the WAKEUP tape blocks.

Figure 17. Format for the WHIPS interval tapes which contain randomly spaced 3-minute intervals of data (1 per hour on the average) which are collected as noise samples.



and the WAKEUP tapes recycled. A sample output from XSTPCHK is shown in Fig. 18. Most of the lines of output are self-explanatory. The "error blocks" are for blocks of data which had tape read errors coming off of the WAKEUP tapes during XSTRIP. The "clipped data" lines show the number of data points in a particular block, and for a particular channel, which are equal to -32,768 or 32,767, the maximum and minimum values output by the A/D convertor at Wake. The clipped data in this file is on two SOFAR hydrophones and corresponds to the T-phase arrival from event 824 (see Fig. 11 for event 824). The table of values gives information about each multiplexed in the file which is described as follows: 1) "ch" - multiplexed channel number; 2) "hydr" - hydrophone number; 3) "amp" - preamp/pre-whitening filter identification number; 4) "gain" - gain step of the final stage of the preamp/pre-whitening filter (see previous section on the recording system); 5) "avgval" - the average value of this channel (non-zero due to small but constant DC biases in the amplifiers); 6) "stddev" - the standard deviation of each channel (note the much higher values for the noisier SOFAR hydrophones); 7) "0/blk" - average number of zeros per block (note that channel 3 has most zeros due to its near zero average value and small standard deviation); 8) "0/blk/std" - the standard deviation of the number of zeros per block; and 9) "# clips" - the total number of clipped data points for this channel in this file. The "worst case clock error code" indicates the maximum error between the satellite clock time written in each block header and the actual coordinated Universal Time. The codes are as follows:

0 - less than + 1 msec

1 - less than + 5 msec

```

TAPE FILE NUMBER:      8
WHIPS STRIP TAPE: 20043 WHIPS FILE:      8
NUMBER OF EVENTS IN THIS FILE:      1
EVENT NUMBER(S):      824
NUMBER OF ERRORS READING WAKEUP TAPE(S):      0
ERROR BLOCKS:
NUMBER OF MULTIPLEXED DATA CHANNELS:      8
SAMPLES PER SECOND PER CHANNEL:      80
NUMBER OF SECONDS PER BLOCK:      5.000
TIME-FIRST DATA BLOCK: 1983 03 24 (083) 10:48:00.000
RECORD: 393 CLIPPED DATA CH/#PTS:      7/ 2
RECORD: 395 CLIPPED DATA CH/#PTS:      7/ 5
RECORD: 396 CLIPPED DATA CH/#PTS:      7/ 7
RECORD: 400 CLIPPED DATA CH/#PTS:      8/ 10
RECORD: 401 CLIPPED DATA CH/#PTS:      8/ 12
RECORD: 402 CLIPPED DATA CH/#PTS:      8/ 48
RECORD: 403 CLIPPED DATA CH/#PTS:      8/ 51
RECORD: 404 CLIPPED DATA CH/#PTS:      8/ 10
RECORD: 405 CLIPPED DATA CH/#PTS:      8/ 8
TIME-LAST DATA BLOCK: 1983 03 24 (083) 11:29:55.000
RECORD 506 IS A TRAILER RECORD.
CH HYDR AMP GAIN AVGVAL STDDEV O/BLK O/BLK/STD #CLIPS
1 71 6 9 396.4 35.2 0.00 0.000 0
2 73 9 9 -430.8 66.4 0.00 0.000 0
3 74 0 9 32.2 58.8 4.38 2.202 0
4 75 19 9 391.7 88.6 0.00 0.000 0
5 76 1 9 109.0 238.0 1.07 1.005 0
6 10 13 9 129.3 1363.5 0.59 0.762 0
7 20 11 9 32.6 1388.4 1.95 1.682 14
8 40 18 9 -189.9 2266.2 0.22 0.473 139
THE WORST CASE CLOCK ERROR CODE:      0
FILE:      8
TOTAL RECORDS IN THIS FILE (INCL. HEADER): 506

```

Figure 18. Sample output from program XSTPCHK. Detailed explanation of this figure is given in the text.

3 - less than  $\pm 50$  msec

7 - less than  $\pm 500$  msec

15 - more than  $\pm 500$  msec

A sample output from XINTCHK is shown in Fig. 19. Much less computation is done on the interval data, and the XINTCHK output serves more as a simple log of what has been saved.

#### Strip Tape Copies (XTAPCOP)

As a final step in the preliminary processing, the strip tapes are copied using program XTAPCOP, and the copies are sent to the DARPA Center for Seismic Studies (CSS) in Rosslyn, Virginia. Copies of interval tapes are not currently sent to CSS but may be at some time in the future.

```

RECORD      1 IS A HEADER RECORD.
#BLKS: 21    2-    22 INT: 1983 04 20 (110) 02:18:15-02:20:00 #SEC: 105.000
#BLKS: 36    23-   58 INT: 1983 04 20 (110) 03:38:00-03:41:00 #SEC: 180.000
#BLKS: 36    59-   94 INT: 1983 04 20 (110) 05:20:00-05:23:00 #SEC: 180.000
#BLKS: 36   95-  130 INT: 1983 04 20 (110) 06:47:00-06:50:00 #SEC: 180.000
#BLKS: 36  131-  166 INT: 1983 04 20 (110) 07:03:00-07:06:00 #SEC: 180.000
#BLKS: 36  167-  202 INT: 1983 04 20 (110) 08:07:00-08:10:00 #SEC: 180.000
#BLKS: 36  203-  238 INT: 1983 04 20 (110) 09:57:00-10:00:00 #SEC: 180.000
#BLKS: 36  239-  274 INT: 1983 04 20 (110) 11:18:00-11:21:00 #SEC: 180.000
#BLKS: 36  275-  310 INT: 1983 04 20 (110) 11:41:00-11:44:00 #SEC: 180.000
#BLKS: 36  311-  346 INT: 1983 04 20 (110) 12:28:00-12:31:00 #SEC: 180.000
#BLKS: 36  347-  382 INT: 1983 04 20 (110) 13:13:00-13:16:00 #SEC: 180.000
#BLKS: 36  383-  418 INT: 1983 04 20 (110) 15:03:00-15:06:00 #SEC: 180.000
#BLKS: 36  419-  454 INT: 1983 04 20 (110) 15:54:00-15:57:00 #SEC: 180.000
#BLKS: 36  455-  490 INT: 1983 04 20 (110) 16:22:00-16:25:00 #SEC: 180.000
#BLKS: 36  491-  526 INT: 1983 04 20 (110) 18:23:00-18:26:00 #SEC: 180.000
#BLKS: 36  527-  562 INT: 1983 04 20 (110) 19:30:00-19:33:00 #SEC: 180.000
#BLKS: 36  563-  598 INT: 1983 04 20 (110) 20:48:00-20:51:00 #SEC: 180.000
#BLKS: 36  599-  634 INT: 1983 04 20 (110) 21:40:00-21:43:00 #SEC: 180.000
#BLKS: 36  635-  670 INT: 1983 04 20 (110) 22:29:00-22:32:00 #SEC: 180.000
#BLKS: 36  671-  706 INT: 1983 04 20 (110) 23:10:00-23:13:00 #SEC: 180.000
#BLKS: 36  707-  742 INT: 1983 04 20 (110) 23:55:00-23:58:00 #SEC: 180.000
#BLKS: 36  743-  778 INT: 1983 04 21 (111) 01:07:00-01:10:00 #SEC: 180.000
#BLKS: 36  779-  814 INT: 1983 04 21 (111) 01:33:00-01:36:00 #SEC: 180.000
#BLKS: 36  815-  850 INT: 1983 04 21 (111) 02:26:00-02:29:00 #SEC: 180.000
#BLKS: 36  851-  886 INT: 1983 04 21 (111) 04:15:00-04:18:00 #SEC: 180.000
#BLKS: 36  887-  922 INT: 1983 04 21 (111) 05:04:00-05:07:00 #SEC: 180.000
#BLKS: 36  923-  958 INT: 1983 04 21 (111) 06:13:00-06:16:00 #SEC: 180.000
#BLKS: 36  959-  994 INT: 1983 04 21 (111) 07:27:00-07:30:00 #SEC: 180.000
#BLKS: 36  995-1030 INT: 1983 04 21 (111) 08:13:00-08:16:00 #SEC: 180.000
#BLKS: 36 1031-1066 INT: 1983 04 21 (111) 10:04:00-10:07:00 #SEC: 180.000
#BLKS: 36 1067-1102 INT: 1983 04 21 (111) 12:04:00-12:07:00 #SEC: 180.000
#BLKS: 36 1103-1138 INT: 1983 04 21 (111) 12:22:00-12:25:00 #SEC: 180.000
#BLKS: 36 1139-1174 INT: 1983 04 21 (111) 12:27:00-12:30:00 #SEC: 180.000
#BLKS: 36 1175-1210 INT: 1983 04 21 (111) 13:15:00-13:18:00 #SEC: 180.000
#BLKS: 36 1211-1246 INT: 1983 04 21 (111) 13:48:00-13:51:00 #SEC: 180.000
#BLKS: 72 1247-1318 INT: 1983 04 21 (111) 14:47:00-14:53:00 #SEC: 360.000
#BLKS: 36 1319-1354 INT: 1983 04 21 (111) 15:19:00-15:22:00 #SEC: 180.000
#BLKS: 36 1355-1390 INT: 1983 04 21 (111) 16:41:00-16:44:00 #SEC: 180.000
#BLKS: 36 1391-1426 INT: 1983 04 21 (111) 18:07:00-18:10:00 #SEC: 180.000
#BLKS: 36 1427-1462 INT: 1983 04 21 (111) 18:53:00-18:56:00 #SEC: 180.000
#BLKS: 36 1463-1498 INT: 1983 04 21 (111) 19:27:00-19:30:00 #SEC: 180.000
#BLKS: 36 1499-1534 INT: 1983 04 21 (111) 19:38:00-19:41:00 #SEC: 180.000
#BLKS: 36 1535-1570 INT: 1983 04 21 (111) 21:02:00-21:05:00 #SEC: 180.000
#BLKS: 36 1571-1606 INT: 1983 04 21 (111) 22:03:00-22:06:00 #SEC: 180.000
#BLKS: 36 1607-1642 INT: 1983 04 21 (111) 22:18:00-22:21:00 #SEC: 180.000
#BLKS: 36 1643-1678 INT: 1983 04 22 (112) 00:08:00-00:11:00 #SEC: 180.000
#BLKS: 36 1679-1714 INT: 1983 04 22 (112) 00:18:00-00:21:00 #SEC: 180.000

```

Figure 19. Sample output from program XINTCHK showing some of the 3-minute intervals saved on a WHIPS interval tape. The first interval shown, blocks 2-22, contains only 105 seconds because part of that interval was written to the previous interval tape. Another interval, blocks 1247-1318, contains 360 seconds and represents two contiguous 3-minute intervals.

#### ACKNOWLEDGEMENTS

This system has been sponsored primarily by the Air Force Office of Scientific Research with supplemental funds provided by the U.S. Arms Control and Disarmament Agency. Appreciation is expressed to Dan Walker, George Sutton, Paul Jubinski, Grant Blackinton and Joe Gettrust for their respective contributions towards the design and implementation of this system. Firmin Oliveira successfully programmed most of the WAKEUP and WHIPS software in less time than seemed possible. Al David, Bonnie Jose, and Kentron Corporation have provided excellent day to day operation of the system at Wake.

APPENDIX X

## WAKE HYDROPHONE INFORMATION PROCESSING SYSTEM (WHIPS) EVENT LISTING

5 JUL 83

KEY: INFORMATION SOURCES - PDE=NEIS PDECARD, MON=NEIS MONTHLY LIST, ICS=ICS LIST, HEL=HELICORDER, OTH=OTHER  
 EVENT TYPE - EQ=EARTHQUAKE, NX=NUCLEAR EXPLOSION, SX=SCIENTIFIC EXPLOSION, OT=OTHER, UN=UNKNOWN  
 PHASES - A=P, B=PO, C=S, D=SO, E=T, F=OTHER

EVNT	*****ORIGIN	TIME*****	**COORDINATES**	*****LOCATION*****	DEP	"MAGNI"	INF	EV	*****SAVED*****	**STRIP**					
"NO"	YR*MO*DA*	JUL*HR*MN*SECS	**LAT*** **LON***	*****DESCRIPTION*****	KM	BDY*SRF	SRC	TP	*****INTERVAL*****	MNS	TAPE/FILE				
0001	82	09	252	03:06:44.8	38.299N	137.670E	SOUTH OF HONSHU, JAPAN	481	5.8	PDE	EQ	ABDE	03:08-03:50	43	20001/06
0002	82	09	252	05:43:52.1	3.306S	177.566E	GILBERT ISLANDS REGION	33	5.4	PDE	EQ	ABDE	05:44-06:22	39	20001/07
0003	82	09	252	06:48:21.2	35.597S	182.453W	SOUTHERN PACIFIC OCEAN.	18	5.1	PDE	EQ	A	06:49-07:09	21	20001/08
0004	82	09	252	12:49:08.4	43.563N	146.606E	KURIL ISLANDS	33	4.7	PDE	EQ	ABD	12:50-13:17	20	20001/09
0005	82	09	252	15:42:22.0	15.493N	147.571E	MARIANA ISLANDS REGION	33	5.4	PDE	EQ	ABDE	15:41-16:12	32	20001/10
0006	82	09	252	16:09:30.3	15.518N	147.593E	MARIANA ISLANDS REGION	33	5.2	PDE	EQ	ABDE	16:09-16:39	31	20001/11
0007	82	09	252	16:13:59.7	15.638N	147.648E	MARIANA ISLANDS	33	5.1	PDE	EQ	ABDE	16:13-16:44	32	20001/12
0008	82	09	252	16:40:13.1	22.183S	169.446E	LOYALTY ISLANDS	33	5.5	PDE	EQ	ABDE	16:43-16:54	12	20001/13
0009	82	09	252	16:43:15.2	3.437S	177.650E	GILBERT ISLANDS	33	5.1	PDE	EQ	ABDE	16:43-17:02	48	20001/14
0010	82	09	253	01:20:37.5	55.161N	161.673E	NEAR EAST COAST OF KAMCHATKA	33	5.0	PDE	EQ	ABDE	01:23-11:13	51	20002/01
0011	82	09	253	13:41:42.2	2.447N	126.910E	MOLUCCA PASSAGE 46 DEGS.	45	4.8	PDE	EQ	A	13:45-13:56	12	20002/02
0012	82	09	254	06:31:48.6	26.620S	176.644W	SOUTH OF FIJI ISLANDS 49 DEGS.	33	5.2	PDE	EQ	A	06:41-07:08	28	20002/03
0013	82	09	254	06:57:44.6	26.803S	176.210W	SOUTH OF FIJI ISLANDS 49 DEGS.	33	5.0	PDE	EQ	A	07:01-07:13	13	20002/04
0014	82	09	254	13:59:07.0	15.611N	147.818E	MARIANA ISLANDS	38	4.2	PDE	EQ	ABD	13:58-14:27	38	20002/05
0015	82	09	255	03:42:43.1	42.031N	142.702E	HOKKAIDO, JAPAN	66	4.8	PDE	EQ	ABD	03:44-03:59	16	20002/06
0016	82	09	255	07:22:39.3	19.727S	177.914W	FIJI ISLANDS	577	5.1	PDE	EQ	A	07:25-07:47	13	20002/07
0017	82	09	255	08:46:06.0	26.952S	176.475W	SOUTH OF FIJI	33	5.1	PDE	EQ	A	08:56-09:01	12	20002/08
0018	82	09	255	09:22:23.2	52.671N	166.937W	FOX ISLANDS, ALEUTIAN ISLANDS.	33	5.7	PDE	EQ	ABDE	09:26-10:18	53	20002/09
0019	82	09	255	11:59:52.6	52.783N	166.772W	FOX ISLANDS, ALEUTIAN ISLANDS.	33	5.2	PDE	EQ	ABDE	12:03-12:56	54	20002/10
0020	82	09	255	13:03:10.2	8.820N	126.837E	MOLUCCA PASSAGE	78	4.9	PDE	EQ	A	13:12-13:31	28	20002/11
0021	82	09	255	16:58:38.8	52.847N	166.977W	FOX ISLANDS, ALEUTIAN ISLANDS.	33	5.5	PDE	EQ	ABDE	16:53-17:46	54	20002/12
0022	82	09	255	16:46:57.7	17.992S	178.496W	FIJI ISLANDS.	597	4.3	PDE	EQ	A	16:49-17:01	13	20003/01
0023	82	09	256	18:03:36.3	37.526N	141.306E	NEAR COAST OF HONSHU, JAPAN.	62	5.0	PDE	EQ	ABDE	18:04-18:47	44	20003/02
0024	82	09	256	19:08:51.6	3.520S	177.622E	GILBERT ISLANDS.	33	5.2	PDE	EQ	ABDE	19:09-19:47	39	20003/03
0025	82	09	257	03:26:04.9	15.495N	147.722E	MARIANA ISLANDS.	38	4.8	PDE	EQ	ABD	03:25-03:38	14	20003/04
0026	82	09	257	03:53:42.6	3.442S	177.667E	GILBERT ISLANDS.	33	5.4	PDE	EQ	ABDE	03:54-04:32	39	20003/05
0027	82	09	257	05:11:49.4	31.077S	179.615W	KERMADEC ISLANDS.	78	5.4	PDE	EQ	A	05:21-05:48	28	20003/06
0028	82	09	257	11:37:18.6	43.729N	148.138E	HOKKAIDO, JAPAN.	161	5.2	PDE	EQ	ABDE	11:33-12:06	48	20003/07
0029	82	09	257	12:42:23.8	27.017S	176.480W	KERMADEC ISLANDS.	33	5.0	PDE	EQ	A	12:46-12:57	12	20003/08
0030	82	09	257	18:17:02.4	7.247S	149.056E	EAST PAPUA NEW GUINEA.	33	5.0	PDE	EQ	ABDE	18:18-19:04	47	20003/09
0031	82	09	257	21:18:38.5	7.368S	12.499W	ASCENSION ISLAND.	10	4.9	PDE	EQ	A	21:28-21:47	28	20003/10
0032	82	09	258	02:22:57.5	14.515S	78.842W	PERU, NB 6.3 (BRK).	152	5.9	PDE	EQ	A	22:32-20:51	28	20004/01
0033	82	09	258	02:34:09.2	21.518S	169.308E	LOYALTY ISLANDS.	67	5.6	PDE	EQ	A	22:37-22:48	12	20004/02
0034	82	09	258	03:31:54.1	12.022N	143.743E	SOUTH OF MARIANA ISLANDS	33	4.9	PDE	EQ	ABD	23:32-00:08	29	20004/03
0035	82	09	258	08:20:38.5	38.103N	138.966E	SOUTH OF HONSHU, JAPAN.	378	5.1	PDE	EQ	ABDE	08:21-08:52	42	20004/04
0036	82	09	259	03:07:58.5	3.568S	177.684E	GILBERT ISLANDS.	33	4.8	PDE	EQ	ABD	03:08-03:22	15	20004/05
0037	82	09	259	08:23:23.2	15.335S	173.283W	TONGA ISLANDS.	129	5.5	PDE	EQ	A	08:26-08:37	12	20004/06
0038	82	09	259	09:21:11.0	5.261S	152.059E	NEW BRITAIN.	63	5.2	PDE	EQ	ABDE	09:22-10:03	42	20004/07
0039	82	09	259	11:41:00.9	3.351S	177.602E	GILBERT ISLANDS.	33	5.2	PDE	EQ	ABDE	11:41-12:19	39	20004/08
0040	82	09	259	12:27:38.7	7.294S	127.056E	BANDA SEA.	389	5.0	PDE	EQ	A	12:31-12:42	12	20004/09
0041	82	09	259	13:20:39.3	6.870N	125.882E	MINDANAO, PHILIPPINE ISLANDS.	169	5.1	PDE	EQ	A	13:31-13:43	13	20004/10
0042	82	09	259	16:46:02.2	3.397S	177.557E	GILBERT ISLANDS.	33	4.7	PDE	EQ	ABD	16:46-17:14	29	20004/11
0043	82	09	259	16:07:53.3	41.411N	160.095E	DOWNHOLE NEAR KURIL IS.	0	0.0	OTH	SX	AE	06:08-06:44	37	0/000
0044	82	09	259	16:08:35.8	41.715N	160.077E	DOWNHOLE NEAR KURIL IS.	0	0.0	OTH	SX	AE	09:01-09:37	37	0/000
0045	82	09	259	12:08:24.7	42.017N	160.033E	DOWNHOLE NEAR KURIL IS.	0	0.0	OTH	SX	AE	12:08-12:37	38	20001/01
0046	82	09	259	15:01:23.3	42.317N	160.010E	DOWNHOLE NEAR KURIL IS.	0	0.0	OTH	SX	AE	15:01-15:38	38	20001/02
0047	82	09	259	18:01:00.5	42.605N	159.971E	DOWNHOLE NEAR KURIL IS.	0	0.0	OTH	SX	AE	18:01-18:38	38	20001/03
0048	82	09	259	21:00:23.5	42.883N	159.905E	DOWNHOLE NEAR KURIL IS.	0	0.0	OTH	SX	AE	21:00-21:30	39	20001/04
0049	82	09	259	22:00:57.9	43.203N	159.793E	DOWNHOLE NEAR KURIL IS.	0	0.0	OTH	SX	AE	00:01-00:39	39	20001/05
0050	82	09	255	22:45:04.2	44.252N	160.776E	KURILS DOWNHOLE - 240# SHOT	0	0.0	OTH	SX	AE	22:45-23:24	48	20002/12
0051	82	09	255	23:01:00.5	44.276N	160.826E	KURILS DOWNHOLE - 240# SHOT	0	0.0	OTH	SX	AE	23:01-23:48	48	20003/01
0052	82	09	255	23:03:02.3	44.316N	160.925E	KURILS DOWNHOLE - 240# SHOT	0	0.0	OTH	SX	AE	23:17-23:56	48	20003/02
0053	82	09	255	23:09:05.4	44.338N	160.982E	KURILS DOWNHOLE - 240# SHOT	0	0.0	OTH	SX	AE	23:33-00:12	48	20003/03
0054	82	09	255	23:49:05.4	44.359N	161.037E	KURILS DOWNHOLE - 240# SHOT	0	0.0	OTH	SX	AE	23:49-00:20	48	20003/04
0055	82	09	256	00:05:07.1	44.359N	161.037E	KURILS DOWNHOLE - 240# SHOT	0	0.0	OTH	SX	AE	00:05-00:44	48	20003/05
0056	82	09	256	02:57:48.1	11.151S	162.212E	SOLOMON ISLANDS	69	5.2	PDE	EQ	ABDE	02:59-03:43	45	20005/01
0057	82	09	256	04:15:21.7	17.725S	172.756W	TONGA IS. REG.	33	5.2	PDE	EQ	A	04:24-04:44	21	20005/02
0058	82	09	256	09:40:41.2	3.400S	177.608E	GILBERT IS. REG.	33	4.7	PDE	EQ	ABD	09:41-10:09	29	20005/03
0059	82	09	256	13:28:25.6	23.446S	179.947W	S. OF FIJI IS.	555	5.9	PDE	EQ	A	13:37-13:57	21	20005/04
0060	82	09	256	15:38:16.6	11.857S	117.188E	S. OF SUMBAWA IS.	33	5.1	PDE	EQ	A	15:43-15:54	12	20005/05
0061	82	09	256	20:21:03.1	23.426S	179.611W	S. OF FIJI IS.	33	5.3	PDE	EQ	A	20:24-20:35	12	20005/06
0062	82	09	256	14:25:03.3	3.488S	177.679E	GILBERT IS. REG.	33	5.0	PDE	EQ	ABDE	14:25-15:04	48	20005/07
0063	82	09	256	15:00:41.3	7.676S	127.477E	BANDA SEA	165	5.4	PDE	EQ	A	15:04-15:15	12	20005/08
0064	82	09	256	18:19:35.9	36.110N	141.454E	NR. E. COAST HONSHU, JAPAN	33	4.7	PDE	EQ	ABD	18:21-18:48	28	20005/09
0065	82	09	256	21:20:19.2	26.950S	176.461W	S. OF FIJI IS.	116	5.2	PDE	EQ	A	21:24-21:35	12	20005/10
0066	82	09	256	12:57:45.3	26.924S	175.814W	S. OF TONGA IS.	33	5.5	PDE	EQ	ABDE	13:01-14:06	66	20005/11
0067	82	09	256	13:48:32.5	26.870S	175.934W	S. OF TONGA IS.	33	5.1	PDE	EQ	A	13:52-14:04	33	20005/12
0068	82	09	256	13:56:06.6	54.612S	143.723E	W. OF MACQUARIE IS.	18	5.7	PDE	EQ	A	14:05-		

# WAKE HYDROPHONE INFORMATION PROCESSING SYSTEM (WHIPS) EVENT LISTING

5 JUL 83

KEY: INFORMATION SOURCES - PDE=NEIS PDECARD, MON=NEIS MONTHLY LIST, ICS=ICS LIST, MEL=HELICORDER, OTH=OTHER  
 EVENT TYPE - EQ=EARTHQUAKE, NX=NUCLEAR EXPLOSION, SX=SCIENTIFIC EXPLOSION, OT=OTHER, UN=UNKNOWN  
 PHASES - A=P, B=PO, C=S, D=SO, E=T, F=OTHER

EVNT	*****ORIGIN TIME*****	*****COORDINATES*****	*****LOCATION*****	DEP	MAGNI	INF	EV	*****SAVED*****	*****STRIP*****	
NO	YR-MO-DA-JUL-MN-SECS	*****LAT*****	*****LONG*****	*****DESCRIPTION*****	KM	BDY	SRC	TP	PHASES*****INTERVAL*****MMS TAPE/FILE	
0101	02 09 27 270 12:37:38.4	39.278N	73.784E	TAIJIK-SINKIANG BORDER REGION.	33	4.8	4.8	PDE	EQ A	12:45-12:56 12 200877 01
0102	02 09 27 270 12:37:12.7	10.327N	126.150E	PHILIPPINE IS. REGION.	54	5.8	5.8	PDE	EQ A	21:48-21:51 12 202277 02
0103	02 09 28 271 05:07:15.7	3.029S	177.554E	GILBERT IS. REGION.	33	4.9	5.0	PDE	EQ ABD	05:07-05:21 12 202277 03
0104	02 09 28 271 15:14:36.0	24.173S	176.754W	SOUTH OF FIJI IS.	40	6.0	6.1	PDE	EQ AE	15:18-16:19 62 202277 04
0105	02 09 28 271 22:42:20.6	15.685N	147.658E	MARIANA IS. REGION.	33	5.1	5.0	PDE	EQ ABDE	22:41-23:12 32 202277 05
0106	02 09 28 271 22:48:05.4	15.722N	147.761E	MARIANA IS. REGION.	33	4.7	5.0	PDE	EQ ABDE	22:47-23:00 14 202277 06
0107	02 09 29 272 04:24:16.1	37.346N	72.942E	TAJIK SSR	33	5.4	4.9	PDE	EQ A	04:31-04:43 13 202277 07
0108	02 09 29 272 05:53:33.8	37.297N	73.258E	TAJIK SSR	33	4.8	5.0	PDE	EQ A	06:01-06:12 12 202277 08
0109	02 09 29 272 09:29:47.2	25.139N	141.751E	VOLCANO ISLANDS REGION.	103	4.9	5.0	PDE	EQ ABD	09:38-09:44 15 202277 09
0110	02 09 29 272 13:38:00.1	37.091N	116.045W	SOUTHERN NEVADA	55	5.8	4.5	PDE	EQ NX	13:36-13:47 12 202277 10
0111	02 09 29 272 19:03:37.3	7.268S	155.723E	SOLOMON IS.	23	6.1	4.4	PDE	EQ ABDE	19:04-19:46 42 202277 11
0112	02 09 29 272 20:46:49.9	7.275S	155.894E	SOLOMON IS.	42	5.8	5.0	PDE	EQ ABDE	20:43-21:29 42 202277 12
0113	02 09 30 273 01:44:06.0	6.981S	155.750E	SOLOMON IS.	42	5.8	5.0	PDE	EQ ABDE	01:45-02:26 12 202277 13
0114	02 09 30 273 02:20:30.0	21.528S	177.980W	FIJI IS. REG.	400	4.4	5.0	PDE	EQ A	02:31-02:42 12 202277 14
0115	02 09 30 273 05:44:49.1	30.051N	73.996E	TAJIK-SINKIANG BORDER REGION.	104	4.8	5.0	PDE	EQ A	05:52-06:03 12 202277 15
0116	02 09 30 273 14:23:58.5	14.658S	173.204W	SAMOA IS. REGION.	20	5.6	5.5	PDE	EQ A	14:26-14:33 13 202277 16
0117	02 10 01 274 16:53:51.6	37.797N	139.476E	HONSHU, JAPAN	150	5.1	5.0	PDE	EQ ABDE	16:55-17:39 45 202277 17
0118	02 10 02 275 02:29:13.0	27.722N	139.052E	BONIN ISLANDS REGION	405	4.2	5.0	PDE	EQ ABD	02:29-02:44 16 202277 18
0119	02 10 02 275 04:54:07.5	8.083S	110.027E	SUMBAWA ISLAND REGION	33	4.9	5.0	PDE	EQ A	04:59-05:10 12 202277 19
0120	02 10 02 275 08:26:25.5	14.730S	167.204E	VANUATU ISLANDS	152	5.5	5.0	PDE	EQ A	08:29-08:39 12 202277 20
0121	02 10 03 276 01:12:58.0	5.646S	129.099E	BANDA SEA	220	5.0	5.0	PDE	EQ A	01:16-01:27 12 202277 21
0122	02 10 03 276 08:41:29.4	3.372S	177.553E	GILBERT ISLANDS REGION	33	5.0	4.7	PDE	EQ ABDE	08:42-08:28 39 202277 22
0123	02 10 03 276 11:02:04.3	9.377S	152.347E	DENTRECASTEAUX ISLANDS REGION	39	5.1	5.0	PDE	EQ A	11:03-11:15 13 202277 23
0124	02 10 03 276 16:10:09.3	55.963N	149.967W	GULF OF ALASKA	33	4.2	5.0	PDE	EQ A	16:22-16:33 12 202277 24
0125	02 10 03 276 19:59:34.0	6.460S	150.038E	NEW BRITAIN REGION	42	5.2	5.0	PDE	EQ ABDE	20:01-20:44 44 202277 25
0126	02 10 03 276 22:26:34.0	0.142S	110.407E	SUMBAWA ISLAND REGION	33	4.7	5.0	PDE	EQ A	22:31-23:47 12 202277 26
0127	02 10 03 276 23:29:31.2	42.064N	140.761E	HOKKAIDO, JAPAN REGION.	152	4.7	5.0	PDE	EQ ABD	23:31-23:47 17 202277 27
0128	02 10 04 277 01:40:53.2	51.771N	176.009W	ANDREANOF ISL. ALEUTIAN ISL.	62	5.4	5.0	PDE	EQ ABDE	01:49-01:37 49 202277 28
0129	02 10 04 277 01:40:53.2	51.771N	176.009W	ANDREANOF ISL. ALEUTIAN ISL.	94	5.4	5.0	PDE	EQ A	01:55-01:06 12 202277 29
0130	02 10 04 277 15:23:26.9	5.042N	126.744E	LOVALTY ISLAND REGION	33	5.1	5.0	PDE	EQ A	15:26-15:37 12 202277 30
0131	02 10 04 277 15:23:26.9	22.684S	171.192E	LOVALTY ISLAND REGION	33	4.9	5.0	PDE	EQ A	16:23-16:33 12 202277 31
0132	02 10 05 278 03:10:53.0	0.217N	122.244E	MINAHASSA PENINSULA	221	4.0	5.0	PDE	EQ A	03:22-03:33 12 202277 32
0133	02 10 05 278 08:09:16.7	3.410S	177.591E	GILBERT ISL. REGION	33	5.3	5.0	PDE	EQ ABDE	08:09-08:48 40 202277 33
0134	02 10 05 278 09:14:41.3	15.642S	167.930E	VANUATU ISL. REGION	91	5.9	5.0	PDE	EQ ABDE	09:16-10:05 50 202277 34
0135	02 10 05 278 10:15:15.4	30.229S	170.056W	KERMADEC ISL	146	5.5	5.0	PDE	EQ A	10:15-10:30 12 202277 35
0136	02 10 05 278 12:04:13.2	4.239N	126.657E	TALAUD ISLANDS	95	5.3	5.0	PDE	EQ A	12:07-12:18 12 202277 36
0137	02 10 05 278 19:46:27.6	33.149N	136.922E	NEAR S. COAST OF SOUTH HONSHU	391	4.7	5.0	PDE	EQ ABD	19:47-20:03 17 202277 37
0138	02 10 05 278 22:17:19.9	30.161S	179.304W	KERMADEC ISL. REGION	325	4.9	5.0	PDE	EQ A	22:21-22:32 12 202277 38
0139	02 10 05 278 22:25:56.0	22.017S	171.107E	LOVALTY ISL. REGION	45	5.6	5.4	PDE	EQ A	22:29-22:40 12 202277 39
0140	02 10 06 279 21:13:12.0	22.005S	171.241E	LOVALTY IS. REGION	33	5.5	5.1	PDE	EQ A	21:16-21:27 12 202277 40
0141	02 10 07 280 01:52:29.3	23.376N	94.349E	BURMA-INDIA BORDER REGION	90	4.7	5.0	PDE	EQ A	01:50-02:09 12 202277 41
0142	02 10 07 280 07:15:56.9	7.163S	125.910E	BANDA SEA	510	6.2	5.0	PDE	EQ A	07:19-07:31 13 202277 42
0143	02 10 07 280 09:26:01.4	3.496S	177.516E	GILBERT IS. REGION	26	4.7	5.0	PDE	EQ ABD	09:26-09:48 15 202277 43
0144	02 10 07 280 11:02:17.4	32.348N	137.455E	SOUTH OF HONSHU, JAPAN.	300	5.1	5.0	PDE	EQ ABDE	11:02-11:46 44 202277 44
0145	02 10 07 280 13:40:19.2	3.546S	177.679E	GILBERT IS. REGION	29	4.9	4.4	PDE	EQ ABD	13:40-13:55 16 202277 45
0146	02 10 07 280 21:57:03.3	32.143N	142.301E	SOUTH OF HONSHU, JAPAN.	33	4.8	5.0	PDE	EQ ABD	21:57-22:12 16 202277 46
0147	02 10 08 281 13:34:57.2	26.356N	99.849E	YUNNAN PROVINCE, CHINA	40	5.0	4.5	PDE	EQ A	13:40-13:51 12 202277 47
0148	02 10 08 281 18:45:39.4	23.314S	179.052E	SOUTH OF FIJI IS.	650	5.1	5.0	PDE	EQ A	18:48-18:59 12 202277 48
0149	02 10 08 281 18:59:11.0	37.504N	72.095E	TAJIK SSR	33	5.2	5.0	PDE	EQ A	19:06-19:18 12 202277 49
0150	02 10 09 282 00:53:15.2	40.147N	143.742E	OFF EAST COAST OF HONSHU, JAPA	33	4.8	4.5	PDE	EQ ABD	00:54-01:09 16 202277 50
0151	02 10 09 282 10:53:02.1	3.519S	177.708E	GILBERT IS. REGION	33	5.3	4.7	PDE	EQ ABD	10:53-10:32 40 202277 51
0152	02 10 09 282 19:40:23.0	3.470S	177.675E	GILBERT IS. REGION	33	5.3	4.4	PDE	EQ ABDE	19:41-20:19 39 202277 52
0153	02 10 09 282 22:09:11.7	16.565S	167.479E	VANUATU IS.	33	5.1	4.7	PDE	EQ A	22:11-22:22 12 202277 53
0154	02 10 10 283 04:59:56.0	61.555N	112.033E	CENTRAL SIBERIA	5	5.3	5.0	PDE	EQ NX	05:05-05:16 12 202277 54
0155	02 10 10 283 12:41:00.2	17.762S	178.573W	FIJI IS. REGION	596	4.1	5.0	PDE	EQ A	12:43-12:54 12 202277 55
0156	02 10 10 283 17:23:03.0	40.171N	143.002E	OFF EAST COAST OF HONSHU, JAPA	20	5.4	5.2	PDE	EQ ABDE	17:24-18:06 43 202277 56
0157	02 10 10 283 20:36:20.6	7.222S	129.621E	BANDA SEA	149	4.0	5.0	PDE	EQ A	20:39-20:51 13 202277 57
0158	02 10 11 284 07:14:58.1	73.368N	54.532E	NOVAYA ZEMLYA	5	5.6	3.6	PDE	EQ NX	07:22-07:33 12 202277 58
0159	02 10 11 284 10:25:35.2	62.551S	166.066E	BALENYI IS. REGION	10	5.0	4.9	PDE	EQ A	10:33-10:44 12 202277 59
0160	02 10 11 284 16:34:47.0	27.439S	175.441W	KERMADEC IS. REGION	45	5.2	5.0	PDE	EQ A	16:38-16:50 12 202277 60
0161	02 10 12 285 04:49:38.9	37.200N	69.704E	AFGHANISTAN-USSR BORDER REGION	33	4.0	5.0	PDE	EQ A	04:57-05:09 12 202277 61
0162	02 10 12 285 10:52:49.3	14.156N	175.637E	TONGA IS.	190	4.7	5.0	PDE	EQ A	10:44-09:54 12 202277 62
0163	02 10 13 286 10:52:49.3	14.156N	175.637E	TONGA IS.	33	5.1	5.0	PDE	EQ A	10:55-10:07 12 202277 63
0164	02 10 14 287 21:40:19.5	27.405N	139.037E	BONIN IS. REGION	495	5.1	5.0	PDE	EQ ABDE	21:40-22:20 41 202277 64
0165	02 10 14 287 21:59:44.4	30.449N	133.501E	SEA OF JAPAN	416	4.3	5.0	PDE	EQ ABD	22:01-22:10 18 202277 65
0166	02 10 15 288 00:54:09.9	5.049N	126.242E	MINDANAO, PHILIPPINE IS.	94	5.3	5.0	PDE	EQ A	00:57-01:08 12 202277 66
0167	02 10 15 288 10:58:39.0	32.071N	125.756W	NORTH PACIFIC OCEAN.	10	5.1	4.4	PDE	EQ A	11:04-11:15 12 202277 67
0168	02 10 16 289 01:53:30.9	5.544S	146.247E	EAST PAPUA NEW GUINEA REGION	76	5.3	5.0	PDE	EQ ABDE	01:55-02:40 46 202277 68
0169	02 10 16 289 03:02:50.3	34.601N	139.411E	NEAR S. COAST OF HONSHU, JAPAN	133	4.7	5.0	PDE	EQ ABD	03:04-03:19 16 202277 69
0170	02 10 16 289 05:59:57.2	46.727N	40.162E	SOUTHWESTERN USSR	5	5.2	3.0	PDE	EQ NX	06:00-06:19 12 202277 70
0171	02 10 16 289 06:04:57.1	46.723N	40.222E	SOUTHWESTERN USSR	5	5.3	3.0	PDE	EQ NX	06:13-06:24 12 202277 71
0172	02 10 16 289 06:09:57.1	46.740N	40.258E	SOUTHWESTERN USSR	5	5.2	3.1	PDE	EQ NX	06:10-06:29 12 202277 72
0173	02 10 16 289 06:14:57.1	46.707N	40.230E	SOUTHWESTERN USSR	5	5.4	3.1	PDE	EQ NX	06:23-06:34 12 202277 73
0174	02 10 16 289 06:02:54.3	23.321S	171.604E	LOVALTY IS. REGION	33	5.0	4.2	PDE	EQ A	06:06-06:17 12 202277 74
0175	02 10 16 289 09:46:56.0	36.406N	71.228E	AFGHANISTAN-USSR BORDER REGION	230	4.6	5.0	PDE	EQ A	09:54-09:25 12 202277 75
0176	02 10 17 290 10:12:09.0	49.628N	155.919E	KURIL IS.	47	5.5	4.9	PDE	EQ ABDE	10:13-10:59 47 202277 76
0177</										



## WAKE HYDROPHONE INFORMATION PROCESSING SYSTEM (WHIPS) EVENT LISTING

5 JUL 83

KEY: INFORMATION SOURCES - PDE=NEIS PDECARD, MON=NEIS MONTHLY LIST, ICS=ICS LIST, MEL=MELICORDER, OTH=OTHER  
 EVENT TYPE - EQ=EARTHQUAKE, NX=NUCLEAR EXPLOSION, SX=SCIENTIFIC EXPLOSION, OT=OTHER, UN=UNKNOWN  
 PHASES - A=P, B=PO, C=S, D=SO, E=T, F=OTHER

EVNT	*****ORIGIN TIME*****	*****COORDINATES*****	*****LOCATION*****	DEP	MAGNI	INF	EV	*****SAVED*****	***STRIP**			
NO	YR-MO-DA-JUL-HR-MN-SECS	LAT-LON	*****DESCRIPTION*****	KM	BDY	SFR	SRC	TP	PHASES*****INTERVAL*****	INS	TAPE/FILE	
0201	02 10 24 297 16:09:05.5	3.739S 131.194E	WEST IRIAN REG.	33	4.9	0.0	PDE	EQ	A	16:17-16:23	12	2001/1/12
0202	02 10 24 297 22:28:20.5	53.752S 141.746E	W. OF MACQUARIE IS.	10	4.0	5.3	PDE	EQ	A	22:35-22:46	12	2001/1/13
0203	02 10 25 298 12:30:04.5	18.198S 173.920E	TONGA ISLANDS	142	4.6	0.0	PDE	FO	A	12:33-12:44	12	2001/1/14
0204	02 10 25 298 12:30:04.5	18.198S 173.920E	TONGA ISLANDS	142	4.6	0.0	PDE	FO	A	12:33-12:44	12	2001/1/14
0205	02 10 25 298 14:26:49.5	4.802S 152.327E	NEW BRITAIN REG.	86	5.4	0.0	PDE	EQ	ABDE	14:27-15:08	42	2001/1/16
0206	02 10 25 298 19:23:52.0	23.684S 179.251E	S. OF FIJI ISLANDS	673	4.8	0.0	PDE	EQ	A	19:26-19:37	12	2001/1/17
0207	02 10 25 298 22:26:04.4	36.322N 120.500E	CENTRAL CALIFORNIA	11	5.4	5.2	PDE	EQ	ABD	22:32-23:56	25	2001/1/18
0208	02 10 26 299 07:33:37.6	85.992N 84.821E	NORTH OF SEVERNAYA ZEMLYA	10	4.6	0.0	PDE	EQ	A	07:39-07:51	12	2001/1/19
0209	02 10 26 299 12:44:18.1	7.446S 105.653E	JAVA	119	5.6	0.0	PDE	EQ	A	12:50-13:01	12	2001/1/20
0210	02 10 27 300 05:45:32.3	46.096N 152.478E	KURIL IS.	33	4.9	0.0	PDE	EQ	ABD	05:46-06:52	17	2001/1/21
0211	02 10 27 300 18:38:13.9	28.484N 121.596E	PHILIPPINE IS. REGION	33	4.9	0.0	PDE	EQ	A	18:39-18:44	12	2001/1/22
0212	02 10 27 300 15:36:36.3	23.838N 105.007E	YUNNAN PROVINCE, CHINA	33	4.9	0.0	PDE	EQ	A	15:33-16:44	12	2001/1/23
0213	02 10 27 300 15:48:15.0	36.389N 69.465E	MINDU KUSH	33	5.2	5.1	PDE	EQ	A	15:41-15:52	12	2001/1/24
0214	02 10 28 301 03:28:36.5	37.355N 134.807E	SEA OF JAPAN	51	4.0	0.0	PDE	EQ	A	03:28-04:09	42	2001/1/25
0215	02 10 28 301 15:38:15.2	7.992S 109.144E	JAVA	90	5.1	0.0	PDE	EQ	A	15:35-15:47	12	2001/1/26
0216	02 10 28 301 18:38:29.2	46.447N 144.867E	SEA OF OKHOTSK	204	4.4	0.0	PDE	EQ	ABD	18:31-18:40	16	2001/1/27
0217	02 10 28 302 03:42:15.5	4.569S 152.462E	NEW BRITAIN REGION	100	5.1	0.0	PDE	EQ	ABDE	03:43-04:24	42	2001/1/28
0218	02 10 29 302 01:04:44.9	16.998S 173.768E	TONGA ISLANDS	124	4.0	0.0	PDE	EQ	A	01:07-01:18	12	2001/1/29
0219	02 10 29 302 03:47:25.4	6.051S 132.426E	BANDA SEA	190	5.6	0.0	PDE	EQ	A	03:50-04:01	12	2001/1/30
0220	02 10 29 302 08:13:06.0	8.114S 107.172E	JAVA	33	5.1	4.0	PDE	EQ	A	08:19-08:30	12	2001/1/31
0221	02 10 30 303 16:38:02.1	12.176S 167.432E	SANTA CRUZ ISLANDS	327	5.3	0.0	PDE	EQ	ABDE	16:31-17:16	46	2001/2/01
0222	02 10 31 304 02:36:58.6	11.630S 117.722E	SOUTH OF SUNBAWA ISLAND	33	5.1	0.0	PDE	EQ	A	02:42-02:53	12	2001/2/02
0223	02 10 31 304 02:40:26.6	10.662S 169.088E	VANUATU ISLANDS	289	4.7	0.0	PDE	EQ	ABD	02:50-03:00	19	2001/2/03
0224	02 10 31 304 01:38:41.2	6.642S 138.508E	BANDA SEA	100	5.0	0.0	PDE	EQ	A	01:34-01:45	12	2001/2/04
0225	02 10 31 304 02:40:13.5	2.944N 96.126E	NORTHERN SUMATERA	61	5.5	0.0	PDE	EQ	A	02:54-03:05	12	2001/2/05
0226	02 10 31 304 18:40:52.0	35.921N 82.516E	TIBET	33	5.2	5.1	PDE	EQ	A	18:47-18:59	13	2001/2/06
0227	02 10 31 304 19:12:46.2	9.672N 126.095E	MINDANAO, PHILIPPINE IS.	60	4.7	0.0	PDE	EQ	A	19:15-19:26	12	2001/2/07
0228	02 10 31 304 22:17:38.2	6.057S 105.540E	SUNDA STRAIT	69	5.0	0.0	PDE	EQ	A	22:23-22:34	12	2001/2/08
0229	02 11 01 305 08:47:55.2	31.397N 141.755E	SOUTH OF HONSHU, JAPAN	33	4.2	0.0	PDE	EQ	ABD	08:48-09:02	15	2001/2/09
0230	02 11 01 305 23:31:56.2	25.823S 179.751E	SOUTH OF FIJI IS.	543	4.9	0.0	PDE	EQ	A	23:34-23:46	13	2001/2/10
0231	02 11 02 306 07:48:27.7	12.397N 125.666E	SAMAR, PHILIPPINE IS.	33	5.1	4.2	PDE	EQ	A	07:43-07:54	12	2001/2/11
0232	02 11 02 306 18:38:04.6	55.494S 124.485E	EASTERN IS. CORDILLERA	33	5.1	4.2	PDE	EQ	ABDE	18:46-19:02	17	2001/2/12
0233	02 11 03 307 14:48:24.5	3.235S 139.692E	WEST IRIAN	33	5.3	0.0	PDE	EQ	A	14:56-15:01	12	2001/2/13
0234	02 11 03 307 18:07:47.9	25.167S 179.724E	SOUTH OF FIJI IS.	486	5.3	0.0	PDE	EQ	A	18:10-18:22	13	2001/2/14
0235	02 11 04 308 03:08:32.1	22.705N 121.643E	TAIWAN REGION	143	5.0	0.0	PDE	EQ	A	03:11-03:22	12	2001/2/15
0236	02 11 04 308 09:29:53.3	44.088N 147.992E	KURIL IS.	38	5.7	5.1	PDE	EQ	ABDE	09:31-09:44	44	2001/2/16
0237	02 11 04 308 15:54:13.1	38.548N 143.424E	OFF EAST COAST OF HONSHU, JAPAN	33	5.4	4.9	PDE	EQ	ABDE	15:55-16:37	43	2001/2/17
0238	02 11 04 308 18:49:17.3	15.260S 167.469E	VANUATU IS.	115	5.2	0.0	PDE	EQ	A	18:51-19:02	12	2001/2/18
0239	02 11 05 309 03:58:32.1	3.598S 177.703E	GILBERT IS. REGION	33	5.0	0.0	PDE	EQ	ABDE	03:51-04:29	39	2001/2/19
0240	02 11 05 309 04:52:02.3	3.633S 128.671E	CERAM	114	5.3	0.0	PDE	EQ	A	04:55-05:06	12	2001/2/20
0241	02 11 05 309 06:31:53.0	26.185S 178.216E	NORFOLK IS. REGION	33	5.7	0.0	PDE	EQ	A	06:35-06:46	12	2001/2/21
0242	02 11 05 309 06:31:53.0	26.185S 178.216E	NORFOLK IS. REGION	33	5.7	0.0	PDE	EQ	A	06:35-06:46	12	2001/2/21
0243	02 11 05 309 16:59:38.0	7.155S 129.622E	BANDA SEA	143	5.2	0.0	PDE	EQ	A	16:25-16:39	15	2001/2/22
0244	02 11 06 310 07:45:49.2	3.556N 126.631E	TALAUD IS.	63	5.2	0.0	PDE	EQ	A	07:49-07:58	12	2001/2/23
0245	02 11 07 311 07:21:35.6	20.216S 173.002E	TONGA IS. REGION	33	5.1	5.1	PDE	EQ	A	07:24-07:36	13	2001/2/24
0246	02 11 07 311 08:38:38.5	6.482S 132.262E	BANDA SEA	107	5.0	0.0	PDE	EQ	A	08:41-08:53	13	2001/2/25
0247	02 11 07 311 15:31:56.4	3.985S 154.479E	NORTH OF SOLOMON IS.	488	4.6	0.0	PDE	EQ	ABD	15:32-15:47	16	2001/2/26
0248	02 11 08 312 07:56:02.2	25.375S 177.167E	SOUTH OF FIJI IS.	150	5.2	0.0	PDE	EQ	A	07:59-08:10	12	2001/2/27
0249	02 11 08 312 09:44:06.9	55.789S 27.061E	SOUTH OF SANDWICH IS. REGION	33	5.4	5.3	PDE	EQ	A	09:53-10:12	20	2001/2/28
0250	02 11 08 312 11:35:42.1	8.855S 119.268E	FLORES IS. REGION	103	5.1	0.0	PDE	EQ	A	11:40-11:51	12	2001/2/29
0251	02 11 08 312 16:48:07.4	55.040N 165.687E	KOMANDORSKY IS. REGION	33	5.2	0.0	PDE	EQ	ABDE	16:42-17:32	51	2001/3/01
0252	02 11 08 312 16:48:07.4	55.040N 165.687E	KOMANDORSKY IS. REGION	33	5.0	0.0	PDE	EQ	ABDE	16:49-17:27	39	2001/3/02
0253	02 11 08 312 18:35:34.8	4.027N 127.035E	TALAUD IS.	161	5.4	0.0	PDE	EQ	A	18:30-18:49	12	2001/3/03
0254	02 11 09 313 08:46:56.1	21.303S 170.734E	FIJI IS. REGION	556	5.2	0.0	PDE	EQ	A	08:49-08:58	12	2001/3/04
0255	02 11 09 313 08:36:35.4	7.236N 94.437E	NICOBAR IS. REGION	33	5.2	4.7	PDE	EQ	A	08:43-08:54	12	2001/3/05
0256	02 11 09 313 09:25:28.4	3.447S 177.708E	GILBERT IS. REGION	33	5.2	0.0	PDE	EQ	ABDE	09:25-10:04	40	2001/3/06
0257	02 11 10 314 13:23:16.0	33.903N 137.077E	KURIL IS.	33	5.1	0.0	PDE	EQ	ABD	13:37-00:22	44	2001/3/07
0258	02 11 10 314 13:23:16.0	33.903N 137.077E	KURIL IS.	347	4.6	0.0	PDE	EQ	ABD	13:24-13:48	17	2001/3/08
0259	02 11 10 314 21:20:45.0	15.454S 176.022E	FIJI IS. REGION	33	5.5	5.7	PDE	EQ	A	21:23-21:34	12	2001/3/09
0260	02 11 11 315 08:43:45.7	6.677S 101.671E	SOUTHWEST OF SUMATERA	33	6.1	5.9	PDE	EQ	A	08:50-09:01	12	2001/3/10
0261	02 11 11 315 01:55:37.2	44.237N 149.515E	KURIL IS.	46	6.4	5.2	PDE	EQ	ABDE	01:56-02:39	44	2001/3/11
0262	02 11 11 315 02:01:15.1	44.338N 149.488E	KURIL IS.	41	6.0	5.2	PDE	EQ	ABDE	02:02-02:35	44	2001/3/12
0263	02 11 11 315 02:52:09.3	44.113N 149.595E	KURIL IS.	41	6.3	5.2	PDE	EQ	ABD	02:53-03:35	43	2001/3/13
0264	02 11 11 315 04:14:34.6	44.217N 149.314E	KURIL IS.	33	5.0	0.0	PDE	EQ	ABD	04:15-04:50	44	2001/3/14
0265	02 11 11 315 11:55:58.9	6.190S 145.369E	EAST PAPUA NEW GUINEA REG.	42	5.4	0.0	PDE	EQ	ABD	11:57-12:14	47	2001/3/15
0266	02 11 11 315 21:22:22.4	27.431S 176.735E	KERMADEC IS. REGION	44	5.6	4.6	PDE	EQ	A	21:25-21:36	12	2001/3/16
0267	02 11 12 316 12:16:05.2	1.478N 126.455E	MOLUCCA PASSAGE	33	5.1	0.0	PDE	EQ	A	12:19-12:30	12	2001/3/17
0268	02 11 12 316 19:17:00.1	37.024N 116.032E	SOUTHERN NEVADA	33	4.4	0.0	PDE	EQ	NX	19:23-19:34	12	2001/3/18
0269	02 11 12 316 22:00:54.0	42.753N 150.075E	KURIL IS. REGION	33	5.1	0.0	PDE	EQ	ABDE	22:10-22:52	43	2001/3/19
0270	02 11 13 317 01:20:59.2	17.079S 176.306E	FIJI IS. REGION	33	5.0	4.9	PDE	EQ	A	01:22-01:35	13	2001/3/20
0271	02 11 13 317 05:43:47.4	3.305S 146.035E	BISMARCK SEA	7	5.3	5.1	PDE	EQ	ABDE	05:45-06:20	44	2001/3/21
0272	02 11 13 317 07:31:29.1	10.568S 167.241E	VANUATU ISLANDS	36	5.0	0.0	PDE	EQ	A	07:34-07:45		

## WAKE HYDROPHONE INFORMATION PROCESSING SYSTEM (WHIPS) EVENT LISTING.

5 JUL 83

KEY: INFORMATION SOURCES - PDE-NEIS PDECARD, NON-NEIS MONTHLY LIST, ICS-ICS LIST MEL-MELI ORDER, OTH-OTHER  
 EVENT TYPE - EQ-EARTHQUAKE, NX-NUCLEAR EXPLOSION, SX-SCIENTIFIC EXPLOSION, O'-OTHER, UN-UNKNOWN  
 PHASES - A-P, B-PO, C-S, D-SO, E-T, F-OTHER

EVNT	*****ORIGIN TIME*****	*****COORDINATES*****	*****LOCATION*****	DEP	MA	4	INF	EV	*****SAVED*****	*****STRIP*****
NO	*****NO-DA-JUL-HR-MN-SECS*****	*****LAT-LON*****	*****DESCRIPTION*****	KM	BDY	SRC	TY	PHASES	*****INTERVAL*****	*****MNS TAPE/FILE*****
0301	02 11 21 325	23:27:11.7	55.432N 163.222E	OFF EAST COAST OF KAMCHATKA	35	5.7	6.1	PDE E	ABDE	23:29-00:20 52 20016/ 09
0302	02 11 22 326	00:25:20.3	55.627N 163.153E	OFF EAST COAST OF KAMCHATKA	33	4.7	8.0	PDE E	ABD	00:27-00:44 18 20016/ 10
0303	02 11 22 326	00:28:03.7	7.255S 132.145E	TANIMBAR ISL. REGION	85	5.5	1.0	PDE E	A	00:31-00:42 12 20016/ 11
0304	02 11 22 326	01:07:59.0	39.712N 77.718E	SOUTHERN SINKIANG PROV., CHINA	33	5.1	1.0	PDE E	A	01:15-01:26 12 20016/ 11
0305	02 11 22 326	01:26:27.7	55.667N 163.221E	OFF EAST COAST OF KAMCHATKA	33	4.7	3.0	PDE E	ABD	01:28-01:45 18 20016/ 11
0306	02 11 22 326	05:32:51.2	23.740S 175.064W	SOUTH OF FIJI IS.	82	5.4	7.0	PDE E	A	05:36-05:47 12 20016/ 13
0307	02 11 22 326	05:19:48.4	32.250S 178.273W	SOUTH OF KERMADEC IS.	30	5.3	1.0	PDE E	A	06:24-06:35 12 20016/ 14
0308	02 11 22 326	23:00:04.6	32.203S 178.484W	SOUTH OF KERMADEC IS.	80	5.1	2.0	PDE E	A	23:12-23:23 12 20017/ 01
0309	02 11 23 327	06:45:47.0	3.744S 101.700E	SOUTHERN SUMATRA	75	5.1	2.0	PDE E	A	06:52-07:03 12 20017/ 02
0310	02 11 23 327	18:59:29.0	23.955S 175.470W	TONGA IS. REGION	30	5.2	0.0	PDE E	A	19:03-19:14 12 20017/ 03
0311	02 11 25 329	07:31:13.9	3.307S 177.639E	GILBERT IS. REGION	33	5.2	0.0	PDE E	ABDE	07:31-08:08 40 20017/ 04
0312	02 11 25 329	18:00:59.6	36.732N 71.474E	AFGHANISTAN-USSR BORDER REGION	124	4.7	0.0	PDE E	A	18:16-18:27 12 20017/ 05
0313	02 11 25 329	18:55:29.1	38.006N 132.263E	SOUTHEAST OF SHIKOKU, JAPAN	30	4.0	2.0	PDE E	ABD	18:57-19:13 17 20017/ 06
0314	02 11 26 330	16:00:27.3	11.057N 142.647E	SOUTH OF MARIANA IS.	33	4.4	0.0	PDE E	ABD	16:09-16:22 14 20017/ 07
0315	02 11 26 330	16:52:01.0	5.020N 125.812E	MINDANAO, PHILIPPINE IS.	10	5.0	2.0	PDE E	A	16:55-17:06 12 20017/ 08
0316	02 11 26 330	17:45:33.0	55.084S 144.220W	SOUTH PACIFIC CORDILLERA	10	5.7	5.3	PDE E	A	17:53-18:04 12 20017/ 09
0317	02 11 27 331	02:19:09.0	32.463S 178.263W	SOUTH OF KERMADEC IS.	52	5.5	1.0	PDE E	A	02:23-02:35 13 20017/ 10
0318	02 11 27 331	03:30:42.1	55.764S 144.309W	SOUTH PACIFIC CORDILLERA	10	5.3	2.0	PDE E	A	03:38-03:49 12 20017/ 11
0319	02 11 27 331	09:55:38.0	50.174N 147.792E	SEA OF OKHOTSK	623	5.6	2.0	PDE E	ABDE	09:56-10:46 51 20017/ 12
0320	02 11 27 331	11:13:51.3	5.296N 125.829E	MINDANAO, PHILIPPINE IS.	142	5.1	1.0	PDE E	A	11:16-11:28 13 20017/ 13
0321	02 11 27 331	14:11:46.3	36.535N 71.609E	AFGHANISTAN-USSR BORDER REGION	181	4.2	0.0	PDE E	A	14:19-14:30 12 20017/ 14
0322	02 11 27 331	17:02:44.2	23.544S 175.286W	TONGA IS. REGION	33	5.2	0.0	PDE E	A	17:05-17:17 12 20017/ 15
0323	02 11 27 331	20:30:27.7	39.018N 148.033E	HONSHU, JAPAN	33	4.8	0.0	PDE E	ABD	20:31-20:47 17 20017/ 16
0324	02 11 28 332	11:04:06.9	6.608S 150.523E	NEW BRITAIN REGION	33	5.0	1.0	PDE E	ABDE	11:05-11:49 45 20017/ 17
0325	02 11 28 332	19:05:30.2	2.912S 129.481E	CELESTES	33	5.0	1.0	PDE E	ABD	19:08-19:20 13 20017/ 18
0326	02 11 29 333	14:02:50.6	6.464S 154.399E	SOLOMON IS.	33	5.0	2.0	PDE E	ABD	14:04-14:15 16 20017/ 19
0327	02 11 30 334	02:16:43.9	20.436S 178.035W	FIJI IS. REGION	542	5.2	2.0	PDE E	A	02:19-02:30 12 20017/ 20
0328	02 11 30 334	02:00:00.0	2.000E 2.000E	PROBABLY MARIANAS	2	0.0	0.0	HEL E	BD	06:52-07:19 26 20017/ 21
0329	02 11 30 334	14:03:00.5	32.449S 178.133W	SOUTH OF KERMADEC IS.	30	5.2	0.0	PDE E	A	14:07-14:18 12 20017/ 22
0330	02 11 30 334	18:54:20.6	9.449S 121.595E	FLORES IS. REGION	224	4.7	0.0	PDE E	A	18:50-19:09 12 20017/ 23
0331	02 11 30 334	19:08:32.2	51.977N 158.918E	NEAR EAST COAST OF KAMCHATKA	33	4.7	0.0	PDE E	ASD	19:10-19:26 17 20017/ 23
0332	02 12 01 335	00:39:44.4	31.047N 131.762E	KYUSHU, JAPAN	35	5.0	5.1	PDE E	ABDE	00:41-00:59 49 20018/ 01
0333	02 12 02 336	03:20:14.1	1.199S 23.722W	CENTRAL MID-ATLANTIC RIDGE	10	5.2	4.9	PDE E	A	03:29-03:48 29 20018/ 01
0334	02 12 02 336	09:43:53.7	51.927N 170.473W	FOX IS., ALEUTIAN IS.	33	5.5	4.7	PDE E	ABDE	09:46-10:37 52 20018/ 02
0335	02 12 02 336	15:24:50.1	36.217N 142.629E	OFF EAST COAST OF HONSHU JAPAN	33	4.7	0.0	PDE E	ABD	15:26-15:41 16 20018/ 02
0336	02 12 02 336	19:36:56.4	4.542S 130.980E	WEST IRIAN	33	5.6	5.3	PDE E	A	19:39-19:58 12 20018/ 03
0337	02 12 03 337	00:56:10.0	3.009S 151.969E	NEW IRELAND REGION	255	4.9	0.0	PDE E	ABD	00:56-01:11 16 20018/ 04
0338	02 12 03 337	01:38:42.5	23.580S 175.762W	TONGA IS. REGION	33	5.3	5.9	PDE E	A	01:42-01:53 12 20018/ 05
0339	02 12 03 337	16:49:56.6	9.057S 120.340E	SUMBA IS. REGION	33	5.1	1.0	PDE E	A	16:54-17:05 12 20018/ 07
0340	02 12 03 337	22:30:00.1	13.350S 167.206E	VANUATU IS.	26P	5.7	1.0	PDE E	A	22:31-22:42 12 20018/ 06
0341	02 12 04 338	02:07:27.9	3.715S 148.022E	WEST IRIAN	33	5.1	0.0	PDE E	A	02:09-02:20 12 20018/ 09
0342	02 12 04 338	07:45:00.4	4.944N 126.055E	TALAUD ISLANDS	10	5.0	2.0	PDE E	A	07:48-07:59 12 20018/ 10
0343	02 12 04 338	23:23:44.4	22.937N 142.691E	VOLCANO IS. REGION	270	4.7	0.0	PDE E	ABDE	23:23-23:59 12 20018/ 11
0344	02 12 05 339	01:03:49.9	0.059S 126.434E	MOLUCCA SEA	50	4.9	0.0	PDE E	A	01:07-01:18 12 20018/ 12
0345	02 12 05 339	03:37:12.6	49.907N 78.843E	EASTERN SAKHAKH SSR	84	5.0	0.0	PDE E	ABDE	03:49-05:32 44 20018/ 14
0346	02 12 05 339	05:48:24.1	9.074S 161.101E	SOLOMON ISLANDS	33	5.0	5.0	PDE E	A	05:08-05:19 12 20018/ 15
0347	02 12 05 339	05:04:53.5	23.659S 175.461W	TONGA ISLANDS REGION	33	5.4	0.0	PDE E	A	10:43-11:55 13 20018/ 16
0348	02 12 05 339	13:42:12.0	11.009S 165.126E	SANTA CRUZ ISLANDS	33	5.4	5.2	PDE E	A	15:04-15:15 12 20018/ 17
0349	02 12 05 339	15:00:36.0	23.624S 175.627W	TONGA ISLANDS REGION	33	5.5	5.7	PDE E	A	15:56-16:07 12 20018/ 18
0350	02 12 05 339	15:52:22.6	23.489S 175.001W	TONGA ISLANDS REGION	33	5.5	5.7	PDE E	A	15:56-16:07 12 20018/ 18
0351	02 12 06 340	14:03:31.6	36.321N 141.262E	NEAR EAST COAST OF HONSHU, JAP	59	4.7	0.0	PDE E	ABD	14:04-14:19 16 20018/ 20
0352	02 12 06 341	05:43:49.6	36.025N 114.025W	SOUTHERN NEVADA	5	0.0	0.0	PDE E	A	09:58-10:01 12 20018/ 21
0353	02 12 07 341	12:12:09.1	45.551N 146.050E	KURIL ISLANDS	117	4.0	0.0	PDE E	ABD	12:13-12:29 17 20018/ 22
0354	02 12 08 342	02:01:34.1	14.235N 145.126E	MARIANA ISLANDS	66	4.9	0.0	PDE E	ABD	02:01-02:54 14 20018/ 23
0355	02 12 08 342	05:01:12.6	3.473S 177.577E	GILBERT ISLANDS REGION	33	5.1	0.0	PDE E	A	05:04-11:06 13 20018/ 24
0356	02 12 08 342	16:30:51.0	0.632N 119.918E	MINDANASSA PENINSULA	87	5.0	0.0	PDE E	A	16:34-16:46 13 20018/ 25
0357	02 12 08 342	18:04:47.1	41.364S 07.626E	WEST CHILE RISE	10	5.4	0.0	PDE E	A	18:14-18:33 20 20018/ 26
0358	02 12 09 343	01:41:07.6	29.009S 112.655W	EASTERN ISLAND REGION	10	5.6	5.9	PDE E	ABDE	01:50-03:42 113 20018/ 27
0359	02 12 09 343	05:20:40.1	3.481S 177.616E	GILBERT ISLANDS REGION	33	5.6	5.2	PDE E	ABDE	05:29-06:07 39 20018/ 28
0360	02 12 09 343	10:39:40.3	21.025S 168.527E	LOYALTY ISLANDS	33	5.4	5.0	PDE E	A	10:42-10:53 12 20018/ 29
0361	02 12 09 343	18:50:35.7	47.033N 155.246E	KURIL ISLANDS REGION	33	5.2	0.0	PDE E	ABDE	19:00-19:43 44 20018/ 31
0362	02 12 10 344	14:49:35.7	45.177N 148.613E	KURIL ISLANDS	119	4.9	0.0	PDE E	ABD	14:50-15:06 17 20018/ 32
0363	02 12 10 344	15:28:00.0	37.030N 116.072W	SOUTHERN NEVADA	8	4.0	0.0	PDE E	A	15:26-15:37 12 20018/ 33
0364	02 12 10 344	17:20:59.9	26.442S 176.570W	SOUTH OF FIJI ISLANDS	33	5.2	5.1	PDE E	A	17:24-17:36 13 20018/ 34
0365	02 12 10 344	02:00:00.0	0.000N 0.000E	PROBABLY MARIANAS PO SO T	0	0.0	0.0	HEL E	BDE	19:10-19:44 35 20018/ 35
0366	02 12 10 344	02:00:00.0	0.000N 0.000E	PROBABLY MARIANAS PO SO T	0	0.0	0.0	HEL E	BDE	23:19-00:02 49 20018/ 36
0367	02 12 11 345	16:46:31.4	11.377S 119.813E	SOUTH OF SUMBA ISLAND	33	5.7	1.0	PDE E	A	16:51-17:02 12 20018/ 37
0368	02 12 12 346	17:10:09.2	17.018N 145.616E	MARIANA ISLANDS	326	4.9	0.0	PDE E	ABD	17:09-17:42 34 20018/ 38
0369	02 12 13 347	02:50:51.6	63.275S 61.237W	SOUTH SHETLAND ISLANDS	33	5.7	5.4	PDE E	A	03:00-03:19 20 20018/ 39
0370	02 12 13 347	09:12:49.4	14.750N 44.207E	WESTERN ARABIAN PENINSULA	10	5.9	6.0	PDE E	A	09:22-11:41 140 20018/ 40
0371	02 12 13 347	10:25:05.5	10.111S 178.476W	FIJI IS. REGION	845	4.7	0.0	PDE E	A	10:27-10:38 12 20018/ 41
0372	02 12 14 348	02:37:10.5	20.535S 169.407E	TONGA IS. REGION	207	5.2	0.0	PDE E	A	02:39-02:51 13 20018/ 42
0373	02 12 14 348	12:02:05.0	23.053S 175.005W	SOUTH OF FIJI IS.	33	5.4	5.6	PDE E	A	12:05-12:17 13 20018/ 43
0374	02 12 14 348	23:11:07.7	23.197S 178.612E	SOUTH OF FIJI IS.	548	5.9	0.0	PDE E	A	23:13-23:25 13 20018/ 44
0375	02 12 15 349	10:17:21.0	10.177S 178.321W	FIJI IS. REGION	652	5.0	0.0	PDE E	A	10:19-10:32 12 20018/ 45
0376	02 12 16 350	00:40:48.6	36.242N 69.096E	HINDU KUSH REGION	35	6.2	6.6	PDE E	AE	00:40-02:33 106 20018/ 46
0377	02 12 16 350	05:27:53.1</								

## WAKE HYDROPHONE INFORMATION PROCESSING SYSTEM (WHIPS) EVENT LISTING

5 JUL 83

KEY: INFORMATION SOURCES - PDE-NEIS PDECARD, MON-NEIS MONTHLY LIST, ICS-ICS LIST, MEL-MELICORDE, OTH-OTHER  
 EVENT TYPE - EQ-EARTHQUAKE, NX-NUCLEAR EXPLOSION, SX-SCIENTIFIC EXPLOSION, OT-OTH.R, UN-UNKNOWN  
 PHASES - A-P, B-PO, C-S, D-SO, E-T, F-OTHER

EVNT NO	ORIGIN VR	TIME MO DA JUL	COORDINATES HR MN SECS	COORDINATES LAT	COORDINATES LON	DESCRIPTION	DPT KM	MAGNI BDY	INF SRF	EV SRC	PHASES	INTERVAL MNS	STRIP TAPE/FILE
0401	02	12	20	354	01:30:30.3	24.860S 175.580W	SOUTH OF TONGA ISLANDS	33	5.5	6.8	PDE EQ AE	01:34-02:36	63 20021/ 03
0402	02	12	20	354	02:50:10.6	23.693S 176.825W	SOUTH OF FIJI ISLANDS	33	5.7	6.3	PDE EQ AE	03:01-04:03	63 20021/ 04
0403	02	12	20	354	05:54:37.5	24.504S 175.985W	SOUTH OF TONGA ISLANDS	33	5.9	5.8	PDE EQ A	05:58-06:04	12 20021/ 05
0404	02	12	20	354	07:14:20.7	24.604S 175.623W	SOUTH OF TONGA ISLANDS	33	5.3	5.8	PDE EQ A	07:18-07:29	12 20021/ 06
0405	02	12	20	354	07:56:42.0	24.542S 175.989W	SOUTH OF TONGA ISLANDS	33	5.6	5.1	PDE EQ A	08:02-08:11	12 20021/ 07
0406	02	12	20	354	12:34:59.3	24.682S 175.991W	SOUTH OF TONGA ISLANDS	33	5.5	5.6	PDE EQ A	12:38-12:52	13 20021/ 08
0407	02	12	20	354	14:35:45.4	24.584S 175.848W	SOUTH OF TONGA ISLANDS	33	5.7	6.0	PDE EQ AE	14:39-14:41	63 20021/ 09
0408	02	12	20	354	18:12:22.9	23.821S 175.631W	TONGA ISLANDS REGION	33	5.5	6.2	PDE EQ AE	18:16-18:17	62 20021/ 10
0409	02	12	21	355	01:10:16.1	42.255N 142.396E	HONAIKAI JAPAN REGION	53	4.7	0.0	PDE EQ ABD	01:19-01:35	17 20021/ 11
0410	02	12	21	355	01:19:29.0	24.672S 175.743W	SOUTH OF TONGA ISLANDS	33	5.2	5.4	PDE EQ A	02:23-02:34	12 20021/ 12
0411	02	12	21	355	05:48:10.7	3.494S 142.925E	NEAR N COAST PAPUA NEW GUINEA	17	5.1	0.0	PDE EQ ABDE	05:58-06:35	46 20021/ 13
0412	02	12	21	355	05:10:23.1	16.172S 172.569W	SAMOA ISLANDS REGION	33	5.2	0.0	PDE EQ A	05:12-05:24	12 20021/ 14
0413	02	12	21	355	07:31:47.0	24.239S 175.707W	SOUTH OF TONGA ISLANDS	33	5.0	0.0	PDE EQ A	07:35-07:45	12 20021/ 15
0414	02	12	21	355	12:00:46.6	29.221N 81.333E	NEPAL	33	4.7	0.0	PDE EQ A	12:16-12:27	12 20021/ 16
0415	02	12	21	355	16:12:10.3	24.744S 175.776W	SOUTH OF TONGA ISLANDS	33	5.3	5.7	PDE EQ A	16:16-16:27	12 20021/ 17
0416	02	12	21	355	18:00:27.1	23.622S 175.622W	TONGA ISLANDS REGION	33	5.3	5.2	PDE EQ A	18:04-18:15	12 20021/ 18
0417	02	12	21	355	18:43:25.0	23.999S 175.899W	TONGA ISLANDS REGION	33	5.1	0.0	PDE EQ A	18:47-18:58	12 20021/ 19
0418	02	12	21	355	23:35:27.9	37.172N 71.743E	AFGHANISTAN-USSR BORDER REGION	160	4.0	0.0	PDE EQ A	23:42-23:54	13 20021/ 20
0419	02	12	22	356	00:32:35.3	23.251S 179.835E	SOUTH OF FIJI ISLANDS	573	5.5	0.0	PDE EQ A	00:35-00:40	12 20021/ 21
0420	02	12	23	357	00:10:30.1	24.479S 176.210W	SOUTH OF FIJI ISLANDS	33	5.6	5.3	PDE EQ A	00:14-00:25	12 20021/ 22
0421	02	12	23	357	02:14:13.2	23.812S 175.949W	TONGA ISLANDS REGION	33	5.4	5.4	PDE EQ A	02:17-02:29	13 20021/ 23
0422	02	12	23	357	03:20:30.0	24.507S 176.895W	SOUTH OF FIJI ISLANDS	33	5.4	5.3	PDE EQ A	03:24-03:35	12 20021/ 24
0423	02	12	23	357	05:47:24.9	24.186S 175.816W	SOUTH OF TONGA ISLANDS	33	5.1	0.0	PDE EQ A	05:51-05:52	12 20021/ 25
0424	02	12	23	357	09:41:47.0	23.778S 175.326W	TONGA ISLANDS REGION	33	5.3	5.1	PDE EQ A	09:45-09:56	12 20021/ 26
0425	02	12	23	357	13:05:16.5	23.596S 175.445W	TONGA ISLANDS REGION	33	5.5	5.4	PDE EQ A	13:09-13:20	12 20021/ 27
0426	02	12	24	358	04:10:24.2	24.455S 175.183E	SOUTH OF FIJI ISLANDS	33	5.2	5.1	PDE EQ A	04:14-04:25	12 20021/ 28
0427	02	12	24	358	06:17:07.0	27.165N 71.794E	AFGHANISTAN-USSR BORDER REGION	148	4.6	0.0	PDE EQ A	06:21-06:32	13 20021/ 29
0428	02	12	24	358	10:10:22.6	44.896N 149.511E	KURIL ISLANDS	56	5.2	0.0	PDE EQ ABDE	10:14-10:25	44 20021/ 30
0429	02	12	24	358	23:31:03.0	52.521N 173.311E	NEAR ISLANDS, ALEUTIAN ISLANDS	74	5.2	0.0	PDE EQ A	23:32-23:44	13 20021/ 31
0430	02	12	25	359	00:00:00.0	0.000N 0.000E	POSSIBLY NEAR WAKE ISLAND	0.0	0.0	0.0	HEL EC BDE	00:00-00:00	12 20021/ 32
0431	02	12	25	359	04:19:31.9	0.717S 134.871E	WEST IRAN REGION	51	4.7	0.0	PDE EQ A	04:22-04:33	12 20021/ 33
0432	02	12	25	359	07:53:39.3	4.377S 131.454E	BANDA SEA	33	5.1	4.4	PDE EQ A	07:56-08:08	13 20021/ 34
0433	02	12	25	359	12:20:00.0	8.431S 123.004E	FLORIS ISLAND REGION	22	5.6	5.8	PDE EQ A	12:22-12:43	12 20021/ 35
0434	02	12	25	359	16:51:47.3	26.575N 95.040E	BURMA-INDIA BORDER REGION	33	5.2	0.0	PDE EQ A	16:57-17:09	13 20021/ 36
0435	02	12	26	360	02:29:36.5	45.252N 151.200E	KURIL ISLANDS	33	5.0	0.0	PDE EQ ABDE	02:32-02:43	44 20021/ 37
0436	02	12	26	360	02:22:07.0	23.985S 175.174W	TONGA ISLANDS REGION	33	5.1	0.0	PDE EQ A	02:23-02:35	13 20021/ 38
0437	02	12	26	360	02:42:00.3	3.637S 177.692E	GILBERT ISLANDS REGION	33	4.9	0.0	PDE EQ ABDE	02:42-02:51	40 20021/ 39
0438	02	12	26	360	03:35:14.3	50.070N 79.895E	EASTERN KAZAKH SSR	0.0	5.7	0.0	PDE NX A	03:42-03:53	12 20021/ 40
0439	02	12	26	360	05:29:34.0	41.011N 61.693E	UZBEK SSR	33	4.9	0.0	PDE EQ A	05:37-05:45	12 20021/ 41
0440	02	12	26	360	09:24:42.7	4.553S 143.850E	PAPUA NEW GUINEA	102	5.3	0.0	PDE EQ ABDE	09:26-09:42	47 20021/ 42
0441	02	12	26	360	16:19:57.6	38.278N 141.696E	NEAR EAST COAST OF HONSHU JAPAN	73	5.1	0.0	PDE EQ ABDE	16:21-16:33	43 20021/ 43
0442	02	12	26	360	20:59:56.3	3.302S 177.796E	GILBERT ISLANDS REGION	33	4.7	0.0	PDE EQ ABDE	20:59-21:10	39 20021/ 44
0443	02	12	27	361	01:32:57.6	19.005N 145.000E	MARIANA ISLANDS	600	5.3	0.0	PDE EQ ABDE	01:32-01:45	39 20021/ 45
0444	02	12	27	361	01:50:42.0	11.439S 162.325E	SOLOMON ISLANDS	78	5.0	0.0	PDE EQ ABDE	01:52-02:06	45 20021/ 46
0445	02	12	28	362	02:00:00.0	0.000N 0.000E	POSSIBLE MARIANAS PO.SO.T	0.0	0.0	0.0	HEL EC BDE	02:00-02:00	30 20021/ 47
0446	02	12	27	361	07:07:29.4	34.116N 139.120E	NEAR S. COAST OF HONSHU JAPAN	33	5.0	0.0	PDE EQ ABDE	07:08-07:15	44 20021/ 48
0447	02	12	27	361	11:33:18.0	33.823N 139.451E	SOUTH OF HONSHU JAPAN	21	5.2	5.0	PDE EQ ABDE	11:34-12:16	45 20021/ 49
0448	02	12	27	361	14:07:43.0	34.233N 139.243E	NEAR S. COAST OF HONSHU JAPAN	33	5.6	0.0	PDE EQ ABDE	14:08-14:51	44 20021/ 50
0449	02	12	28	362	01:23:47.6	33.101N 129.361E	SOUTH OF HONSHU JAPAN	20	5.0	4.1	PDE EQ ABDE	01:25-02:07	47 20021/ 51
0450	02	12	28	362	01:52:31.3	33.707N 139.447E	SOUTH OF HONSHU JAPAN	21	5.3	5.5	PDE EQ ABDE	01:53-02:35	43 20021/ 52
0451	02	12	28	362	02:12:14.1	33.578N 139.540E	SOUTH OF HONSHU JAPAN	15	5.2	0.0	PDE EQ ABDE	02:13-02:25	43 20021/ 53
0452	02	12	28	362	06:37:42.0	33.739N 139.465E	SOUTH OF HONSHU JAPAN	20	5.9	6.1	PDE EQ ABDE	06:38-07:20	43 20021/ 54
0453	02	12	28	362	07:30:07.5	22.355N 102.860E	BURMA-CHINA BORDER REGION	26	5.2	0.0	PDE EQ A	07:35-07:46	12 20021/ 55
0454	02	12	28	362	08:00:00.0	25.577N 99.379E	YUNNAN PROVINCE, CHINA	30	5.0	0.0	PDE EQ A	08:05-08:17	13 20021/ 56
0455	02	12	28	362	10:03:46.3	18.007N 145.762E	MARIANA ISLANDS	217	4.6	0.0	PDE EQ ABDE	10:03-10:35	33 20021/ 57
0456	02	12	28	362	13:49:29.5	19.950N 121.423E	PHILIPPINE ISLANDS REGION	39	5.9	5.9	PDE EQ A	13:52-14:04	13 20021/ 58
0457	02	12	28	362	15:53:51.5	23.605S 175.702W	TONGA ISLANDS REGION	33	5.3	5.6	PDE EQ A	15:57-16:08	12 20021/ 59
0458	02	12	28	362	16:29:36.3	33.636N 139.674E	SOUTH OF HONSHU JAPAN	33	4.5	5.7	PDE EQ ABDE	16:38-17:12	43 20021/ 60
0459	02	12	28	362	21:19:05.0	3.363S 177.713E	GILBERT ISLANDS REGION	33	5.1	0.0	PDE EQ ABDE	21:19-21:50	40 20021/ 61
0460	02	12	28	362	21:51:05.1	23.384S 175.635W	TONGA ISLANDS REGION	33	5.0	0.0	PDE EQ A	21:54-22:06	13 20021/ 62
0461	02	12	28	362	23:37:06.4	18.194S 170.514W	FIJI ISLANDS REGION	627	4.8	0.0	PDE EQ A	23:39-23:52	12 20021/ 63
0462	02	12	29	363	00:09:20.0	38.344N 79.022E	TIBET-INDIA BORDER REGION	33	4.8	0.0	PDE EQ A	00:16-00:27	12 20021/ 64
0463	02	12	29	363	02:10:55.0	17.717S 177.446W	FIJI ISLANDS REGION	419	5.1	0.0	PDE EQ A	02:13-02:24	12 20021/ 65
0464	02	12	29	363	07:02:31.4	33.724N 139.255E	SOUTH OF HONSHU JAPAN	20	5.5	5.3	PDE EQ ABDE	07:03-07:45	43 20021/ 66
0465	02	12	29	363	12:17:45.9	33.702N 139.296E	SOUTH OF HONSHU JAPAN	22	5.3	4.6	PDE EQ ABDE	12:19-13:01	43 20021/ 67
0466	02	12	29	363	14:05:40.9	14.066N 120.323E	LUZON PHILIPPINE ISLANDS	107	5.5	0.0	PDE EQ A	14:09-14:20	12 20021/ 68
0467	02	12	29	363	15:14:59.6	34.049N 140.396E	NEAR EAST COAST OF HONSHU JAPAN	33	5.0	0.0	PDE EQ ABDE	15:16-15:57	42 20021/ 69
0468	02	12	29	363	15:21:20.9	29.941N 70.136E	PAKISTAN	33	5.0	4.9	PDE EQ A	15:29-15:40	12 20021/ 70
0469	02	12	29	363	16:50:41.0	6.504S 154.529E	SOLOMON ISLANDS	33	5.1	0.0	PDE EQ ABDE	16:59-17:41	43 20021/ 71
0470	02	12	30	364	00:51:21.0	24.154S 174.969W	SOUTH OF TONGA ISLANDS	64	4.9				

## WAKE HYDROPHONE INFORMATION PROCESSING SYSTEM (WHIPS) EVENT LISTING

5 JUL 83

KEY: INFORMATION SOURCES - PDE=NEIS PDECARD, MON=NEIS MONTHLY LIST, ICS=ICS LIST, MEL=HELICORDER, OTH=OTHER  
 EVENT TYPE - EQ=EARTHQUAKE, NX=NUCLEAR EXPLOSION, SX=SCIENTIFIC EXPLOSION, OT=OTHER, UN=UNKNOWN  
 PHASES - A=P, B=PO, C=S, D=SO, E=T, F=OTHER

EVNT	*****ORIGIN TIME*****	*****COORDINATES*****	*****LOCATION*****	DEP	MAGNI	INF	EV	*****SAVED*****	*****STRIP*****		
NO	VR=MO=DA=JUL=MM=SS	LAT=LONG	*****DESCRIPTION*****	KM	BOY=SRF	SRC	TP	*****PHASES*****	*****INTERVAL*****	*****MNS*****	*****TAPE/FILE*****
0501	03 01 06 006 17:21:26.4	8.349N 147.327E	CAROLINE ISLANDS REGION	33	5.0	0.0	PDE EQ ABDE	17:21-17:55	35	20026/ 02	
0502	03 01 06 006 18:02:30.0	14.066N 146.997E	MARIANA ISLANDS	33	4.5	0.0	PDE EQ ABD	18:02-18:14	13	20026/ 03	
0503	03 01 06 006 19:56:44.9	19.668S 176.599W	FUJI ISLANDS REGION	285	5.1	0.0	PDE EQ A	19:56-20:10	12	20026/ 04	
0504	03 01 06 006 20:29:30.4	31.356N 82.220E	TIBET	33	4.7	0.0	PDE EQ A	20:29-20:47	12	20026/ 05	
0505	03 01 07 007 09:17:35.6	3.248N 126.857E	TALAUD ISLANDS	63	5.2	0.0	PDE EQ A	09:17-09:31	12	20026/ 06	
0506	03 01 07 007 18:10:56.9	36.001N 139.747E	HONSHU JAPAN	67	5.0	0.0	PDE EQ ABDE	18:10-18:23	44	20026/ 07	
0507	03 01 07 007 23:40:24.7	26.863S 176.653W	SOUTH OF FUJI ISLANDS	33	5.3	5.3	PDE EQ A	23:40-23:52	12	20026/ 08	
0508	03 01 08 008 06:35:12.2	3.116S 177.675E	GILBERT ISLANDS REGION	33	4.9	0.0	PDE EQ ABD	06:35-06:50	16	20026/ 09	
0509	03 01 08 008 08:10:34.0	17.958S 178.117W	FUJI ISLANDS REGION	681	5.1	0.0	PDE EQ A	08:10-08:24	13	20026/ 10	
0510	03 01 08 008 10:51:33.3	36.423N 78.651E	HINDU KUSH REGION	195	4.0	0.0	PDE EQ A	10:51-11:10	17	20026/ 11	
0511	03 01 08 008 10:02:00.0	0.000N 0.000E	PROBABLE BONIN ISLANDS	0.0	0.0	0.0	HEL NX BDE	11:00-11:37	38	20026/ 12	
0512	03 01 08 008 11:21:29.6	15.324S 173.397W	TONGA ISLANDS	33	6.1	6.3	PDE EQ AE	11:24-12:18	51	20026/ 13	
0513	03 01 08 008 15:04:55.2	3.164S 146.255E	BISMARCK SEA	9	5.5	6.1	PDE EQ AE	15:06-15:46	43	20026/ 14	
0514	03 01 08 008 16:21:14.2	55.265N 163.182E	OFF EAST COAST OF KAMCHATKA	33	5.0	0.0	PDE EQ ABDE	16:23-17:13	51	20026/ 15	
0515	03 01 08 008 17:42:47.3	55.057N 163.225E	OFF EAST COAST OF KAMCHATKA	33	5.2	5.1	PDE EQ ABDE	17:45-18:35	51	20026/ 16	
0516	03 01 09 009 12:44:07.3	43.929N 142.687E	HOKKAIDO JAPAN REGION	281	4.7	0.0	PDE EQ ABDE	12:45-13:31	47	20027/ 01	
0517	03 01 09 009 18:36:53.5	35.922N 139.565E	NEAR S. COAST OF HONSHU JAPAN	188	5.0	0.0	PDE EQ ABDE	18:38-19:21	44	20027/ 02	
0518	03 01 09 009 21:03:54.2	55.111N 163.381E	OFF EAST COAST OF KAMCHATKA	33	5.4	6.0	PDE EQ ABDE	21:06-21:56	51	20027/ 03	
0519	03 01 10 010 01:57:55.7	1.944S 133.740E	WEST IRIAN REGION	33	5.3	5.7	PDE EQ ABDE	02:00-02:52	53	20027/ 04	
0520	03 01 10 010 05:12:51.0	9.620N 122.087E	NEGROS PHILIPPINE ISLANDS	42	5.1	0.0	PDE EQ A	05:16-05:27	12	20027/ 05	
0521	03 01 10 010 12:32:21.9	27.299S 63.390W	SANTIAGO DEL ESTERO PROV. ARG	559	5.8	0.0	PDE EQ A	12:41-13:01	21	20027/ 06	
0522	03 01 11 011 06:12:43.4	3.417S 177.640E	GILBERT ISLANDS REGION	33	4.9	0.0	PDE EQ ABD	06:13-06:27	15	20027/ 07	
0523	03 01 11 011 10:49:00.0	3.365N 122.338E	CELEBES SEA	642	5.2	0.0	PDE EQ ABD	10:51-11:03	13	20027/ 08	
0524	03 01 12 012 01:02:20.5	3.417S 177.597E	GILBERT ISLANDS REGION	33	4.7	0.0	PDE EQ ABD	01:03-01:17	15	20027/ 09	
0525	03 01 12 012 03:20:25.0	27.031N 96.962E	BURMA-INDIA BORDER REGION	33	4.9	0.0	PDE EQ A	03:24-03:45	12	20027/ 10	
0526	03 01 12 012 05:29:45.7	56.988N 162.481E	NEAR EAST COAST OF KAMCHATKA	33	4.9	0.0	PDE EQ A	05:32-06:49	19	20027/ 11	
0527	03 01 12 012 09:11:58.0	24.481S 175.824E	SOUTH OF TONGA ISLANDS	33	4.7	0.0	PDE EQ ABD	09:14-09:26	12	20027/ 12	
0528	03 01 12 012 12:22:25.6	26.849N 97.940E	BURMA	33	5.3	5.1	PDE EQ A	12:28-12:39	12	20027/ 13	
0529	03 01 12 012 16:10:32.9	4.357S 150.248E	NEW BRITAIN REGION	567	4.7	0.0	PDE EQ ABDE	16:19-17:01	43	20027/ 14	
0530	03 01 12 012 16:41:21.0	54.924N 162.869E	NEAR EAST COAST OF KAMCHATKA	33	4.9	0.0	PDE EQ ABD	16:43-17:02	18	20027/ 15	
0531	03 01 13 013 09:23:47.5	35.785S 182.832E	SOUTHERN PACIFIC OCEAN	18	5.4	5.1	PDE EQ ABD	09:23-10:08	35	20027/ 16	
0532	03 01 13 013 15:05:05.3	44.498N 148.150E	KURIL ISLANDS	33	5.1	0.0	PDE EQ ABDE	15:06-15:49	44	20027/ 17	
0533	03 01 13 013 16:30:33.9	6.590S 154.157E	SOLOMON ISLANDS	33	4.0	0.0	PDE EQ ABD	16:31-16:46	16	20028/ 01	
0534	03 01 14 014 10:20:53.3	56.054N 154.239W	KODIAK ISLAND REGION	33	5.5	5.9	PDE EQ ABDE	10:24-10:26	63	20028/ 02	
0535	03 01 15 015 08:16:51.3	7.402N 124.592E	MINDANAO PHILIPPINE ISLANDS	35	5.6	4.6	PDE EQ A	08:20-08:31	12	20028/ 03	
0536	03 01 15 015 08:39:32.3	33.264N 135.974E	NEAR S. COAST OF SOUTH. HONSHU	413	5.5	0.0	PDE EQ ABDE	08:40-09:25	46	20028/ 04	
0537	03 01 15 015 08:49:54.3	52.039N 160.154E	OFF EAST COAST OF KAMCHATKA	33	5.6	0.0	PDE EQ ABDE	08:51-09:42	52	20028/ 05	
0538	03 01 15 015 08:52:10.0	6.296S 131.117E	TANIMBAR ISLANDS REGION	46	5.3	0.0	PDE EQ A	08:52-09:34	12	20028/ 06	
0539	03 01 15 015 16:55:30.6	2.742N 124.202E	CELEBES SEA	375	4.9	0.0	PDE EQ A	16:58-17:05	12	20028/ 07	
0540	03 01 15 015 19:40:08.1	9.117S 124.157E	TIMOR	92	4.9	0.0	PDE EQ A	19:44-19:55	12	20028/ 08	
0541	03 01 16 016 02:27:52.1	7.221S 129.491E	BANDA SEA	186	5.2	0.0	PDE EQ A	02:31-02:42	12	20028/ 09	
0542	03 01 16 016 13:10:44.5	17.203S 176.929W	FUJI ISLANDS REGION	33	5.7	5.3	PDE EQ A	13:13-13:24	12	20028/ 10	
0543	03 01 16 016 22:10:11.6	5.449S 147.055E	EAST PAPUA NEW GUINEA REGION	229	6.0	0.0	PDE EQ ABDE	22:11-22:56	46	20028/ 11	
0544	03 01 17 017 09:40:16.0	5.405S 146.525E	EAST PAPUA NEW GUINEA REGION	174	5.4	0.0	PDE EQ ABDE	09:41-10:26	46	20028/ 12	
0545	03 01 17 017 11:55:38.4	26.427N 126.241E	RUKYU ISLANDS	33	5.1	0.0	PDE EQ A	11:57-12:09	15	20028/ 13	
0546	03 01 17 017 12:41:29.3	30.092N 128.193E	RUKYU ISLANDS	9	6.0	7.0	PDE EQ AF	12:45-14:44	128	20028/ 14	
0547	03 01 17 017 19:01:08.3	25.662N 126.219E	RUKYU ISLANDS	74	4.9	0.0	PDE EQ A	19:08-19:19	12	20028/ 15	
0548	03 01 18 018 02:22:54.7	49.618S 114.920W	EASTER ISLAND CORDILLERA	18	5.1	5.3	PDE EQ ABD	02:31-03:05	35	20029/ 01	
0549	03 01 18 018 15:23:33.0	58.023S 124.274W	SOUTH SANDWICH ISLANDS REGION	33	6.0	6.5	PDE EQ AF	15:28-17:27	122	20029/ 02	
0550	03 01 18 018 17:42:04.2	6.812S 128.187E	BANDA SEA	318	5.0	0.0	PDE EQ A	17:45-17:56	12	20029/ 03	
0551	03 01 19 019 11:50:10.3	10.618S 166.142E	HINDU KUSH REGION	288	4.4	0.0	PDE EQ A	22:59-23:18	12	20029/ 04	
0552	03 01 19 019 12:09:39.1	25.253N 91.853E	SANTA CRUZ ISLANDS	153	5.0	0.0	PDE EQ ABDE	11:51-12:35	45	20029/ 05	
0553	03 01 19 019 13:38:29.0	55.095N 160.762E	INDIA-BANGLADESH BORDER REGION	33	4.9	0.0	PDE EQ A	12:16-12:27	12	20029/ 06	
0554	03 01 19 019 15:22:06.9	5.741S 154.372E	KAMCHATKA	58	5.0	0.0	PDE EQ ABDE	13:48-14:31	55	20029/ 07	
0555	03 01 20 020 12:45:32.2	20.754N 142.379E	SOLOMON ISLANDS	112	5.4	0.0	PDE EQ A	12:23-21:04	42	20029/ 08	
0556	03 01 20 020 12:45:32.2	20.754N 142.379E	BANDA SEA	153	5.0	0.0	PDE EQ A	10:06-10:17	12	20029/ 09	
0557	03 01 20 020 12:45:32.2	20.754N 142.379E	BONIN ISLANDS REGION	33	5.0	0.0	PDE EQ ABDE	12:46-13:23	38	20029/ 10	
0558	03 01 21 021 05:04:42.0	4.263N 124.559E	ANDAMAN ISL., ALEUTIAN ISL.	69	4.5	0.0	PDE EQ ABD	22:24-23:48	17	20029/ 11	
0559	03 01 21 021 05:04:42.0	4.263N 124.559E	CELEBES SEA	366	4.7	0.0	PDE EQ A	05:07-05:18	12	20029/ 12	
0560	03 01 21 021 05:04:42.0	4.263N 124.559E	HOKKAIDO JAPAN REGION	72	5.2	0.0	PDE EQ ABDE	10:27-11:12	46	20029/ 13	
0561	03 01 21 021 05:04:42.0	4.263N 124.559E	EAST PAPUA NEW GUINEA	33	5.4	5.2	PDE EQ ABDE	14:22-15:05	46	20029/ 14	
0562	03 01 21 021 05:04:42.0	4.263N 124.559E	GILBERT ISLANDS REGION	33	5.1	4.0	PDE EQ ABDE	18:01-18:48	48	20029/ 15	
0563	03 01 22 022 01:24:33.9	6.654S 103.000E	SOUTHWEST OF SUMATRA	33	5.4	5.5	PDE EQ A	01:30-01:42	13	20029/ 16	
0564	03 01 22 022 01:24:33.9	6.654S 103.000E	SOUTHWEST OF SUMATRA	33	5.4	5.5	PDE EQ A	01:34-01:45	12	20029/ 17	
0565	03 01 22 022 06:44:36.5	6.753S 102.993E	SOUTHWEST OF SUMATRA	29	5.6	6.1	PDE EQ AF	06:46-08:17	98	20029/ 18	
0566	03 01 22 022 06:44:36.5	6.753S 102.993E	SOUTHWEST OF SUMATRA	33	5.2	0.0	PDE EQ A	07:02-07:13	12	20029/ 19	
0567	03 01 22 022 08:44:21.5	26.299S 178.745E	SOUTH OF FUJI ISLANDS	594	5.0	0.0	PDE EQ A	08:47-08:58	12	20029/ 20	
0568	03 01 23 023 04:31:36.9	11.584N 141.732E	WEST CAROLINE ISLANDS	33	4.9	0.0	PDE EQ ABDE	04:32-05:09	38	20029/ 21	
0569	03 01 23 023 09:00:36.6	46.319N 150.161E	KURIL ISLANDS	162	4.0	0.0	PDE EQ ABDE	08:09-08:54	46	20029/ 22	
0570	03 01 23 023 10:46:53.7	2.838N 120.507E	HALMAHERA	33	5.0	0.0	PDE EQ A	10:49-11:01	13	20029/ 23	
0571	03 01 23 023 16:36:30.7	37.277S 95.243W	SOUTHERN PACIFIC OCEAN	18	5.6	0.0	PDE EQ ABD	16:46-17:23	38	20029/ 24	
0572	03 01 23 023 17:01:31.9	37.161S 95.147W	SOUTHERN PACIFIC OCEAN	18	5.1	0.0	PDE EQ ABD	17:10-17:40	39	20029/ 25	
0573	03 01 24 024 08:17:30.6	16.184N 95.149W	OAXACA MEXICO	45	6.3	6.6	PDE EQ AE	08:26-10:18	113	20031/ 01	
0574	03 01 24 024 08:02:00.0	0.000N 0.000E	POSSIBLE NUCLEAR TEST	0.0	0.0	0.0	HEL NX AE	08:45-09:05	25	20031/ 02	
0575	03 01 24 024 13:02:37.1	51.342N 176.308E	RAT ISL., ALEUTIAN ISL.	33	5.4	5.7	PDE EQ ABDE	13:04-13:51	88	20031/ 03	
0576	03 01 24 024 15:04:16.3	54.664N 160.435E	NEAR EAST COAST OF KAMCHATKA	33	4.7	0.0	PDE EQ ABDE	15:06-15:56	51	20031/ 04	
0577	03 01 24 024 16:13:21.7	51.433N 176.262E	RAT ISL.,								

## WAKE HYDROPHONE INFORMATION PROCESSING SYSTEM (WHIPS) EVENT LISTING

8 JUL 83

KEY: INFORMATION SOURCES - PDE=NEIS PDECARD, MON=NEIS MONTHLY LIST, ICS=ICS LIST, HEL=HELICORDER, OTW=OTHER  
 EVENT TYPE - EQ=EARTHQUAKE, NX=NUCLEAR EXPLOSION, SX=SCIENTIFIC EXPLOSION, OT=OTHER, UN=UNKNOWN  
 PHASES - A=P, B=PO, C=S, D=SO, L=T, F=OTHER

EVNT	*****ORIGIN TIME*****	*****COORDINATES*****	*****LOCATION*****	DEP	MAGNI	INF	EV	*****SAVED*****	*****STRIP*****
NO	VR=MO=DA=JUL=HR=MM=SECS	LAT=LON	*****DESCRIPTION*****	KM	BDV	SRC	TP	PHASES=INTERVAL=MNS	TAPE/FILE
0601	03 01 20 020 14:23:05.4	18.740S 165.813E	SANTA CRUZ ISLANDS	79	5.6	PDE	EQ ABDE	14:24-15:00	45 20032/ 13
0602	03 01 20 020 15:05:34.9	20.735N 139.318E	BONIN ISLANDS REGION	443	5.1	PDE	EQ ABDE	15:06-15:46	41 20032/ 13
0603	03 01 20 020 21:01:37.3	3.030S 177.057E	GILBERT ISLANDS REGION	33	4.9	PDE	EQ ABD	21:02-21:16	15 20032/ 14
0604	03 01 29 029 00:07:01.8	17.613S 179.869E	FII ISLANDS	634	4.8	PDE	EQ A	00:08-00:20	13 20032/ 15
0605	03 01 29 029 02:44:10.2	36.505N 141.400E	NFAR E. COAST OF MONSHU JAPAN	58	5.0	PDE	EQ ABDE	02:45-03:27	43 20032/ 16
0606	03 01 29 029 09:54:57.2	48.214N 146.151E	SEA OF OKHOTSK	488	4.8	PDE	EQ ABDE	09:56-10:44	49 20033/ 01
0607	03 01 29 029 10:02:14.7	48.214N 146.177E	SEA OF OKHOTSK	478	4.9	PDE	EQ ABDE	10:03-10:51	49 20033/ 01
0608	03 01 29 029 17:47:52.4	17.515S 179.886E	FII ISLANDS	638	4.8	PDE	EQ A	17:49-18:01	13 20033/ 02
0609	03 01 30 030 01:26:05.9	5.420N 94.942E	NORTHERN SUMATERA	82	5.2	PDE	EQ A	01:32-01:43	12 20033/ 03
0610	03 01 30 030 13:29:54.2	18.365S 161.231E	SOLOMON ISLANDS	98	4.8	PDE	EQ ABD	13:31-13:46	16 20033/ 04
0611	03 01 30 030 22:45:39.9	33.369N 148.796E	SOUTH OF MONSHU JAPAN	49	5.7	PDE	EQ ABDE	22:46-23:27	42 20033/ 05
0612	03 01 31 031 05:32:21.1	7.397S 128.743E	BANDA SEA	103	5.3	PDE	EQ A	05:35-05:47	13 20033/ 05
0613	03 01 31 031 21:17:31.4	3.398S 177.616E	GILBERT ISLANDS REGION	29	5.0	PDE	EQ ABDE	21:18-21:56	39 20033/ 07
0614	03 00 00 000 00:00:00.0	0.000N 0.000E	PROBABLE MARIANAS PO. SO. T	0	0.0	HEL	NX A	22:27-22:52	38 20033/ 08
0615	03 01 32 032 00:07:07.7	3.486S 140.147E	WEST IRIAN	33	5.1	PDE	EQ ABDE	00:09-01:57	49 20033/ 09
0616	03 01 32 032 01:47:20.4	37.156N 135.080E	SEA OF JAPAN	374	4.2	PDE	EQ ABDE	14:48-15:36	49 20033/ 10
0617	03 01 32 032 15:38:06.0	4.675S 144.042E	NEAR N COAST OF PAPUA NEW GUIN	68	5.3	PDE	EQ ABDE	15:40-16:25	46 20033/ 11
0618	03 01 32 032 20:44:06.1	27.032N 92.870E	INDIA-CHINA BORDER REGION	33	5.2	PDE	EQ A	20:50-21:01	12 20033/ 12
0619	03 02 04 035 06:31:16.3	1.513N 127.259E	MALAYAN	158	5.4	PDE	EQ A	06:34-06:45	12 20033/ 13
0620	03 02 04 035 15:21:57.0	4.386S 152.040E	NEW BRITAIN REGION	43	5.4	PDE	EQ ABDE	15:23-16:03	41 20033/ 14
0621	03 02 04 035 19:05:59.6	18.393S 124.384E	TIMOR	33	5.4	PDE	EQ A	19:10-19:21	12 20033/ 15
0622	03 02 05 036 03:51:58.0	5.504S 153.019E	NEW IRELAND REGION	47	5.0	PDE	EQ ABDE	03:53-04:34	42 20034/ 01
0623	03 02 05 036 15:47:19.6	6.525S 154.065E	SOLOMON ISLANDS	51	5.0	PDE	EQ ABDE	15:48-16:30	43 20034/ 02
0624	03 02 05 036 17:07:53.1	3.375S 177.567E	GILBERT ISLANDS REGION	33	5.1	PDE	EQ ABDE	17:08-17:46	39 20034/ 03
0625	03 02 05 036 23:51:46.1	3.369S 177.670E	GILBERT ISLANDS REGION	33	5.0	PDE	EQ ABDE	23:52-00:38	39 20034/ 04
0626	03 02 06 037 01:52:33.5	36.107N 68.997E	HINDU KUSH REGION	89	5.1	PDE	EQ A	02:00-02:11	12 20034/ 05
0627	03 02 06 037 16:15:29.6	3.314S 177.066E	GILBERT ISLANDS REGION	33	4.8	PDE	EQ ABD	16:16-16:38	15 20034/ 06
0628	03 02 07 038 01:21:02.0	18.291S 161.063E	SOLOMON ISLANDS	89	5.3	PDE	EQ ABDE	01:22-02:06	45 20034/ 07
0629	03 02 07 038 11:07:26.9	26.495S 177.799W	SOUTH OF FIJI ISLANDS	181	5.3	PDE	EQ A	11:11-11:22	12 20034/ 08
0630	03 02 07 038 16:53:30.3	49.331N 155.627E	KURIL ISLANDS	33	5.2	PDE	EQ ABDE	16:55-17:48	46 20034/ 09
0631	03 02 07 038 16:56:33.8	7.041S 129.055E	BANDA SEA	180	5.0	PDE	EQ A	17:00-17:11	12 20034/ 10
0632	03 02 08 039 02:00:00.0	0.000N 0.000E	POSSIBLE NUCLEAR TEST	0	0.0	HEL	NX A	17:59-18:13	15 20034/ 11
0633	03 02 08 039 10:23:54.2	29.708S 178.464W	KERMADEC ISLANDS	483	5.7	PDE	EQ A	10:27-10:38	12 20034/ 12
0634	03 02 08 039 21:26:00.0	32.710N 135.939E	NFAR S. COAST OF S. MONSHU	486	4.8	PDE	EQ ABDE	21:27-22:52	46 20034/ 13
0635	03 02 08 039 02:51:19.5	26.420N 126.158E	NUKUYU ISLANDS	135	4.5	PDE	EQ A	00:53-01:02	13 20034/ 14
0636	03 02 08 039 02:51:19.5	26.420N 126.158E	HAWAII	27	4.7	PDE	EQ ABDE	02:05-02:54	55 20034/ 15
0637	03 02 08 039 05:50:42.9	51.675N 159.752E	OFF EAST COAST OF KAMCHATKA	33	5.7	PDE	EQ ABDE	07:00-07:47	48 20034/ 16
0638	03 02 08 039 10:19:58.9	6.352S 147.627E	EAST PAPUA NEW GUINEA REGION	59	5.3	PDE	EQ ABDE	10:21-11:06	46 20034/ 17
0639	03 02 08 039 14:06:19.2	45.926N 143.962E	HOKKAIDO JAPAN REGION	252	5.2	PDE	EQ ABDE	14:07-14:54	48 20034/ 18
0640	03 02 08 039 16:17:47.9	1.675S 96.473E	SOUTHWEST OF SUMATERA	15	5.3	PDE	EQ A	16:24-16:35	12 20034/ 19
0641	03 02 08 039 21:38:52.1	20.403S 177.867W	FII ISLANDS REGION	643	5.0	PDE	EQ A	21:39-21:44	12 20035/ 01
0642	03 02 09 040 05:43:36.0	19.546N 120.488E	PHILIPPINE ISLANDS REGION	33	5.4	PDE	EQ A	05:47-05:58	12 20035/ 02
0643	03 02 09 040 05:54:00.0	19.563N 120.535E	PHILIPPINE ISLANDS REGION	33	5.4	PDE	EQ A	05:57-06:08	12 20035/ 03
0644	03 02 09 040 07:02:31.6	7.592S 156.078E	SOLOMON ISLANDS	36	5.6	PDE	EQ ABDE	07:03-07:45	43 20035/ 04
0645	03 02 09 040 13:31:34.1	19.534N 120.438E	PHILIPPINE ISLANDS REGION	33	5.1	PDE	EQ A	13:34-13:46	13 20035/ 05
0646	03 02 09 040 02:00:00.0	0.000N 0.000E	PROBABLE BONIN ISLANDS	0	0.0	HEL	NX A	14:01-14:38	38 20035/ 06
0647	03 02 11 042 01:33:01.8	49.075N 153.933E	KURIL ISLANDS	177	4.7	PDE	EQ ABDE	01:34-02:21	48 20035/ 07
0648	03 02 11 042 04:34:18.2	5.741S 133.762E	APOE ISLANDS REGION	33	5.6	PDE	EQ A	04:37-04:48	12 20035/ 08
0649	03 02 11 042 16:00:00.1	37.051N 116.045W	SOUTHERN NEVADA	0	0.0	PDE	NX A	16:06-16:17	12 20035/ 09
0650	03 02 11 042 17:41:02.7	20.784S 170.283W	FII ISLANDS REGION	513	5.1	PDE	EQ A	17:43-17:54	12 20035/ 10
0651	03 02 12 043 05:17:10.7	36.390N 71.053E	AFGHANISTAN-USSR BORDER REGION	278	4.6	PDE	EQ A	05:24-05:35	12 20035/ 11
0652	03 02 12 043 09:47:10.0	5.610N 126.444E	MINDANAO PHILIPPINE ISLANDS	38	5.8	PDE	EQ AE	09:50-09:45	56 20035/ 12
0653	03 02 12 043 11:20:07.1	5.522N 125.555E	MINDANAO PHILIPPINE ISLANDS	33	5.0	PDE	EQ A	11:31-11:42	12 20035/ 13
0654	03 02 12 043 22:50:24.5	23.709N 105.086E	YUNNAN PROVINCE CHINA	33	4.6	PDE	EQ A	23:03-23:14	12 20035/ 14
0655	03 02 13 044 01:40:13.2	39.988N 75.097E	SOUTHERN SINKIANG PROV CHINA	33	5.6	PDE	EQ AE	01:47-03:26	100 20035/ 15
0656	03 02 13 044 02:52:52.2	39.992N 75.275E	SOUTHERN SINKIANG PROV CHINA	33	5.2	PDE	EQ A	02:50-02:11	12 20035/ 16
0657	03 02 13 044 02:59:03.3	39.916N 75.280E	SOUTHERN SINKIANG PROV CHINA	33	4.4	PDE	EQ A	02:46-02:57	12 20035/ 17
0658	03 02 13 044 04:10:52.9	39.962N 75.128E	SOUTHERN SINKIANG PROV CHINA	33	4.5	PDE	EQ ABDE	04:26-04:37	12 20035/ 18
0659	03 02 13 044 06:35:38.0	13.036N 144.977E	MARIANA ISLANDS	189	5.6	PDE	EQ ABDE	07:35-07:09	35 20035/ 19
0660	03 02 13 044 07:13:11.0	40.005N 124.023E	HONGKONG-SINKIANG BORDER REGION	33	4.9	PDE	EQ A	07:38-07:41	12 20036/ 01
0661	03 02 13 044 14:23:01.1	5.520N 126.521E	MINDANAO PHILIPPINE ISLANDS	33	5.0	PDE	EQ A	14:26-14:37	12 20036/ 02
0662	03 02 13 044 15:10:12.1	11.410N 126.215E	PHILIPPINE ISLANDS REGION	33	5.1	PDE	EQ A	15:13-15:24	12 20036/ 03
0663	03 02 14 045 03:23:10.6	10.479N 140.934E	WEST CAROLINE ISLANDS	33	5.8	PDE	EQ ABDE	03:24-03:02	39 20036/ 04
0664	03 02 14 045 01:29:52.3	1.640N 126.409E	MOLUCCA PASSAGE	56	5.2	PDE	EQ A	01:33-01:44	12 20036/ 05
0665	03 02 14 045 03:20:03.3	84.956N 159.191W	SOUTH OF ALASKA	33	5.9	PDE	EQ AE	03:23-04:21	69 20036/ 06
0666	03 02 14 045 06:00:01.3	22.412S 169.766E	LOVALTY ISLANDS REGION	75	5.0	PDE	EQ A	06:11-06:22	12 20036/ 07
0667	03 02 14 045 09:10:03.7	54.971N 159.212W	SOUTH OF ALASKA	33	5.9	PDE	EQ AE	09:13-09:11	59 20036/ 08
0668	03 02 14 045 23:40:12.0	51.004N 175.571E	RAT ISLANDS, ALEUTIAN ISLANDS	91	4.6	PDE	EQ ABD	23:50-02:06	17 20036/ 09
0669	03 02 15 046 01:14:35.4	10.236S 161.308E	SOLOMON ISLANDS	78	5.2	PDE	EQ ABDE	01:15-01:59	45 20036/ 10
0670	03 02 16 047 09:50:35.3	25.329S 179.624E	SOUTH OF FIJI ISLANDS	478	5.4	PDE	EQ A	09:53-10:04	12 20036/ 11
0671	03 02 17 048 00:16:01.8	43.939N 83.018E	NORTHERN SINKIANG PROV CHINA	33	5.1	PDE	EQ A	00:22-00:34	13 20036/ 12
0672	03 02 17 048 02:00:00.0	0.000N 0.000E	PROBABLE BONIN ISL. PO SO T	0	0.0	HEL	NX A	15:28-15:54	35 20036/ 13
0673	03 02 17 048 16:10:48.7	21.370S 174.469W	TONGA ISLANDS	41	5.9	PDE	EQ A	16:14-16:25	12 20036/ 14
0674	03 02 17 048 17:00:00.0	37.163N 116.063W	SOUTHERN NEVADA	0	0.0	PDE	NX A	17:06-17:17	12 20036/ 15
0675	03 02 18 049 03:53:37.6	23.068N 143.959E	VOLCANO ISLANDS REGION	33	4.9	PDE	EQ ABD	03:53-04:07	15 20036/ 16
0676	03 02 18 049 14:51:20.9	7.307N 125.185E	MINDANAO PHILIPPINE ISLANDS	33	5.3	PDE	EQ A	14:54-15:05	12 20036/ 17
0677	03 02 18 049 19:31:34.9	5.055S 183.242E	POSSIBLE NUCLEAR TEST	0	0.0	HEL	NX A	19:32-20:13	42 20036/ 18
0678	03 02 19 050 15:57:19.2	24.053N 122.629E	NEW IRELAND REGION	33	5.2	PDE	EQ ABDE	16:00-16:11	12 20036/ 19
0679	03 02 19 050 20:14:22.6	0.710N 124.023E	MINDANAO PHILIPPINE ISLANDS	564	5.0	PDE	EQ A	20:16-20:28	13 20036/ 20
0680	03 02 19 050 21:40:39.9	4.507S 137.065E	WEST IRIAN	81	4.0	PDE	EQ ABD	21:43-22:00	18 20036/ 01
0681	03 02 20 051 01:21:35.6	43.440N 147.453E	KURIL ISLANDS	33	5.0				

## WAKE HYDROPHONE INFORMATION PROCESSING SYSTEM (WHIPS) EVENT LISTING

6 JUL 83

KEY: INFORMATION SOURCES - PDE=NEIS PDECARD, MON=NEIS MONTHLY LIST, ICS=ICS LIST, MEL=HELICORDER, OTH=OTHER  
 EVENT TYPE - EQ=EARTHQUAKE, NX=NUCLEAR EXPLOSION, SX=SCIENTIFIC EXPLOSION, OT=OTHER, UN=UNKNOWN  
 PHASES - A=P, B=PO, C=S, D=SO, E=T, F=OTHER

SVMT	*****ORIGIN TIME*****	*****COORDINATES*****	*****LOCATION*****	DEF	MAGNI	INT	EV	*****SAVED*****	*****STRIP*****
NO	VR=NO*DA*JUL*HR*MM*SECS	LAT*LONG	*****DESCRIPTION*****	KM	BDY=SRF	SRC	TP	PHASES**INTERVAL**MNS	TAPE/FILE
0701	03 02 25 056 05:16:06.1	23.5475 176.339W	SOUTH OF FIJI ISLANDS	33	5.0	4.6	PDE EQ A	05:19-05:31	13 28037/ 21
0702	03 02 25 056 08:37:08.1	35.040N 79.038E	EASTERN KASHMIR	33	4.9	0.0	PDE EQ A	08:44-08:55	12 28037/ 22
0703	03 02 25 056 16:33:11.1	7.372S 107.116E	JAVA	90	5.0	0.0	PDE EQ A	16:39-16:50	12 28037/ 23
0704	03 02 25 056 22:03:54.9	5.423S 146.026E	EAST PAPUA NEW GUINEA REGION	222	6.0	0.0	PDE EQ ABDE	22:05-22:50	46 28037/ 24
0705	03 02 25 056 22:49:52.1	10.757S 69.582W	NORTHERN CHILE	144	5.9	0.0	PDE EQ A	22:59-23:10	20 28037/ 25
0706	03 02 26 057 02:05:36.9	22.419N 121.234E	TAIWAN REGION	37	5.1	4.5	PDE EQ A	02:08-02:20	13 28037/ 26
0707	03 02 26 057 03:01:26.4	31.931N 131.670E	KYUSHU JAPAN	52	5.2	4.6	PDE EQ ABDE	03:03-03:51	49 28037/ 27
0708	03 02 26 057 05:32:04.6	3.217S 136.053E	WEST IRIAN	33	4.0	0.0	PDE EQ ABDE	05:34-05:51	18 28037/ 28
0709	03 02 26 057 06:01:16.5	10.030S 172.206W	TONGA ISLANDS REGION	33	5.1	0.0	PDE EQ A	06:04-06:15	12 28037/ 29
0710	03 02 26 057 07:10:59.2	49.231N 155.617E	KURIL ISLANDS	67	6.0	0.0	PDE EQ ABDE	07:12-07:57	46 28037/ 30
0711	03 02 26 057 11:42:48.7	50.524S 162.796E	AUCKLAND ISLANDS REGION	10	5.4	0.0	PDE EQ A	11:49-12:00	12 28037/ 31
0712	03 02 26 057 12:08:00.0	0.000N 0.000E	UNKNOWN P PHASE	0	0.0	0.0	HEL UN A	12:05-12:34	10 28037/ 32
0713	03 02 26 057 20:07:40.4	38.973N 72.015E	AFGHANISTAN-USSR BORDER REGION	33	5.3	5.1	PDE EQ A	20:15-20:26	12 28037/ 33
0714	03 02 26 057 10:11:04.7	36.099N 141.902E	NEAR E COAST OF HONSHU JAPAN	33	4.7	0.0	PDE EQ ABD	10:12-10:26	15 28037/ 34
0715	03 02 27 058 12:14:19.1	35.072N 139.948E	NEAR S COAST OF HONSHU JAPAN	64	5.9	0.0	PDE EQ ABDE	12:15-12:50	44 28037/ 35
0716	03 02 27 058 20:33:08.5	32.638N 76.567E	KASHMIR-TIBET BORDER REGION	52	5.3	4.9	PDE EQ A	20:40-20:51	12 28037/ 36
0717	03 02 28 059 05:44:24.3	44.164N 148.039E	KURIL ISLANDS	41	5.0	5.9	PDE EQ A	05:45-06:29	45 28037/ 37
0718	03 02 28 059 09:01:12.0	40.002N 72.153E	KIRGHIZ SSR	33	4.9	0.0	PDE EQ A	09:08-09:20	13 28037/ 38
0719	03 02 28 059 10:33:14.3	20.102N 142.219E	BONIN ISLANDS REGION	33	5.0	0.0	PDE EQ ABDE	10:33-10:11	39 28037/ 39
0720	03 02 28 059 22:17:58.6	4.005S 142.244E	PAPUA NEW GUINEA	103	5.3	0.0	PDE EQ ABDE	22:19-23:07	49 28037/ 40
0721	03 03 01 060 02:02:19.5	39.168N 54.594E	TURKISH SSR	33	4.0	0.0	PDE EQ A	02:11-02:22	12 28037/ 41
0722	03 03 01 060 09:02:17.3	31.066N 141.637E	SOUTH OF HONSHU JAPAN	33	5.0	5.4	PDE EQ ABDE	09:03-09:41	39 28037/ 42
0723	03 03 01 060 13:22:31.6	20.610N 95.982E	INDIA-CHINA BORDER REGION	33	5.0	0.0	PDE EQ A	13:20-13:39	12 28037/ 43
0724	03 03 01 060 19:26:45.4	5.715S 104.314E	SOUTHERN SUMATRA	33	5.0	0.0	PDE EQ A	19:32-19:44	13 28037/ 44
0725	03 03 02 061 02:08:00.0	0.000N 0.000E	PROBABLE MARIANAS	0	0.0	0.0	HEL UN BDE	02:08-02:19	30 28037/ 45
0726	03 03 02 061 07:07:41.4	11.595S 77.027W	NEAR COAST OF PERU	64	5.5	0.0	PDE EQ A	07:17-07:36	20 28037/ 46
0727	03 03 02 061 09:11:22.1	37.249N 141.974E	NEAR E COAST OF HONSHU JAPAN	33	4.7	0.0	PDE EQ ABD	09:12-09:27	16 28037/ 47
0728	03 03 03 062 01:51:19.5	10.019S 170.206W	FIJI ISLANDS REGION	550	5.2	0.0	PDE EQ A	01:53-02:42	12 28037/ 48
0729	03 03 03 062 02:02:21.4	11.433N 139.073E	WEST CAROLINE ISLANDS	45	5.0	0.0	PDE EQ ABDE	02:03-02:04	48 28037/ 49
0730	03 03 03 062 02:30:31.0	6.152S 100.783E	SOUTHWEST OF SUMATRA	33	5.6	5.4	PDE EQ A	02:37-02:48	12 28037/ 50
0731	03 03 03 062 03:32:13.0	43.928N 85.697E	NORTHERN SINKIANG PROV CHINA	33	5.6	0.0	PDE EQ A	03:30-03:50	13 28037/ 51
0732	03 03 03 062 16:42:54.6	41.763N 143.425E	HOKKAIDO JAPAN REGION	33	5.2	0.0	PDE EQ ABD	16:44-17:20	45 28037/ 52
0733	03 03 03 062 17:43:08.4	39.413N 143.373E	OFF E COAST OF HONSHU JAPAN	33	4.9	0.0	PDE EQ ABD	17:44-17:59	16 28037/ 53
0734	03 03 04 063 14:11:36.0	39.563N 143.132E	OFF E COAST OF HONSHU JAPAN	33	5.2	5.6	PDE EQ ABDE	14:12-14:55	44 28037/ 54
0735	03 03 04 063 19:06:12.9	14.265S 14.319W	SOUTH ATLANTIC RIDGE	10	5.2	5.3	PDE EQ ABD	19:15-20:19	65 28037/ 55
0736	03 03 04 063 20:08:00.0	0.000N 0.000E	PROBABLE MARIANAS	0	0.0	0.0	HEL UN BDE	20:08-09:13	12 28037/ 56
0737	03 03 05 064 09:57:04.0	10.794S 115.054E	SOUTH OF BALI ISLAND	33	5.0	5.3	PDE EQ A	11:46-11:57	12 28037/ 57
0738	03 03 05 064 16:37:53.6	39.141N 64.586E	UZEK SSR	33	4.0	0.0	PDE EQ A	16:47-16:59	13 28037/ 58
0739	03 03 05 064 21:01:47.1	22.650N 93.971E	SOUTHERN HONSHU JAPAN	97	4.0	0.0	PDE EQ A	21:34-21:49	16 28037/ 59
0740	03 03 05 064 21:32:20.0	35.575N 136.147E	SOUTHERN HONSHU JAPAN	49	4.0	0.0	PDE EQ ABD	21:51-22:39	45 28037/ 60
0741	03 03 05 064 21:50:06.0	49.547N 150.782E	NORTHWEST OF KURIL ISLANDS	347	4.9	0.0	PDE EQ ABDE	22:25-23:10	46 28037/ 61
0742	03 03 06 065 02:23:57.7	6.144S 147.300E	EAST PAPUA NEW GUINEA REGION	84	5.0	0.0	PDE EQ ABDE	06:33-06:44	12 28037/ 62
0743	03 03 07 066 05:30:26.1	9.561N 126.071E	MINDANAO PHILIPPINE ISLANDS	07	5.0	0.0	PDE EQ A	05:11-15:24	14 28037/ 63
0744	03 03 07 066 15:12:22.3	10.297N 146.551E	MARIANA ISLANDS	70	4.0	0.0	PDE EQ ABD	13:22-14:00	39 28037/ 64
0745	03 03 08 067 13:21:46.8	3.476S 177.631E	GILBERT ISLANDS REGION	33	5.0	0.0	PDE EQ ABDE	10:30-19:17	48 28037/ 65
0746	03 03 08 067 18:30:07.7	3.507S 177.707E	GILBERT ISLANDS REGION	32	5.1	0.0	PDE EQ ABDE	20:24-20:50	35 28037/ 66
0747	03 03 08 067 22:24:25.2	13.770N 144.747E	MARIANA ISLANDS	100	5.0	0.0	PDE EQ ABDE	23:31-23:42	12 28037/ 67
0748	03 03 08 067 23:27:57.5	7.094S 129.261E	BANDA SEA	101	5.4	0.0	PDE EQ A	00:11-00:22	12 28037/ 68
0749	03 03 09 068 05:45:46.2	7.210S 107.762E	JAVA	110	5.4	0.0	PDE EQ A	17:10-18:03	46 28037/ 69
0750	03 03 09 068 17:16:27.7	5.050S 145.697E	EAST PAPUA NEW GUINEA REGION	202	5.0	0.0	PDE EQ ABDE	00:29-01:12	44 28037/ 70
0751	03 03 10 069 00:27:49.4	43.011N 147.441E	KURIL ISLANDS	42	6.2	5.0	PDE EQ ABDE	05:40-05:59	12 28037/ 71
0752	03 03 10 069 05:46:06.0	14.645S 167.202E	VANUATU ISLANDS	33	5.3	0.0	PDE EQ A	12:01-12:12	12 28037/ 72
0753	03 03 10 069 11:50:19.9	5.411N 126.760E	MINDANAO PHILIPPINE ISLANDS	33	5.4	5.6	PDE EQ A	00:33-00:52	20 28037/ 73
0754	03 03 11 070 02:24:09.3	10.249S 13.430W	ASCENSION ISLAND REGION	10	4.0	0.0	PDE EQ A	03:12-03:58	47 28037/ 74
0755	03 03 11 070 03:10:42.1	6.992S 147.374E	EAST PAPUA NEW GUINEA REGION	66	5.9	0.0	PDE EQ ABDE	23:05-23:16	12 28037/ 75
0756	03 03 11 070 23:02:36.5	5.372N 126.623E	MINDANAO PHILIPPINE ISLANDS	60	5.2	0.0	PDE EQ A	00:52-01:03	12 28037/ 76
0757	03 03 12 071 00:44:44.6	36.435N 78.059E	HINDU KUSH REGION	234	4.5	0.0	PDE EQ A	00:57-01:55	59 28037/ 77
0758	03 03 12 071 02:53:40.2	4.037S 127.914E	BANDA SEA	33	5.9	6.0	PDE EQ AE	01:40-02:30	59 28037/ 78
0759	03 03 12 071 03:36:36.6	4.103S 127.918E	BANDA SEA	33	5.3	5.2	PDE EQ ABDE	07:02-07:54	53 28037/ 79
0760	03 03 12 071 07:00:15.0	52.325N 170.119W	FOX ISL. ALEUTIAN ISL.	63	5.0	0.0	PDE EQ A	07:24-07:36	13 28037/ 80
0761	03 03 12 071 07:21:50.2	5.395S 126.671E	MINDANAO PHILIPPINE ISLANDS	33	5.6	5.9	PDE EQ A	08:52-09:03	12 28037/ 81
0762	03 03 12 071 08:49:45.7	10.008S 160.120E	VANUATU ISLANDS	33	5.0	0.0	PDE EQ A	12:33-12:45	13 28037/ 82
0763	03 03 12 071 12:37:17.5	4.202N 120.175E	BANDA SEA	33	4.0	0.0	PDE EQ A	14:30-14:41	12 28037/ 83
0764	03 03 12 071 14:25:27.2	31.575N 104.239E	SICHUAN PROVINCE CHINA	21	5.2	0.0	PDE EQ A	14:40-15:00	13 28037/ 84
0765	03 03 12 071 14:45:17.0	4.100S 120.050E	BANDA SEA	33	5.0	4.6	PDE EQ A	21:11-21:23	13 28037/ 85
0766	03 03 12 071 21:05:15.7	0.671N 93.009E	NICOBAR ISLANDS REGION	33	4.0	0.0	PDE EQ ABD	22:14-22:27	14 28037/ 86
0767	03 03 12 071 22:14:15.4	21.733N 143.070E	MARIANA ISLANDS REGION	31	5.2	5.1	PDE EQ ABDE	02:55-03:39	45 28037/ 87
0768	03 03 13 072 02:54:10.0	5.109S 147.610E	EAST PAPUA NEW GUINEA REGION	33	5.1	0.0	PDE EQ ABDE	05:20-06:09	50 28037/ 88
0769	03 03 13 072 05:10:56.0	52.371N 157.475E	KAMCHATKA	40	4.0	0.0	PDE EQ ABD	09:10-09:25	16 28037/ 89
0770	03 03 13 072 09:00:51.6	42.220N 142.606E	HOKKAIDO JAPAN REGION	33	4.6	0.0	PDE EQ ABD	10:07-10:24	18 28037/ 90
0771	03 03 13 072 10:05:45.2	52.321N 157.398E	KAMCHATKA	33	4.0	0.0	PDE EQ ABD	10:00-10:24	17 28037/ 91
0772	03 03 13 072 10:06:14.0	52.407N 157.478E	KAMCHATKA	33	5.0	0.0	PDE EQ ABDE	20:00-20:57	46 28037/ 92
0773	03 03 13 072 20:05:57.7	54.117N 159.172E	NEAR E COAST OF KAMCHATKA	63	5.0	0.0	PDE EQ ABDE	20:21-21:06	50 28037/ 93
0774	03 03 13 072 20:20:00.0	41.563N 142.050E	HOKKAIDO JAPAN REGION	142	4.7	0.0	PDE EQ ABD	23:32-23:46	17 28037/ 94
0775	03 03 13 072 23:30:14.6	51.973N 170.063E	RAT ISL. ALEUTIAN ISL.	33	4.9	4.0	PDE EQ A	12:04-12:15	12 28037/ 95
0776	03 03 14 073 11:55:20.2	39.292N 54.633E	TURKISH SSR	33	5.2	5.0	PDE EQ A	12:11-12:32	12 28037/ 96
0777	03 03 14 073 12:12:40.5	39.257N 54.522E	TURKISH SSR	33	5.0	0.0	PDE EQ A	19:05-19:16	12 28037/ 97
0778	03 03 14 073 14:15:36.0	3.327S 177.524E	GILBERT ISLANDS REGION	33	5.0	0.0	PDE EQ A	21:17-22:09	53 28037/ 98
0779	03 03 14 073 19:02:06.5	4.175S 127.024E	BANDA SEA	33	5.1	0.0	PDE EQ ABDE	12:41-12:52	12 28037/ 99
0780	03 03 14 073 21:14:54.3	52.34							



# MAKE HYDROPHONE INFORMATION PROCESSING SYSTEM (WNIPS) EVENT LISTING

5 JUL 83

KEY: INFORMATION SOURCES - PDE=NEIS PDECARD, MON=NEIS MONTHLY LIST, ICS=ICS LIST, HEL=HELICORDER, OTH=OTHER  
 EVENT TYPE - EQ=EARTHQUAKE, NX=NUCLEAR EXPLOSION, SX=SCIENTIFIC EXPLOSION, OT=OTHER, UN=UNKNOWN  
 PHASES - A=P, B=PO, C=S, D=SO, E=T, F=OTHER

EVNT	*****ORIGIN TIME*****	*****COORDINATES*****	*****LOCATION*****	DEP	MAGNIT	INF	EV	*****SAVED*****	*****STRIP*****			
NO	YR-MO-DA-JUL-HR-MN-SECS	LAT-LON	*****DESCRIPTION*****	KM	BDY	SRF	SRC	TP	PHASES	INTERVAL	MNS	TAPE/FILE
0001	03 03 19 070 22:59:47.1	4.8265 153.812E	NEW IRELAND REGION	119	4.8	B	PDE	EQ	ABD	23:00-23:15	16	20042/-11
0002	03 03 20 079 11:24:48.4	2.375N 126.800E	MOLUCCA PASSAGE	58	5.5	B	PDE	EQ	A	11:20-11:39	12	20042/-12
0003	03 03 20 079 13:45:49.8	4.7275 153.125E	NEW IRELAND REGION	85	5.9	B	PDE	EQ	ABDE	13:46-14:27	42	20042/-13
0004	03 03 20 079 16:24:13.3	10.8275 177.762W	FIJI ISLANDS REGION	632	5.8	B	PDE	EQ	A	16:26-16:37	12	20042/-14
0005	03 03 20 079 17:44:07.1	18.8045 177.679W	FIJI ISLANDS REGION	634	4.9	B	PDE	EQ	A	17:46-17:57	12	20042/-15
0006	03 03 21 080 04:06:24.0	5.8315 153.698E	NEW IRELAND REGION	88	5.5	B	PDE	EQ	ABDE	04:07-04:48	42	20042/-16
0007	03 03 21 080 07:44:17.6	21.6685 175.321W	TONGA ISLANDS	70	6.3	B	PDE	EQ	A	07:47-07:59	13	20042/-17
0008	03 03 21 080 07:57:10.4	7.3425 128.928E	BANDA SEA	143	5.6	B	PDE	EQ	A	08:00-08:12	13	20042/-18
0009	03 03 21 080 15:23:42.7	36.582N 78.593E	HINDU KUSH REGION	166	4.2	B	PDE	EQ	A	15:31-15:42	12	20042/-19
0010	03 03 21 080 15:49:52.0	21.3945 175.452W	TONGA ISLANDS	70	5.4	B	PDE	EQ	A	15:53-16:04	12	20042/-20
0011	03 03 22 081 01:32:20.6	51.297N 178.481W	ANDREANOF ISL. ALEUTIAN ISL.	33	4.9	B	PDE	EQ	ABD	01:34-01:50	17	20042/-21
0012	03 03 22 081 20:17:07.5	53.211N 162.259E	OFF EAST COAST OF KAMCHATKA	33	4.7	B	PDE	EQ	ABD	20:19-20:35	17	20042/-22
0013	03 03 23 082 06:09:29.6	6.6185 154.612E	SOLOMON ISLANDS	41	5.7	6.2	PDE	EQ	ABDE	06:10-06:52	43	20042/-23
0014	03 03 23 082 06:40:32.1	6.6635 154.559E	SOLOMON ISLANDS	55	5.2	B	PDE	EQ	ABDE	06:41-07:23	43	20042/-24
0015	03 03 23 082 06:26:55.2	6.6275 154.585E	SOLOMON ISLANDS	35	5.4	5.6	PDE	EQ	ABDE	06:28-06:59	42	20042/-25
0016	03 03 23 082 12:11:23.9	37.811N 71.487E	AFGHANISTAN-USSR BORDER REGION	122	5.2	B	PDE	EQ	A	12:10-12:38	13	20042/-26
0017	03 03 23 082 14:04:52.1	6.7825 154.528E	SOLOMON ISLANDS	68	5.2	B	PDE	EQ	ABDE	14:06-14:47	42	20042/-27
0018	03 03 23 082 16:07:21.2	3.3755 177.491E	GILBERT ISLANDS REGION	27	4.8	B	PDE	EQ	ABD	16:07-16:21	15	20042/-28
0019	03 03 23 082 21:54:36.3	37.224N 138.125E	NEAR W. COAST OF HONSHU JAPAN	54	4.9	B	PDE	EQ	ABD	21:56-22:11	16	20042/-29
0020	03 03 24 083 07:01:42.9	18.5515 159.821E	LOCAL PO. SO. T	8	8.0	B	HEL	EQ	BDE	07:22-08:51	30	20042/-30
0021	03 03 24 083 07:24:12.5	7.6155 187.173E	SOLOMON ISLANDS	151	4.9	B	PDE	EQ	ABD	07:30-07:10	16	20042/-31
0022	03 03 24 083 08:44:53.9	6.6825 154.564E	SOLOMON ISLANDS	57	4.9	B	PDE	EQ	A	07:30-07:41	12	20042/-32
0023	03 03 24 083 12:47:40.5	4.7215 153.336E	NEW IRELAND REGION	88	5.2	B	PDE	EQ	ABDE	08:46-09:27	42	20042/-33
0024	03 03 24 083 12:44:35.2	18.8145 163.992E	SOLOMON ISLANDS	74	4.9	B	PDE	EQ	ABD	10:48-11:29	42	20042/-34
0025	03 03 24 083 12:44:35.2	18.8145 163.992E	SOLOMON ISLANDS	74	4.9	B	PDE	EQ	ABD	12:25-12:41	17	20042/-35
0026	03 03 25 084 07:01:42.9	18.5515 159.821E	PROBABLE MARIANAS PO. SO. T	8	8.0	B	HEL	EQ	BDE	27:10-28:39	30	20042/-36
0027	03 03 25 084 13:02:14.2	6.4945 151.722E	NEW BRITAIN REGION	164	5.4	B	PDE	EQ	A	07:47-07:58	12	20042/-37
0028	03 03 25 084 19:33:54.1	0.3955 124.680E	TIMOR	45	5.3	B	PDE	EQ	ABDE	13:01-13:44	44	20042/-38
0029	03 03 25 084 21:41:54.0	6.4925 155.118E	SOLOMON ISLANDS	169	4.8	B	PDE	EQ	A	19:37-19:49	13	20042/-39
0030	03 03 26 085 10:51:43.4	39.135N 144.502E	N.W. IRAN-USSR BORDER REGION	123	5.1	B	PDE	EQ	ABDE	21:42-22:24	43	20042/-40
0031	03 03 26 085 12:46:47.7	5.1855 153.597E	NEW IRELAND REGION	33	4.6	B	PDE	EQ	A	11:00-11:20	21	20042/-41
0032	03 03 26 085 14:57:49.3	1.167N 126.586E	MOLUCCA PASSAGE	70	4.9	B	PDE	EQ	ABD	12:47-13:02	16	20042/-42
0033	03 03 26 085 17:19:37.5	4.6315 143.878E	PAPUA NEW GUINEA	73	5.2	B	PDE	EQ	A	15:01-15:12	12	20042/-43
0034	03 03 26 085 18:42:46.8	42.847N 141.795E	HOKKAIDO JAPAN REGION	181	4.5	B	PDE	EQ	ABD	17:21-17:37	17	20042/-44
0035	03 03 26 085 20:28:00.0	37.381N 116.460W	SOUTHERN NEVADA	88	4.4	B	PDE	EQ	ABD	10:44-10:50	17	20042/-45
0036	03 03 27 086 02:42:41.4	34.268N 92.644E	QINGHAI PROVINCE CHINA	8	5.1	B	PDE	NX	A	20:26-20:37	12	20042/-46
0037	03 03 27 086 09:04:13.5	27.514N 141.378E	BONIN ISLANDS REGION	33	4.5	B	PDE	EQ	A	02:40-03:08	13	20042/-47
0038	03 03 27 086 10:32:00.1	4.0385 153.568E	NEW IRELAND REGION	38	4.8	B	PDE	EQ	ABD	09:05-09:29	15	20042/-48
0039	03 03 27 086 20:05:07.6	6.0935 148.451E	NEW BRITAIN REGION	95	4.9	B	PDE	EQ	ABD	18:33-18:47	15	20042/-49
0040	03 03 28 087 17:58:16.6	26.308N 127.311E	RYUKYU ISLANDS	62	5.3	B	PDE	EQ	A	19:20-19:31	12	20042/-50
0041	03 03 28 087 21:38:27.2	12.985N 146.354E	SOUTH OF MARIANA ISLANDS	33	4.7	B	PDE	EQ	ABD	23:30-23:51	14	20042/-51
0042	03 03 29 088 04:53:29.4	36.443N 131.589E	KYUSHU JAPAN	33	4.9	B	PDE	EQ	ABD	04:55-05:11	17	20042/-52
0043	03 03 29 088 20:55:47.0	6.9845 154.887E	SOLOMON ISLANDS	33	5.1	B	PDE	EQ	ABDE	22:57-23:38	42	20042/-53
0044	03 03 30 089 09:49:09.9	1.572N 122.513E	MINAHASSA PENINSULA	40	5.4	5.1	PDE	EQ	A	08:53-09:04	12	20042/-54
0045	03 03 30 089 06:46:22.5	48.081N 75.033E	KIRGHIZ-KINJIANG BORDER REGION	33	4.9	4.9	PDE	EQ	A	08:53-07:05	13	20042/-55
0046	03 03 30 089 12:02:52.3	6.6375 154.568E	SOLOMON ISLANDS	33	4.8	B	PDE	EQ	ABD	12:04-12:18	15	20042/-56
0047	03 03 30 089 16:13:35.2	39.884N 75.480E	SOUTHERN XINJIANG CHINA	33	4.8	B	PDE	EQ	A	16:21-16:32	12	20042/-57
0048	03 03 30 089 18:55:49.1	5.9195 142.222E	PAPUA NEW GUINEA	33	5.2	B	PDE	EQ	ABDE	10:50-10:46	49	20042/-58
0049	03 03 31 089 13:24:45.6	34.281N 135.033E	NEAR S. COAST OF SOUTH HONSHU	382	4.9	B	PDE	EQ	ABDE	13:25-14:11	47	20042/-59
0050	03 03 31 089 18:55:49.1	5.9195 142.222E	PAPUA NEW GUINEA	33	5.2	B	PDE	EQ	ABDE	13:25-14:11	47	20042/-60
0051	03 04 01 091 01:04:59.0	10.534N 145.086E	MARIANA ISLANDS	102	5.1	B	PDE	EQ	ABDE	01:04-01:36	33	20044/-1
0052	03 04 01 091 02:05:02.0	8.082N 135.082E	PROBABLE BONIN PO. SO. T	8	8.0	B	HEL	EQ	BDE	20:43-21:12	30	20044/-2
0053	03 04 01 091 03:12:35.5	3.1235 135.207E	WEST IRAN	33	5.0	B	PDE	EQ	A	04:20-04:32	13	20044/-3
0054	03 04 01 091 05:01:18.3	54.059N 162.314E	NEAR EAST COAST OF KAMCHATKA	92	4.9	B	PDE	EQ	ABD	05:11-05:26	16	20044/-4
0055	03 04 01 091 06:49:01.9	24.7115 176.196W	SOUTH OF FIJI ISLANDS	40	5.4	5.0	PDE	EQ	A	06:52-07:04	13	20044/-5
0056	03 04 01 091 21:04:38.6	6.3275 154.533E	SOLOMON ISLANDS	44	4.6	B	PDE	EQ	ABD	21:05-21:20	16	20044/-6
0057	03 04 01 091 21:55:44.8	36.393N 70.734E	HINDU KUSH REGION	215	4.8	B	PDE	EQ	A	22:03-22:14	12	20044/-7
0058	03 04 01 091 22:58:02.7	0.731N 83.115W	COSTA RICA	33	6.6	7.2	PDE	EQ	AE	02:59-05:08	138	20044/-8
0059	03 04 01 091 10:14:53.0	0.671N 124.181E	MINAHASSA PENINSULA	174	5.0	B	PDE	EQ	A	10:18-10:29	12	20044/-9
0060	03 04 01 091 19:14:05.2	51.997N 179.255E	RAT ISL. ALEUTIAN ISL.	116	5.6	B	PDE	EQ	ABDE	19:16-20:04	49	20044/-10
0061	03 04 01 091 19:26:24.5	51.889N 176.919W	ANDREANOF ISL. ALEUTIAN ISL.	68	5.3	B	PDE	EQ	ABDE	19:20-20:17	50	20044/-11
0062	03 04 01 091 07:45:07.9	30.517N 70.334E	AFGHANISTAN-USSR BORDER REGION	33	4.9	B	PDE	EQ	A	07:52-08:04	13	20044/-12
0063	03 04 01 091 02:51:34.9	6.738N 94.011E	NORTHERN SUMATERA	85	6.5	B	PDE	EQ	A	02:50-03:09	12	20044/-13
0064	03 04 01 091 03:03:35.0	5.752N 94.798E	NORTHERN SUMATERA	74	5.8	B	PDE	EQ	A	03:10-03:21	12	20044/-14
0065	03 04 01 091 02:05:02.0	8.082N 135.082E	PROBABLE BONIN PO. SO. T	8	8.0	B	HEL	EQ	BDE	05:25-05:54	30	20044/-15
0066	03 04 01 091 06:50:59.5	5.585N 94.648E	NORTHERN SUMATERA	76	5.8	B	PDE	EQ	A	07:05-07:16	12	20044/-16
0067	03 04 01 091 19:04:20.8	52.923N 159.916E	OFF EAST COAST OF KAMCHATKA	38	6.0	5.5	PDE	EQ	ABDE	19:06-19:58	45	20044/-17
0068	03 04 01 091 19:40:04.1	7.0575 129.379E	BANDA SEA	144	5.8	B	PDE	EQ	A	19:51-20:02	12	20044/-18
0069	03 04 01 091 23:12:47.0	49.399N 155.648E	KURIL ISLANDS	50	6.1	5.5	PDE	EQ	ABDE	23:14-23:59	46	20044/-19
0070	03 04 01 091 23:50:59.6	15.8195 167.274E	VANUATU ISLANDS	127	6.1	5.0	PDE	EQ	ABDE	00:00-00:09	50	20044/-20
0071	03 04 01 091 02:55:24.6	41.631N 70.763E	KIRGHIZ SSR	33	5.1	B	PDE	EQ	A	01:03-01:14	12	20044/-21
0072	03 04 01 091 06:50:33.5	40.062N 75.205E	KIRGHIZ-KINJIANG BORDER REGION	33	5.4	5.6	PDE	EQ	A	06:57-07:09	13	20044/-22
0073	03 04 01 091 07:07:23.5	39.074N 75.449E	SOUTHERN XINJIANG CHINA	33	4.8	B	PDE	EQ	A	07:14-07:26	13	20044/-23
0074	03 04 01 091 07:40:38.3	5.438N 126.698E	MINDANAO PHILIPPINE ISLANDS	41	5.1	B	PDE	EQ	A	07:43-07:54	12	20044/-24
0075	03 04 01 091 21:49:08.0	26.489N 126.488E	RYUKYU ISLANDS	121	4.7	B	PDE	EQ	ABD	21:41-21:58	18	20044/-25
0076	03 04 01 091 06:50:23.7	6.1715 149.065E	NEW BRITAIN REGION	53	4.8	4.7	PDE	EQ	ABD	06:51-07:07	17	20044/-26
0077	03 04 01 091 00:11:10.0	36.438N 71.477E	AFGHANISTAN-USSR BORDER REGION	101	4.7	B	PDE	EQ	A	02:15-02:27	13	20044/-27
0078	03 04 01 091 12:30:36.6	5.5485 153.568E	NEW IRELAND REGION	68	4.6	B	PDE	EQ	ABD	10:31-10:46	16	20044/-28
0079	03 04 01 091 12:49:38.4	39.974N 75.129E	SOUTHERN XINJIANG CHINA	33	4.7	B	PDE	EQ	A	12:56-13:07	12	20044/-29
0080	03 04 01 091 18:00:08.2	21.6145 179.391W	FIJI ISLANDS REGION	636	4.9	B	PDE	EQ	A	18:10-18:21	12	20044/-30
0081	03 04 01											

## WAKE HYDROPHONE INFORMATION PROCESSING SYSTEM (WHIPS) EVENT LISTING

13 AUG 83

KEY: INFORMATION SOURCES - PDE=NEIS PDECARD, MON=NEIS MONTHLY LIST, ICS=ICS LIST, HEL=HELICORDER, OTH=OTHER  
 EVENT TYPE - EQ=EARTHQUAKE, NX=NUCLEAR EXPLOSION, SX=SCIENTIFIC EXPLOSION, OT=OTHER, UN=UNKNOWN  
 PHASES - A=P, B=PU, C=S, D=SO, E=T, F=OTHER

EVNT	*****ORIGIN TIME*****	*****COORDINATES*****	*****LOCATION*****	DEF	"MAGNI"	INF	EV	*****SAVED*****	*****STRIP*****	
"NO"	YY-MM-DD-JUL-HR-MN-SECS	"LAT" "LONG"	"DESCRIPTION"	KM	BDY-SRF	SRC	TP	PHASES	INTERVAL-MNMS	TAPE/FILE
0901	03 04 12 102 22:44:49.5	5.1515 153.637E	NEW IRELAND REGION	55	5.3	5.5	PDE EQ ABDE	22:45-23:26	42 22247/ 01	
0902	03 04 13 103 14:44:09.5	10.5595 164.683E	SANTA CRUZ ISLANDS REGION	33	5.0	4.9	PDE EQ A	14:45-14:56	12 22247/ 02	
0903	03 04 13 103 15:26:37.0	14.577N 145.904E	MARIANA ISLANDS	50	4.7	0.0	PDE EQ ABD	15:26-15:39	14 22247/ 03	
0904	03 04 13 103 19:41:24.5	46.941N 145.638E	NORTHWEST OF KURIL ISLANDS	354	4.5	0.0	PDE EQ ABDE	19:42-20:29	48 22247/ 04	
0905	03 04 13 103 21:07:22.0	22.016N 94.537E	BUPIA	130	4.7	0.0	PDE EQ A	21:13-21:24	12 22247/ 05	
0906	03 04 14 104 02:46:26.7	14.011N 140.967E	MARIANA ISLANDS	33	4.5	0.0	PDE EQ ABD	02:46-02:58	13 22247/ 06	
0907	03 04 14 104 04:03:48.3	18.431S 165.225E	SANTA CRUZ ISLANDS	33	5.0	4.4	PDE EQ A	04:05-04:16	12 22247/ 07	
0908	03 04 14 104 06:09:38.4	36.360N 71.112E	AFGHANISTAN-USSR BORDER REGION	224	4.6	0.0	PDE EQ A	06:17-06:28	12 22247/ 08	
0909	03 04 14 104 09:12:01.2	35.953N 69.969E	HINDU KUSH REGION	70	4.7	0.0	PDE EQ A	09:19-09:31	13 22247/ 09	
0910	03 04 14 104 10:24:12.2	22.126S 175.002E	TONGA ISLANDS REGION	33	5.2	5.1	PDE EQ A	10:27-10:39	13 22247/ 10	
0911	03 04 14 104 10:00:00.0	0.000N 0.000E	PROBABLE MARIANAS PO. SO. T	0	0.0	0.0	HEL EQ BDE	11:18-11:47	32 22247/ 11	
0912	03 04 14 104 19:05:00.1	37.073N 116.046W	SOUTHERN NEVADA	0	5.7	0.0	PDE NX A	19:11-19:22	12 22247/ 12	
0913	03 04 14 104 23:01:12.2	0.275N 126.113E	MOLUCCA PASSAGE	64	5.0	0.0	PDE EQ A	23:04-23:15	12 22247/ 13	
0914	03 04 15 105 00:09:36.1	19.095S 175.611W	TONGA ISLANDS	249	5.7	0.0	PDE EQ A	00:12-00:23	12 22247/ 14	
0915	03 04 15 105 04:44:00.7	6.502S 154.948E	SOLOMON ISLANDS	33	5.9	5.5	PDE EQ ABDE	04:45-05:26	42 22247/ 15	
0916	03 04 15 105 09:23:59.1	14.954N 99.142E	SOUTHEAST ASIA	10	5.3	0.0	PDE EQ A	09:30-09:41	12 22247/ 16	
0917	03 04 15 105 14:21:49.0	13.130N 121.971E	MINDORO PHILIPPINE ISLANDS	33	5.3	5.1	PDE EQ A	14:25-14:36	12 22247/ 17	
0918	03 04 15 105 14:51:59.0	53.355N 167.001E	NEAR EAST COAST OF KAMCHATKA	71	5.0	0.0	PDE EQ ABDE	14:54-15:42	49 22247/ 18	
0919	03 04 16 106 12:57:45.6	10.106S 110.052E	SOUTH OF JAVA	23	5.0	5.3	PDE EQ A	13:03-13:14	12 22247/ 19	
0920	03 04 16 106 17:23:29.5	4.795N 127.684E	TALAUD ISLANDS	83	5.1	0.0	PDE EQ A	17:26-17:37	12 22247/ 20	
0921	03 04 16 106 17:28:31.2	41.475N 142.040E	HOKKAIDO JAPAN REGION	62	5.0	0.0	PDE EQ ABDE	17:29-18:14	46 22247/ 21	
0922	03 04 17 107 13:08:14.1	1.779N 99.520E	NORTHERN SUMATRA	178	4.5	0.0	PDE EQ A	13:06-13:17	12 22247/ 22	
0923	03 04 17 107 14:06:56.3	20.747S 169.103E	VANUATU ISLANDS	22	5.4	6.2	PDE EQ ABDE	14:09-15:04	56 22248/ 01	
0924	03 04 17 107 19:14:47.2	36.612N 71.014E	AFGHANISTAN-USSR BORDER REGION	270	4.5	0.0	PDE EQ A	19:22-19:33	12 22248/ 02	
0925	03 04 17 107 20:05:44.9	44.840N 147.615E	KURIL ISLANDS	115	4.9	0.0	PDE EQ ABDE	20:07-20:51	45 22248/ 03	
0926	03 04 17 107 23:16:34.5	22.002N 94.327E	BURMA	241	5.1	0.0	PDE EQ A	23:42-23:53	12 22248/ 04	
0927	03 04 18 108 05:01:19.4	19.094S 175.008E	TONGA ISLANDS	37	6.5	6.2	PDE EQ F	11:00-12:59	122 22248/ 05	
0928	03 04 18 108 10:58:47.9	27.721N 62.058E	SOUTHERN IRAN	191	6.0	0.0	PDE EQ A	13:56-14:07	12 22248/ 06	
0929	03 04 18 108 13:52:13.2	0.275S 126.113E	FLORES ISLAND REGION	70	4.7	0.0	PDE EQ ABD	16:31-16:47	17 22248/ 07	
0930	03 04 18 108 16:29:37.5	52.111N 169.137E	OFF EAST COAST OF KAMCHATKA	213	5.1	0.0	PDE EQ A	17:16-17:27	12 22248/ 08	
0931	03 04 18 108 17:15:04.0	13.639S 167.209E	VANUATU ISLANDS	38	4.9	0.0	PDE EQ ABD	18:29-18:44	16 22248/ 09	
0932	03 04 18 108 18:20:10.0	43.524N 147.698E	KURIL ISLANDS	137	5.2	0.0	PDE EQ ABD	09:12-09:28	17 22248/ 10	
0933	03 04 19 109 09:11:01.1	4.389S 144.059E	NEAR N COAST PAPUA NEW GUINEA	33	4.3	0.0	PDE EQ ABD	14:17-14:30	14 22248/ 11	
0934	03 04 19 109 14:17:59.0	21.492N 145.777E	MARIANA ISLANDS REGION	149	5.0	0.0	PDE EQ ABDE	14:20-15:16	49 22248/ 12	
0935	03 04 19 109 14:26:29.1	14.823S 167.478E	VANUATU ISLANDS	464	4.5	0.0	PDE EQ ABDE	15:05-15:47	42 22248/ 13	
0936	03 04 19 109 15:05:41.2	29.359N 139.727E	SOUTH OF HONSHU JAPAN	186	5.0	0.0	PDE EQ A	15:18-15:29	12 22248/ 14	
0937	03 04 19 109 15:15:10.7	7.253S 129.255E	BANDA SEA	33	4.5	0.0	PDE EQ ABD	16:26-16:42	17 22248/ 15	
0938	03 04 19 109 16:25:27.2	46.449N 153.131E	KURIL ISLANDS	0	5.6	0.0	PDE NX A	18:59-19:10	12 22248/ 16	
0939	03 04 19 109 18:52:50.4	21.064S 138.941W	TUAMOTU ARCHIPELAGO REGION	113	5.1	0.0	PDE EQ ABD	19:17-19:38	22 22248/ 17	
0940	03 04 19 109 19:12:40.7	63.372N 149.950E	CENTRAL ALASKA	282	5.2	0.0	PDE EQ A	11:04-11:15	12 22248/ 18	
0941	03 04 20 110 11:01:39.0	5.521S 129.449E	BANDA SEA	50	4.9	0.0	PDE EQ ABD	16:34-16:48	15 22249/ 01	
0942	03 04 20 110 16:34:32.2	12.423N 143.701E	SOUTH OF MARIANA ISLANDS	95	5.0	0.0	PDE EQ ABDE	13:35-14:11	33 22249/ 02	
0943	03 04 21 111 13:39:24.5	15.539N 146.151E	MARIANA ISLANDS	63	5.2	0.0	PDE EQ A	10:28-10:39	12 22249/ 03	
0944	03 04 21 111 18:25:09.0	0.823N 125.965E	MOLUCCA PASSAGE	0	0.0	0.0	HEL EQ BDE	21:57-22:06	30 22249/ 04	
0945	03 04 22 112 00:00:00.0	0.000N 0.000E	PROBABLE MARIANAS PO. SO. T	0	0.0	0.0	HEL EQ BDE	03:27-03:38	12 22249/ 05	
0946	03 04 22 112 00:37:40.5	14.952N 99.072E	SOUTHEAST ASIA	33	5.0	5.0	PDE EQ A	03:27-03:38	12 22249/ 06	
0947	03 04 22 112 03:21:48.6	14.962N 99.051E	SOUTHEAST ASIA	33	5.2	4.4	PDE EQ A	04:04-04:15	12 22249/ 07	
0948	03 04 22 112 03:56:26.6	39.321N 64.271E	UZZEK SSR	46	4.0	0.0	PDE EQ A	07:54-08:05	12 22249/ 08	
0949	03 04 22 112 07:51:49.0	6.152N 126.984E	MINDANAO PHILIPPINE ISLANDS	59	5.7	0.0	PDE EQ A	10:40-10:51	12 22249/ 09	
0950	03 04 22 112 10:32:41.7	39.250N 68.313E	TADIK SSR	33	4.0	0.0	PDE EQ A			
0951	03 04 22 112 13:53:00.0	37.112N 116.022W	SOUTHERN NEVADA	0	4.0	0.0	PDE NX A	13:59-14:10	12 22249/ 12	
0952	03 04 22 112 18:00:00.0	0.000N 0.000E	PROBABLE BONIN ISL. PO. SO. T	0	0.0	0.0	HEL EQ BDE	14:32-15:01	30 22249/ 13	
0953	03 04 22 112 18:20:24.5	42.369N 87.942E	NORTHERN KINJIAN CHINA	24	5.0	4.1	PDE EQ A	18:34-18:46	13 22249/ 14	
0954	03 04 23 113 00:30:50.3	6.391S 151.053E	NEW BRITAIN REGION	33	5.0	0.0	PDE EQ ABDE	00:32-01:14	43 22249/ 15	
0955	03 04 23 113 04:23:55.6	30.272N 67.943E	PAKISTAN	33	4.7	4.2	PDE EQ A	04:22-04:43	12 22249/ 16	
0956	03 04 23 113 09:28:12.0	11.353S 118.041E	SOUTH OF SUMBAWA ISLAND	21	5.4	0.0	PDE EQ A	09:25-09:36	12 22249/ 17	
0957	03 04 23 113 10:49:54.0	59.529N 68.250E	PAKISTAN	33	4.0	4.3	PDE EQ A	10:50-10:59	12 22249/ 18	
0958	03 04 23 113 23:33:50.0	53.095S 117.830W	EASTER ISLAND CORDILLERA	10	5.0	5.5	PDE EQ ABD	23:42-00:16	35 01/ 02	
0959	03 04 24 114 03:26:39.0	16.354S 177.694W	FUJI ISLANDS REGION	33	4.9	5.6	PDE EQ A	03:29-03:40	12 01/ 02	
0960	03 04 24 114 03:29:18.2	23.918S 176.029W	SOUTH OF FUJI ISLANDS	33	5.9	5.5	PDE EQ A	03:32-03:44	13 01/ 02	
0961	03 04 24 114 04:48:13.0	35.039N 139.776E	NEAR S COAST OF HONSHU JAPAN	90	4.7	0.0	PDE EQ ABD	04:49-05:04	16 01/ 02	
0962	03 04 24 114 09:08:05.6	13.239N 146.329E	SOUTH OF MARIANA ISLANDS	33	5.1	0.0	PDE EQ ABDE	09:08-09:40	33 22249/ 19	
0963	03 04 24 114 09:08:49.0	0.912S 157.649E	SOLOMON ISLANDS	10	5.0	6.2	PDE EQ ABDE	09:12-09:53	44 22249/ 20	
0964	03 04 24 114 15:56:33.1	19.095S 173.219W	TONGA ISLANDS	51	5.1	0.0	PDE EQ A	15:59-16:11	13 22249/ 21	
0965	03 04 25 115 01:59:46.9	53.943N 159.368E	NEAR EAST COAST OF KAMCHATKA	111	4.4	0.0	PDE EQ ABDE	02:01-02:51	51 22249/ 22	
0966	03 04 25 115 11:13:11.5	0.706S 157.396E	SOLOMON ISLANDS	33	5.0	0.0	PDE EQ ABD	11:14-11:57	44 22250/ 01	
0967	03 04 25 115 13:55:50.0	46.391N 142.332E	SAKHALIN ISLAND	311	4.7	0.0	PDE EQ ABD	13:57-14:45	49 22250/ 02	
0968	03 04 25 115 14:00:43.3	51.331N 156.920E	KAMCHATKA	97	5.2	0.0	PDE EQ ABD	14:02-14:49	48 22250/ 03	
0969	03 04 25 115 17:57:01.0	5.456S 146.060E	EAST PAPUA NEW GUINEA	241	5.1	0.0	PDE EQ ABD	17:50-18:43	46 22250/ 04	
0970	03 04 25 115 19:03:47.0	12.777N 123.042E	LUZON PHILIPPINE ISLANDS	23	5.0	4.5	PDE EQ A	19:07-19:18	12 22250/ 05	
0971	03 04 25 115 23:24:20.9	55.010N 160.675E	KAMCHATKA	160	4.7	0.0	PDE EQ ABD	11:17-11:34	18 22250/ 06	
0972	03 04 26 116 11:15:37.6	15.091S 168.365E	VANUATU ISLANDS	33	5.6	5.5	PDE EQ ABD	12:44-12:55	12 22250/ 07	
0973	03 04 26 116 12:30:10.7	6.493S 105.374E	SUNDA STRAIT	123	5.0	0.0	PDE EQ A	15:29-15:40	12 22250/ 08	
0974	03 04 26 116 15:26:40.9	24.632N 122.045E	KURIL ISLANDS	155	4.9	0.0	PDE EQ ABDE	16:03-16:49	47 22250/ 09	
0975	03 04 26 116 16:02:17.5	48.686N 153.465E	KURIL ISLANDS	67	4.9	0.0	PDE EQ A	16:10-16:30	13 22250/ 10	
0976	03 04 26 116 18:15:37.0	24.220N 121.741E	TAIWAN	40	4.9	0.0	PDE EQ ABD	00:08-00:03	16 22250/ 11	
0977	03 04 27 117 00:46:51.6	6.318S 151.310E	NEW BRITAIN REGION	161	4.7	0.0	PDE EQ A	16:35-16:47	13 22250/ 12	
0978	03 04 27 117 16:20:19.3	36.228N 70.760E	HINDU KUSH REGION	21	5.5	5.6	PDE EQ A	17:24-17:35	12 22250/ 13	
0979	03 04 27 117 17:20:35.1	20.969S 174.532W	TONGA ISLANDS	120	4.9	0.0	PDE EQ ABDE	00:59-09:46	46 22250/ 14	
0980	03 04 28 118 00:50:06.0	51.119N 156.331E	KAMCHATKA	100						



## WAKE HYDROPHONE INFORMATION PROCESSING SYSTEM (WHIPS) EVENT LISTING

13 AUG 83

KEY: INFORMATION SOURCES - PDE=NEIS PDECARD, MON=NEIS MONTHLY LIST, ICS=ICS LIST, HEL=HELICORDER, OTH=OTHER  
 EVENT TYPE - EQ=EARTHQUAKE, NX=NUCLEAR EXPLOSION, SX=SCIENTIFIC EXPLOSION, OT=OTHER, UN=UNKNOWN  
 PHASES - A-P, B-PO, C-S, D-SO, E-T, F-OTHER

EVNT	*****ORIGIN TIME*****	*****COORDINATES*****	*****LOCATION*****	DEP	MAGNI	INF	EV	*****SAVED*****	*****STRIP*****
NO	VR*MO*DA*JUL*HR*MM*SECS	*LAT* *LON*	*DESCRIPTION*	KM	BDV	SRF	SRF	PHASES	INTERVAL
1001	83 05 03 123 02:38:15.4	46.489N 153.492E	KURIL ISLANDS	33	5.1	0.0	PDE EQ ABDE	02:39-03:22	44 202557 02
1002	83 05 03 123 15:39:39.3	20.212S 176.345W	FUJI ISLANDS REGION	593	5.5	0.0	PDE EQ A	15:41-15:53	13 202557 03
1003	83 05 03 123 18:37:13.4	46.297N 153.535E	KURIL ISLANDS	33	6.2	4.7	PDE EQ ABDE	18:38-19:21	44 202557 04
1004	83 05 03 123 21:02:15.2	3.885N 124.503E	TALAUD ISLANDS	64	5.0	0.0	PDE EQ A	21:05-21:16	12 202557 05
1005	83 05 04 124 07:58:25.4	9.443S 143.678E	EAST PAPUA NEW GUINEA REGION	15	5.0	4.9	PDE EQ ABDE	08:00-08:47	46 202557 06
1006	83 05 04 124 14:29:38.3	42.654N 142.979E	HOKKAIDO JAPAN REGION	187	4.7	0.0	PDE EQ ABDE	14:31-15:16	41 202557 07
1007	83 05 05 125 04:43:59.4	33.829S 179.383E	SOUTH OF KERMADEC ISLANDS	97	6.0	0.0	PDE EQ A	04:48-04:59	12 202557 08
1008	83 05 05 125 05:19:45.2	38.762N 72.354E	TADJIK SSR	33	4.9	0.0	PDE EQ A	06:27-06:38	12 202557 09
1009	83 05 05 125 07:14:19.9	3.187S 135.165E	WEST IRIAN REGION	33	5.4	0.0	PDE EQ A	07:17-07:28	12 202557 10
1010	83 05 05 125 15:20:00.0	37.812N 116.089W	SOUTHERN NEVADA	0	4.5	0.0	PDE NX A	15:26-15:37	12 202557 11
1011	83 05 06 126 04:16:15.2	43.107N 145.934E	KURIL ISLANDS	34	5.2	5.0	PDE EQ ABDE	04:17-05:07	44 202557 12
1012	83 05 06 126 11:59:41.4	21.324S 174.152W	TONGA ISLANDS	33	5.2	4.7	PDE EQ A	12:02-12:14	12 202557 13
1013	83 05 06 126 18:24:18.5	15.439N 121.691E	LUZON PHILIPPINE ISLANDS	33	5.6	5.6	PDE EQ A	18:27-18:38	12 202557 14
1014	83 05 07 127 06:11:24.1	6.048S 147.410E	EAST PAPUA NEW GUINEA REGION	119	5.2	0.0	PDE EQ ABDE	06:13-06:57	45 202557 15
1015	83 05 07 127 08:20:39.0	9.702S 159.504E	SOLOMON ISLANDS	33	5.0	0.0	PDE EQ ABDE	08:22-09:05	44 202557 16
1016	83 05 07 127 22:40:16.6	33.480N 144.084E	SOUTH OF HONSHU JAPAN	101	4.5	0.0	PDE EQ ABDE	22:41-23:22	42 202557 17
1017	83 05 07 127 23:58:01.9	24.654N 121.959E	TAIWAN	22	4.8	0.0	PDE EQ A	00:01-00:12	12 202557 18
1018	83 05 08 128 00:26:16.0	36.814N 70.980E	HINDU KUSH REGION	46	4.9	0.0	PDE EQ A	00:34-00:45	12 202557 19
1019	83 05 08 128 15:05:08.6	19.997N 109.340W	REVILLA GIGEDO ISLANDS REGION	10	5.3	5.0	PDE EQ A	15:12-15:23	12 202557 20
1020	83 05 08 128 21:32:48.5	43.010N 146.898E	KURIL ISLANDS	33	5.2	0.0	PDE EQ ABDE	21:32-22:14	43 202557 21
1021	83 05 09 129 15:53:02.7	0.202N 82.925W	PANAMA-COSTA RICA BORDER REGN	36	5.5	6.1	PDE EQ AE	16:02-16:11	130 202557 22
1022	83 05 09 129 28:09:15.1	19.983N 109.453W	REVILLA GIGEDO ISLANDS REGION	10	5.5	6.2	PDE EQ AE	28:16-21:03	98 202557 23
1023	83 05 10 130 00:15:06.2	24.422N 121.586E	TAIWAN	33	5.7	5.4	PDE EQ A	00:18-00:25	12 202557 24
1024	83 05 10 130 01:10:59.2	24.545N 122.029E	TAIWAN REGION	33	5.0	0.0	PDE EQ A	01:22-01:33	12 202557 25
1025	83 05 10 130 11:02:34.7	5.358S 150.915E	NEW BRITAIN REGION	104	6.0	0.0	PDE EQ ABDE	11:03-11:46	44 202557 26
1026	83 05 10 130 18:27:30.6	4.792S 152.508E	NEW BRITAIN REGION	60	5.9	0.0	PDE EQ ABDE	18:28-19:09	45 202557 27
1027	83 05 10 130 19:05:19.4	14.569N 122.352E	LUZON PHILIPPINE ISLANDS	35	5.1	0.0	PDE EQ A	19:05-19:18	17 202557 28
1028	83 05 10 130 19:05:19.4	36.503N 70.151E	HINDU KUSH REGION	218	5.0	0.0	PDE EQ A	19:12-19:24	3 202557 29
1029	83 05 11 131 00:17:13.4	2.302N 129.341E	HALMAHERA	140	5.0	0.0	PDE EQ A	00:28-00:31	12 202557 30
1030	83 05 00 000 00:00:00.0	0.000N 3.000E	UNKNOWN PHASE	0	0.0	0.0	HEL UN F	01:04-01:14	11 202557 31
1031	83 05 11 131 03:26:58.0	37.211N 141.817E	NEAR E COAST OF HONSHU JAPAN	44	4.0	0.0	PDE EQ ABD	03:27-03:42	16 202557 32
1032	83 05 11 131 07:41:44.5	11.949N 143.264E	SOUTH OF MARIANA ISLANDS	35	5.3	4.4	PDE EQ ABDE	07:42-08:16	37 202557 33
1033	83 05 11 131 10:05:06.4	14.726S 167.051E	VANUATU ISLANDS	165	4.0	0.0	PDE EQ ABD	10:06-10:23	18 202557 34
1034	83 05 11 131 20:20:27.1	45.651N 122.820W	WASHINGTON-OREGON BORDER REGN	0	0.0	0.0	PDE EQ A	20:26-20:37	12 202557 35
1035	83 05 11 131 21:40:15.2	21.467S 173.461W	TONGA ISLANDS	33	5.9	5.3	PDE EQ A	21:51-22:03	13 202557 36
1036	83 05 12 132 14:52:02.0	7.072S 103.353E	SOUTHWEST OF SUMATERA	33	5.0	4.7	PDE EQ A	14:58-15:09	12 202557 37
1037	83 05 12 132 21:52:56.4	51.101N 179.150W	ANDREANOF ISLANDS	50	4.9	0.0	PDE EQ ABD	21:54-22:11	18 202557 38
1038	83 05 13 133 10:09:37.0	3.022N 128.098E	NORTH OF HALMAHERA	142	5.5	0.0	PDE EQ A	10:12-10:23	12 202557 39
1039	83 05 13 133 22:54:14.9	6.626S 154.437E	SOLOMON ISLANDS	49	5.0	3.7	PDE EQ ABDE	22:55-23:37	43 202557 40
1040	83 05 14 134 13:29:17.9	40.393N 139.198E	NEAR W COAST OF HONSHU JAPAN	34	5.1	0.0	PDE EQ ABDE	13:38-14:16	47 202557 41
1041	83 05 15 135 00:24:00.5	10.888S 175.719W	TONGA ISLANDS	36	5.0	6.5	PDE EQ AE	00:27-01:23	57 202557 42
1042	83 05 15 135 22:02:14.2	52.022N 179.666E	RAT ISL. ALEUTIAN ISL.	162	4.5	0.0	PDE EQ ABD	22:04-22:22	17 202557 43
1043	83 05 16 136 12:07:54.7	39.415N 64.324E	UZBEK SSR	33	4.0	0.0	PDE EQ A	12:16-12:27	12 202557 44
1044	83 05 16 136 16:30:02.8	43.753N 87.293E	NORTHERN XINJIANG CHINA	33	5.0	0.0	PDE EQ A	16:36-16:47	12 202557 45
1045	83 05 16 136 21:39:47.1	38.489N 144.530E	OFF E COAST OF HONSHU JAPAN	33	5.1	0.0	PDE EQ ABDE	21:40-22:21	43 202557 46
1046	83 05 17 137 11:50:24.4	6.636S 154.135E	SOLOMON ISLANDS	59	5.2	0.0	PDE EQ ABDE	11:51-12:03	43 202557 47
1047	83 05 17 137 20:33:25.3	14.991S 169.042E	VANUATU ISLANDS	51	5.4	4.9	PDE EQ ABDE	20:35-21:23	49 202557 48
1048	83 05 17 137 21:02:13.4	38.693S 177.766W	KERMADEC ISLANDS	33	5.0	0.0	PDE EQ A	21:05-21:18	13 202557 49
1049	83 05 17 137 23:26:33.2	5.432S 159.939E	NEW BRITAIN REGION	118	5.6	0.0	PDE EQ ABDE	23:27-00:10	44 202557 50
1050	83 05 18 138 07:23:23.6	3.366N 126.799E	TALAUD ISLANDS	33	4.7	0.0	PDE EQ A	07:26-07:37	12 202557 51
1051	83 05 18 138 00:21:31.4	0.592N 121.739E	MINAHASSA PENINSULA	131	5.3	0.0	PDE EQ A	00:25-00:36	12 202557 52
1052	83 05 18 138 10:45:24.0	0.359S 121.272E	FLORES ISLAND REGION	209	4.9	0.0	PDE EQ A	10:49-10:58	12 202557 53
1053	83 05 19 139 09:54:37.9	28.172N 133.122E	RYUKYU ISLANDS	33	4.0	0.0	PDE EQ ABD	09:56-10:13	18 202557 54
1054	83 05 19 139 17:48:37.0	51.432N 174.070W	ANDREANOF ISL. ALEUTIAN ISL.	39	5.0	0.0	PDE EQ ABDE	17:50-18:40	51 202557 55
1055	83 05 19 139 21:20:57.0	53.902N 161.299E	OFF EAST COAST OF KAMCHATKA	33	4.4	0.0	PDE EQ ABD	21:23-21:39	17 202557 56
1056	83 05 20 140 04:45:55.1	4.776S 153.524E	NEW IRELAND REGION	101	4.9	0.0	PDE EQ ABD	04:46-05:01	16 202557 57
1057	83 05 20 140 06:09:18.0	53.116N 173.641W	ANDREANOF ISL. ALEUTIAN ISL.	233	4.0	0.0	PDE EQ ABD	06:11-06:28	18 202557 58
1058	83 05 20 140 15:42:06.6	23.291N 132.400E	SOUTHEAST OF SHIKOKU JAPAN	33	4.9	0.0	PDE EQ ABD	15:44-15:59	16 202557 59
1059	83 05 21 141 09:55:44.7	25.315S 179.319E	SOUTH OF FUJI ISLANDS	550	4.9	0.0	PDE EQ A	09:58-10:12	13 202557 60
1060	83 05 21 141 10:46:37.0	35.206N 140.246E	NEAR E COAST OF HONSHU JAPAN	31	5.1	4.5	PDE EQ ABDE	10:47-11:25	43 202557 61
1061	83 05 21 141 10:06:25.2	6.313N 124.368E	MINDANAO PHILIPPINE ISLANDS	71	5.0	0.0	PDE EQ A	10:09-10:20	12 202557 62
1062	83 05 21 141 10:32:44.5	35.169N 140.377E	NEAR E COAST OF HONSHU JAPAN	33	4.5	0.0	PDE EQ ABD	10:33-10:48	12 202557 63
1063	83 05 22 142 11:44:19.4	9.378S 123.765E	SOUTH OF HONSHU JAPAN	93	5.0	0.0	PDE EQ ABD	11:48-11:59	12 202557 64
1064	83 05 22 142 12:15:18.4	29.897N 141.582E	TIMOR	33	4.0	0.0	PDE EQ ABD	12:18-12:35	15 202557 65
1065	83 05 22 142 17:02:46.0	13.577S 167.514E	VANUATU ISLANDS	33	5.2	0.0	PDE EQ ABD	17:04-17:15	12 202557 66
1066	83 05 22 142 17:13:18.9	45.089N 151.095E	KURIL ISLANDS	33	4.0	0.0	PDE EQ ABD	17:14-17:29	16 202557 67
1067	83 05 22 142 19:56:12.6	45.133N 146.292E	KURIL ISLANDS	33	4.0	0.0	PDE EQ ABD	19:57-20:13	17 202557 68
1068	83 05 23 143 06:54:37.9	13.821S 171.294E	VANUATU ISLANDS REGION	183	4.4	0.0	PDE EQ ABD	06:56-07:07	12 202557 69
1069	83 05 23 143 17:55:52.9	37.904N 141.945E	NEAR E COAST OF HONSHU JAPAN	33	5.3	5.0	PDE EQ ABDE	17:57-18:39	43 202557 70
1070	83 05 24 144 00:00:00.0	0.000N 3.000E	PROBABLE HOKKAIDO PO. SO. T	0	0.0	0.0	HEL EQ ABDE	00:03-00:47	46 202557 71
1071	83 05 24 144 05:09:07.7	24.431N 143.295E	VOLCANO HOKKAIDO REGION	33	5.1	4.7	PDE EQ ABDE	05:09-05:44	36 202557 72
1072	83 05 24 144 07:30:36.0	26.910N 140.038E	BONIN ISLANDS REGION	460	4.5	0.0	PDE EQ ABD	07:38-07:53	16 202557 73
1073	83 05 24 144 10:03:25.0	31.356S 178.541W	KERMADEC ISLANDS REGION	33	5.3	0.0	PDE EQ A	10:07-10:19	13 202557 74
1074	83 05 24 144 13:39:49.5	55.605N 160.484E	OFF EAST COAST OF KAMCHATKA	49	4.0	0.0	PDE EQ ABD	13:42-13:59	18 202557 75
1075	83 05 25 145 17:30:58.2	21.912S 130.936W	TUAMOTU ARCHIPELAGO REGION	0	5.9	0.0	PDE NX A	17:37-17:48	12 202557 76
1076	83 05 26 146 03:00:00.0	40.370N 139.153E	NEAR W COAST OF HONSHU JAPAN	33	6.0	7.7	PDE EQ ABDE	03:01-03:47	47 202557 77
1077	83 05 26 146 06:46:03.3	40.930N 139.051E	NEAR W COAST OF HONSHU JAPAN	33	4.6	0.0	PDE EQ ABD	06:47-07:03	17 202557 78
1078	83 05 26 146 09:35:31.4	41.158N 139.063E	HOKKAIDO JAPAN REGION	19	5.2	0.0	PDE EQ ABDE	09:37-10:23	47 202557 79
1079	83 05 26 146 10:12:27.3	41.231N 139.097E	HOKKAIDO JAPAN REGION	33	5.3	0.0	PDE EQ ABDE		

# WAKE HYDROPHONE INFORMATION PROCESSING SYSTEM (WHIPS) EVENT LISTING

13 AUG 83

KEY: INFORMATION SOURCES - PDE=NEIS PDECARD, MON=NEIS MONTHLY LIST, ICS=ICS LIST, MEL=HELICORDER, OTH=OTHER  
 EVENT TYPE - EQ=EARTHQUAKE, NX=NUCLEAR EXPLOSION, SX=SCIENTIFIC EXPLOSION, OT=OTHER, UN=UNKNOWN  
 PHASES - A=P, B=P, C=S, D=SO, E=T, F=OTHER

EVNT	*****ORIGIN TIME*****	*****COORDINATES*****	*****LOCATION*****	DEP	MAGNI	INF	EV	*****SAVED*****	*****STIP*****
NO	VR=NO DA=JUL=NR=MM=SECS	LAT=*****LON=*****	*****DESCRIPTION*****	KM	BDY=SRF	SRC	TP	PHASES=*****INTERVAL*****	MNS TAPE/FILE
1101	03 05 29 149	00:20:32.1	48.398N 133.829E	33	4.6	4.1	PDE EQ ABD	00:30-00:46	17 20250/ 03
1102	03 05 29 149	02:14:02.0	4.227N 122.622E	611	5.5	0.0	PDE EQ A	02:17-02:28	12 20250/ 04
1103	03 05 29 149	04:45:39.6	49.255N 155.375E	33	5.0	5.2	PDE EQ ABDE	04:47-05:32	46 20250/ 05
1104	03 05 29 149	05:26:51.0	36.066N 141.937E	28	5.3	4.1	PDE EQ ABDE	05:27-06:09	43 20250/ 05
1105	03 05 29 149	06:55:32.9	48.442N 125.449W	10	5.1	5.1	PDE EQ A	07:01-07:12	12 20250/ 06
1106	03 05 29 149	07:15:29.6	48.487N 133.966E	28	5.1	0.0	PDE EQ ABDE	07:17-08:03	47 20250/ 07
1107	03 05 29 149	20:53:57.7	42.711N 143.434E	76	5.3	0.0	PDE EQ ABDE	20:55-21:40	46 20250/ 08
1108	03 05 29 149	22:01:49.4	48.674N 139.381E	33	5.6	4.7	PDE EQ ABDE	22:03-22:49	47 20250/ 09
1109	03 05 29 149	22:07:09.1	15.575S 174.977W	302	5.5	0.0	PDE EQ A	22:10-22:21	12 20250/ 09
1110	03 05 30 150	02:25:28.5	41.065N 139.163E	33	4.6	0.0	PDE EQ ABD	02:27-02:43	17 20250/ 10
1111	03 05 30 150	03:33:44.6	49.741N 73.210E	0	5.4	0.0	PDE EQ A	03:40-03:52	13 20250/ 11
1112	03 05 30 150	12:32:41.1	1.094N 125.549E	0	5.4	0.0	PDE EQ A	12:36-12:47	12 20250/ 12
1113	03 05 30 150	14:47:14.2	4.727S 183.232E	97	5.5	0.0	PDE EQ A	14:53-15:04	12 20250/ 13
1114	03 05 30 150	15:54:31.0	52.068N 177.698E	187	5.0	0.0	PDE EQ ABDE	15:56-16:45	57 20250/ 14
1115	03 05 31 151	00:17:33.8	40.595N 139.053E	33	4.7	0.0	PDE EQ ABD	00:19-02:35	17 20250/ 15
1116	03 05 31 151	00:31:11.8	5.092S 149.554E	33	4.7	0.0	PDE EQ ABD	00:33-00:49	17 20250/ 15
1117	03 05 31 151	06:10:09.2	4.768S 153.258E	119	4.5	0.0	PDE EQ ABD	06:10-06:33	15 20250/ 16
1118	03 05 31 151	21:05:44.1	34.602N 79.764E	33	5.0	4.3	PDE EQ A	21:12-21:24	13 20250/ 01
1119	03 05 31 151	21:15:56.2	40.202N 138.948E	25	4.9	0.0	PDE EQ ABD	21:17-21:32	17 20250/ 01
1120	03 05 31 151	23:19:11.1	48.711N 139.473E	18	5.3	0.0	PDE EQ ABDE	23:20-00:06	47 20250/ 02
1121	03 05 31 151	23:22:32.3	48.796N 139.420E	25	5.3	0.0	PDE EQ ABDE	23:24-00:10	47 20250/ 02
1122	03 06 01 152	00:58:46.9	48.419N 139.171E	33	4.9	0.0	PDE EQ ABD	01:02-01:16	17 20250/ 03
1123	03 06 01 152	01:37:02.7	13.762N 122.748E	260	5.5	0.0	PDE EQ A	01:40-01:51	12 20250/ 04
1124	03 06 01 152	02:00:00.1	16.996S 174.713W	228	6.1	0.0	PDE EQ A	02:02-02:13	12 20250/ 05
1125	03 06 01 152	06:40:36.9	39.950N 138.897E	33	4.8	0.0	PDE EQ ABD	06:42-06:58	17 20250/ 06
1126	03 06 01 152	07:14:30.1	48.399N 139.133E	33	4.7	0.0	PDE EQ ABD	07:16-07:31	16 20250/ 07
1127	03 06 01 152	07:30:33.9	51.722N 171.302W	32	4.7	0.0	PDE EQ ABD	07:33-07:49	17 20250/ 07
1128	03 06 01 152	10:50:42.8	15.922S 172.021W	33	5.6	6.1	PDE EQ A	11:01-11:12	12 20250/ 09
1129	03 06 01 152	11:17:40.2	43.919N 80.576E	32	5.1	0.0	PDE EQ A	11:24-11:35	12 20250/ 10
1130	03 06 01 152	13:13:59.0	17.037S 174.614W	223	4.8	0.0	PDE EQ A	13:16-13:27	12 20250/ 11
1131	03 06 02 000	00:00:00.0	0.000N 0.000E	0	0.0	0.0	MEL EQ BDE	15:29-15:58	30 20250/ 12
1132	03 06 02 000	00:00:00.0	0.000N 0.000E	0	0.0	0.0	MEL UN A	20:26-20:35	13 20250/ 13
1133	03 06 02 153	20:51:58.2	24.596S 179.505E	524	5.0	0.0	PDE EQ A	20:54-21:08	13 20250/ 14
1134	03 06 03 154	01:30:04.2	51.164N 177.164W	54	4.6	0.0	PDE EQ ABD	01:32-01:48	17 20250/ 15
1135	03 06 03 154	21:51:52.4	0.636N 119.917E	73	5.0	0.0	PDE EQ A	21:52-22:07	12 20250/ 16
1136	03 06 03 154	22:52:13.6	7.094S 129.184E	202	5.2	0.0	PDE EQ A	22:55-23:06	12 20250/ 17
1137	03 06 04 155	09:34:44.4	27.059N 103.322E	33	5.1	0.0	PDE EQ A	09:42-09:51	12 20250/ 18
1138	03 06 04 155	11:37:40.9	37.391N 115.214W	6	0.0	0.0	PDE EQ A	11:44-11:55	12 20250/ 19
1139	03 06 05 156	00:43:14.3	7.604S 127.621E	184	5.2	0.0	PDE EQ A	00:46-00:58	13 20250/ 20
1140	03 06 05 156	05:34:40.2	6.105S 143.108E	116	5.2	0.0	PDE EQ ABDE	05:36-06:22	47 20250/ 21
1141	03 06 05 156	10:39:38.7	39.235N 75.712E	33	4.9	4.5	PDE EQ A	10:47-10:56	12 20250/ 22
1142	03 06 05 156	13:23:34.2	16.096S 172.987W	33	5.1	4.7	PDE EQ A	13:26-13:37	12 20250/ 23
1143	03 06 05 156	16:26:40.7	15.929S 173.017W	33	5.3	5.1	PDE EQ A	16:29-16:40	12 20250/ 24
1144	03 06 05 156	22:17:03.2	39.433N 73.466E	33	5.0	0.0	PDE EQ A	22:24-22:35	12 20250/ 25
1145	03 06 05 157	03:10:01.4	20.545S 175.569W	620	4.9	0.0	PDE EQ A	03:20-03:31	12 20250/ 26
1146	03 06 05 157	21:40:17.5	45.365N 150.352E	33	5.6	5.1	PDE EQ ABDE	21:41-22:04	44 20250/ 01
1147	03 06 07 158	02:11:32.5	23.951N 122.756E	33	5.1	0.0	PDE EQ A	02:14-02:25	12 20250/ 02
1148	03 06 07 158	06:31:34.3	5.433N 95.187E	110	4.8	0.0	PDE EQ A	06:38-06:49	12 20250/ 03
1149	03 06 07 158	15:57:36.1	32.012N 130.921E	51	0.0	4.7	PDE EQ ABD	15:59-16:15	17 20250/ 04
1150	03 06 08 159	09:54:38.0	5.289S 102.853E	33	5.2	0.0	PDE EQ A	10:00-10:12	13 20250/ 05
1151	03 06 09 160	04:36:58.6	48.014N 139.178E	33	4.9	0.0	PDE EQ ABD	04:38-04:54	17 20250/ 06
1152	03 06 09 160	04:51:00.7	3.076S 129.046E	114	5.2	0.0	PDE EQ A	04:54-05:05	12 20250/ 07
1153	03 06 09 160	10:23:31.9	48.198N 139.003E	33	5.4	0.0	PDE EQ ABD	10:25-11:10	46 20250/ 08
1154	03 06 09 160	12:49:04.1	48.200N 139.054E	33	6.3	5.6	PDE EQ ABDE	12:50-12:36	47 20250/ 09
1155	03 06 09 160	13:04:02.9	40.194N 139.226E	33	6.3	5.6	PDE EQ ABDE	13:05-13:51	47 20250/ 09
1156	03 06 09 160	14:11:05.7	48.403N 137.751E	33	5.0	0.0	PDE EQ ABDE	14:42-15:29	46 20250/ 10
1157	03 06 09 160	17:10:02.0	37.158N 110.009W	0	4.6	0.0	PDE EQ A	17:16-17:27	12 20250/ 10
1158	03 06 09 160	18:46:01.0	51.441N 174.161W	20	6.2	5.0	PDE EQ ABDE	18:48-19:37	50 20250/ 11
1159	03 06 09 160	20:26:01.0	5.995S 122.650E	50	5.5	5.2	PDE EQ A	20:31-20:42	12 20250/ 12
1160	03 06 09 160	20:36:36.9	51.441N 174.148W	26	4.8	0.0	PDE EQ ABD	20:38-20:55	18 20250/ 13
1161	03 06 10 161	02:13:23.0	75.505N 120.682E	10	5.5	5.3	PDE EQ A	02:18-02:30	12 20250/ 12
1162	03 06 10 161	07:20:17.6	40.244N 139.050E	33	5.1	0.0	PDE EQ ABDE	07:21-08:07	47 20250/ 14
1163	03 06 10 161	20:30:27.0	16.275N 149.078E	100	5.1	0.0	PDE EQ ABDE	20:38-21:10	30 20250/ 15
1164	03 06 10 161	22:39:07.3	24.271S 176.203W	33	5.7	5.4	PDE EQ A	22:42-22:54	13 20250/ 01
1165	03 06 10 161	00:00:00.0	0.000N 0.000E	0	0.0	0.0	MEL EQ B	23:26-23:45	20 20250/ 02
1166	03 06 11 162	00:28:13.1	1.615N 126.593E	62	5.1	0.0	PDE EQ A	00:31-00:42	12 20250/ 03
1167	03 06 11 162	03:09:53.9	36.261N 120.466W	2	5.4	5.4	PDE EQ A	03:16-03:27	12 20250/ 04
1168	03 06 11 162	04:54:00.6	4.300S 122.536E	634	5.3	0.0	PDE EQ A	04:57-05:26	12 20250/ 05
1169	03 06 11 162	22:01:26.0	40.712N 139.243E	33	5.0	0.0	PDE EQ ABDE	22:03-22:49	47 20250/ 06
1170	03 06 12 163	02:36:43.5	49.094N 78.964E	0	6.1	4.5	PDE EQ A	02:43-02:55	13 20250/ 07
1171	03 06 12 163	09:14:10.6	12.844S 169.028E	592	5.2	0.0	PDE EQ A	09:15-09:26	12 20250/ 08
1172	03 06 12 163	10:12:43.2	1.527N 127.278E	124	5.6	0.0	PDE EQ A	10:15-10:26	12 20250/ 09
1173	03 06 12 163	19:20:59.6	46.687N 152.637E	33	5.0	0.0	PDE EQ ABDE	19:22-20:06	45 20250/ 10
1174	03 06 13 164	00:52:02.2	48.452N 143.885E	33	4.7	4.7	PDE EQ ABC	00:53-01:08	16 20250/ 11
1175	03 06 13 164	03:54:54.1	45.147N 154.543E	33	5.0	0.0	PDE EQ ABDE	03:56-04:39	44 20250/ 12
1176	03 06 13 164	04:19:38.5	48.405N 143.751E	33	4.9	0.0	PDE EQ ABD	04:22-04:35	16 20250/ 12
1177	03 06 13 164	08:01:38.4	27.255N 65.274E	33	4.9	0.0	PDE EQ A	08:10-08:21	12 20250/ 13
1178	03 06 13 164	09:45:01.1	0.464S 122.633E	179	5.0	0.0	PDE EQ A	09:49-10:00	12 20250/ 14
1179	03 06 14 165	00:59:29.6	53.508S 143.635E	10	5.2	0.0	PDE EQ A	01:06-01:17	12 20250/ 15
1180	03 06 15 166	06:05:55.5	34.109N 92.017E	33	5.1	5.2	PDE EQ A	06:12-06:23	12 20250/ 16
1181	03 06 15 166	06:07:55.3	15.192S 170.686E	40	5.5	5.5	PDE EQ A	06:10-06:22	13 20250/ 16
1182	03 06 15 166	00:00:00.0	0.000N 0.000E	0	0.0	0.0	MEL EQ BDE	07:21-07:50	30 20250/ 17
1183	03 06 15 166	07:33:43.6	5.307N 127.592E	53	5.4	5.0	PDE EQ A	07:36-07:47	12 20250/ 17
1184	03 06 15 166	13:34:06.5	39.320N 64.333E	33	4.9	0.0	PDE EQ A	13:42-13:53	12 20250/ 18
1185	03 06 16 167	11:33:15.4	36.440S 97.443W	10	5.5	5.5	PDE EQ A	11:42-12:01	20 20250/ 19
1186	03 06 17 168	20:55:32.6	41.282N 139.155E	33	5.0	0.0	PDE EQ ABDE	20:57-21:43	47 20250/ 20
1187	03 06 17 168	22:02:31.6	52.234N 159.647E	33	5.6	5.0	PDE EQ ABDE	22:04-22:52	44 20250/ 01
1188	03 06 18 169	03:03:34.0	53.121N 159.748E	33	5.0	0.0	PDE EQ ABDE	03:05-03:54	50 20250/ 02
1189	03 06 18 169	11:29:48.4	5.577S 131.260E	59	5.1	0.0	PDE EQ A	11:33-11:44	12 20250/ 03
1190	03 06 18 169	13:17:56.2	12.255N 143.004E	27	4.9	0.0	PDE EQ ABD	13:18-13:31	14 20250/ 04
1191	03 06 18 169	19:31:12.7	0.247S						

## WAKE HYDROPHONE INFORMATION PROCESSING SYSTEM (WHIPS) EVENT LISTING

13 AUG 83

KEY: INFORMATION SOURCES - PDE=NEIS PDECARD, MON=NEIS MONTHLY LIST, ICS=ICS LIST, MEL=HELICORDER, OTH=OTHER  
 EVENT TYPE - EQ=EARTHQUAKE, NX=NUCLEAR EXPLOSION, SK=SCIENTIFIC EXPLOSION, OT=OTHER, UN=UNKNOWN  
 PHASES - A=P, B=PO, C=S, D=SO, E=T, F=OTHER

EVNT	*****ORIGIN TIME*****	*****COORDINATES*****	*****LOCATION*****	DEP	MAGNI	INF	EV	*****SAVED*****	*****STRIP*****
NO	YR*MO*DA*JUL	HR*MIN*SECS	LAT*SRF*LONG	KM	BDY	TP	PHASES	INTERVAL	MNS TAPE/FILE
1201	03 06 21	172 06:25:27.6	41.315N 139.136E	13	6.6	6.0	PDE EQ ABDE	06:27-07:13	47 28863/ 01
1202	03 06 21	172 06:46:50.1	41.385N 139.345E	33	5.4	0.0	PDE EQ ABDE	06:48-07:34	47 01 00
1203	03 06 21	172 07:04:22.2	41.358N 139.349E	33	5.5	0.0	PDE EQ ABDE	07:06-07:52	47 01 00
1204	03 06 21	172 07:13:51.4	41.320N 139.270E	33	5.4	0.0	PDE EQ ABDE	07:15-08:01	47 01 00
1205	03 06 21	172 08:12:15.3	41.380N 139.596E	33	4.6	0.0	PDE EQ ABD	08:13-09:29	17 01 00
1206	03 06 21	172 08:16:05.7	41.380N 139.421E	33	4.8	0.0	PDE EQ ABD	08:17-08:33	17 01 00
1207	03 06 21	172 08:26:28.0	5.483S 151.037E	105	5.2	0.0	PDE EQ ABDE	08:27-11:10	44 01 00
1208	03 06 21	172 08:38:46.7	24.045N 122.853E	33	4.9	0.0	PDE EQ A	08:41-08:53	13 01 00
1209	03 06 21	172 11:29:55.5	41.735N 139.168E	20	5.2	0.0	PDE EQ ABDE	11:31-12:18	46 01 00
1210	03 06 21	172 11:32:12.7	7.122S 129.983E	111	4.8	0.0	PDE EQ A	11:35-11:46	12 01 00
1211	03 06 21	172 11:36:57.5	15.436S 173.451W	33	5.1	0.0	PDE EQ A	11:39-11:51	13 01 00
1212	03 06 21	172 14:31:50.9	24.877N 122.467E	32	5.3	4.7	PDE EQ A	14:34-14:46	13 01 00
1213	03 06 21	172 14:40:05.5	24.253N 122.488E	24	5.0	6.3	PDE EQ A	14:51-15:02	12 01 00
1214	03 06 21	172 15:49:41.9	6.260N 125.335E	342	0.0	0.0	PDE EQ A	15:52-16:03	12 01 00
1215	03 06 21	172 16:02:21.3	41.521N 139.488E	33	4.0	0.0	PDE EQ ABD	16:04-16:20	17 01 00
1216	03 06 21	172 17:06:52.1	29.705N 129.362E	164	5.9	0.0	PDE EQ ABDE	17:06-17:56	51 01 00
1217	03 06 21	173 04:34:20.8	41.378N 139.277E	33	5.0	0.0	PDE EQ ABDE	04:36-05:22	47 01 00
1218	03 06 22	173 04:36:34.3	41.047N 139.161E	27	5.3	0.0	PDE EQ ABDE	04:38-05:24	47 01 00
1219	03 06 22	173 05:39:33.9	41.455N 139.381E	33	4.0	0.0	PDE EQ ABD	05:41-05:57	17 01 00
1220	03 06 22	173 14:32:07.4	50.315N 142.257E	33	4.0	0.0	PDE EQ ABD	14:34-14:51	18 01 00
1221	03 06 22	173 15:28:23.4	41.340N 139.224E	18	5.1	0.0	PDE EQ ABDE	15:22-16:08	47 01 00
1222	03 06 22	173 20:15:46.8	40.033N 138.974E	17	5.3	4.1	PDE EQ ABDE	20:17-21:03	47 01 00
1223	03 06 22	173 21:38:27.0	41.165N 139.335E	33	4.4	0.0	PDE EQ ABD	21:40-21:56	17 01 00
1224	03 06 23	174 01:45:03.5	51.366N 179.024W	33	4.0	0.0	PDE EQ ABD	01:47-02:03	17 01 00
1225	03 06 23	174 11:00:38.0	41.556N 141.956E	79	4.9	0.0	PDE EQ ABD	11:02-11:17	16 01 00
1226	03 06 23	174 12:05:18.4	51.763N 139.599E	18	5.5	5.6	PDE EQ A	12:08-12:19	12 01 00
1227	03 06 23	174 19:40:23.1	26.760S 177.171W	54	5.0	4.8	PDE EQ A	19:44-19:55	12 01 00
1228	03 06 24	175 02:09:28.0	4.669S 182.562E	33	5.1	0.0	PDE EQ A	02:15-02:26	12 01 00
1229	03 06 24	175 07:18:21.9	21.723N 103.381E	18	6.1	6.5	PDE EQ F	07:18-08:47	90 01 00
1230	03 06 24	175 09:06:46.7	24.197N 122.439E	54	6.0	0.0	PDE EQ A	09:09-09:24	17 01 00
1231	03 06 24	175 09:07:17.2	45.155N 146.921E	97	4.9	0.0	PDE EQ ABD	09:09-09:24	17 01 00
1232	03 06 24	175 12:20:14.6	34.435N 69.609E	33	4.7	0.0	PDE EQ A	12:26-12:39	12 01 00
1233	03 06 24	175 19:55:20.9	23.993N 122.696E	33	5.0	0.0	PDE EQ A	19:56-20:09	12 01 00

EOP...

1234	03 06 25	176 02:32:47.3	29.898S 177.351W	33	5.1	0.0	PDE EQ A	02:38-02:49	12 28864-9
1235	03 06 25	176 10:03:17.6	32.004S 178.798W	46	5.6	5.6	PDE EQ A	10:27-10:39	13 28864-11
1236	03 06 25	176 11:59:45.6	18.058S 177.589W	595	5.1	0.0	PDE EQ A	12:01-12:13	13 28864-12
1237	03 06 25	176 12:50:25.3	32.277N 137.683E	377	5.1	0.0	PDE EQ ABDE	13:51-14:34	44 28864-14
1238	03 06 25	176 00:02:43.0	1.332N 99.918E	205	4.9	0.0	PDE EQ A	00:46-00:57	12 28864-10
1239	03 06 25	176 14:12:54.9	23.103N 123.343E	16	5.4	0.0	PDE EQ A	14:15-14:27	13 28864-14
1240	03 06 25	176 15:04:09.9	22.037S 177.465W	274	5.5	0.0	PDE EQ A	15:07-15:18	10 28864-13
1241	03 06 25	176 19:10:02.2	32.817S 178.679W	33	5.5	0.0	PDE EQ A	19:14-19:26	13 28864-15
1242	03 06 25	176 19:40:55.3	24.001N 122.550E	42	5.5	5.0	PDE EQ A	19:44-19:55	12 28864-16
1243	03 06 25	176 23:14:56.8	7.251S 106.017E	56	5.2	0.0	PDE EQ A	23:21-23:32	12 28864-17
1244	03 06 26	177 02:31:16.2	23.005N 93.758E	73	4.7	0.0	PDE EQ A	02:37-02:48	12 28864-18
1245	03 06 26	177 05:10:20.1	44.931S 167.277E	33	5.1	0.0	PDE EQ A	05:16-05:27	12 28864-19
1246	03 06 26	177 13:56:54.5	41.381N 139.386E	29	4.9	0.0	PDE EQ ABD	13:58-14:14	17 28864-20
1247	03 06 26	177 15:44:23.5	17.055S 167.470E	45	5.2	5.2	PDE EQ A	15:56-16:08	13 28864-21
1248	03 06 26	177 17:45:11.1	20.093N 139.094E	201	4.9	0.0	PDE EQ ABDE	17:45-18:25	41 28865-1
1249	03 06 27	178 00:25:13.2	10.100S 167.666E	50	5.0	0.0	PDE EQ A	00:27-00:39	13 28865-2
1250	03 06 27	178 14:10:05.5	23.047S 179.955W	540	5.3	0.0	PDE EQ A	14:12-14:24	13 28865-3
1251	03 06 28	179 03:25:16.6	60.250N 141.272W	15	5.9	5.4	PDE EQ ABDE	03:38-04:02	71 28865-4
1252	03 06 28	179 17:45:58.2	21.015S 132.950W	0	5.4	0.0	PDE NX A	17:52-18:03	12 28865-5
1253	03 06 28	179 21:55:46.1	22.734S 174.702W	33	5.2	4.9	PDE EQ A	21:59-22:10	12 28865-6
1254	03 06 28	179 23:59:33.4	43.074N 84.075E	33	5.1	4.5	PDE EQ A	00:26-00:37	12 28865-7
1255	03 06 29	180 05:11:57.3	40.190N 139.022E	33	5.1	0.0	PDE EQ ABDE	05:13-05:59	47 28865-8
1256	03 06 29	180 10:55:40.6	36.602N 140.794E	123	4.6	0.0	PDE EQ ABD	10:56-11:11	16 28865-9
1257	03 06 29	180 12:51:37.9	6.916S 129.021E	193	4.2	0.0	PDE EQ A	12:55-13:06	12 28865-10
1258	03 06 29	180 00:00:00.0	0.000E 0.000E	0	0.0	0.0	PDE MEL B	16:14-16:53	40 28865-11
1259	03 06 29	180 22:18:22.6	41.277N 139.358E	33	4.9	0.0	PDE EQ ABD	22:20-22:36	17 28865-12
1260	03 06 30	181 00:53:28.7	10.071N 121.313E	75	5.1	0.0	PDE EQ A	00:56-00:57	12 28865-13
1261	03 06 30	181 13:39:04.5	44.032N 147.049E	47	5.6	5.4	PDE EQ ABDE	13:40-14:23	44 28865-14
1262	03 06 30	181 14:11:23.2	10.540S 174.841W	272	4.8	0.0	PDE EQ A	14:14-14:25	12 28865-15
1263	03 06 30	181 17:37:49.0	2.529N 128.265E	49	5.6	5.4	PDE EQ A	17:40-17:52	13 28865-16
1264	03 06 30	181 18:24:51.5	44.002N 149.519E	33	5.3	5.1	PDE EQ ABDE	18:26-18:38	43 28865-17
1265	03 06 30	181 23:03:50.1	6.910S 155.220E	97	5.1	0.0	PDE EQ ABDE	23:05-23:46	42 28865-18
1266	03 06 30	181 23:10:51.0	44.428N 149.498E	48	5.1	0.0	PDE EQ ABDE	23:12-00:02	43 28865-19
1267	03 06 30	181 23:42:16.9	44.318N 149.586E	33	5.0	0.0	PDE EQ ABDE	23:43-00:02	44 28865-20
1268	03 07 01	182 02:23:11.7	44.502N 149.410E	60	5.4	0.0	PDE EQ ABDE	02:24-03:07	44 28865-21
1269	03 07 01	182 06:35:56.0	32.262N 140.464E	76	4.8	0.0	PDE EQ ABD	06:36-06:51	16 28865-22
1270	03 07 01	182 08:53:55.5	44.256N 149.580E	33	5.0	4.8	PDE EQ ABDE	08:55-09:11	43 28865-23
1271	03 07 01	182 10:46:54.7	44.374N 149.575E	33	5.2	4.7	PDE EQ ABDE	10:48-11:30	43 28865-24
1272	03 07 01	182 22:03:42.0	36.098N 141.057E	53	5.5	0.0	PDE EQ ABDE	22:04-22:47	44 28865-25
1273	03 07 01	182 23:32:00.4	39.961N 139.016E	37	4.6	0.0	PDE EQ ABD	23:33-23:49	17 28865-26
1274	03 07 02	183 05:32:42.6	40.000N 130.965E	33	5.1	0.0	PDE EQ ABDE	05:34-06:20	47 28865-27
1275	03 07 02	183 08:00:00.0	0.000E 0.000E	0	0.0	0.0	PDE MEL B	07:10-07:47	30 28865-28
1276	03 07 02	183 09:34:05.6	5.724N 94.779E	98	5.7	0.0	PDE EQ A	09:42-09:51	12 28865-29
1277	03 07 02	183 11:42:21.9	39.305N 64.301E	33	4.9	0.0	PDE EQ A	11:50-12:01	12 28865-30
1278	03 07 03	184 02:49:26.8	20.157N 127.418E	211	6.1	0.0	PDE EQ A	02:52-03:03	12 28865-31
1279	03 07 03	184 06:11:35.7	5.589S 154.318E	405	5.4	0.0	PDE EQ ABDE	06:12-06:53	42 28865-32
1280	03 07 03	184 07:05:26.1	41.453N 139.347E	33	5.0	0.0	PDE EQ ABDE	07:07-07:53	47 28865-33
1281	03 07 03	184 08:01:22.0	13.093S 167.954E	33	4.9	0.0	PDE EQ A	08:03-08:14	12 28865-34
1282	03 07 03	184 17:14:23.2	9.650N 83.644W	33	5.7	6.1	PDE EQ AE	17:23-19:33	129 28865-35
1283	03 07 03	184 17:48:01.4	24.023N 141.012E	292	4.5	0.0	PDE EQ ABDE	17:48-18:26	39 28865-36

Reproduced from  
 best available copy.

## WAKE HYDROPHONE INFORMATION PROCESSING SYSTEM (WHIPS) EVENT LISTING

27 SEP 83

KEY: INFORMATION SOURCES - PDE=NEIS PDECARD, MON=NEIS MONTHLY LIST, ICS=ICS LIST, HEL=HELICORDER, OTH=OTHER  
 EVENT TYPE - EQ=EARTHQUAKE, NX=NUCLEAR EXPLOSION, SX=SCIENTIFIC EXPLOSION, OT=OTHER, UN=UNKNOWN  
 PHASES - A=P, B=PO, C=S, D=SO, E=T, F=OTHER

EVNT	*****ORIGIN TIME*****	**COORDINATES**	*****LOCATION*****	DEF	*MAGNI*	INF	EV	*****SAVED*****	*STRIP**
*NO*	VR=MO=DA=JUL=NR=MM=SECS	*LAT=*****LON**	*****DESCRIPTION*****	KM	BDY=SRF	SRC	TP	PHASES=INTERVAL=**MNS	TAPE-FIL
1204	03 07 03 104 20:24:41.5	24.372N 122.499E	TAIWAN REGION	65.5	2.0	PDE	EQ A	20:27-20:39	13 20066-1
1205	03 07 04 105 11:32:46.2	55.569S 27.942W	SOUTH SANDWICH ISLANDS REGION	33.5	5.4	PDE	EQ A	11:42-12:01	20 20066-2
1206	03 07 04 105 20:51:19.6	49.753N 155.610E	KURIL ISLANDS	40.5	0.0	PDE	EQ ABDE	20:52-21:30	47 20066-3
1207	03 07 04 105 22:00:34.0	4.415N 126.736E	TALAUJ ISLANDS	100.5	1.0	PDE	EQ A	22:03-22:14	12 20066-4
1208	03 07 05 106 05:58:21.4	55.596S 123.453W	EASTER ISLAND CORDILLERA	10.5	3.0	PDE	EQ AE	06:07-06:08	117 20066-5
1209	03 07 05 106 08:54:40.0	26.431N 126.947E	RYUKYU ISLANDS	33.5	5.3	PDE	EQ ABDE	08:57-09:46	50 20066-6
1210	03 07 05 106 09:57:30.0	24.201S 174.894W	SOUTH OF TONGA ISLANDS	33.5	5.0	PDE	EQ A	10:01-10:12	12 20066-7
1211	03 07 05 106 11:11:41.1	22.551S 171.015E	LOYALTY ISLANDS REGION	45.6	0.0	PDE	EQ AE	11:14-12:11	56 20066-8
1212	03 07 05 106 11:49:02.0	22.718S 170.931E	LOYALTY ISLANDS REGION	51.5	1.0	PDE	EQ A	11:52-12:03	12 20066-9
1213	03 07 05 106 12:55:05.0	22.713S 171.042E	LOYALTY ISLANDS REGION	33.5	4.0	PDE	EQ A	12:58-13:09	12 20066-10
1214	03 07 05 106 16:37:06.0	57.021S 25.629W	SOUTH SANDWICH ISLANDS REGION	33.5	7.5	PDE	EQ A	16:46-17:05	20 20066-11
1215	03 07 05 106 18:24:15.4	22.921S 171.061E	LOYALTY ISLANDS REGION	40.5	2.0	PDE	EQ A	03:27-03:38	12 20066-12
1216	03 07 06 107 04:54:36.5	21.807S 174.022W	TONGA ISLANDS	33.5	3.0	PDE	EQ A	04:58-05:09	12 20066-13
1217	03 07 06 107 07:47:12.8	12.012N 144.759E	MARIANA ISLANDS	146.5	0.0	PDE	EQ ABDE	07:47-08:21	35 20066-14
1218	03 07 06 107 17:59:54.7	11.632S 166.347E	SANTA CRUZ ISLANDS	33.5	2.0	PDE	EQ A	18:01-18:12	12 20066-15
1219	03 07 06 107 18:19:31.7	1.715N 98.148E	NORTHERN SUMATRA	84.5	3.0	PDE	EQ A	18:25-18:37	13 20066-16
1220	03 07 06 108 00:00:00.0	0.000N 0.000E	UNKNOWN PO. SO. T	0.0	0.0	HEL	EQ BDE	00:00-01:27	40 20066-17
1221	03 07 07 108 01:02:57.0	22.633S 171.002E	LOYALTY ISLANDS REGION	55.5	3.0	PDE	EQ A	01:06-01:17	12 20066-18
1222	03 07 07 108 03:35:05.5	12.203N 125.749E	SAMAR PHILIPPINE ISLANDS	40.5	0.0	PDE	EQ A	03:38-03:49	12 20066-19
1223	03 07 07 108 05:29:48.4	22.613S 170.058E	LOYALTY ISLANDS REGION	64.5	1.0	PDE	EQ A	05:32-05:44	13 20066-20
1224	03 07 07 108 13:33:53.5	19.203S 177.301W	FIJI ISLANDS REGION	377.5	3.0	PDE	EQ A	13:36-13:47	12 20066-21
1225	03 07 07 108 15:35:45.4	22.602S 170.961E	LOYALTY ISLANDS REGION	33.5	1.0	PDE	EQ A	15:38-15:50	13 20066-22
1226	03 07 07 108 16:05:40.0	22.561S 170.722E	LOYALTY ISLANDS REGION	41.5	4.0	PDE	EQ AE	16:08-17:05	56 20066-23
1227	03 07 08 109 00:58:11.7	2.398N 128.424E	HALMEHERA	157.5	3.0	PDE	EQ A	01:01-01:12	12 20066-24
1228	03 07 08 109 18:05:00.1	21.802S 173.300W	TONGA ISLANDS	33.5	5.0	PDE	EQ A	18:08-18:19	12 20066-25
1229	03 07 08 109 19:38:12.1	19.472S 169.072E	VANUATU ISLANDS	152.5	2.0	PDE	EQ A	19:42-19:53	12 20066-26
1230	03 07 08 109 19:38:12.1	19.472S 169.072E	PROBABLE MARIANAS PO. SO. T	0.0	0.0	HEL	EQ BDE	19:38-19:57	30 20066-27
1231	03 07 09 100 18:30:39.0	6.432S 146.605E	EAST PAPUA NEW GUINEA REGION	110.5	1.0	PDE	EQ ABDE	18:32-19:10	47 20066-28
1232	03 07 10 191 03:59:57.0	51.327N 53.286E	EUROPEAN USSR	0.5	3.0	PDE	EQ A	04:06-04:19	12 20066-29
1233	03 07 10 191 04:04:57.0	51.336N 53.290E	EUROPEAN USSR	0.5	4.0	PDE	EQ A	04:13-04:24	12 20066-30
1234	03 07 10 191 04:05:57.1	51.357N 53.321E	EUROPEAN USSR	0.5	2.0	PDE	EQ A	04:18-04:29	12 20066-31
1235	03 07 10 191 17:15:46.6	27.401N 128.286E	RYUKYU ISLANDS	58.5	4.0	PDE	EQ A	17:22-17:33	12 20066-32
1236	03 07 10 191 17:15:46.6	27.401N 128.286E	PROBABLE MARIANAS PO. SO. T	0.0	0.0	HEL	EQ BDE	17:01-17:20	32 20066-33
1237	03 07 11 192 10:35:26.0	41.340N 139.495E	HOKKAIDO JAPAN REGION	33.5	4.0	PDE	EQ ABD	10:37-10:53	17 20066-34
1238	03 07 11 192 12:56:28.1	60.896S 52.935W	SOUTH SHELTER ISLANDS	10.5	6.0	PDE	EQ AE	13:05-15:45	161 20066-35
1239	03 07 11 192 21:10:23.0	40.522N 77.625E	KIRGHIZ-KOSTANG BORDER REGION	33.5	0.0	PDE	EQ A	21:25-21:36	12 20066-36
1240	03 07 12 193 14:56:55.3	38.033N 141.095E	NEAR E COAST OF HONSHU JAPAN	33.5	4.0	PDE	EQ ABD	14:56-15:13	16 20066-37
1241	03 07 12 193 15:10:03.3	61.033N 147.379W	SOUTHERN ALASKA	37.6	1.0	PDE	EQ ABDE	15:14-16:22	69 20066-38
1242	03 07 13 194 11:09:42.2	36.302N 70.991E	HINDU KUSH REGION	131.4	7.0	PDE	EQ A	11:17-11:26	12 20066-39
1243	03 07 13 194 15:07:40.0	6.623S 106.342E	JAVA	127.5	0.0	PDE	EQ A	15:13-15:24	12 20066-40
1244	03 07 14 195 09:48:36.0	18.957S 175.699W	TONGA ISLANDS	275.5	1.0	PDE	EQ A	09:51-10:02	12 20066-41
1245	03 07 14 195 15:47:46.5	5.532N 126.406E	MINDANAO PHILIPPINE ISLANDS	43.5	6.0	PDE	EQ AE	19:58-20:46	57 20066-42
1246	03 07 15 196 03:10:03.1	18.965S 168.362E	VANUATU ISLANDS	33.5	1.0	PDE	EQ A	03:28-03:32	13 20066-43
1247	03 07 15 196 03:55:53.9	52.288N 176.913W	ANDREANOF ISL. ALEUTIAN ISL.	127.5	2.0	PDE	EQ ABDE	03:57-04:47	51 20066-44
1248	03 07 15 196 04:46:56.5	21.799N 103.425E	SOUTHEAST ASIA	33.5	5.0	PDE	EQ A	04:54-05:05	12 20066-45
1249	03 07 15 196 07:48:59.4	60.282N 140.897W	SOUTHEASTERN ALASKA	15.5	1.0	PDE	EQ A	07:53-08:05	13 20066-46
1250	03 07 15 196 10:39:08.3	23.005N 121.439E	TAIWAN	36.5	0.0	PDE	EQ A	10:42-10:53	12 20066-47
1251	03 07 15 196 12:45:38.2	5.465N 126.540E	MINDANAO PHILIPPINE ISLANDS	47.5	5.0	PDE	EQ A	18:48-18:59	12 20066-48
1252	03 07 16 197 02:32:16.0	5.495N 126.530E	MINDANAO PHILIPPINE ISLANDS	30.5	2.0	PDE	EQ A	02:35-02:46	12 20066-49
1253	03 07 16 197 07:55:24.6	7.106S 129.361E	BANDA SEA	150.5	4.0	PDE	EQ A	07:50-08:10	13 20066-50
1334	03 07 16 197 11:25:11.7	7.704S 126.744E	BANDA SEA	176.5	2.0	PDE	EQ A	11:20-11:40	13 20071-11
1335	03 07 16 197 14:09:47.5	0.156S 121.786E	MINAHASSA PENINSULA	71.5	2.0	PDE	EQ A	14:13-14:24	12 20071-12
1336	03 07 16 197 15:50:07.3	10.901S 177.556E	FIJI ISLANDS	11.6	4.0	PDE	EQ A	15:52-16:04	13 20071-13
1337	03 07 16 197 17:19:22.2	44.876N 140.071E	EASTERN SEA OF JAPAN	246.4	0.0	PDE	EQ ABDE	17:20-18:00	49 20071-14
1338	03 07 16 197 18:17:11.4	0.141S 121.664E	MINAHASSA PENINSULA	49.5	0.0	PDE	EQ A	18:21-18:32	12 20071-15
1339	03 07 16 197 23:20:22.2	7.418S 100.233E	JAVA	130.4	9.0	PDE	EQ A	23:34-23:45	12 20071-16
1340	03 07 17 190 01:33:40.1	0.104S 121.679E	MINAHASSA PENINSULA	54.5	0.0	PDE	EQ A	01:37-01:48	12 20071-17
1341	03 07 17 190 01:56:52.0	49.230N 155.669E	KURIL ISLANDS	96.5	0.0	PDE	EQ ABDE	01:50-02:43	46 20071-18
1342	03 07 17 190 05:22:52.0	5.379N 126.555E	MINDANAO PHILIPPINE ISLANDS	45.5	3.0	PDE	EQ A	05:26-05:37	12 20071-19
1343	03 07 17 190 05:44:45.5	0.115S 121.665E	MINAHASSA PENINSULA	54.5	2.0	PDE	EQ A	05:48-05:59	12 20071-20
1344	03 07 17 190 06:29:19.0	10.479S 177.784W	FIJI ISLANDS REGION	691.5	1.0	PDE	EQ A	06:31-06:42	12 20071-21
1345	03 07 17 190 10:14:26.1	0.056S 121.727E	MINAHASSA PENINSULA	51.5	2.0	PDE	EQ A	10:18-10:29	12 20071-22
1346	03 07 17 190 10:21:54.0	7.144S 129.546E	BANDA SEA	103.4	9.0	PDE	EQ A	10:25-10:36	12 20071-23
1347	03 07 17 190 13:15:52.6	0.024S 121.771E	MINAHASSA PENINSULA	33.5	0.0	PDE	EQ A	13:19-13:31	13 20071-24
1348	03 07 17 190 14:47:05.6	23.500S 179.051E	SOUTH OF FIJI ISLANDS	554.5	0.0	PDE	EQ A	14:49-15:01	13 20071-25
1349	03 07 17 190 16:01:54.1	0.003S 121.763E	MINAHASSA PENINSULA	52.5	2.0	PDE	EQ A	16:05-16:17	13 20071-26
1350	03 07 17 190 19:04:19.3	0.081S 121.748E	MINAHASSA PENINSULA	62.5	4.0	PDE	EQ A	19:08-19:19	12 20071-27
1351	03 07 17 190 21:06:24.7	36.335N 70.838E	HINDU KUSH REGION	216.4	9.0	PDE	EQ A	21:13-21:25	13 20071-28
1352	03 07 17 190 21:56:21.4	31.256S 170.283W	KERMADEC ISLANDS REGION	87.5	3.0	PDE	EQ A	22:02-22:12	13 20071-29
1353	03 07 17 190 22:10:23.1	0.079S 121.689E	MINAHASSA PENINSULA	49.5	4.0	PDE	EQ A	22:14-22:25	12 20071-30
1354	03 07 17 190 23:02:49.7	22.707S 170.130W	SOUTH OF FIJI ISLANDS	335.5	2.0	PDE	EQ A	23:05-23:17	12 20071-31
1355	03 07 18 190 01:35:19.0	0.042N 121.641E	MINAHASSA PENINSULA	51.5	1.0	PDE	EQ A	01:39-01:50	12 20071-32
1356	03 07 18 190 02:14:14.7	0.110S 121.697E	MINAHASSA PENINSULA	62.5	4.0	PDE	EQ A	02:18-02:29	12 20071-33
1357	03 07 18 190 05:11:25.1	37.253N 141.613E	NEAR E COAST OF HONSHU JAPAN	42.5	2.0	PDE	EQ ABDE	05:12-05:54	43 20071-34
1358	03 07 18 190 05:20:06.5	0.120S 121.727E	MINAHASSA PENINSULA	62.5	0.0	PDE	EQ A	05:32-05:43	12 20071-35
1359	03 07 18 190 07:27:56.0	0.114S 121.787E	MINAHASSA PENINSULA	62.5	4.0	PDE	EQ A	07:31-07:43	13 20071-36
1360	03 07 18 190 09:41:20.2	0.040S 121.742E	MINAHASSA PENINSULA	54.5	1.0	PDE	EQ A	09:45-09:56	12 20071-37
1361	03 07 18 190 12:49:33.2	0.178S 121.692E	MINAHASSA PENINSULA	63.5	0.0	PDE	EQ A	12:53-13:04	12 20071-38
1362	03 07 18 190 13:40:26.3	0.031S 121.649E	MINAHASSA PENINSULA	75.5	3.0	PDE	EQ A	13:44-13:55	12 20071-39
1363	03 07 18 190 14:57:52.6	0.066S 121.743E	MINAHASSA PENINSULA	62.5	1.0	PDE	EQ A	15:01-15:13	13 20071-40
1364	03 07 18 190 18:09:03.6</								

## WAKE HYDROPHONE INFORMATION PROCESSING SYSTEM (WHIPS) EVENT LISTING

19 DEC 83

KEY: INFORMATION SOURCES - PDE=NEIS PDECARD, MON=NEIS MONTHLY LIST, ICS=ICS LIST, HEL=HELICORDER, OTH=OTHER  
EVENT TYPE - EQ=EARTHQUAKE, NX=NUCLEAR EXPLOSION, SK=SCIENTIFIC EXPLOSION, OT=OTHER, UN=UNKNOWN  
PHASES - A=P, B=PO, C=S, D=SO, E=T, F=OTHER

EVNT \*\*\*\*\*ORIGIN TIME\*\*\*\*\* \*\*COORDINATES\*\* \*\*\*\*\*LOCATION\*\*\*\*\* DEP \*MAGNI\* INF EV \*\*\*\*\*SAVED\*\*\*\*\* \*STRIP\*  
\*NO\* \*VR\*MO\*DA\*JUL\*HR\*MIN\*SECS \*LAT\* \*LON\* \*KM\* \*BDV\*SRF SRC TP PHASES\*\*INTERVAL\*\*MMS TAPE-FIL

1304	03	07	22	203	02:25:48.2	0.5525	121.717E	MINAHASSA PENINSULA	53	5.0	0.0	PDE	EQ	A	02:29-02:48	12	22073-8
1305	03	07	22	203	02:36:43.9	14.6625	167.251E	VANUATU ISLANDS	193	5.4	0.0	PDE	EQ	ABDE	02:38-03:26	49	22073-8
1306	03	07	22	203	02:39:55.3	36.223N	120.395W	CENTRAL CALIFORNIA	7	6.0	5.7	PDE	EQ	ABD	02:46-03:18	25	22073-8
1307	03	07	22	203	06:36:14.6	0.1985	121.678E	MINAHASSA PENINSULA	32	5.1	0.0	PDE	EQ	A	06:48-06:51	12	22073-9
1308	03	07	23	204	08:29:48.0	0.1435	121.619E	MINAHASSA PENINSULA	46	5.2	0.0	PDE	EQ	A	08:33-08:44	12	22073-10
1309	03	07	23	204	08:56:13.4	0.2235	121.596E	MINAHASSA PENINSULA	62	5.1	0.0	PDE	EQ	A	08:56-09:11	12	22073-11
1310	03	07	23	204	15:06:48.4	12.441N	144.081E	SOUTH OF MARIANA ISLANDS	41	4.9	0.0	PDE	EQ	ABD	15:07-15:28	14	22073-12
1311	03	07	23	204	22:57:24.2	0.1335	121.681E	MINAHASSA PENINSULA	62	5.1	0.0	PDE	EQ	A	22:57-23:12	12	22073-13
1312	03	07	24	205	00:52:25.5	27.904S	176.480W	KERMADEC ISLANDS REGION	73	5.3	0.0	PDE	EQ	A	00:56-01:07	12	22073-14
1313	03	07	24	205	05:59:35.2	43.693N	150.378E	KURIL ISLANDS REGION	33	5.0	0.0	PDE	EQ	ABDE	05:41-12:22	43	22073-15
1314	03	07	24	205	09:48:44.1	6.1835	154.634E	SOLOMON ISLANDS	414	4.9	0.0	PDE	EQ	ABDE	09:41-12:22	43	22073-16
1315	03	07	24	205	10:58:37.0	51.921N	158.926E	NEAR EAST COAST OF KAMCHATKA	65	4.6	0.0	PDE	EQ	ABD	11:02-11:16	12	22073-17
1316	03	07	24	205	14:52:33.3	39.739N	139.453E	NEAR W COAST OF HONSHU JAPAN	190	5.2	0.0	PDE	EQ	ABDE	14:53-15:39	47	22073-18
1317	03	07	24	205	17:58:07.4	19.356S	176.076W	FUJI ISLANDS REGION	288	4.8	0.0	PDE	EQ	A	17:52-18:04	13	22073-19
1318	03	07	24	205	23:07:38.7	53.852N	158.391E	NEAR EAST COAST OF KAMCHATKA	101	6.1	0.0	PDE	EQ	ABDE	23:09-23:59	51	22073-20
1319	03	07	24	205	23:38:08.3	0.1675	119.579E	FLORES ISLANDS REGION	33	5.0	5.9	PDE	EQ	A	23:42-23:54	13	22073-21
1320	03	07	25	206	02:31:48.0	36.220N	120.390W	CENTRAL CALIFORNIA	8	5.6	5.3	PDE	EQ	A	22:37-22:48	12	22074-1
1321	03	07	25	206	23:17:44.1	40.102N	139.001E	NEAR W COAST OF HONSHU JAPAN	33	5.0	0.0	PDE	EQ	ABDE	23:15-23:06	47	22074-2
1322	03	07	26	207	11:01:59.2	0.0445	121.776E	MINAHASSA PENINSULA	57	5.2	4.0	PDE	EQ	A	11:05-11:17	13	22074-3
1323	03	07	26	207	20:14:51.6	0.655N	120.076E	MINAHASSA PENINSULA	43	5.3	4.5	PDE	EQ	A	20:19-20:30	12	22074-4
1324	03	07	28	209	01:40:33.3	20.149S	176.255W	KERMADEC ISLANDS REGION	31	5.6	5.4	PDE	EQ	A	01:44-01:56	13	22074-5
1325	03	07	28	209	03:00:59.0	0.685N	120.092E	MINAHASSA PENINSULA	41	5.0	0.0	PDE	EQ	A	03:05-03:16	12	22074-6
1326	03	07	28	209	05:58:11.1	43.725N	147.668E	KURIL ISLANDS	34	5.2	5.0	PDE	EQ	ABDE	05:59-10:42	44	22074-7
1327	03	07	28	209	15:06:44.1	42.805N	142.647E	HOKKAI DO JAPAN REGION	59	5.2	0.0	PDE	EQ	ABDE	15:08-15:50	45	22074-8
1328	03	07	28	209	19:20:24.1	22.403S	171.430E	LOVATY ISLANDS REGION	159	5.2	0.0	PDE	EQ	A	19:31-19:42	12	22074-9
1329	03	07	29	210	11:25:27.0	0.7525	185.629E	SUNDA STRAIT	33	5.5	4.0	PDE	EQ	A	11:26-11:37	12	22074-10
1330	03	07	29	210	13:26:54.3	14.328N	146.518E	MARIANA ISLANDS	89	5.0	0.0	PDE	EQ	ABD	13:26-13:35	14	22074-11
1331	03	07	29	210	14:21:35.6	4.9175	145.376E	NEAR N COAST PAPUA NEW GUINEA	161	4.0	0.0	PDE	EQ	ABDE	14:23-14:26	16	22074-12
1332	03	07	29	210	19:24:23.6	32.322N	140.087E	SOUTH OF HONSHU JAPAN	51	5.0	0.0	PDE	EQ	ABDE	19:25-20:05	41	22074-13
1333	03	07	29	210	20:25:58.7	5.394N	126.567E	MINDANAO PHILIPPINE ISLANDS	50	5.2	4.5	PDE	EQ	A	20:29-20:40	12	22074-14
1334	03	07	30	211	03:35:09.6	0.1595	121.720E	MINAHASSA PENINSULA	75	5.0	0.0	PDE	EQ	A	03:39-03:50	12	22074-15
1335	03	07	30	211	07:07:14.6	0.1445	121.709E	MINAHASSA PENINSULA	63	5.0	0.0	PDE	EQ	A	07:11-07:22	12	22074-16
1336	03	07	30	211	08:09:52.6	52.451N	170.580W	FOX ISLANDS ALEUTIAN ISLANDS	50	5.2	4.3	PDE	EQ	ABDE	08:12-08:23	52	22074-17
1337	03	07	30	211	11:24:41.7	56.414N	162.801E	NEAR EAST COAST OF KAMCHATKA	33	4.6	0.0	PDE	EQ	ABD	11:27-11:44	18	22074-18
1338	03	07	31	212	00:08:24.9	0.616N	120.103E	MINAHASSA PENINSULA	33	5.3	4.4	PDE	EQ	A	00:12-00:23	12	22074-19
1339	03	07	31	212	09:09:21.3	0.964N	123.931E	MINAHASSA PENINSULA	272	5.1	0.0	PDE	EQ	A	09:12-09:23	12	22074-20
1340	03	07	31	212	10:26:08.2	20.142S	126.869W	SOUTH PACIFIC OCEAN	10	6.0	5.3	PDE	EQ	ABD	10:33-11:02	26	22074-21
1341	03	07	31	212	11:57:50.0	20.120S	127.080W	SOUTH PACIFIC OCEAN	10	5.4	0.0	PDE	EQ	ABD	12:05-12:32	26	22075-1
1342	03	07	31	212	16:32:33.9	5.628N	94.784E	NORTHERN SUMATERA	96	5.0	0.0	PDE	EQ	A	16:35-16:52	12	22075-2
1343	03	07	31	212	21:05:10.5	19.247N	145.435E	MARIANA ISLANDS	163	5.0	0.0	PDE	EQ	ABDE	21:04-21:37	34	22075-3
1344	03	07	31	212	23:14:55.7	16.921N	147.190E	MARIANA ISLANDS REGION	52	5.2	4.8	PDE	EQ	ABDE	23:14-23:45	32	22075-4
1345	03	07	31	212	23:14:55.7	0.000N	0.000E	PROBABLE MARIANAS PO. SO. T	0	0.0	0.0	PDE	EQ	ABDE	23:15-23:45	32	22075-5
1346	03	07	31	212	23:14:55.7	3.3915	145.835E	NEAR N COAST PAPUA NEW GUINEA	33	5.0	5.1	PDE	EQ	ABDE	23:15-23:45	45	22075-6
1347	03	07	31	212	23:14:55.7	0.000N	0.000E	MINAHASSA PENINSULA	62	5.2	0.0	PDE	EQ	A	11:18-11:29	12	22075-7
1348	03	07	31	212	23:14:55.7	0.000N	0.000E	MINAHASSA PENINSULA	156	6.1	0.0	PDE	EQ	A	22:28-22:31	12	22075-8
1349	03	07	31	212	23:14:55.7	45.174N	153.482E	KURIL ISLANDS REGION	68	5.4	0.0	PDE	EQ	ABDE	06:05-06:51	43	22075-9
1350	03	07	31	212	23:14:55.7	7.1915	117.398E	BALI SEA	500	5.4	0.0	PDE	EQ	A	12:47-12:58	12	22075-10
1351	03	07	31	212	23:14:55.7	16.469S	177.615E	FUJI ISLANDS	33	5.1	0.0	PDE	EQ	A	13:17-13:29	12	22075-11
1352	03	07	31	212	23:14:55.7	27.378N	120.447E	RYUKYU ISLANDS	49	5.4	0.0	PDE	EQ	A	22:18-22:21	12	22075-12
1353	03	07	31	212	23:14:55.7	11.205S	162.380E	SOLOMON ISLANDS	33	4.9	0.0	PDE	EQ	ABD	07:14-07:29	16	22075-13
1434	03	08	03	215	13:33:00.0	37.119N	116.009W	SOUTHERN NEVADA	0	4.2	0.0	PDE	NX	A	13:39-13:50	12	22075-14
1435	03	08	03	215	18:17:44.3	17.362S	167.703E	VANUATU ISLANDS	49	5.4	5.5	PDE	EQ	ABDE	18:28-19:10	51	22075-15
1436	03	08	03	215	22:29:44.6	22.280S	7.463E	S ATLANTIC OCEAN GOOD ANTIPODE	10	5.1	0.0	PDE	EQ	A	22:38-22:57	20	22075-16
1437	03	08	03	215	23:18:29.6	21.624N	143.048E	MARIANA ISLANDS REGION	309	5.0	0.0	PDE	EQ	ABDE	23:18-23:53	36	22075-17
1438	03	08	03	215	23:25:27.6	21.669N	143.054E	MARIANA ISLANDS REGION	305	4.0	0.0	PDE	EQ	ABDE	23:25-23:52	36	22075-18
1439	03	08	03	215	15:18:16.0	0.2745	120.278E	TIMOR SEA	50	4.0	0.0	PDE	EQ	A	15:19-15:38	12	22075-19
1440	03	08	05	217	00:33:44.7	52.708N	159.770E	OFF EAST COAST OF KAMCHATKA	33	5.4	7.7	PDE	EQ	ABDE	00:35-01:24	50	22076-1
1441	03	08	05	217	05:25:43.7	17.276S	167.791E	VANUATU ISLANDS	33	5.3	5.7	PDE	EQ	ABDE	05:28-05:18	51	22076-2
1442	03	08	05	217	06:21:42.4	3.589S	62.171W	WESTERN BRAZIL	21	5.5	5.3	PDE	EQ	A	06:31-06:50	20	22076-3
1443	03	08	05	217	07:02:41.3	17.216S	167.027E	VANUATU ISLANDS	33	5.2	5.2	PDE	EQ	ABDE	07:05-07:55	51	22076-4
1444	03	08	05	217	08:29:32.3	7.727S	123.548E	BANDA SEA	274	4.0	0.0	PDE	EQ	A	08:33-08:44	12	22076-5
1445	03	08	05	217	08:26:49.3	16.134N	93.886W	CHIAPAS MEXICO	06	5.6	0.0	PDE	EQ	A	08:35-02:46	12	22076-6
1446	03	08	05	217	15:43:52.6	48.176N	24.720E	AEGEAN SEA	10	6.3	7.1	PDE	EQ	AF	15:48-17:47	120	22076-7
1447	03	08	05	217	22:06:03.9	44.413N	149.100E	KURIL ISLANDS	33	5.2	0.0	PDE	EQ	ABDE	22:07-22:50	44	22076-8
1448	03	08	05	217	22:37:54.9	6.556S	130.127E	BANDA SEA	161	5.0	0.0	PDE	EQ	A	22:41-22:52	12	22076-9
1449	03	08	05	217	22:48:21.7	6.336S	149.236E	NEW BRITAIN REGION	54	4.9	4.4	PDE	EQ	ABD	02:49-03:05	17	22076-10
1450	03	08	05	217	26:27:25.3	31.112N	140.548E	SOUTH OF HONSHU JAPAN	127	4.0	0.0	PDE	EQ	ABD	06:28-06:42	15	22076-11
1451	03	08	05	217	33:47:58.0	35.466N	130.911E	HONSHU JAPAN	33	5.0	5.3	PDE	EQ	ABDE	03:48-04:32	44	22076-12
1452	03	08	05	217	16:54:11.2	27.521S	173.332W	SOUTH ATLANTIC RIDGE	10	5.2	0.0	PDE	EQ	A	17:03-17:22	20	22076-13
1453	03	08	05	217	23:59:00.0	7.532S	120.273E	BANDA SEA	173	5.0	0.0	PDE	EQ	A	00:27-00:38	12	22076-14
1454	03	08	05	217	10:21:10.6	0.3995	132.598E	WEST IRIAN REGION	33	5.2	5.0	PDE	EQ	ABDE	10:23-19:16	5	

## WAKE HYDROPHONE INFORMATION PROCESSING SYSTEM (WHIPS) EVENT LISTING

19 DEC 83

KEY: INFORMATION SOURCES - PDE=NEIS PDECARD, MON=NEIS MONTHLY LIST, ICS=ICS LIST, MEL=HELICORDER, OTH=OTHER  
 EVENT TYPE - EQ=EARTHQUAKE, NX=NUCLEAR EXPLOSION, SX=SCIENTIFIC EXPLOSION, OT=OTHER, UN=UNKNOWN  
 PHASES - A=P, B=PO, C=S, D=SO, E=T, F=OTHER

EVNT	*****ORIGIN TIME*****	*****COORDINATES*****	*****LOCATION*****	DEP	MAGNI	INF	EV	*****SAVED*****	*****STRIP*****
NO	VR=MO=DA=JUL=HR=MM=SECS	*****LAT*****LON*****	*****DESCRIPTION*****	KM	BDY=SRF	SRC	TP	PHASES=INTERVAL=MMNS	TAPE=FILE
1484	03 08 18 238 08:38:18.2	19.4165 172.779W	TONGA ISLANDS REGION	33	6.3	5.0	PDE EQ A	08:33-08:44	12 20070-9
1485	03 08 18 238 09:42:30.1	3.8355 151.293E	NEW IRELAND REGION	33	6.2	5.0	PDE EQ ABDE	09:43-10:24	42 20076-10
1486	03 08 18 238 16:05:48.3	3.7485 151.344E	NEW IRELAND REGION	33	5.2	5.0	PDE EQ ABDE	16:05-16:47	42 20078-11
1487	03 08 18 238 16:09:58.6	73.373N 54.839E	NOVAYA ZEMLYA	5	5.9	4.1	PDE NX A	16:17-16:28	12 20078-11
1488	03 08 00 000 00:00:00.0	0.000N 0.000E	PROBABLE MARIANAS PO SO T	0	0.0	0.0	MEL EQ BDE	17:37-18:06	38 20076-12
1489	03 08 10 238 19:46:49.6	3.7865 151.190E	NEW IRELAND REGION	33	5.2	4.9	PDE EQ A	19:47-19:59	13 20076-13
1490	03 08 19 231 14:35:34.3	2.175N 127.078E	MOLUCCA PASSAGE	55	5.2	4.3	PDE EQ A	14:38-14:49	12 20076-14
1491	03 08 00 000 00:00:00.0	0.000N 0.000E	PROBABLE BONIN ISL. PO SO T	0	0.0	0.0	MEL EQ BDE	08:54-01:38	37 20076-15
1492	03 08 00 000 00:00:00.0	0.000N 0.000E	PROBABLE JAPAN PO SO T	0	0.0	0.0	MEL EQ BDE	05:24-00:05	42 20079-1
1493	03 08 20 232 06:19:28.2	8.5585 117.569E	SUMBAWA ISLAND REGION	134	5.5	5.0	PDE EQ A	06:24-06:35	12 20079-2
1494	03 08 20 232 13:08:31.7	27.860N 141.807E	BONIN ISLANDS REGION	35	5.8	5.5	PDE EQ ABDE	13:29-13:46	38 20079-3
1495	03 08 20 232 14:48:30.2	58.865N 156.160E	KURIL ISLANDS	120	5.8	5.0	PDE EQ ABDE	14:50-15:37	48 20079-4
1496	03 08 20 232 17:15:06.6	18.1175 179.734W	FUJI ISLANDS REGION	659	4.7	0.0	PDE EQ A	17:17-17:28	12 20079-5
1497	03 08 20 232 17:15:24.4	39.328N 73.611E	TAJIK-KINJIANG BORDER REGION	33	4.9	4.4	PDE EQ A	17:22-17:34	13 20079-6
1498	03 08 21 233 06:18:55.0	4.519N 127.789E	TALAUD ISLANDS	83	5.8	5.0	PDE EQ A	06:21-06:33	13 20079-6
1499	03 08 21 233 08:34:45.8	3.714N 126.620E	TALAUD ISLANDS	48	5.8	5.6	PDE EQ A	08:37-08:49	13 20079-7
1500	03 08 21 233 17:21:13.6	7.3845 121.185E	FLORES SEA	541	5.1	0.0	PDE EQ A	17:25-17:36	12 20079-8
1501	03 08 21 233 18:58:19.2	28.782S 112.653W	EASTER ISLAND REGION	10	5.4	5.5	PDE EQ A	19:06-19:18	13 20079-9
1502	03 08 21 233 22:57:31.4	23.481S 177.180W	SOUTH OF FUJI ISLANDS	169	5.5	5.0	PDE EQ A	23:00-23:12	13 0-0
1503	03 08 22 234 04:58:11.9	31.880N 141.710E	SOUTH OF HONSHU JAPAN	33	4.5	0.0	PDE EQ ABD	04:59-05:13	15 0-0
1504	03 08 22 234 05:53:26.0	14.027S 166.969E	VANUATU ISLANDS	112	5.5	5.0	PDE EQ ABDE	05:55-06:43	49 0-0
1505	03 08 22 234 09:09:42.3	7.819S 138.811E	TANIMBAR ISLANDS REGION	33	5.8	5.0	PDE EQ A	09:13-09:24	12 20080-1
1506	03 08 22 234 12:38:21.4	7.208N 34.422W	CENTRAL MID-ATLANTIC RIDGE	18	5.1	0.0	PDE EQ A	12:47-13:07	21 20080-2
1507	03 08 22 234 12:39:06.7	53.861N 160.493E	NEAR EAST COAST OF KAMCHATKA	33	5.4	0.0	PDE EQ ABDE	12:41-13:38	50 20080-2
1508	03 08 22 234 23:00:42.5	16.209S 167.903E	VANUATU ISLANDS	105	5.1	0.0	PDE EQ ABDE	23:02-23:52	51 20080-3
1509	03 08 22 234 23:16:30.0	3.507S 146.644E	BISMARCK SEA	29	5.4	5.5	PDE EQ ABDE	23:18-00:01	44 20080-3
1510	03 08 23 235 11:15:16.9	5.917S 150.996E	NEW BRITAIN REGION	52	5.1	4.0	PDE EQ ABDE	11:16-11:59	44 20080-4
1511	03 08 23 235 12:12:16.9	24.567N 95.200E	BURMA	126	5.1	0.0	PDE EQ A	12:18-12:29	12 20080-5
1512	03 08 23 235 23:39:41.0	5.912S 151.068E	NEW BRITAIN REGION	51	6.3	5.8	PDE EQ ABDE	23:41-00:23	43 20080-6
1513	03 08 24 236 13:36:38.9	48.385N 124.767W	NEAR COAST OF NORTHERN CALIF	38	5.5	5.7	PDE EQ ABDE	13:42-14:59	78 20080-7
1514	03 08 24 236 20:19:51.3	3.627N 122.258E	CELEBES SEA	621	4.8	0.0	PDE EQ A	20:22-20:33	12 20080-8
1515	03 08 25 237 00:12:58.0	5.427S 150.919E	NEW BRITAIN REGION	112	5.1	0.0	PDE EQ ABDE	00:14-00:56	43 20080-9
1516	03 08 25 237 07:03:08.3	5.945S 151.008E	NEW BRITAIN REGION	48	5.5	0.0	PDE EQ ABDE	07:04-07:47	44 20080-10
1517	03 08 25 237 11:05:38.0	39.152N 74.052E	SOUTHERN KINJIANG CHINA	33	5.0	4.9	PDE EQ A	11:03-11:24	12 20080-11
1518	03 08 25 237 20:23:32.6	33.498N 131.430E	KYUSHU JAPAN	121	6.1	0.0	PDE EQ ABDE	20:25-21:14	50 20080-12
1519	03 08 00 000 00:00:00.0	0.000N 0.000E	PROBABLE BONIN ISL. PO SO T	0	0.0	0.0	MEL EQ BDE	01:13-01:52	40 20080-1
1520	03 08 26 238 02:34:34.0	2.847S 139.097E	NEAR N COAST OF WEST IRIAN	76	5.4	0.0	PDE EQ A	02:36-02:47	12 20080-2
1521	03 08 26 238 08:18:15.1	3.684N 127.143E	TALAUD ISLANDS	33	5.2	0.0	PDE EQ A	08:21-08:32	12 20080-3
1522	03 08 26 238 18:20:32.0	20.785S 169.583E	VANUATU ISLANDS	100	5.3	0.0	PDE EQ ABDE	18:23-19:17	55 20080-4
1523	03 08 00 000 00:00:00.0	0.000N 0.000E	PROBABLE MARIANAS PO SO T	0	0.0	0.0	MEL EQ BDE	01:49-02:29	41 20080-5
1524	03 08 27 239 04:14:20.8	20.642S 178.023W	FUJI ISLANDS REGION	620	4.7	0.0	PDE EQ A	04:16-04:28	13 20080-6
1525	03 08 27 239 11:50:29.8	8.174N 126.005E	MINDANAO PHILIPPINE ISLANDS	55	5.2	0.0	PDE EQ A	11:53-12:04	12 20080-7
1526	03 08 27 239 12:31:40.9	85.517N 90.603E	NORTH OF SEVERNAYA ZEMLYA	10	4.7	4.8	PDE EQ A	12:38-12:49	12 20080-8
1527	03 08 27 239 18:49:58.3	8.186N 125.962E	MINDANAO PHILIPPINE ISLANDS	33	5.5	6.0	PDE EQ ABDE	18:50-19:49	60 20080-9
1528	03 08 28 240 11:30:14.7	46.197N 151.544E	KURIL ISLANDS	75	5.5	0.0	PDE EQ ABDE	11:31-12:15	45 20080-10
1529	03 08 28 240 13:19:32.5	44.972N 148.771E	KURIL ISLANDS	33	5.8	0.0	PDE EQ ABDE	13:28-14:04	45 20080-11
1530	03 08 29 241 05:19:24.5	3.430S 148.091E	BISMARCK SEA	33	5.2	5.0	PDE EQ ABDE	05:20-06:02	43 20080-12
1531	03 08 29 241 10:10:31.0	35.830N 121.353W	CENTRAL CALIFORNIA	0	5.3	0.0	PDE EQ ABDE	10:16-11:37	82 20080-1
1532	03 08 00 000 00:00:00.0	0.000N 0.000E	PROBABLE KURILS	0	0.0	0.0	MEL EQ BDE	10:12-10:54	43 20080-2
1533	03 08 29 241 15:36:13.6	9.561N 126.337E	MINDANAO PHILIPPINE ISLANDS	49	5.3	4.1	PDE EQ A	15:39-15:50	12 0-0
1534	03 08 30 242 05:57:01.5	6.360S 130.485E	BANDA SEA	136	5.1	0.0	PDE EQ A	06:00-06:11	12 0-0
1535	03 08 30 242 06:50:16.6	16.683S 172.075W	SAMOA ISLANDS REGION	35	6.1	5.7	PDE EQ ABD	08:53-09:11	19 0-0
1536	03 08 30 242 10:39:27.3	25.071N 94.722E	BURMA-INDIA BORDER REGION	63	5.6	0.0	PDE EQ A	10:45-10:56	12 0-0
1537	03 08 30 242 22:15:59.6	9.558S 158.018E	SOLOMON ISLANDS	76	5.8	0.0	PDE EQ ABDE	22:17-23:00	44 0-0
1538	03 08 31 243 19:40:11.2	12.514N 144.238E	SOUTH OF MARIANA ISLANDS	33	4.3	3.9	PDE EQ ABDE	19:48-20:15	36 0-0
1539	03 08 31 243 22:20:07.4	53.503N 163.622W	UNITAK ISLAND REGION	33	5.1	0.0	PDE EQ A	22:23-23:34	12 0-0
1540	03 08 00 000 00:00:00.0	0.000N 0.000E	PROBABLE MARIANAS	0	0.0	0.0	MEL EQ BDE	09:21-09:54	34 0-0
1541	03 08 01 244 14:00:00.0	37.273N 116.355W	SOUTHERN NEVADA	0	5.4	0.0	PDE NX A	14:06-14:17	12 0-0
1542	03 08 02 245 03:05:40.2	36.624N 148.932E	NEAR E COAST OF HONSHU JAPAN	68	5.1	0.0	PDE EQ ABDE	03:06-03:49	44 0-0
1543	03 08 02 245 04:09:39.0	52.363N 175.517W	ANDREANOF ISL. ALEUTIAN ISL.	112	4.7	0.0	PDE EQ ABD	04:11-04:28	18 0-0

EOP..

 Reproduced from  
 best available copy.

END

FILMED

3-84

DTIC